POCKET-TYPE PRESTRESSED BRICKWORK RETAINING WALLS

NABEEL AL-ZAFER ALGAHTANI, BSc, ME.

A thesis submitted for the degree of
Doctor of Philosophy

Department of Civil Engineering and Building Science

The University of Edinburgh

May 1992


بسم الله الرحمن الرحيم

ACKNOWLEDGEMENT

Praise be to God, Lord of the universe, by his will the accomplishment of this study was made possible; and may His blessing and peace be upon His Prophets Mohammed, Jesus, Moses....etc.

To my parents, family and relatives who gave me all the support, love and care in my study in the U.S.A and the U.K. I pray The Most Generous to reward you.

I would like to express my profound gratitude to the **Saline Water Conversion Corporation** in Saudi Arabia staff members, Especially, his Excellency Abdullah Algelakah, for granting me the scholarship that enabled me to pursue my Phd.

I would like also to extend my utmost gratitude to the following people: Professor and Head of Department - J. Michael Rotter, for his personal attention, encouragement and contiuous support, Professor M. Forde, Dr. R. Royles, Mrs. B. McWilliam, Mrs. G. Temple, Mrs. C. Corsie, Mr. J. Baxter, Mr. J. Hutcheson, Dr. F. Khalaf, Dr. K. El-deeb (Thank You Khaled), Mr. N. Naghoj, Mr. R. Duarte, Mr. S. George, Miss. D. Duarte, Dr. J. Uduehi and Dr. B. Kumar, The department technicians and to all my friends that I have not mentioned personally (please forgive me).

Finally, I am particularly grateful to the most important people without whom this work would not have reached its present form: Professor A.W. Hendry and Dr. D.R. Fairbairn, for their guidance, supplying useful references, their open-door policy and invaluable advice in the most

difficult time of the research, no written word could do you justice, God bless you.

The work of this thesis is dedicated to my younger brother who passed away during the process of the work. First Lieutenant **Adel Algahtani.**

ABSTRACT

This thesis presents the results of a study into the behaviour of post-tensioned pocket type brickwork retaining walls. An analytical and experimental study was carried out to examine the behaviour of the wall up to failure. The programme of work considered the effect of the following parameters on the performance of the wall:-

i) Vertical concentrated eccentric load.

ii) Percentage area of steel.

iii) Pocket spacing and wall slenderness.

iv) Type of wall bond.

The effect of the last three parameters on deflection, cracking and ultimate load were studied. The following experimental work was carried out to examine the above parameters :-

i) Nine full-scale six course prisms consisting of three with open pocket, three with concrete infill and three solid brickwork to be tested in axial compression .

ii) Two full scale beams with the bed joints running parallel to the direction of the induced prestressing load.

iii) Six full scale beams/slabs with the bed joints running perpendicular to the direction of the induced prestressing load.

iv) Six half-scale retaining walls.

v) A comprehensive series of control tests, on mortar and grout specimens, single course prisms and small wallets, were undertaken to determine the non-linear deformation characteristics and compressive strengths of brickwork masonry.

The theoretical investigation was based on the following theories:-

i) Finite Element Analysis

ii) Direct Method

iii) Stress Block Analysis

iv) Yield Line Analysis

The results of the analyses were compared with those based on the Code of Practice, B.S. 5628, Part 2, 1985. A computer program was written in Fortran to predict the ultimate moment of the wall panels, using predicted equilibrium equations. Good agreement was found between the theoretical and experimental results. The results show that post-tensioned pocket type brickwork retaining walls have a large nominal strength, largely due to the presence of prestressing forces and the behaviour of the walls as homogenous cantilevers. The most effective pocket spacing was found to be h/3, and the maximum spacing should be limited to give an aspect ratio which is greater than 1.15.

The study confirms the applicability of prestressed brick masonry for structures such as slabs and retaining walls irrespective of the type of brickwork bond.

CONTENTS

NOTATION

a	Shear Span
A,B,C	Cross-sectional Area of Section
A_{ps}	Area of prestressed reinforcement
b	Width of Section
C	Compressive Force in Section
d	Effective Depth of Prestressing Strand
e	Eccentricity of Prestress Force
E	Elastic Modulus of Brickwork
f	Compressive Stress in Brickwork
F_k	Characteristic Compressive Strength of Masonry
f_m	Compressive Strength of Brickwork
f_{pu}	2% Proof Stress of Prestressing Strand
f_{sy}	Yield Stress of the Reinforcement
f_v	Characteristic Shear Strength of Masonry
h	Total Depth of Section
i	Value for the type of boundary conditions assumed
la	Lever Arm
L	Length between Pockets
M	Bending Moment
M_{cr}	Cracking Moment
M_p	Panel Bending Moment of Resistance
M_u	Ultimate Moment
n	Neutral Axis Depth
P	Prestressing Force or External Load
S_m	Average spacing of crack
T_s	Tensile Force in Steel
v	Shear Stress
V	Shear Force

W Crack Width

X_1-X_4 Coefficients of Stress/Strain Relationship of Brickwork

x,y,z Co-ordinate Axes

α Aspect Ratio, $= \frac{\text{h(wall height)}}{\text{L}}$

γ_{mm} and γ_{ms} are material partial safety factors for masonry and steel respectively

β Overlap Prestressing Force Factor

$\beta_1 - \beta_4$ Degree of Tension Stiffening

ε Strain in Brickwork

ε_1 & ε_2 Strains in Top and Bottom Fibres of Sections

ε_m Ultimate Compressive Strain in brickwork

ε_{ma} Strain on the Brickwork at Tendon Level Due to Applied Load

ε_{me} Total Strain on the Brickwork at Tendon Level due to the Prestressing Load

ε_{p1} and ε_{p2} Prestress Strains

ε_s Total Strain in Prestressing Strand

ε_{sa} Total Strain due to the Applied Load

ε_{sam} Average Additional Strain after Cracking

ε_{sm} Average Strain after Cracking at Certain Level

ε_{sy} Strain in the Reinforcement at the Yield Stress

λ_1, λ_2 and λ_3 Stress Block Factors

ϕ Rotation or Curvature

ϕ_{av} Average Curvature

ϕ_p Curvature due to Prestress

σ Stress

σ_1, σ_2 and σ_3 Principal Stresses

μ Orthogonal Strength Ratio

ρ Ratio of Steel in Section

CHAPTER 1

INTRODUCTION

1.1 Historical Background

1.1.1 Plain Masonry

Masonry is a composite structural material consisting of stone, brick or block bonded solids with mortar joints and is the oldest construction material recorded by mankind dating back more than 20,000 years. The first recorded manufacture of sunbaked clay bricks has been attributed to the Samarians some 5500 years ago (Baker, 1981). Ancient Egypt was probably the oldest civilisation to use stone masonry e.g. in building the Pyramids. The existence of Stonehenge in Wiltshire, England is another historical acknowledgement of the very early use of masonry in construction.

Brickwork masonry has a comparatively high compressive strength but very low tensile strength compared to other structural materials. Its use was therefore limited to the compressive loading in structures such as walls, columns and arches, where the section was designed under conditions where the flexural and tensile strength of the section were not taken into account. As a result, the design process introduced limitations on the strength and serviceability of the structure. Up to the early 19th century, lateral loads were not of great concern. The minimum cross-sectional thickness of a brick wall was 1.5 bricks, based on calculations for gravity loads only. The foundations were built very thick using natural stone blocks.

Between 1951 and 1957, Swiss design engineers used brickwork to construct an 18 storey building. To increase the shear strength and

lateral stability of the wall, a 150mm thick cross-section was adopted for the wall with special reorientation of the brickwork panel (Baker, 1987). According to Cajdert (1980), the first reported compressive tests on brickwork were performed at the Watertown Arsenals in the U.S.A. about 1885. When masonry carries both compressive and lateral loads, the effect of the compressive load is to increase the flexural strength of the wall, thus preventing the wall from collapse as a result of the development of cracks.

The Ronan Point disaster in 1968 demanded the introduction of stricter building regulations in the U.K. Furthermore, an extensive research programme was introduced to study the lateral strength of brick walls with consequent publications by the British Ceramic Research Association and the Civil Engineering Department at the University of Edinburgh under Professor Hendry. According to Hendry (1990), the economic success of masonry construction has been achieved, not only by the rationalisation of structural design, but also because the walls which comprise a building structure can perform several functions within a framed structure. Masonry walls simultaneously provide structure, sub-division of space, thermal and acoustic insulation, as well as fire and weather protection. The material is relatively cheap and durable, can provide infinite flexibility in plan form and offer an attractive external appearance.

1.1.2 Reinforced Brickwork

In 1825, Marc Brunel supervised the construction of two 15.20 metre diameter reinforced brickwork shafts as part of a Tunnel under the River Thames. Even though the project has since experienced considerable settlement, the brickwork shafts still stand tall with no developed cracks

(Schneider and Dickey, 1980, Plummer and Blume, 1953). Some years after Brunel's work (1837), Pasley reported on the flexural strength of reinforced brickwork compared to unreinforced brickwork structures. His study was based on several brickwork beams built with and without steel reinforcement (Schneider and Dickey, 1980).

In 1912 the Expanded Metal Co. carried out a lateral load test on a reinforced brickwork slab, as reported by Cajde t,(1980).

Many researchers however consider that the actual beginning of modern reinforced brickwork technology can be attributed to the work published by Brebner in 1923. His work covered experimental and theoretical analyses of reinforced brickwork beams, columns and slabs (Plummer and Blume, 1953).

Interest in reinforced brickwork in the U.K. began following work carried out at the Building Research Station in 1938. However, due to the outbreak of the Second World War, progress in reinforced brickwork research was very limited. In 1985, however the introduction of a Code of Practice based on limit state design philosophy signalled a resurgence of interest. From that point, reinforced brickwork became a competitor to reinforced concrete in some construction applications. The advantages of using reinforced brickwork as opposed to unreinforced brickwork can be summarised as follows:

1) The adddition of steel reinforcement can improve the performance of brickwork as a compressive material. Reinforced brickwork has greater flexural strength and shear strength compared to plain brickwork structures.

2) The addition of steel reinforcement changes the behaviour of the brickwork from brittle to ductile and produces an improved performance in strain and crack resistance as well as a higher tensile strength compared to plain brickwork.

3) With the removal of load, any cracks tend to close up and the brickwork maintains its serviceability and structural life.

4) Reinforced brickwork is essential in seismic areas where plain brickwork is considered inapplicable.

5) Brickwork as a material has more aesthetic appeal than concrete.

6) Haseltine and Tutt (1977) carried out a cost consideration study in which they compared a number of reinforced brickwork walls with corresponding reinforced concrete retaining walls. Their results showed that the reinforced brickwork walls were considerably cheaper than the reinforced concrete structures.

1.1.3 Prestressed Brickwork

Safety and economics are the main design objectives for modern structural elements along with a development towards the use of higher strength materials. Such action reduces the cross-sectional dimensions of the elements with consequent savings in materials. Although concrete block and brickwork masonry are high compressive strength materials, valuable savings can be achieved by the use of high tensile steel which produces a significant improvement in resistance to cracking and deflection at service loads. In 1888, W. Dohring introduced the concept of prestressing concrete by using tensioned wires to produce small slabs and beams (Leonardt, 1964; Abeles, 1964). Further attempts, however to use prestressing concrete techniques have been ineffective. In 1928, Fressyinet suggested that most of the advantages acheived by prestressing were lost due to concrete creep and concluded that high

tensile steel must be used to overcome this problem. A greater allowance could then be made in the elongation of the wires to compensate for the losses due to creep. The first application of prestressing to brickwork masonry is attributed to Felix J. Samuely in 1953, when he attempted to stiffen the piers of tall side walls of a school assembly hall (Samuely, 1953). Results from a study of prestressed brickwork by Jasker in 1961, show that prestressed brickwork can be used economically for walls subjected to lateral earth pressure (Jasker, 1964). A water tank, 12 m in diameter and 4.9m deep, was designed by Foster in 1967 with side walls composed of brickwork with vertical and concentrated load. The design of the prestressed brickwork followed a procedure similar to that for prestressed concrete (Foster, 1970). In 1969, Thomas carried out three separate series of tests on prestressed clay bricks and hollow block beams. His experiments were mainly on beams consisting of brick 'soldiers' using high tensile steel wires threaded through the perforations in the bricks. His conclusion was that post-tensioned brickwork beams behave in a similar way to concrete beams, therefore they can be used successfully for beams and floor slabs (Thomas, 1969). Several experimental studies were also carried out by Curtin et Al (1975) on prestressed brickwork diaphragm walls. The theoretical work was based on an elastic analysis. Both the experimental and theoretical approximation method showed that prestressed diaphragm walls have a considerable flexural strength capacity. Since then, three major research studies have been completed at the Department of Civil Engineering of Edinburgh University. Experimental and theoretical work was carried out to study the behaviour of prestressed and partially prestressed brickwork beams up to failure load. They confirmed that the performance of the beams was satisfactory and that their behaviour could be predicted using

existing theories for prestressed and partially prestressed concrete (Pedreschi, 1983; Walker, 1987; Uduehi, 1989).

The limit state design Code of Practice for reinforced and prestressed masonry, BS 5628, was published in 1985. The code provision for cracking of prestressed sections is very strict. Consideration must also be given to anchorage reinforcement in the design of the brick/block masonry section. According to Professor Hendry (1991), it is necessary to take careful account of creep in the design of prestressed masonry walls. It has been shown that concrete block masonry creeps considerably more than fired clay masonry. Concrete block masonry also shrinks whereas clay expands so that the losses in prestress for block masonry are much higher than for brick masonry.

The main advantages of prestressed brickwork can be summarised as follows:

1) Since the prestressing stresses counteract the stresses caused by the external loads, higher external loads are attained prior to structural cracks and deformation.
2) Prestressed brickwork beams have a much higher shear strength than reinforced brickwork beams.
3) The high tensile steel produces a greater ductility, thus providing to the structure with obvious signs of pending failure.

1.1.4 Retaining Walls

A retaining wall may be defined as a structure which primarily resists lateral earth pressure. Some may carry vertical loads in addition to their own weight. Such walls may be constructed of stone, brick, block, reinforced or prestressed masonry or concrete.

Reinforced brickwork retaining walls can be constructed with three types of cross-section, namely grouted cavity, Quetta bond and pocket-type construction. Pocket-type walls are the most common as they are the most efficient in resisting lateral earth pressure. Cavity and Quetta bonds are more suited as wall partitions in large storage tanks.

According to Phipps (1991), there are three basic types of prestressed wall, namely solid wall, cavity wall and the wall with geometrical cross-section shown in Fig. 1.1. In the solid wall, the ducts for the prestressing tendons are built into the body of the wall; in the cavity wall type, the tendons are placed in the open cavity. Such a wall has been successfully tested by Witt and Aryamanesh at the University of Manchester Institute of Science and Technology in 1979. A geometric cross-section wall is one in which the masonry units are laid out in a particular pattern and so have an irregular cross-section. Details of various cross-sections and different types of retaining wall are given elsewhere (Roberts et Al, 1983; Curtin et Al, 1988; Hendry 1991).

In this study, the pocket-type retaining wall was selected for investigation Fig. 6.2.2, since the pocket-type wall is the most efficient in resisting lateral earth pressure. A large amount of research has already been carried out to investigate the cost considerations. These results show that pocket-type retaining walls are economical compared to grouted cavity, mass brickwork, Quetta bond and reinforced concrete walls (Maurenbrecher et al, 1976; Haseltine et al, 1977; Drinkwater et al, 1982). In 1984, an extensive study was carried out by Tellett to study the structural behaviour of reinforced brickwork pocket-type retaining walls. The results of tests on six full scale walls showed that the

performance of the walls was satisfactory, especially when compared to results based on design recommendations given in the draft British Standard for reinforced and prestressed masonry, BS 5628: Part 2. The design for shear however appears to be unduly conservative when applied to pocket-type retaining walls (Tellett, 1984).

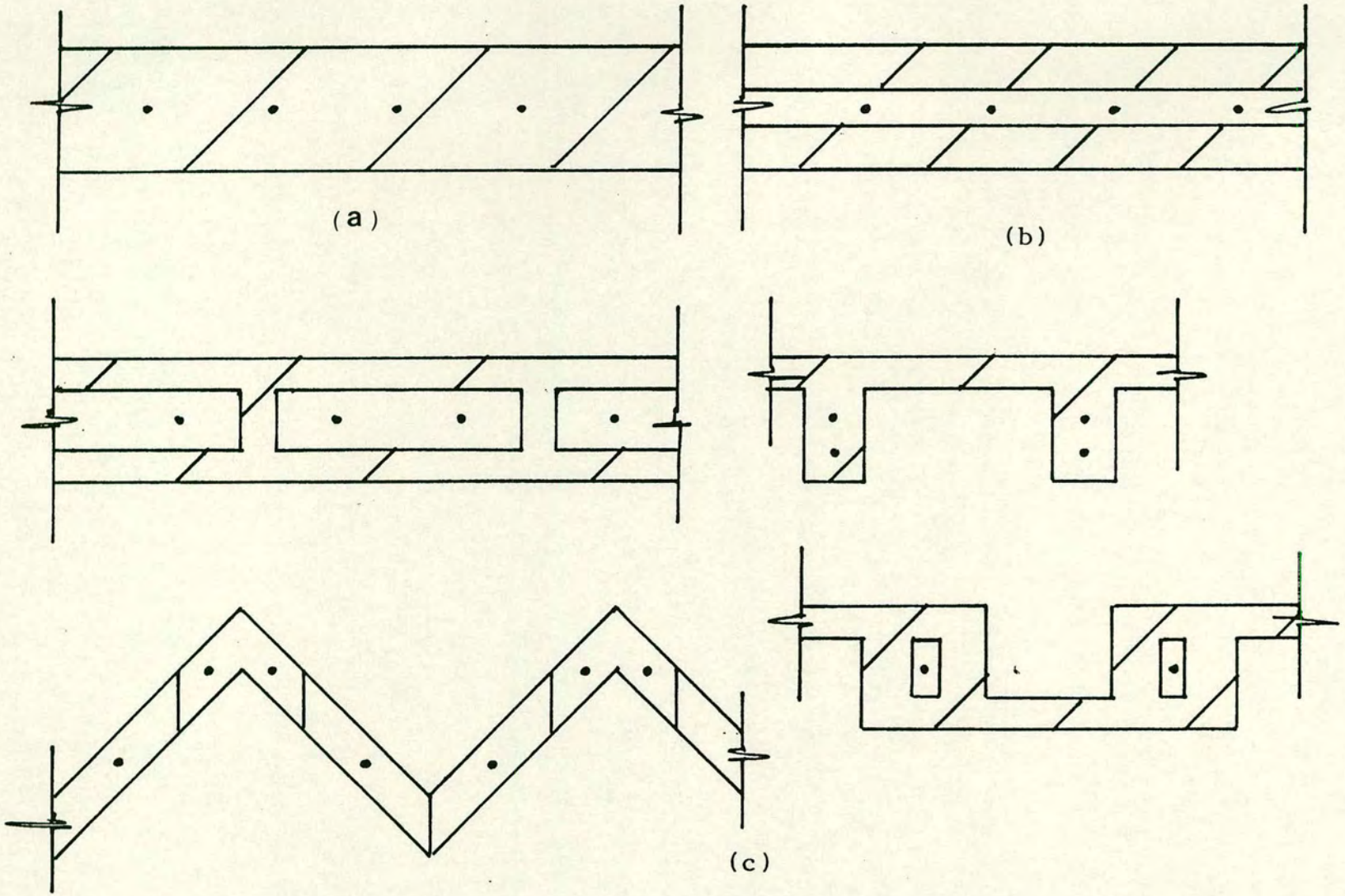

Figure 1.1: The three basic types of prestressed walls
(a) Solid Wall; (b) Cavity wall (c) Geometric Walls

CHAPTER 2

LITERATURE REVIEW & OUTLINE OF PRESENT WORK

2.1 GENERAL

A considerable amount of research has already been published in the field of prestressed masonry. However, up to the present only a limited amount of research work has been published on prestressed brickwork retaining walls. Most of the research on retaining walls has been on prestressed masonry diaphragm walls.

This chapter presents a summary of the research work which has been carried out on prestressed retaining walls and in the field of prestressed masonry in general.

2.2 LITERATURE REVIEW

2.2.1 Retaining Wall Structures

Most recent research on the application of prestressing techniques to brickwork has been essentially concerned to stabilise walls subjected to lateral loads. Precompression is applied by means of a high tensile bar cast into the foundation and passed through a cavity in the wall. At the top of the wall, the rod is threaded and prestress is transferred to the wall via a nut and torque wrench. Neil (1966) used this technique to stabilise the external walls of a factory in Darlington. The walls were 7.3m high with a prestress of 0.7 N/mm^2, applied axially. the prestressing rods passed through the bottom flange of a steel fasica beam at the top of the wall. After prestressing, the fascia beams were welded to steel columns designed to carry all the vertical loads. Adopting this form of construction eliminated the need for buttress steel framing and limited the thickness of the cross-section to 275mm. Curtin et al

(1982) described the construction of a hall of dimensions, 25m long x 15m wide x 8.5m high. A Clerestory window at the top of the wall was requested by the architect, so that the top of the wall could not be propped. The wall had to be designed as a free cantilever with a wall thickness of 665 mm. The reinforcement steel of 32 mm diameter induced an axial precompression of $0.5N/mm^2$. The results obtained for the wall behaviour has encouraged the adoption of 665 mm as a workable design thickness for all post-tensioned diaphragm walls.

In 1982, Bradshaw reported on the design of post-tensioned diaphragm wall in a multi-purpose farm building. The wall was 2.5 m high and the total size of the building 30 m square. The prestressed wall was designed as a cantilever wall required to retain grain. Since the direction of the load was constant, the steel was placed eccentrically with a prestress of $0.3N/mm^2$. The wall achieved a remarkable strength capacity and the selection of acid resistant bricks provided added resistance against acid attack from the stored crop. In 1971, Foster introduced a design for a 5 m high circular brickwork water tank as a solution to the problem of providing on site water for fire fighting. The architect designed and constructed the prestressed tank based on previous studies and applications of prestressed masonry. The tank has a wall thickness of 229 mm and is prestressed in both the horizontal and vertical directions to 2.0 N/mm^2 and 1.0 N/mm^2 respectively. The bricks were laid in Flemish bond and the vertical tendons were placed at 180 mm centres in a continuous vertical cavity in the wall. Due to the hydraulic stress distribution, a water-proof render was applied at the base of the tank.

Curtin and Phipps (1982) carried out experimental work on two full-scale post-tensioned brickwork diaphragm walls. Each wall consisted of two 7.26 m high x 7.62 m long x 0.45 m wide brickwork diaphragm walls built side by side. 40 mm diameter steel bars were cast into a common reinforced concrete foundation. The load was then applied by means of an air bag sandwiched between the walls. The tops of the walls were restrained from lateral movement, and the walls assumed to behave as propped cantilevers under uniform loading. The degree of precompression varied from 0 - 1.38 N/mm^2. The effect of the degree of prestressing on the formation of cracks in flexure defines the serviceability limit of the walls. Test results were in a good agreement with results calculated using simple elastic theory developed from the theoretical prediction of the cracking load at all levels of prestress. After cracking, the prestressed wall showed a considerable amount of strength against lateral load.

Curtin and Howard (1988) carried out tests on a 6 m high x 3.375 m long prestressed brick diaphragm wall. The cross-section of the walls consisted of a 557 mm deep double leaf cellular cantilever with single brick cross ribs built with Class A engineering bricks bedded in designation (i) mortar. Tensile steel bars,40 mm diameter, were placed vertically down through the cells. The free standing cantilever retaining walls were subjected to lateral loading. A diagonal tensile failure occurred due to the development of a 1 metre high hairline crack which appeared in the lower section of the cross ribs. Test results revealed only minor deflections and a high percentage of recovery on removal of the lateral load. The authors concluded that the post-tensioned brick diaphragm wall provided a remarkable structural performance in which a large increase in lateral loading was acheived as a result of improvements

in the ductility and stiffness of the wall. The flexural strength and shear strength were much higher than values based on B.S. 5628.

Al-Manasseer and Neis (1988) reported on the results of tests which were carried out on six reinforced and prestressed walls. The six masonry walls, of dimensions 1200 x 2400 mm, were constructed using standard 190mm masonry blocks. Four walls were post-tensioned using various configurations of No. 9 American Strands (16.9mm diameter), while the other two panels were constructed using various combinations of 10mm ϕ deformed bars. The average ultimate strength of the strands was 90kN and a force of 80% of ultimate strength was used for prestressing. The panels were simply supported and laterally loaded under a midpoint static load. It was observed that after unloading, the post-tensioned panels recovered their original shape, while the reinforced panels remained permanently deformed. The authors thus recommended the use of post-tensioned panels for repeated or cyclic loading. It was further observed that the deflection under elastic conditions was less than 1.1 mm for both the reinforced and post-tensioned panels. These results therefore indicate that reinforced and post-tensioned masonry panels do in fact act as ductile structures.

Work by Hobbs and Daou (1988) was carried out on post-tensioned T-section brickwork retaining walls. The cross-section and bonding pattern of the model wall design is shown in Fig. 2.1. The bonding pattern was chosen to minimise the number of internal straight joints whilst using a small number of special bricks. The walls were built on a reinforced concrete foundation. The joint thickness in the model brickwork was 3 mm. The mix proportions were 1: 0.13: 3.1: 0.97, cement:lime:sand:water by weight. The clay brick dimensions were 18.5 mm thick x 30mm wide x 64mm long. The bricks were specially cut by

the manufacturer from high quality engineering bricks. The compressive strength of the bricks was 129 N/mm^2. The prestressing steel rods were 12.7mm in diameter with an ultimate tensile strength of 960 N/mm^2 and an initial modulus of elasticity of 200 kN/mm^2. The walls were subjected to a lateral eight point loading system designed to simulate earth pressure loading. The initial design was carried out according to BS.5628: Part 2, using a specially written computer program. The authors concluded that the provisions in the current code of practice for shear strength calculation produce considerable restrictions. There is a real need therefore for further investigation into the behaviour of such walls with respect to assessing their ultimate bending moment and shear force capacity.

Ambrose et al (1988) reported on the results of tests on a 3 metre high x 3.14 metre long cantilevered prestressed brickwork diaphragm wall. The wall cross-section was divided into three equal cells as shown in Fig. 2.1. Blockley wire cut facing bricks were used together with a 1:1.5:4.5 mortar. The brick compressive strength was 92.5N/mm^2 and the prestressing rods were 32 mm diameter mild steel, threaded to fit into the anchorage point in a strong floor. Two rods were isolated in each cell with an eccentricity of 50 mm measured from the centre line of the wall. A purpose made p.v.c. bag was placed between the back of the wall and the timber faced steel reaction frame. When filled with water the bag provided the lateral hydrostatic loading. The initial prestressing forces were reduced at a constant rate in each of the eight tests. A design method for this type of construction was proposed based on simple elastic theory. The main conclusion drawn from this work was that any increase in the level of prestress increases the wall stability and

strength. There was no evidence that small shear lag effects were present adjacent to the flanges of the diaphragm.

2.2.2 Prestressed Brickwork Beams

The work of Thomas (1963) was considered to be the first on prestressed masonry. He tested two post-tensioned brickwork beams as part of a study into the feasibility of the construction of a suspended floor system. In the first of these tests, the beam was built from three whole bricks laid as soldiers Fig. 2.2. The tensile reinforcement was six 7 mm diameter steel rods. The reinforcement was threaded through the ungrouted lowest perforation. An initial prestressing force of 67 kN was applied which induced a maximum compressive stress of 7.2 N/mm^2. The beam was simply supported and subjected to a static central point load over a span of 2.515 m. The beam was loaded to 18.30 kN, then unloaded, and the prestressing force then increased to 107 kN. On reloading the beam, failure occurred at a load of 17.2 kN. Failure of the second beam occurred in the anchorage zone during the prestressing operation. The author proposed that a larger cross-sectional area be used, alternatively the vertical reinforcement placed in the anchorage zone.

In 1965, Plowman carried out tests on 13 prestressed brickwork beams. The beams were built as shown in Fig. 2.2. The tensile reinforcement was placed within the lower 'kern' limit to avoid the introduction of tensile stresses during prestressing. The author used bricks of strengths varying between 26.5 and 54.7 N/mm^2, and a prestressing force varying between 17.8 and 93.6kN. The design of the cross-section did not allow for grouting of the tensile steel. All the beams were simply supported and tested under a point load over a span of 3.048 m. Eleven of the

beams failed in flexure. The other two beams failed during the prestressing stage. The author calculated the factor of safety for each beam taking the working load as the load causing decompression. As the wires were unbonded, the factor of safety was 2, taking into account both maximum and minimum eccentricities. In 1966, L.S. Ng also carried out preliminary tests on three post-tensioned masonry beams constructed from extruded clay units Fig. 2.2. Due to the tensile splitting problem mentioned in previous research work, an epoxy resin was used to bond the clay units together anticipating that the bond would exhibit a smaller lateral strain thus delaying any tensile splitting of the beam. The prestressing forces were either 34 or 43 kN. The beams were then tested under four point loading over a span of 3.050 m with point loads applied at the third points. All three beams failed in flexure by crushing of the compression zone. An average load factor of 3.5 was obtained based on the load causing decompression of the prestressed steel. As a result of this work, a British patent was taken out on a prestressed ceramic flooring system (Thomas, 1969).

In 1970, Mehta and Fincher carried out tests on five prestressed brickwork beams. The beams were fabricated in a "U" configuration. The bonding pattern and prestressing force were varied. The tensile reinforcement consisted of three 10mm diameter, seven wire strands. The prestressing force was varied between 94 and 187kN. All five beams were tested under central point loading over a span of 1.829 m. The flexural design and shear design of the beams were based on the American Building Codes and the deflection analysis was based on a strength of material approach. The elastic modulus of the brickwork was derived from tests on axially loaded brickwork prisms. For the theoretical analysis, the author assumed the following :

(i) The beam self weight can be neglected

(ii) No prestress losses

(iii) Masonry and concrete infill have the same elastic properties, even though the concrete infill forms 25% of the beam section.

The predicted values were within 20% of the experimental results, with all beams failures corresponding to the predicted shear strengths. The experimental deflections were between 1.46 and 2.36 times greater than the predicted results.

The authors concluded that the recovery attained after unloading was a result of the strong bond between the masonry and concrete infill, and that the coursing pattern had little effect on the deflection.

Williams and Phipps (1982) carried out tests on six brick masonry box beams. The beams were tested horizontally to represent the behaviour of masonry diaphragm walls. The tensile reinforcement was a 40mm diameter Macalloy bar passed through the ungrouted cavity. The prestressing forces were varied from 132 to 330 kN resulting in compressive stresses of between 1.11 and 2.79 N/mm^2. The beams were tested under four point loading over a span of 4.8 m. Five of the beams failed in flexure due to crushing of the compression zone whilst the sixth beam, which had the highest prestress force, failed as a slender column with the cracking occurring in the outer compression face. The addition of cross ribs increased the ultimate moment capacity of the beams. An empirical relationship between the steel stress and the neutral axis depth at failure was obtained based on the experimental results. The neutral axis depth and the ultimate moment of the beam were calculated simply by considering the equilibrium of the tensile and

compressive forces. Good agreement was obtained between the experimental and theoretical results. Nevertheless, further experimental work is needed to justify the empirical relationship.

Pedreschi (1983), carried out extensive research work into the behaviour of post-tensioned brickwork beams. A total of 51 full scale beams were tested to study the behaviour of post-tensioned brickwork beams with varying brick strength, mortar grade, steel area, prestressing force and a/d ratio. A large number of material tests on prisms were carried out to obtain the properties of brickwork in which the bed joints run parallel to the direction of the induced prestressing load. The beams were tested under four point loading over spans of between 2 and 6 m. Two types of beam sections were used, and the concrete infill occupied a maximum of 10% of the cross-section area. A theoretical approach based on using a non-linear stress-strain relationship for the prestressed concrete beam material properties was assumed. The ultimate flexural moment, deflection and crack widths were predicted using the actual stress-strain relationship of the brickwork prisms and tensile reinforcement. An experimental study into the shear strength of the beams showed that the plastic method adopted for predicting the shear strength of prestressed concrete can be applied to brickwork beams. Following the work of Pedreschi, many researchers carried out studies into the behaviour of prestressed brickwork beams and are reported elsewhere (Roumani and Phipps, 1983; Robson, 1983; Phipps, 1986). Between 1983 and 1987, an extensive study was carried out by Walker into the behaviour of partially prestressed brickwork beams. Forty-one full scale beams were tested to study their behaviour with variable area of steel, prestressing force, partial prestressing ratio, cover to non-tensioned steel, brick strength and mortar strength. The beam section adopted was similar to

the section used by Pedreschi with a modification to bring the tensile reinforcement closer to the beam soffit. The grout occupied 18% of the beam cross-section area and the beams were tested under four point loading. Thirty-seven beams failed in flexural tension and 12 in shear. An interactive programme was developed to predict the ultimate moment, moment-curvature relationship, deflection and crack widths of reinforced, fully and partially prestressed brickwork beams. The programme was based on a direct method of analysis using the actual stress-strain relationships of the brickwork prisms and the tensile reinforcement. The experimental results were in good agreement with the theoretical analysis. The author recommended that more experimental and theoretical work was required to study the shear strength of partially and fully prestressed brickwork beams.

In 1989, Uduehi conducted a comparative study into the structural behaviour of fully and partially prestressed beams of brickwork and concrete and the shear strength of partially prestressed brickwork beams. A total of 29 full scale brickwork and concrete beams with identical cross-sections and material properties were tested. The beams were tested under four point loading over spans of between 1.65 and 6.2 m. The author observed that when the failure was due to flexural tension, the ultimate moment and deflection of fully and partially prestressed brickwork and concrete beams were similar up to failure. The shear strength of a prestressed brickwork beam was lower than that of a corresponding concrete beam. The concept of the compressive force path can be applied to estimate the shear strength of fully and partially prestressed brickwork beams. The ultimate strength in flexure and the deflection can be predicted for fully and partially prestressed brickwork beams assuming flexural theory and a direct method using the stress-

strain relationship and compressive strength of brickwork. Non-linear finite element analysis using a material model modified to account for the behaviour of the brickwork gave values which were in good agreement with the experimental results.

2.3 SCOPE OF PRESENT INVESTIGATION

Having regard for the work described in the foregoing sections, the research undertaken in this study has concentrated on the behaviour of prestressed brickwork pocket-type structures subjected to flexural and shear forces up to failure. This form of construction has been adopted for its economic and advantages in grouting the cross-section. No previous work has been found on the behaviour of post-tensioned pocket-type brickwork beams or retaining walls. This is reflected in the Code of Practice where no cost-effective recommendations are given for cracking of prestressed brickwork retaining walls (or for pocket spacing in pocket-type walls). This investigation considers in detail the influence of the following variables upon the ultimate moment, deflection and cracking of the retaining walls:

(i) Percentage area of steel.

(ii) Pocket spacing and wall slenderness.

(iii) Types of wall bonds.

To examine the above parameters the following experimental work was carried out:-

i) 9 full scale, six course prisms.

ii) 2 full scale beams with the bed joints running parallel to the direction of the induced prestressing load.

iii) 6 full scale beam/slabs with the bed joints running perpendicular to the direction of the induced prestressing load.

iv) 6 half-scale retaining walls to study the combined effects of shear and flexure at the base of the wall.

In conjunction with this work a comprehensive series of small tests were undertaken on mortar and grout specimens, single course prisms and small wallettes to determine the non-linear deformation characteristics and compressive strength of the brickwork. For economic reasons it was not possible use full scale test structures, therefore to complement the investigation, a theoretical study was carried out. This parametric analysis cosisted of the following :

i) An advanced finite element package (London University Stresss Analysis System), each with its graphic part package, MYSTRO . This package and its graphics was implemented on a VAX 8550 at the University of Edinburgh Computer Centre. A plane stress material model developed for concrete and modified to take account of the behaviour of brickwork was used in a three dimensional geometrical and material non-linear finite element analysis.

ii) A computer program based on predicted equilibrium equations was written to calculate the pocket spacing for post-tensioned pocket-type brickwork retaining walls.

The results of the experimental and theoretical (finite element, direct method and yield line) analyses were compared to those based on the Code of Practice B.S.5628: Part 2: 1985. The investigation therefore presents a detailed study into the behaviour of post-tensioned pocket-type brickwork beams/slabs and retaining walls.

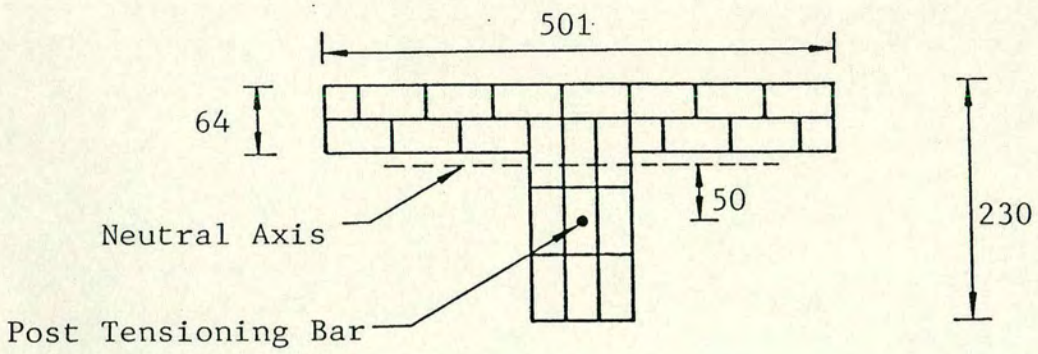

Cross-section details of T section brickwork retaining wall

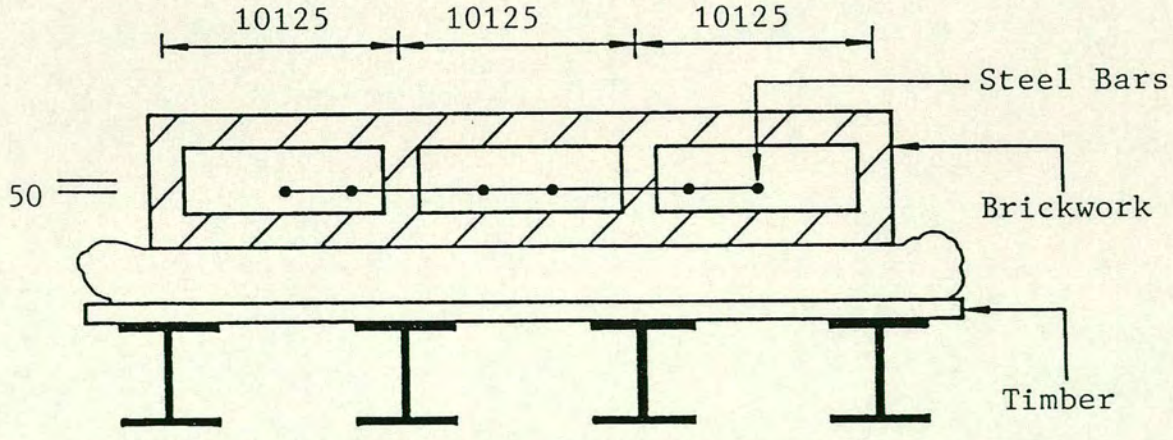

Cross-section details of diaphragm brickwork retaining wall

Figure 2.1

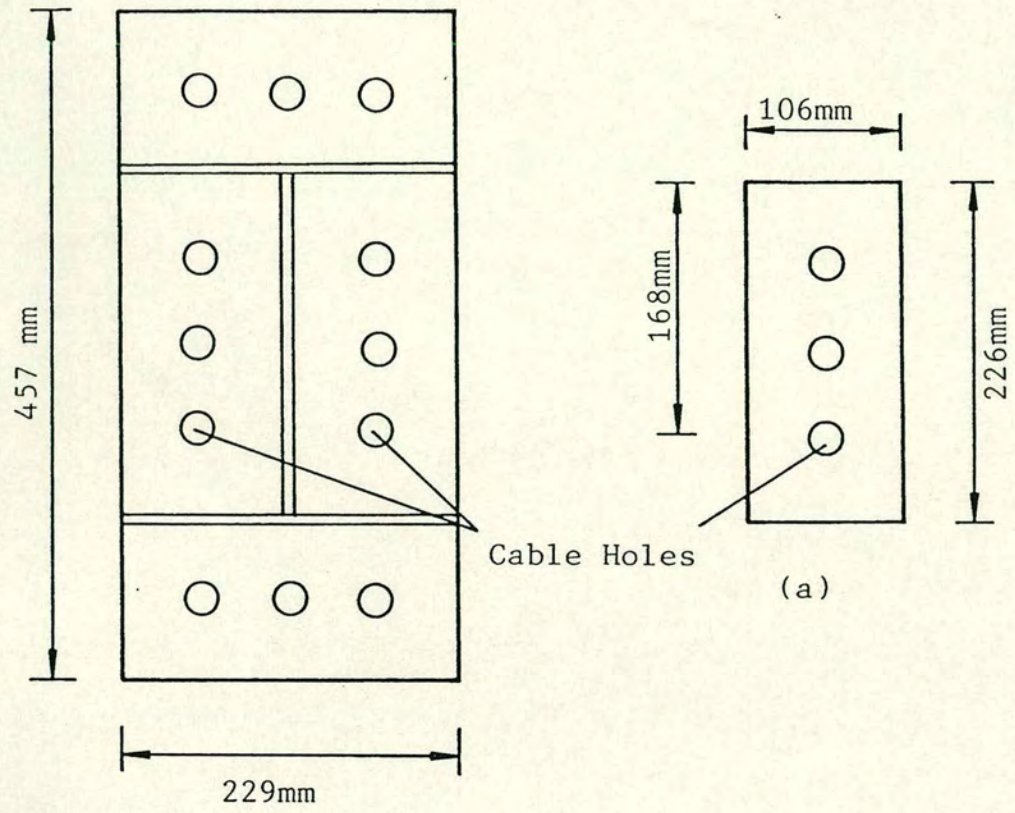

Beam section of K. Thomas

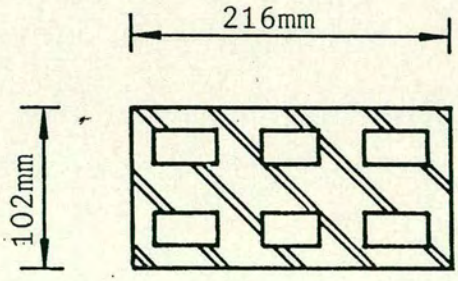

Beam section of L.S NG

Figure 2.2

CHAPTER THREE

MATERIAL PROPERTIES

3.1 General

In this chapter, a brief description is given of the results of tests carried out to determine the properties of the materials used in this investigation. Due to the method of construction of the walls, compressive stresses are developed normal to the bedjoint which lead to the standard practice of testing bricks flat.

Three different types of prism and small wallette prisms were loaded axially to determine the compressive strength and flexural strength of the brickwork. The stress/strain relationships for the brickwork and tensile reinforcement were predicted and mathematically idealised in the form of polynomial for the brickwork and a tri-linear relationship for the strand. A number of plain unreinforced brickwork prisms were tested in flexure to determine the modulus of rupture of the beam. These values are given in table 3.5.

3.2 Properties of the Bricks

Two kinds of bricks were used in the construction of the structures. In the case of the six course prisms, beams and beam/slab structures, extruded three hole bricks of high strength were used Fig. 3.1a. The average percentage area of perforation was 14.9. In the case of the retaining walls, solid clay bricks were used (dimensions shown in Fig. 3.1b). The bricks were specially cut by the manufacturer from good quality engineering bricks. Compressive strength tests were carried out in three orthogonal directions in accordance with the B.S. 3291. The compressive strengths obtained by applying a direct axial stress on the

face, edge and end of the specimens are given in Table 3.1. The average "five" hour boiling water absorption is also included.

3.3 Sand, Mortar and Concrete Infill

3.3.1 Sand

The sieve analysis for the concrete sand used is given in Table 3.6. Test results show agreement with the overall limits given in B.S.882:1983.

3.3.2 Mortar

A 1:$\frac{1}{4}$:3 (cement:lime:sand) mix by volume was used in the construction of each beam. (Satti, 1972) advised the use of this mix if flexural tensile strength was a critical factor. The mortar mix was designed to conform to designation (i) in B.S.5628 with a grading conforming to B.S.1200. The water content was added as needed to give a workable mix. For each mix, 102 mm cubes were cast, cured in water and then tested at 28 days Table 6.1

3.3.3 Concrete Mix

A 1:$\frac{1}{4}$:3 (cement:lime:sand) mix by volume was used for constructing the post-tensioned brickwork retaining walls. For all other structures, a 1:2$\frac{1}{2}$:2 (cement:sand:coarse aggregate) concrete mix by volume was used. The water content was adjusted to provide a workable slump. Combex 100 was added to the mix to reduce the effects of shrinkage and to shorten the setting time. After every mix a number of 102 mm cubes were cast and cured. Table 6.1 shows the seven day compressive strength test results.

3.4 Properties of Brickwork

3.4.1 Experimental Observations and Discussion

Several types of prism were built to determine the compressive strength, flexural strength and deformation properties of the brickwork structures table 3.3 & figs 3.7,8. Six course prisms were built to determine the non-linear deformation characteristics and compressive strength of the material properties of brickwork. These results were used in the open pocket and concrete infill pocket six course prism analysis. A number of single course prisms were built, and the non-linear deformation characteristics and compressive strength results used in the theoretical and experimental analysis of the beams and beam/slab. Due to the possibility of strain gradient effect, such a prism loaded axially is not truly representative of the compressive strength of the prestressed walls. Never-the-less, it was thought to be the most accurate representation compared to any other prism type (Walker, 1987). Half scale prisms and wallette prisms were built to determine the non-linear deformation characteristics, compressive strength and flexural strength of the material properties of brickwork. These results were used in the experimental and theoretical analysis of the half scale retaining walls.

The prisms were built alongside each related structure, using the same mortar mix. Each prism was capped above and below with a rich mortar mix. 6mm thick plywood sheets were placed between the prisms and the platens of the testing machine to ensure an evenly distributed load. Strain measurements were taken on the prism using a 150mm Demec gauge. The strain readings were taken at increments of 10% of the ultimate load.

In the single course prisms, cracks were initiated at approximately 70-75% of the ultimate load. These cracks were due to tensile stresses in the direction of the applied load. In the six course prisms, cracks were initiated at the vertical mortar joints, followed by splitting of the prisms into two or three separate prisms, followed by sudden failure. Table 3.8 presents the compressive strength of the brickwork prisms. Due to the danger of sudden failure, it was not possible to take the ultimate strain reading. The ultimate strain was predicted by mathematical extrapolation of the experimental stress-strain relationship in which the stress-strain relationship was plotted from the average reading at each load increment Figs 3.7, 3.9 , 3.11. The modulus of elasticity was obtained from the stress-strain relationship curve by applying linear regression analysis up to approximately 25% of the ultimate load.

3.4.2 Non-Dimensional Stress/Strain Relationship

The direct method and stress block analysis are both dependent on the stress/strain relationship of the brickwork prisms. In order to use the above mentioned methods to calculate the deformations and ultimate strength of prestressed brickwork structures, it was necessary to have the relationship expressed in mathematical form. Figs 3.8, 3.10, 3.12 present the idealised stress relationship for the brickwork. The plot of the curves was obtained by normalising the stresses and strains by their maximum values. A regression analysis was carried out on all the non-dimensional data points. Figs 3.7, 3.9,. 3.11 present the stress-strain curves. Figs 3.8, 3.10, 3.12 present the non-dimensional stress-strain curves and the best fit statistic equations. An important use of the non-dimensional stress/strain curve is the prediction of the stress block factors λ_1 and λ_2 which are used to describe the distribution of the

compressive forces in the compressive zone of the structure. λ_1 is equal to the area under the non-dimensional stress/strain curve Table 3.9.

$$\lambda_1 = \int_0^{1.0} (x_1 + x_2(\varepsilon/\varepsilon_m) + x_3(\varepsilon/\varepsilon_m)^2 + x_4(\varepsilon/\varepsilon_m)^3 \, d\, \varepsilon/\varepsilon_m)$$

λ_2 is the centroid of the area under the non-dimensional stress/strain curve.

$$\lambda_2 = 1.0 - \frac{\int_0^{1.0} \varepsilon/\varepsilon_m(x_1 + x_2(\varepsilon/\varepsilon_m) + x_3(\varepsilon/\varepsilon_m)^2 + x_4(\varepsilon/\varepsilon_m)^3) d\, \varepsilon/\varepsilon_m}{\lambda_1}$$

3.5 Properties of Prestressing Strand

Two types of tensile reinforcement were used in the experimental work. The 5.0 mm diameter strand was used for the post-tensioned brickwork retaining walls, while the 10.9 mm diameter strands were used for the beams and beam/slabs structures. The strands were tested under uniaxial tension and the strains measured by electrical resistance gauges attached to the strand. Figs 3.4, 3.6 present the stress-strain relationship obtained from a laboratory test. Figs 3.3, 3.5 present the stress-strain relationship after idealisation into a tri-linear form to be used in the analysis.

	BRICK TYPE	
	High	Medium 1/2 size bricks
BED JOINT		
Ave. Comp. Strength N/mm^2	100.81	35.59
Range N/mm^2	93.33-119.05	31.41-38.51
Standard Deviation N/mm^2	8.38	1.99
Coefficient of Variance	7.56	5.59
STRETCHER FACE		
Ave. Comp. Strength N/mm^2	58.58	30.99
Range N/mm^2	53.67-68.03	27.02-33.59
Standard Deviation N/mm^2	5.22	1.94
Coefficient of Variance	8.91	6.26
HEADER FACE		
Ave. Comp. Strength N/mm^2	29.63	24.55
Range N/mm^2	27.46-31.75	19.95-29.55
Standard Deviation N/mm^2	3.01	6.09
Coefficient of Variance	10.59	24.55
ABSORPTION TESTS		
24 Absorption % by weight	2.86	10.294
Range % by weight	2.50-3.09	9.79-10.93
Standard Deviation by weight	0.2134	0.3594
Coefficient of Variance	7.46	3.49

Table 3.1 Compressive Strength and Absorption of Bricks

Specimen No.	Elastic Modulus kN/mm^2	Ultimate Strength N/mm^2	0.2% Proof Stress N/mm^2
1	205	1744	1580
2	207	1745	1610
3	198	1709	1520
4	201	1720	1603
Average	203	1730	1578

Table 3.2 Summary of tests on Strand 5.0mm

	Medium Strength 1/2 size bricks	
Specimen No.	Plane of failure parallel to bed joints N/mm^2	Plane of failure perpendicular to bed joints N/mm^2
1	0.72	1.85
2	0.53	1.48
3	0.51	2.24
4	0.60	2.18
5	0.80	1.61
Average N/mm^2	0.632	1.87
Std. Deviation N/mm^2	0.13	0.34
Coeff. of Variance	19.74	18.00
Orthogonal Ratio μ	0.34	0.34

Table 3.3 Flexural Strength Tests

Specimen No.	Elastic Modulus kN/mm^2	Ultimate Strength N/mm^2	0.2% Proof Stress N/mm^2
1	215	1800	1650
2	221	1830	1700
3	205	1800	1655
4	209	1780	1600
Average	213	1803	1651

Table 3.4 Summary of Tests on Strand 10.9mm

Specimen No.	High Strength Brick	Medium Strength 1/2 size brick
1	1.73	1.85
2	1.35	1.48
3	1.01	2.24
4	1.13	2.18
5	1.84	1.61
Average N/mm^2	1.41	1.87
Std. Deviation N/mm^2	0.364	0.34
Coef. of Variance	26.00	18.00

Table 3.5 Modulus of Rupture

Test Sieve	% by weight passing through sieve	
	Test Result	B.S. 1200 Limit
5.0mm	100	100
2.36mm	100	90-100
1.18mm	96	70-100
600mm	69	40-80
300mm	20	5-40
150mm	8	0-10

Table 3.6 Sieve analysis of sand

Brick Type	Prism Type	Compressive Strength	Ultimate Strain	Average	Elastic Modulus Ave kN/mm^2
High Strength	six	30.87 31.29 27.91	0.0025 0.0027 0.0025	0.0026	25.00
High Strength	Single	26.37 24.65 23.26 26.49 24.00	0.0025 0.0022 0.0025 0.0025 0.0025	0.0025	21.00
Medium Strength 1/2 scale	single	20.00 17.35 20.50 19.34 20.33	0.0053 0.0054 0.0045 0.0042 0.0038	0.0046	10.00
Medium Strength 1/2 scale	Wallettes	20.66 15.07 17.65	0.0046 0.0053 0.0043	0.0047	7.50

Table 3.7 Summary of Stress/Strain Characteristics

Brick Type	High Strength	High Strength	Medium Strength $\frac{1}{2}$ scale test	Medium strength $\frac{1}{2}$ scale test
Mortar type	1:$\frac{1}{4}$:3	1:$\frac{1}{4}$:3	1:$\frac{1}{4}$:3	1:3
Prism type	Six course	Single course	Single course	Walletttes
Compressive Strength N/mm^2	30.87 31.29 27.91 - -	28.37 24.65 23.26 27.49 20.00	20.00 17.35 20.50 19.34 20.33	20.66 15.07 17.65 - -
Average N/mm^2	30.02	24.75	19.50	17.79
Std. Deviation	1.84	3.37	1.28	2.80
Coeff. of Variance	6.13	12.14	6.58	15.73

Table 3.8 Compressive Strength of Brickwork Prisms

Brick Type	Mortar	Prism	fm N/mm^2	Ultimate Strain	X_1	X_2	X_3	X_4	λ_1	λ_2
High	$1:\frac{1}{4}:3$	Six	30	0.0026	0	-2.4	1.41	0	0.73	0.387
High	$1:\frac{1}{4}:3$	Single	24.75	0.0025	0	2.3	-1.6	0.3	0.69	0.379
Medium $\frac{1}{2}$ scale	$1:\frac{1}{4}:3$	Single	19.50	0.0046	-.0217	-1.783	0.783	0	0.64	0.370

Table 3.9 Non-dimensional stress/strain characteristics

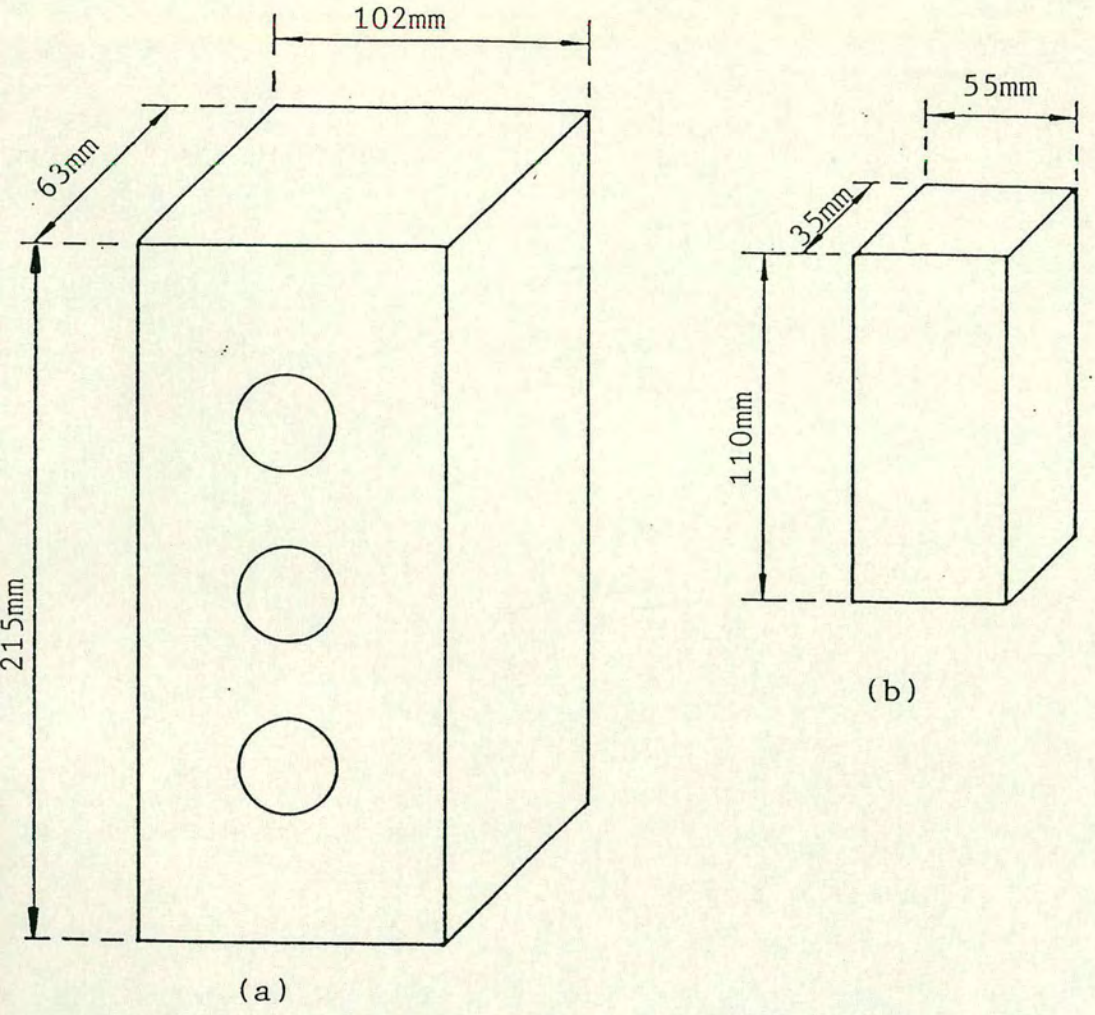

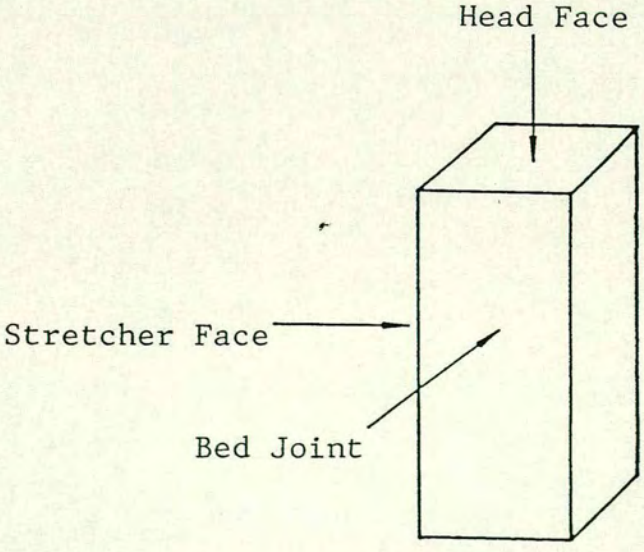

Figure 3.1 Direction of Compressive Tests

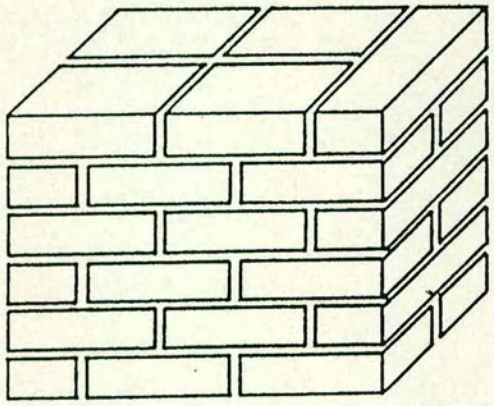

Solid six course prism

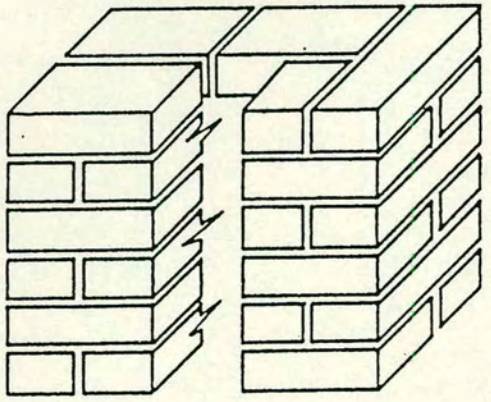

Open pocket prism

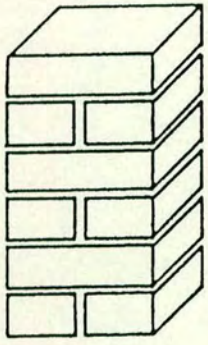

Single course prism

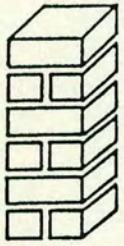

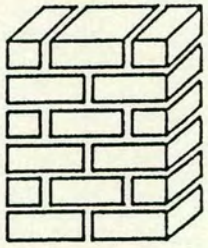

½ scale prisms

Figure 3.2 Isometric View of Prism Types

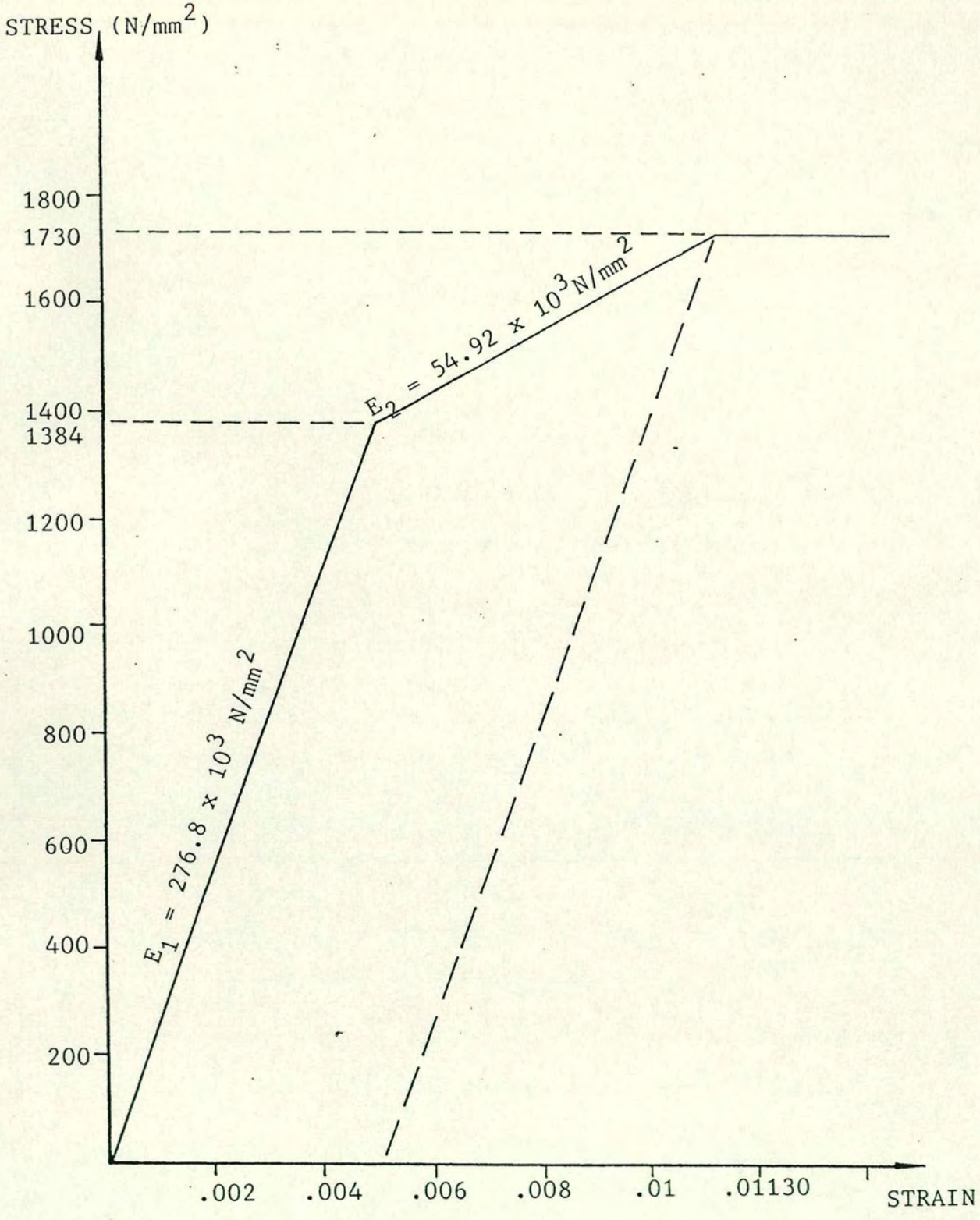

Figure 3.3 Stress strain curve for 5.0mm tendon (Code)

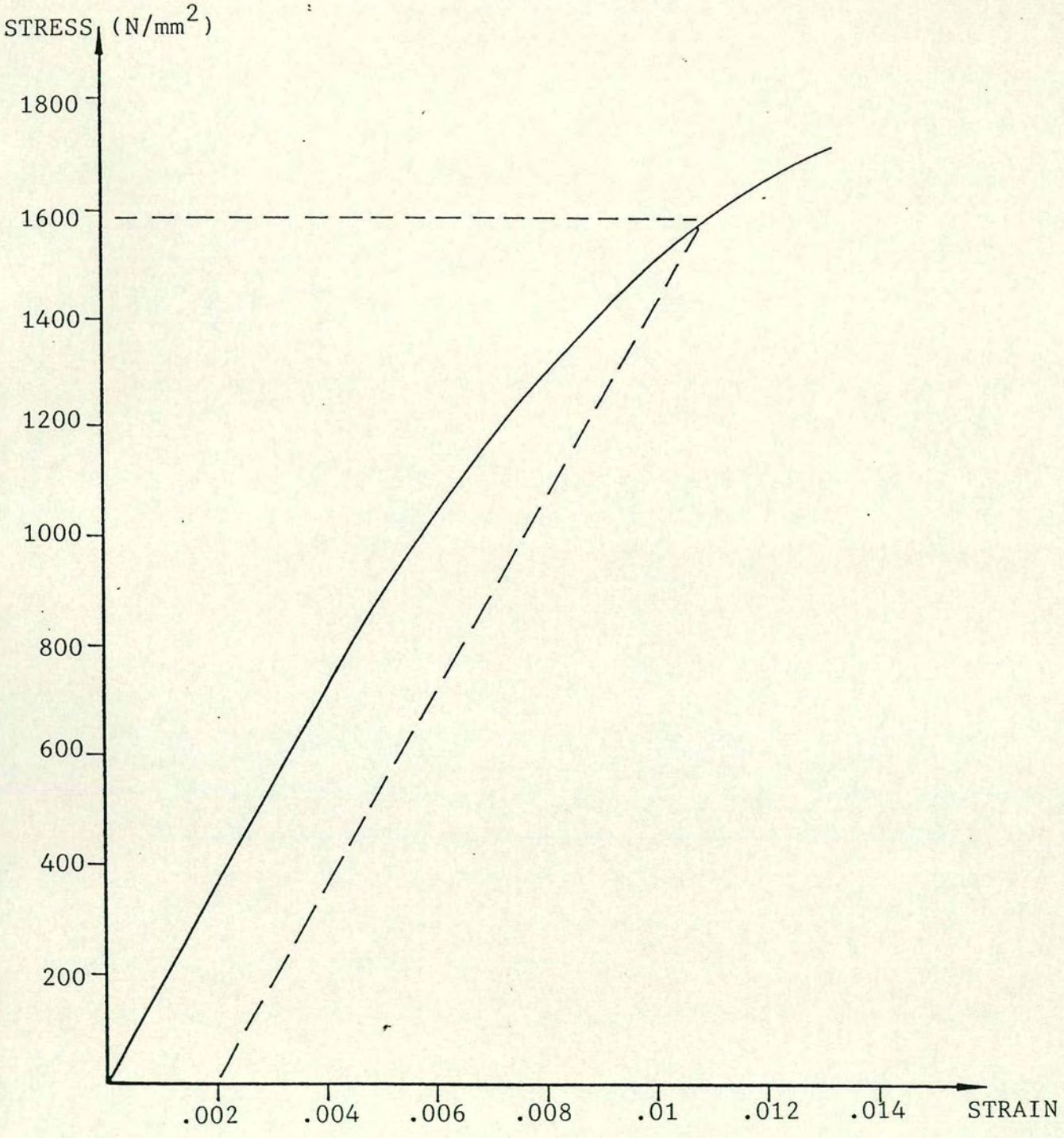

Figure 3.4 Stress Strain Curve for 5.0mm Tendon

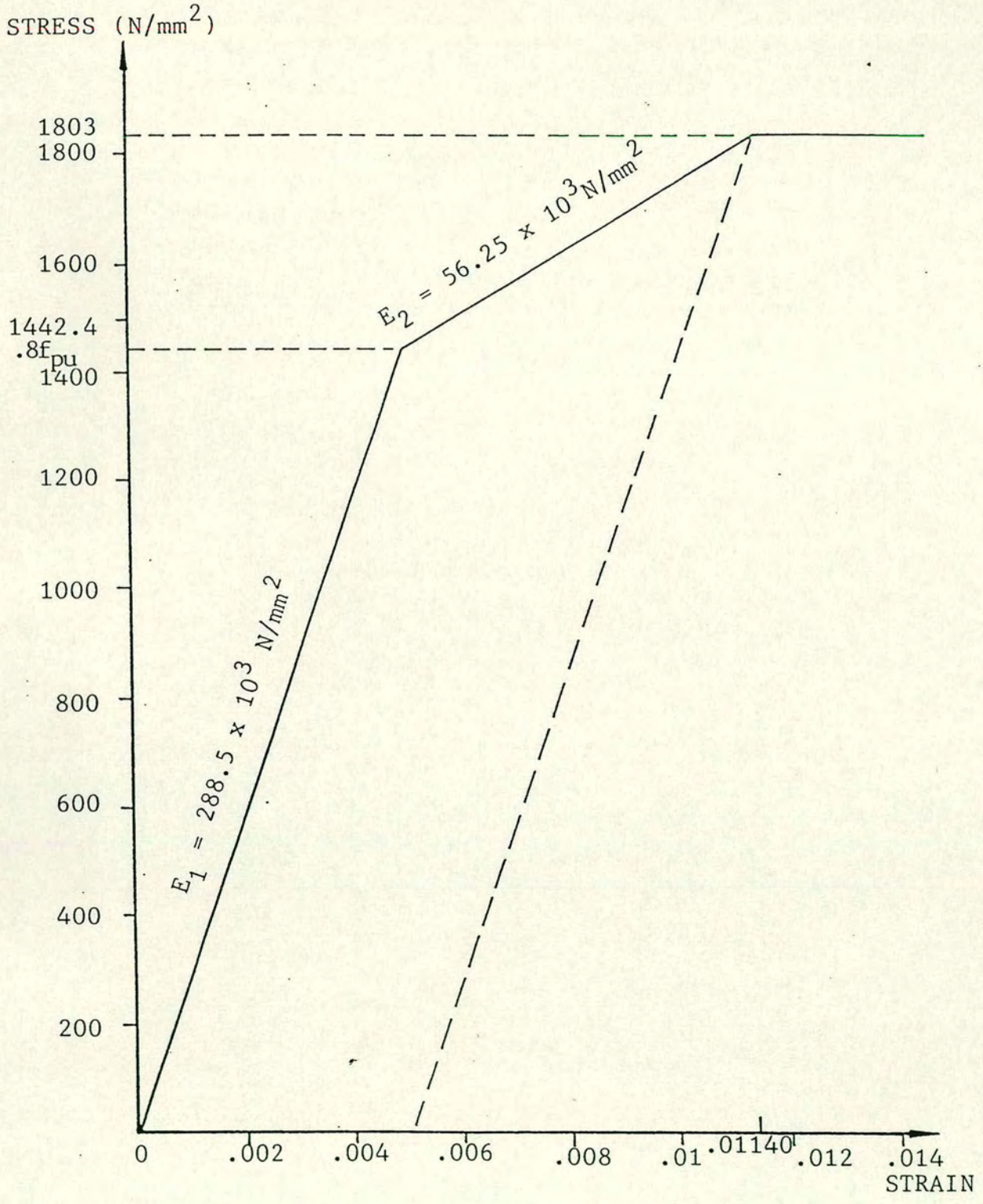

Figure 3.5 Stress strain curve for 10.9mm tendon (Code)

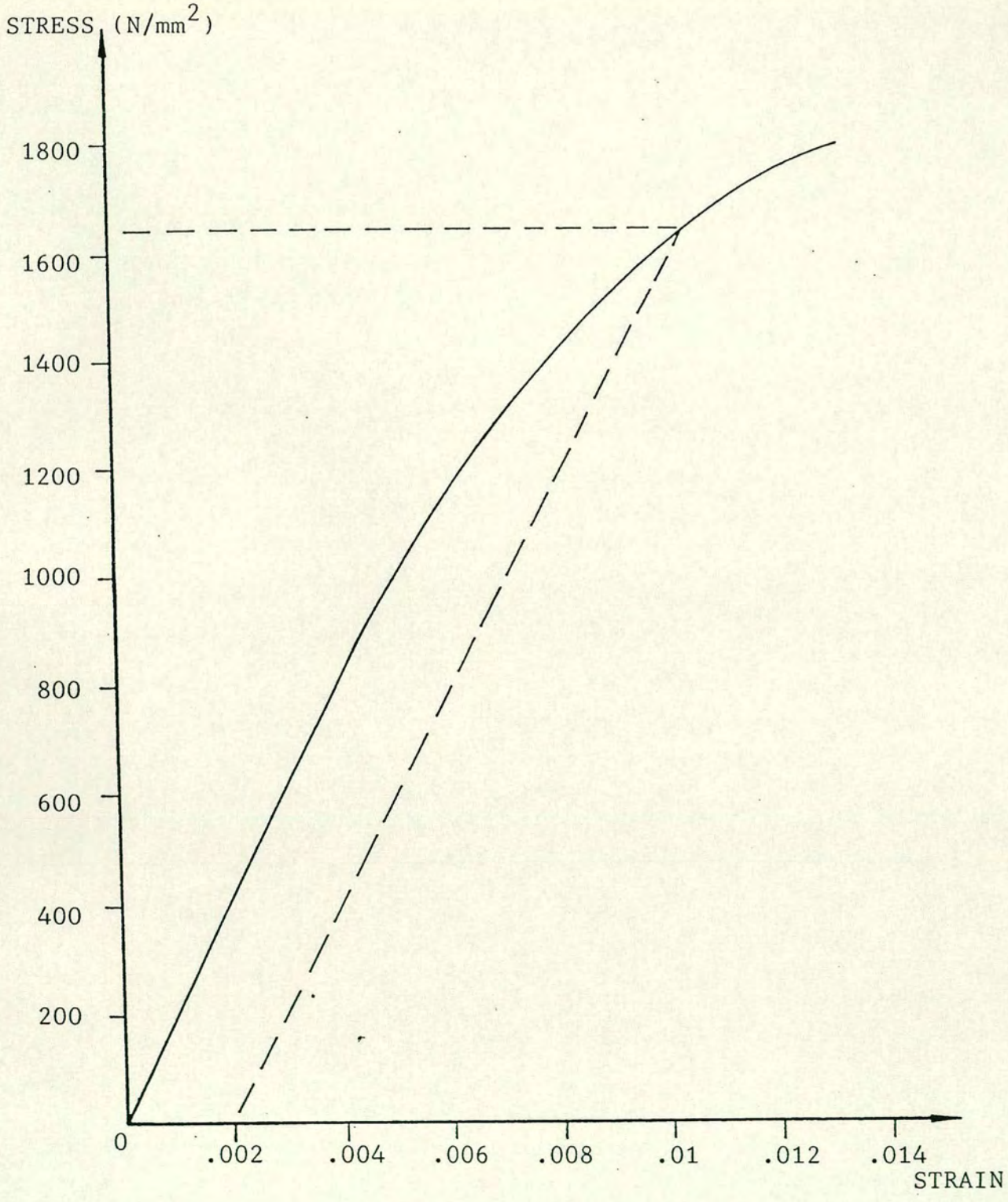

Figure 3.6 Stress strain curve for 10.9mm tendon

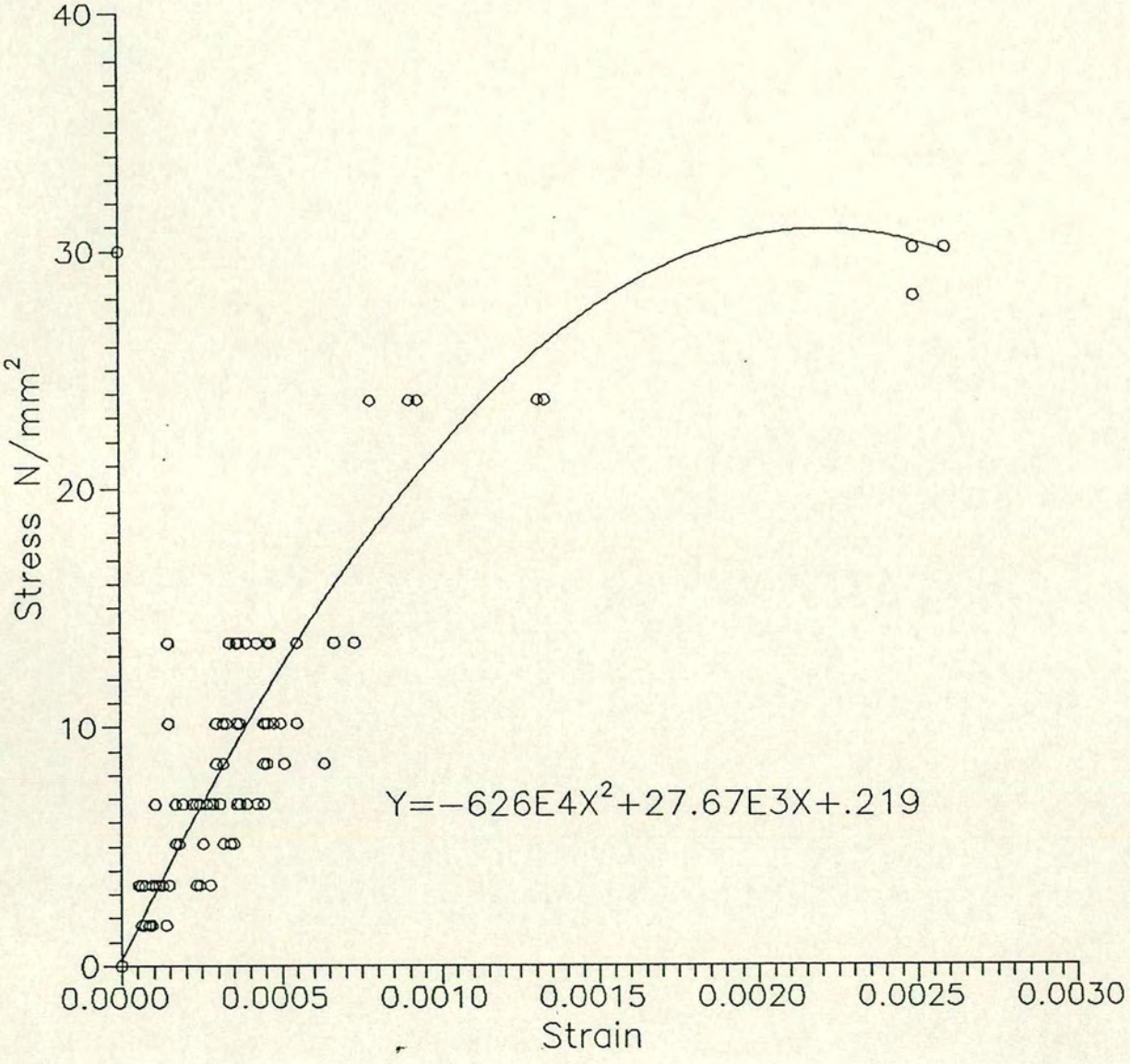

Stress–strain curve for six course brickwork prisms.

Figure 3–7

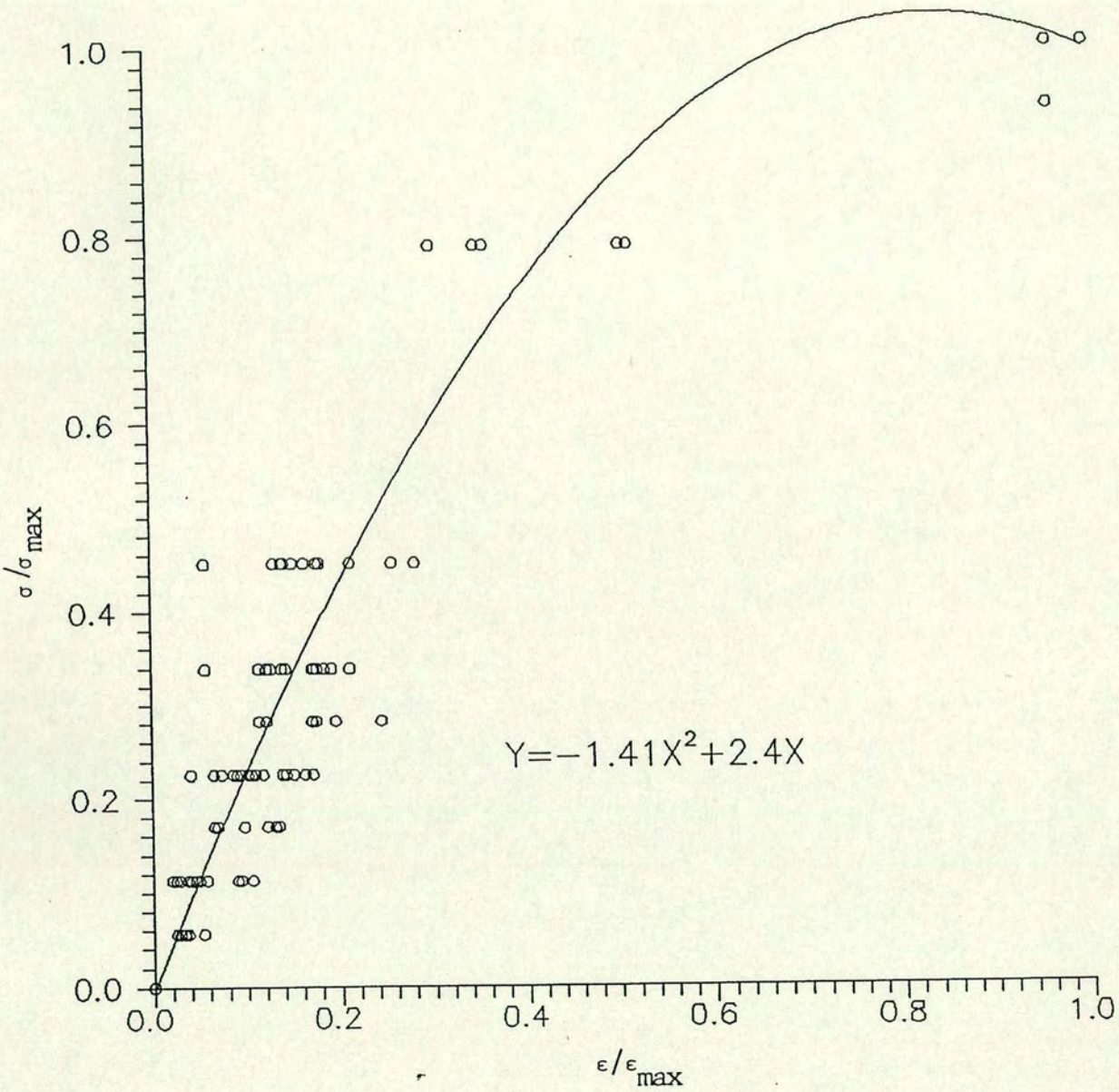

Non dimensional stress–strain curve for six course brickwork prisms.

Figure 3–8

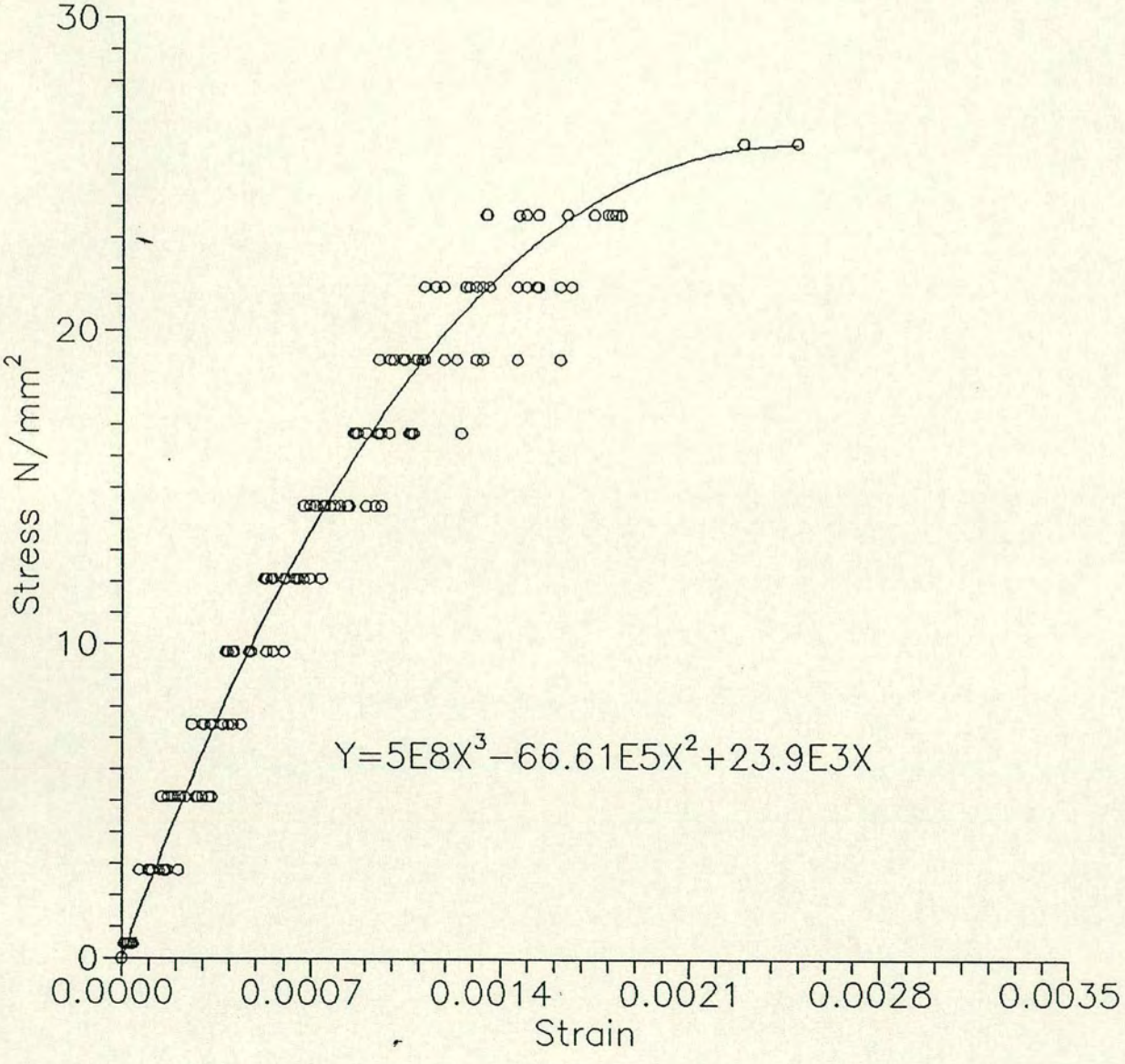

Stress–strain curve for single course brickwork prisms.

Figure 3–9

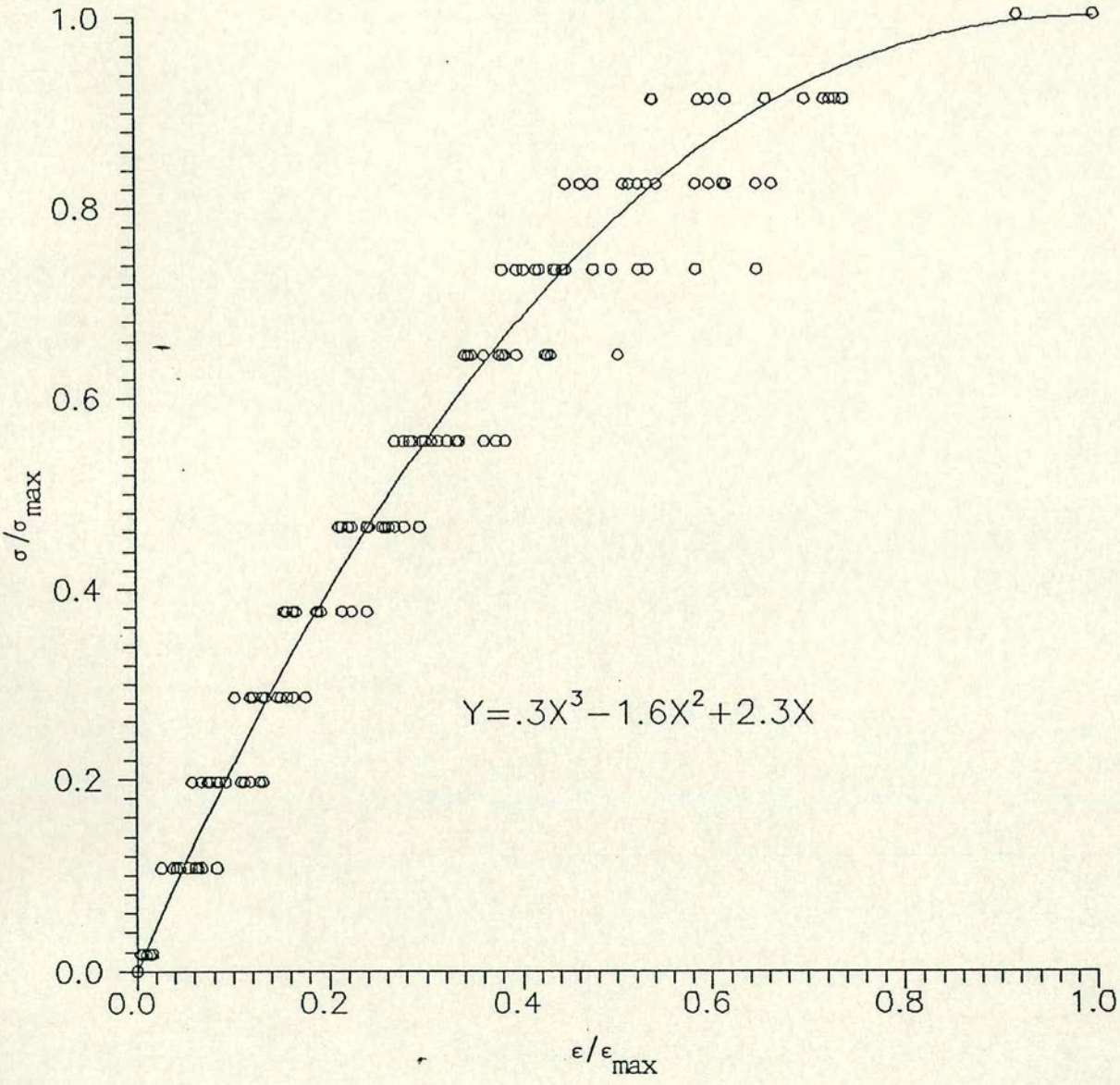

Non dimensional stress–strain curve for single course brickwork prisms.

Figure 3–10

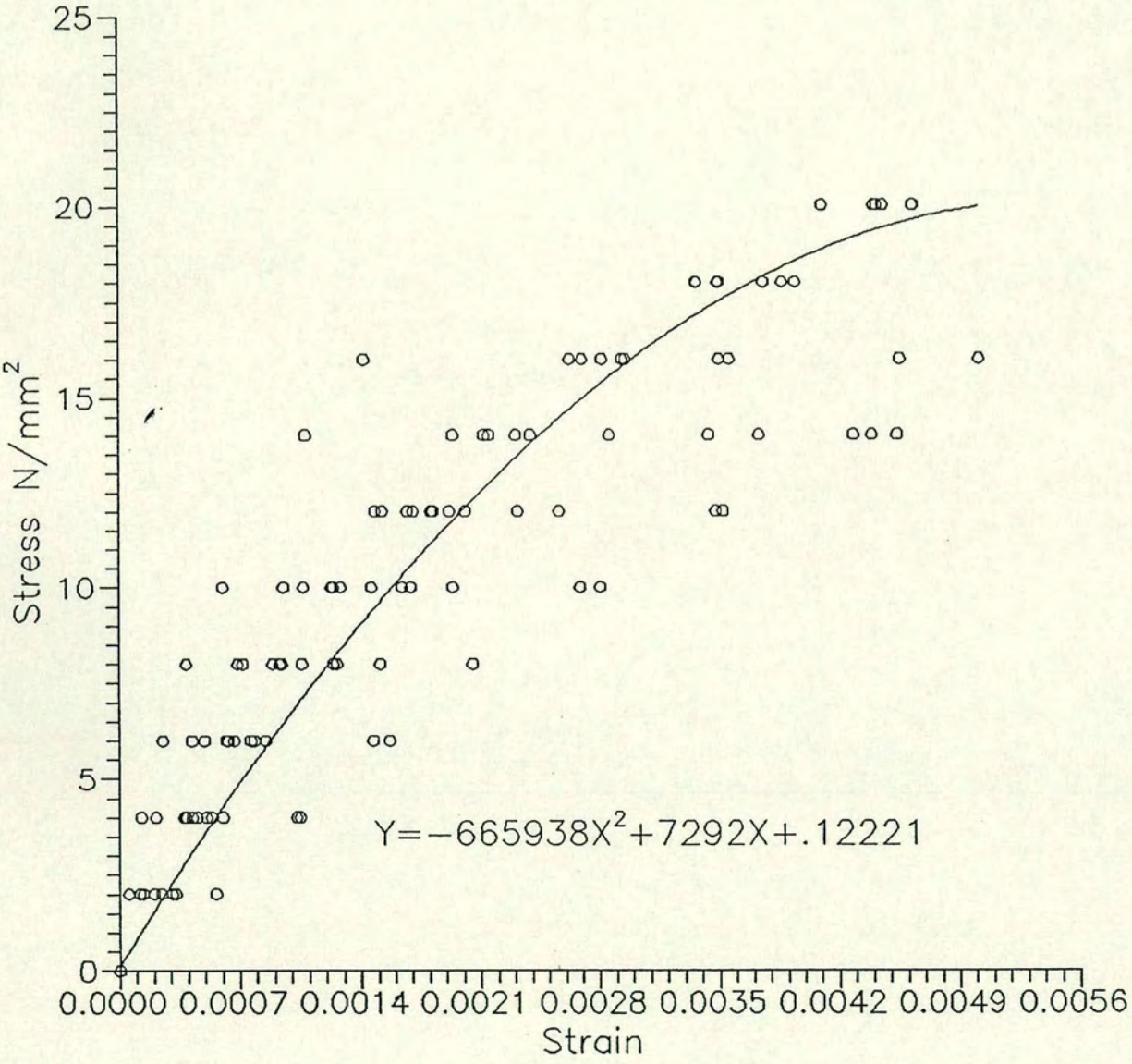

Stress–strain curve for single course brickwork prisms (1/2 scale bricks).

Figure 3–11

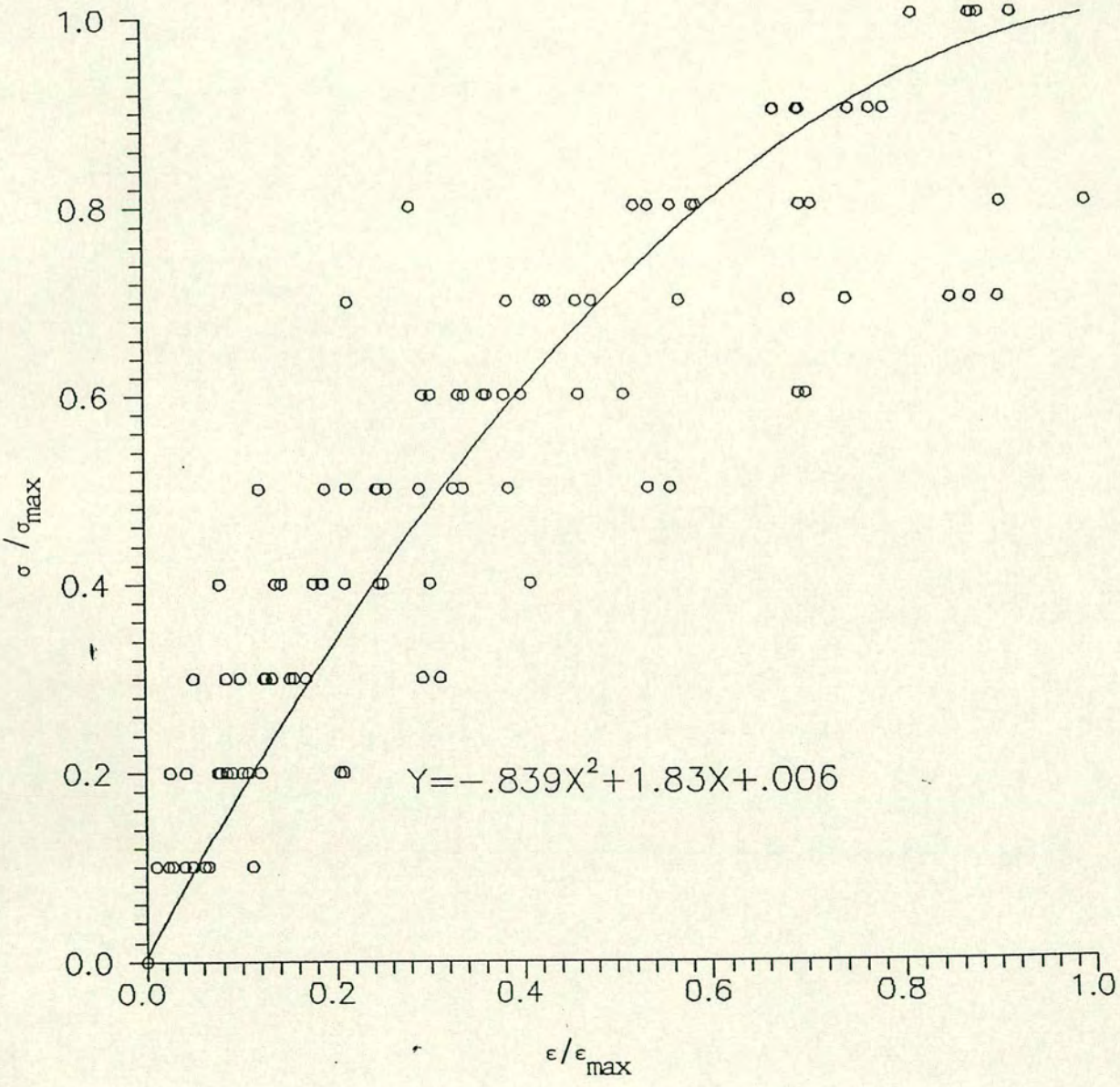

Non dimensional stress–strain curve for single course brickwork prisms (1/2 scale bricks).

Figure 3–12

CHAPTER 4

EXPERIMENTAL TECHNIQUES

4.1 GENERAL

The experimental work involved several types of structure. Chapter 4 describes the construction details and testing methods adopted for each structural member.

4.2 CONSTRUCTIONAL DETAILS

4.2.1 Prisms

Nine prisms were constructed, three open pocket and three formed pocket, Fig. 3.2. The open pocket prisms have a cross-section consisting of four whole bricks and one half brick. The vertical pocket is formed by omitting a half brick having the same described cross-section with concrete infill. The cross-section of the last three prisms consists of six whole bricks built in English bond with no pocket formed in it.

Each prism consists of six courses fabricated vertically on a flat surface. No more than three prisms were constructed at any time. When the brickwork was completed, wooden shuttering was clamped to the rear face of the concrete infill prisms. Concrete was poured into the pockets and subsequently compacted by the vibrator to prevent air pockets forming. Each prism was capped above and below with a rich mortar mix. After construction, the prisms were left undisturbed under a polythene sheet for 28 days prior to testing.

4.2.2 Beams

Two beams with Flemish bond cross-section were fabricated as part of the programme of work, Fig 4.4. The section was similar to the English

bond beams used previously for fully prestressed brickwork beams (Pedreschi, 1983). Results from the two tests were compared to assess the effect of bonding on the behaviour of post-tensioned brickwork beams. Both types have similar dimensions, characteristics and bed joints running parallel to the direction of the induced prestressing load. The Flemish bond beams were fabricated on the floor of the laboratory by an experienced bricklayer. For prestressing and concrete infill purposes, the beams were built upside down. The grouting of the beam was simple as the concrete was poured vertically into the cavity through the perforation in the top course. Pairs of 6 mm diameter mild steel rods were placed at 200 mm centres for the whole length of the beam to avoid shear and anchor zone stress problems. The beam was left under polythene sheets for a minimum of 21 days before prestressing. Thick mild steel plates were bedded at each end of the beam using a rich mortar mix. The tendons were prestressed using CCL XL barrel and wedge type open grips. All tendons were prestressed in stages, up to 50% of the required force at the first stage, then up to 70% of their ultimate load. A slight hairline crack in the bedjoint nearest to the soffit of the beam developed during the prestressing stage. The cracks were an indication of section weakness in the Flemish Bond beams. Prior to testing, during the concrete infill stage, all cracks were completely filled by a rich concrete mix. The possibility of these cracks occurring can be eliminated in future beams by prestressing the strands to only 50% of their ultimate load. Losses of prestress were due to slip of the strand between the wedge during lockoff, elastic shortening and creep of the brickwork. An average of 12% losses was due to slip of the strand, any further losses resulting mainly from elastic shortening and dead load deflection of the beam (creep) prior to testing.

4.2.3 Beams/Slabs

Six beams (two English, two English Garden and two Flemish Garden Bond) were fabricated vertically on top of a steel plate as part of a clamping system designed to prevent structural movement Figs 4.2, 4.3. A vertical pocket was formed by omitting whole or half bricks from the beam's cross-section. All the beams have similar dimensions, characteristics and bed joints running perpendicular to the direction of the induced prestressing load. The beams were fabricated by an experienced bricklayer. The beam was cured under polythene sheets for a minimum of 21 days before prestressing. A compressive force was applied to the beams through the top and bottom steel plates as part of the clamping system. The clamping system was designed to help move the beam to the prestressing area without causing any tensile damage due to its own dead weight. Prior to stressing, the tendons were set in the formed pocket to the required depth. The tendons were anchored to a thick mild steel plate mortared at each end of the beam. The tendons were located at a distance of t/6 from the centre of the beam therefore providing the maximum possible lever arm for the prestressing force without developing tensile stresses. Electrical strain gauges were attached to each of the four tendons in order to monitor the strain in the steel during prestress and testing of the beam. In all the beams the tendons were prestressed horizontally at 21 days to a maximum of 70% of their ultimate load. After prestressing, the pocket was brushed with cement slurry to ensure a good bond between the brickwork and the concrete infill. The concrete infill was compacted using a tamping rod. The beam was left undisturbed under polythene sheets for a further seven days prior to testing.

4.2.4 Walls

Six walls were fabricated vertically on top of a re-useable steel base to which the tendons were anchored Figs 4.5 – 7. The wall cross-section was built in English bond. Around the tendons two vertical pockets in each wall were formed by omitting whole or half bricks from the bond. The walls were built in several stages, with no more than twenty courses laid at each stage. All walls were built with similar dimensions, characteristics and bed joints running perpendicular to the direction of the induced prestressing load. The walls were cured for 21 days under polythene sheet, prior to prestressing. The tendons were anchored to a thick mild steel plate mounted at the top of the wall and prestressed vertically at a distance of t/6 from the centre of the wall thus providing the maximum possible lever arm for the prestressing force without introducing tensile stress. The tendons were prestressed to a maximum of 70% of their ultimate load. After prestressing, the pocket was brushed by cement slurry to ensure a strong bond between the concrete infill and the brickwork shell. Wooden shuttering was then clamped to the rear face of the wall and concrete infill poured into the pockets and compacted by vibrator to prevent air pockets forming. The wall was left under polythene sheets for an extra seven days prior to testing.

4.3 INSTRUMENTATION

4.3.1 Brickwork Strain

In the six course prisms, the Demec points were mainly located at the compression face (front). The strain readings were taken from the first course under the bearing plate up to the sixth course above the base, Fig 4.1. The vertical and horizontal strains were measured at various depths using a demountable Demec gauge over a gauge length of 150 mm. In all cases, the strains were measured within the region of constant

bending moment, using Demec gauges of length 200 mm, on both faces of the beam at various depths across the section. After cracking, the measurements were concentrated in the compression zone to examine any variation in the neutral axis depth for each increment of loading.

Fig. 4.5 shows the arrangement of Demec points on the compression face (front) and the cross-section of the walls. The vertical and horizontal strain readings were recorded using demountable Demec gauges over a gauge length of 100 mm. The strain readings around the base of the wall at the same height as the strain gauges on the reinforcement were used mainly to examine any variation in vertical and horizontal strain on the compression face of the wall. The strain readings on the cross-section of the wall were used mainly to examine the variation in neutral axis depth up to failure load. It was not possible to inspect the strains at the rear of the wall due to the loading arrangement.

Therefore, one advantage of using a three-dimensional finite element analysis is the possibility of modelling the rear of the wall where experimental arrangements make it impossible to obtain actual readings.

4.3.2 Steel Strain

The strain in the prestressing tendons was measured with highly sensitive electrical strain gauges bonded onto a prepared surface on the bar. In each tendon, two strain gauges were positioned diametrically opposite to each other, one for the tension face and the other for compression. For each load increment, the strain gauges were scanned automatically using a data logging system. This provided a check on the behaviour of the structure during the test and up to failure.

4.3.3 Deflection

Displacements were measured using linear voltage displacement transducers with a maximum travel of 50 mm. As the structure approached failure, where deflections were large, the transducers were moved away and the deflection measured using a ruler reading. 10 minutes after each increment reading, the strain and deflection were re-scanned to detect whether the structure exhibited any creep under load. The test results show that creep was very small until close to failure.

For each load increment, the rotation angle was recorded manually using two inclinometers fixed at the first course above the base on both sides of the wall cross-section.

4.3.4 Load Measurement

The load was applied by means of two hydraulic jacks connected to a single feed hydraulic pump. 100 -200 kN load cells were positioned in the test rig just above the jacks to measure the applied load. In the retaining walls, pressure transducers measured the increased pressure in the hydraulic pipe and the hydraulic jack. The detected load measurement was directly scanned onto the data logging system. The loading history of each jack was therefore detected up to failure. Prior to testing, each load cell and pressure transducer was calibrated in a compressing testing machine using a voltmeter.

4.4 TEST RIG AND TEST PROCEDURE

4.4.1 Prisms

The 9 six course prisms had nominal dimensions of 440 mm in height, 550 mm in length and 215 mm thick for brickwork type A. The bearing steel plate had nominal dimensions of 30 mm in thickness, 140 mm in

width and 320 mm in length. The steel bearing plates and the brickwork specimens were mounted on top of freshly made dental plaster to ensure an even distribution of load. A small increment of load was applied immediately to the bearing plate by means of the upper platen of the testing machine to level the brickwork specimens and the bearing plate and fill up the pores underneath. The centre line of the bearing plate was placed at a distance of (t/6) eccentrically to the centre of the wall in the longitudinal direction. The specimens were tested under 4 MN capacity Avery universal compression machine. The load was increased to failure with an average of 8-10 increments of the ultimate load. For each increment, the strain was measured at approximately sixty positions using a mechanical dial gauge of length 150 mm. The crack widths were measured on all faces of the prisms with the use of crack detection moving microscope. In the case of the 3 six course axially loaded prisms, the specimens were positioned in the testing machine so that the centre of the cross-section coincided with the centre line of the upper platen of the testing machine. Adjustments were then made to ensure that the whole cross-section of the specimen was covered and that the load was applied axially.

4.4.2 Beams

All the beams were tested under a four point loading system. The ends of the beam were supported by a pin and roller as shown in Fig.4.2 The distance between loading points was 700 mm for all beam/slabs and 750 mm for the two Flemish beams. This arrangement provided a region of constant moment and is applicable to a retaining wall situation Fig 4.3. All the beams were tested at a minimum age of 28 days, allowing 21 days before prestressing and an extra 7 days for curing of the concrete infill. Prior to testing, the beams were weighed using two 30 kN load

cells. The average weights for the beams and beam/slabs were 1.5 kN/m and 5kN/m respectively. The load was applied in average increments of 10 % to the expected failure load. The applied load was measured by two hydraulic jacks attached by a single feed to a hydraulic pump. To prevent stress concentration, the beam supports and point load were bedded onto a metal plate using a rich mortar mix.

For each increment the load was held constant and the following readings were taken:

(i) Applied load.

(ii) Steel strains.

(iii) Brickwork strains.

(iv) Deflection at supports and at midspan.

After cracking, in addition to the above readings, the crack widths within the constant moment zone were measured with the use of crack detection moving microscope.

4.4.3 Walls

As this investigation is concerned with the deflection and curvature over the full height of the wall up to failure, the loading arrangements were designed to simulate the bending moment and shear force experienced by a retaining wall. The test rig consisted mainly of two items, the steel plate on which the wall was built and the steel reaction frame which carried the loading equipment, Fig. 4.8. The steel plate was placed on the top of two horizontal cross beams bolted to the strong floor. The reaction frame consisted of two vertical standing strong beams bolted to the strong floor and the top part of the reaction frame was stranded using steel wires diagonally to the ground floor.

Each wall was laterally loaded at three horizontal positions using a series of hydraulic jacks connected to pivoted spread beams. The jacks, located at various levels up the wall, were mounted horizontally to the steel reaction frame and applied a load which produced maximum bending moment and shear force at the base of the wall, thus corresponding to a triangular distribution of lateral pressure. In order to ensure an even pressure distribution, freshly made dental plaster was placed between the spreader beam and the wall.

All the walls were tested at a minimum age of 28 days, allowing 21 days before prestressing and a further 7 days for curing. The load was applied in average increments of 10 % the expected failure load. For each increment, the load was held constant for five minutes before the following readings were taken:

(i) Applied load

(ii) Steel strains

(iii) Brickwork strains and the rotation angle at the bottom of the wall

(iv) Deflections at the top and mid-height of the wall

After cracking, the crack propagation and crack width were monitored using crack detection moving microscope. Towards the end of the test, all manual readings were discontinued for safety reasons.

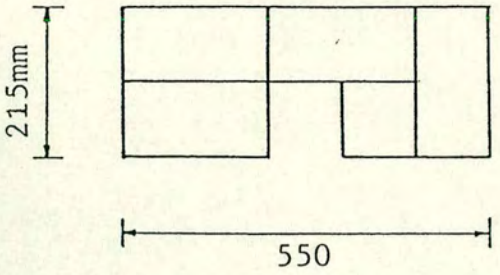

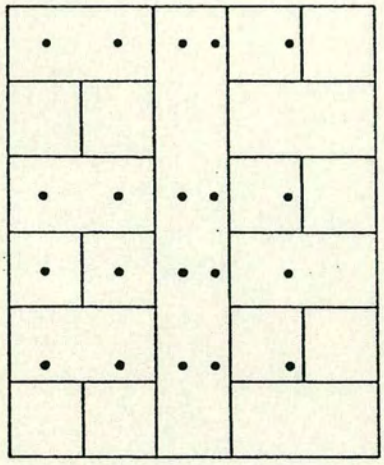

Demecs a) vertical position

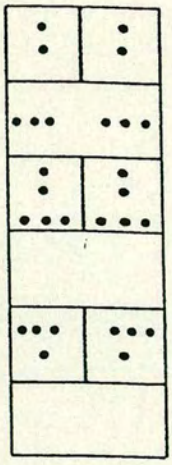

Side View

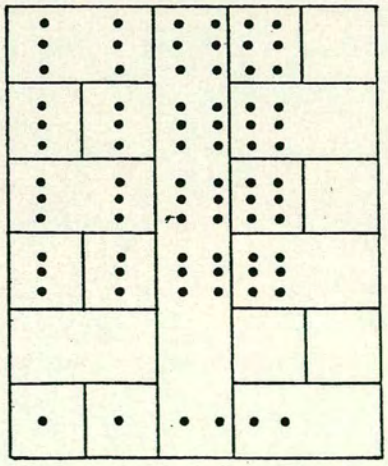

Demecs a) horizontal position

Figure 4.1 Location of Demecs

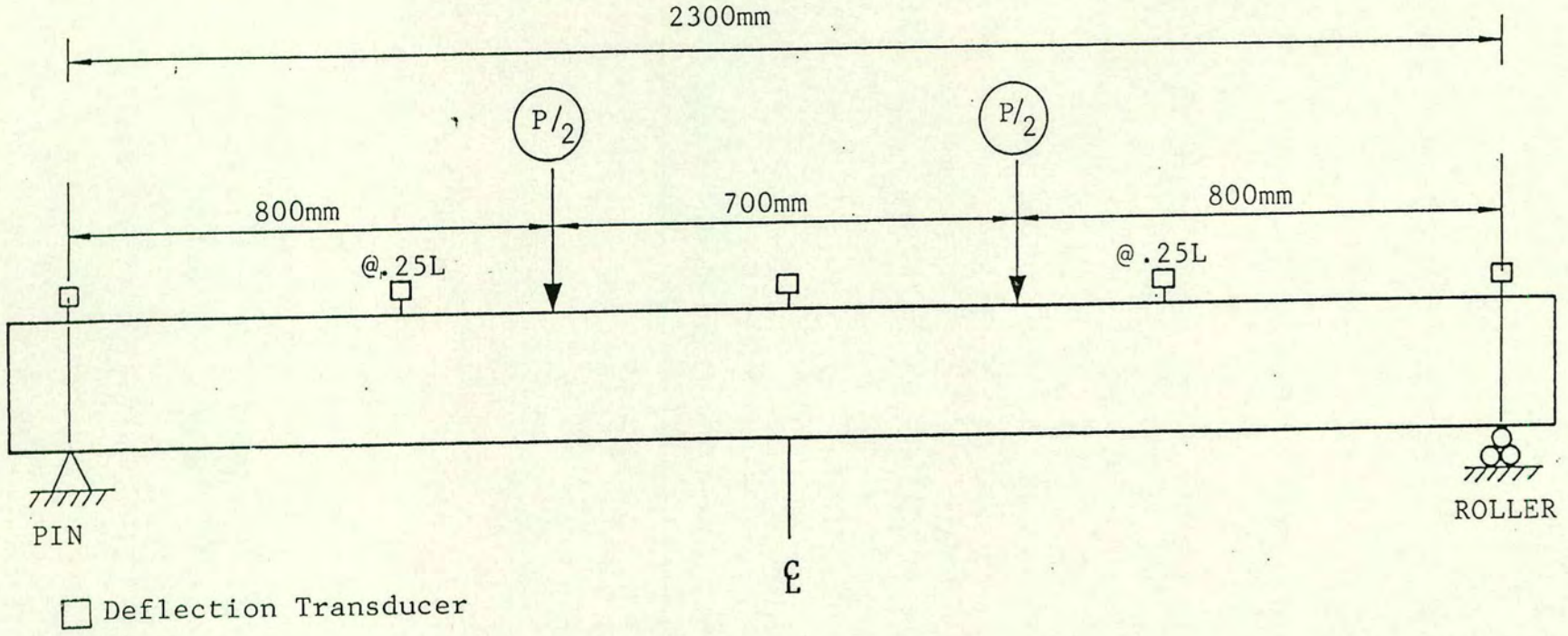

Figure 4.2 Beams 3-8 Test arrangment (Beam/slab)

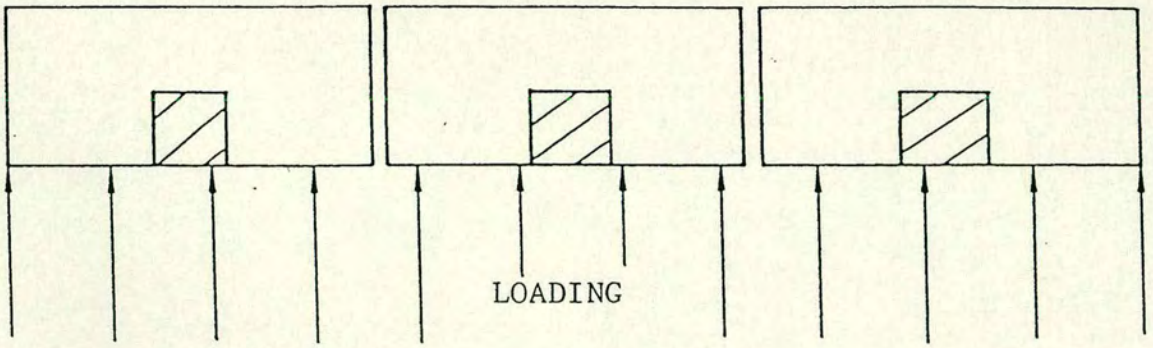

Plane view of pocket type (beam/retaining wall)

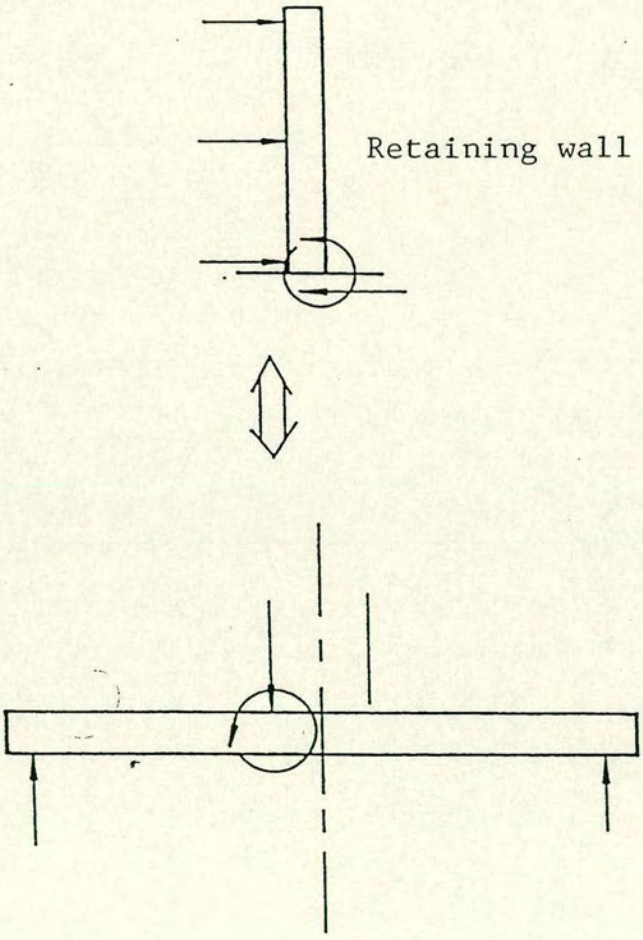

Beam (Two point load)

Figure 4.3

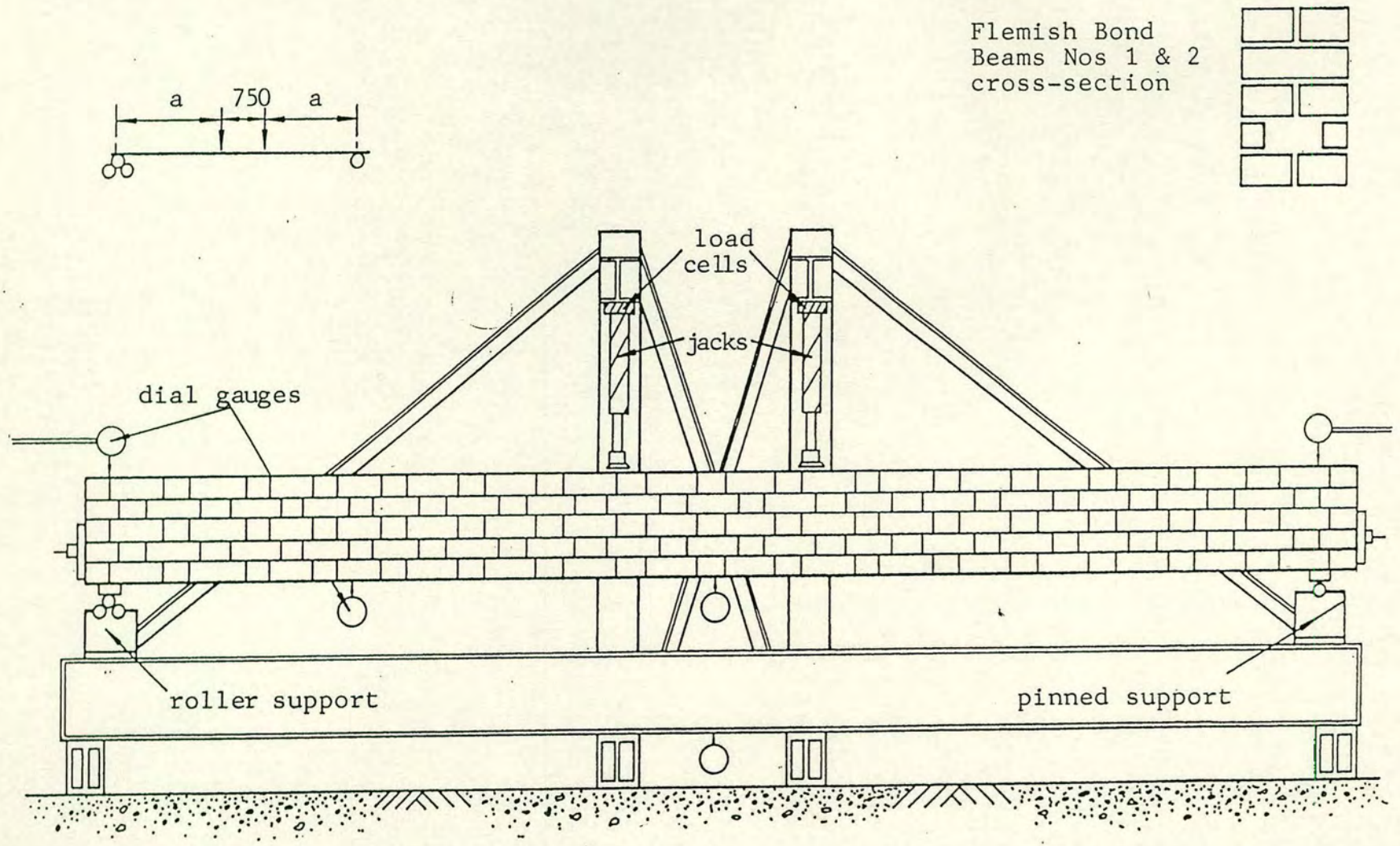

Figure 4.4 Layout of Test Rig

Front View

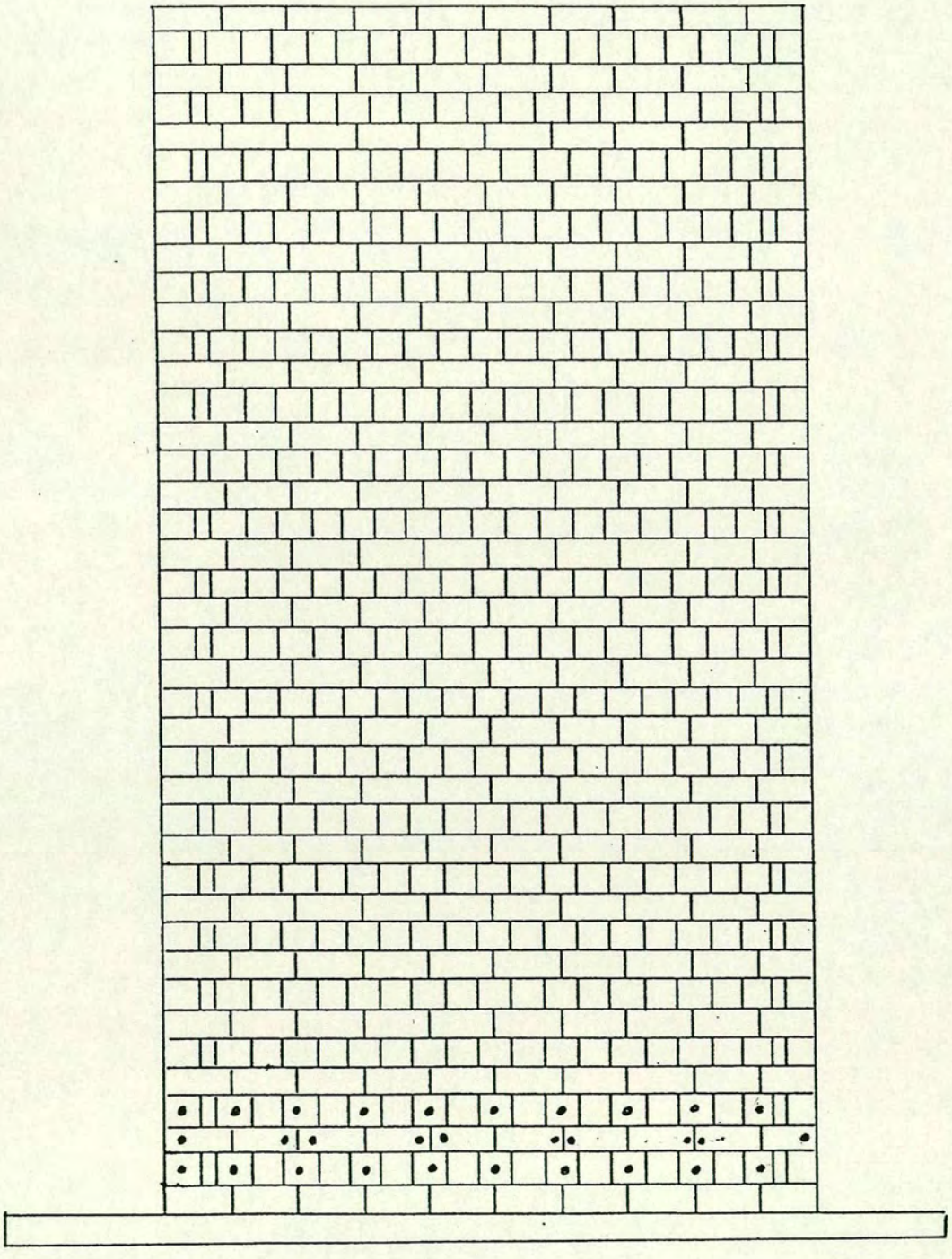

Figure 4.5 Walls - Demec Arrangements

Back View

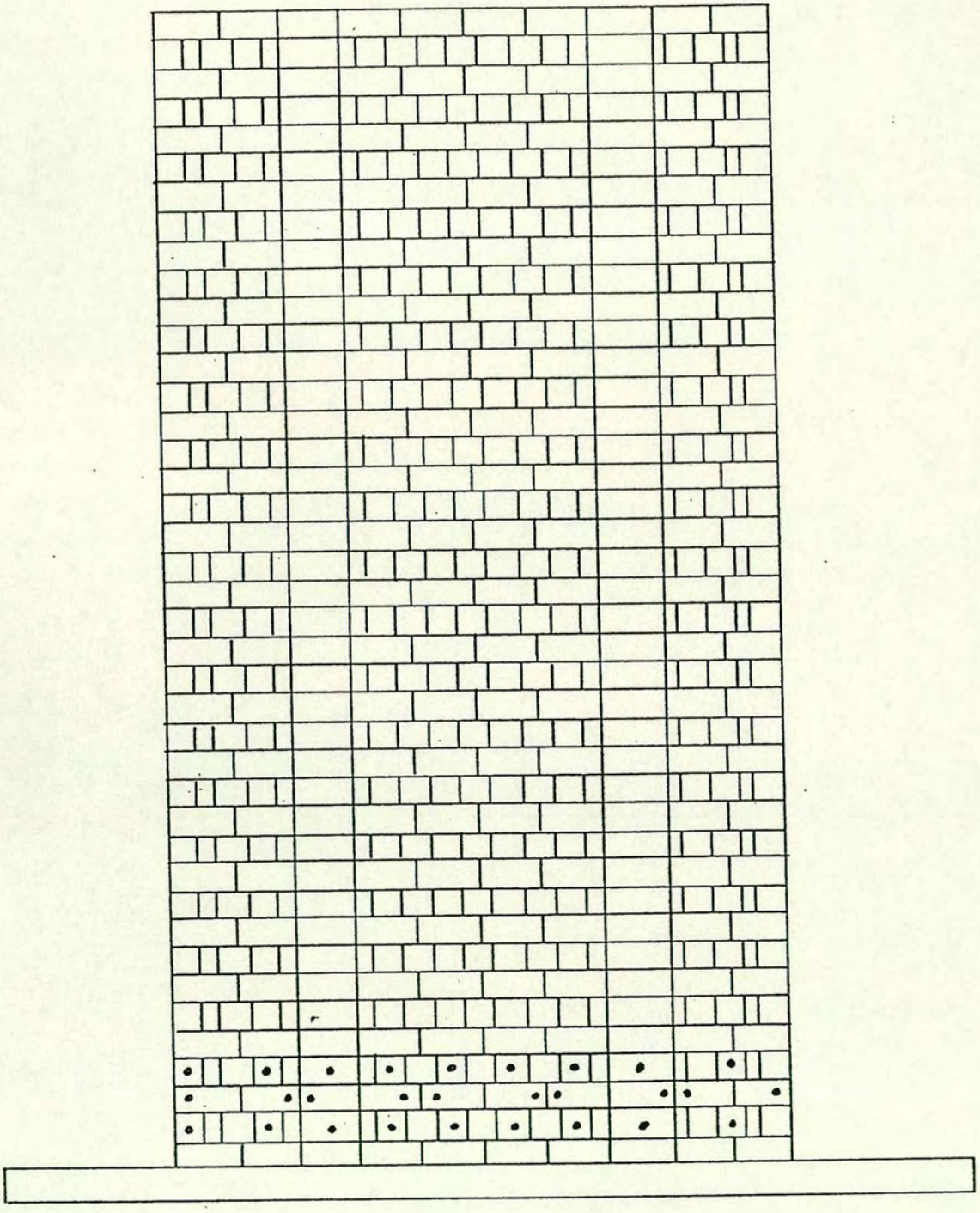

Figure 4.6 Walls - Demec Arrangements

Side View

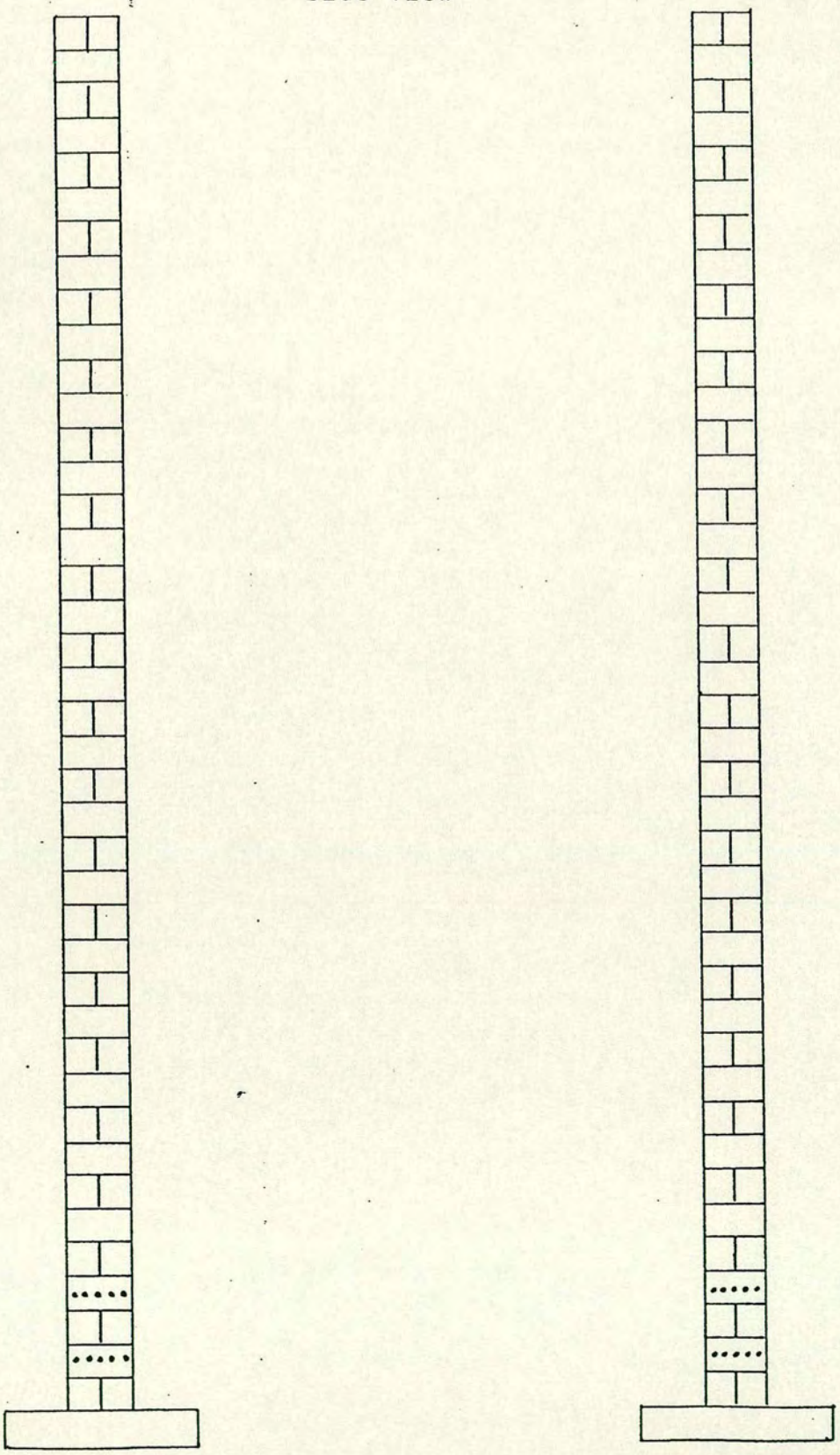

Figure 4.7 Walls - Demec Arrangements

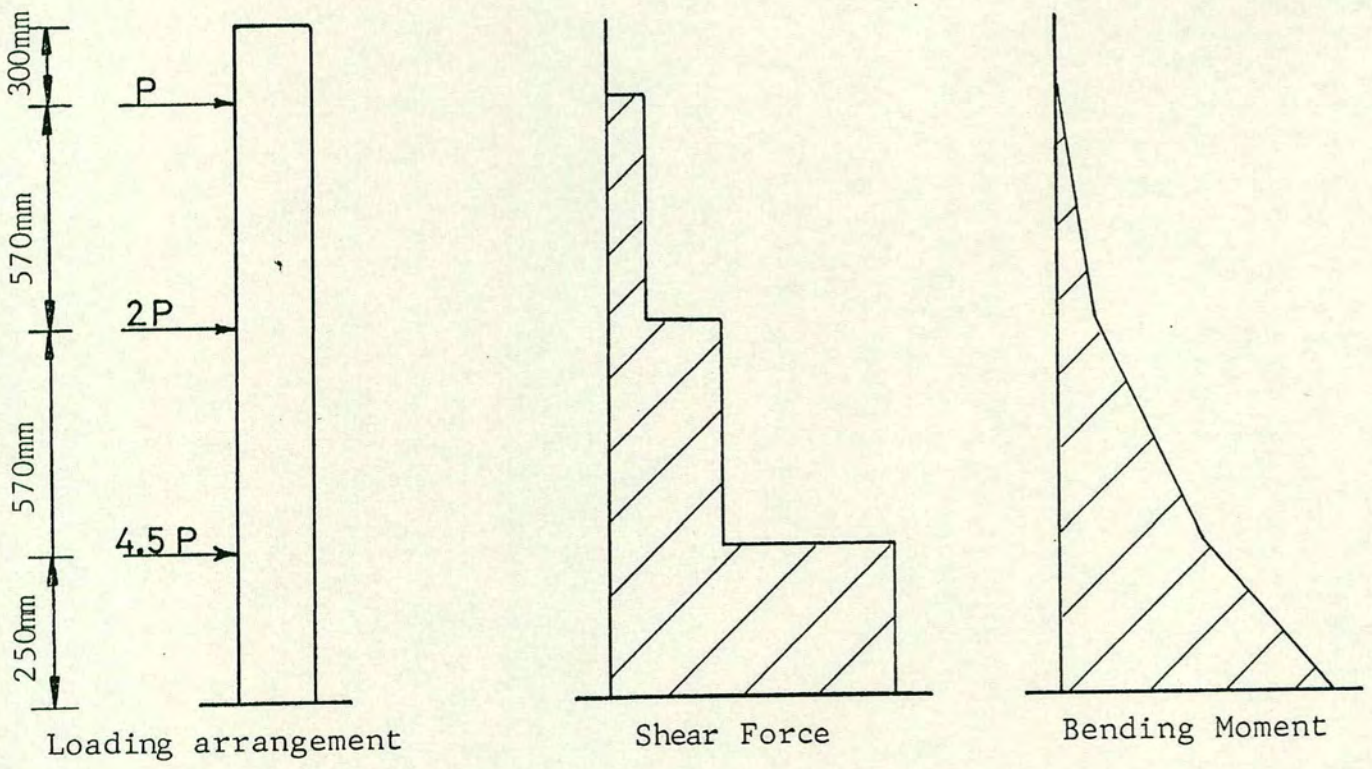

Figure 4.8 Loading arrangment, shear force, and bending moment diagrams

CHAPTER 5

THEORETICAL ANALYSIS

5.1 FINITE ELEMENT ANALYSIS

5.1.1 General

Finite element analysis is probably the only theoretical method that can be used to explain the complicated behaviour of prestressed brickwork retaining walls. The presence of prestressing forces and out of plane pressures cause a complex bi-axial bending behaviour in which the wall spans vertically from the base whilst the brickwork panels span horizontally between the pockets. Only a limited amount of research work has been published which uses finite element analysis to simulate the behaviour of masonry structures. The main aspect in these investigations was the influence of the mortar joints on the brickwork behaviour. Brick is orthotropic material while mortar is an isotropic material, so that brickwork has a non-linear highly anisotropic behaviour. Brickwork is also concerned with additional problems such as creep, shrinkage, cracking, strength variation with age and strength variation within a member. The introduction of tendons can cause additional problems such as bond, anchorage and bond slip. Samarasinghe, Page and Hendry found that the orientation of the bed joint to the principal stresses is of prime importance in the bi-axial tension-compression region typically found in shear walls (Samarasinghe, W. Page, A.W. & Hendry, A.W., 1982). A non-linear finite element program based on a non-linear fracture model of masonry for the analysis of the in-plane behaviour of masonry subjected to concentrated load was developed by Ali and Page (Ali, S.K., 1987). Good agreement was obtained between twenty-four experimental panels, tested under concentric and eccentric strip in-plane concentrated load, and the developed program. The modulus of elasticity

and the strength parameters, particularly the joint bond strength, were found to be the most significant properties. Tellett has developed a non-linear finite element program to analyse pocket-type walls (Tellett, J., 1984). Based on limited information about the uniaxial stress-strain relationships of brickwork in directions other than on the bed face or about the bi-axial behaviour, the author justified the use of a square failure criterion although brickwork is known to be anisotropic. Brickwork under uniaxial compression was assumed to exhibit linear elastic-plastic behaviour and be elastic-brittle under uniaxial tension. Reinforcement was modelled as an elastic plastic material. The theoretical work was in good agreement with the experimental reinforced brickwork retaining panels. But, the analysis was not in good agreement with lightly reinforced two way brickwork panels since tensile membrane action developed. Results showed that it was possible to analyse the two-way unreinforced brickwork panels and arching action in one way spanning panels. Due to the fact that experimental results indicated that a pocket-type retaining wall was unlikely to fail in shear even when heavily reinforced, the finite element program was unable to take into account out-of-plane shear stresses. The finite element program was mainly developed to study a few parameters on the behaviour of reinforced pocket-type walls.

A standard finite element package (London University Stress Analysis System), each with its graphics part package MYSTRO, was used in this research. The package and its graphics partner were implemented on a VAX 8550 at the Edinburgh University Computing Centre. The LUSAS package has an extensive number of facilities, performs several types of analysis and contains a large selection of elements. LUSAS is a general purpose finite element analysis system. A limited number of its facilities

were used in this research work. Two and three-dimensional continuums were used for non-linear geometric and material properties analysis. Material non-linearity means that the stress-strain relationship is non-linear. Geometrical non-linearity means that the data run can have large displacements and small strains or large displacements and large strains. The art of finite element analysis lies in the development of a suitable model idealisation. Analysis form and element discretisation are the functions of computer time and results of acceptable accuracy. Therefore, experience with the package serviceability and implementation is needed to achieve optimum results.

5.1.2 Prisms

A three-dimensional isoparametric solid element (HX8) was idealised for the no fill and concrete infill pocket prisms. Elements with higher order models are capable of modelling curved boundaries. The element is numerically integrated and is capable of modelling a linear anisotropic solid material and non-linear elastic-plastic material properties. The model dimensions and stress units were in millimetres and Newtons respectively. The model height, width and thickness were 420, 200 and 550 mm respectively. The model consisted of 96 elements. This discretisation was one of balance between execution computer time and resultant accuracy. The package gives several analysis options. The options that were selected for the analysis were as follows:
The first option was the invocation of finer numerical integration rules for elements. The second option was using total Lagrangian geometric non-linearity. The third option was the suppression storage of shapes.

The analysis was applied to three-dimensional isoparametric solid elements, each element consisting of 8 nodes and 24 degrees of freedom

(three translations at each node). Brickwork was modelled as an elasto-plastic von Mises yield surface model. This model is used to represent the ductile behaviour of materials which exhibit little volumetric strain. In the explicit (Forward Euler) model the direction of plastic flow is evaluated at the point where the stress increment first reaches the yield surface. The following values were assumed:

Young's Modulus	= 25000 N/MM^2
Poisson's Ratio	= 0.15
Initial uniaxial yield stress	= 25 N/MM^2
Slope of the uniaxial yield stress against effective plastic strain curve	= 6000 and 3000
Limit on the effective plastic strain for which the hardening curve was valid	= 0.0013 and 0.0026
Number of straight line approximations to the hardening curve	= 2

The concrete infill was modelled as an elasto-plastic von Mises yield surface model. The material properties were as follows:

Young's Modulus	= 22500 N/MM^2
Poisson's ratio	= 0.25
initial uniaxial yield stress against effective plastic strain curve	= 16000 and 5210
limit on effective plastic strain for which the hardening curve was valid	= 0.0016 and 0.012
number of straight line approximations to the hardening curve was	= 2

The support conditions that were used to define the boundary conditions were as follows:

(a) The base of the structure was restrained against translation and rotation in all global directions.

(b) The top bearing plate was restrained against translation and rotation in the X and Z directions and free to translate and rotate in the y direction.

LUSAS incorporates a variety of loading types but in this study, distributed loading (face load) was assumed applied at the nodes, and acting on all elements which are connected to that node. The pressure load was applied on the face of the bearing plate elements in the y direction. The pressure load was applied at an eccentricity, e = the thickness of the model/6.

LUSAS provides several types of analysis control. A non-linear control type consisting of several solution orders was used in this analysis. As only one type of loading was applied to the structure, it was practical to use an automatic solution order based on the Newton-Raphson procedure where each iterative calculation is based upon the current tangent stiffness. This solution produces only a small numbers of iterations and a longer computer time for each increment run. The computer time (cpu) to complete each iteration is dependent on the residual force number. The residual force is the sum of the squares of all the residual forces expressed as a percentage of the sum of the square of all the external forces and depend on the structural stiffness (K) and displacement (δ). The external work is the work done by all the residuals acting through the iterative displacement and depends on the magnitude of the structural external force and its distance of travel. The values that were used for the displacement norm, residual force norm and external work norm were 0.1, 0 and 0.001 respectively. The no fill grout pocket prism

finite element analysis data run was completed as above but omitting the grout elements from the element topology data section.

5.1.3 Beam/Slabs

5.1.3.1 A three dimensional continuum (HX8) was idealised for the beam/slabs analysis. Model dimensions and stress units were in millimetres and Newtons respectively. The model length, width and thickness were 3000, 1000 and 200 respectively and the model consisted of 385 elements. This discretisation was one of optimum balance between execution computer time and result accuracy. The element discretisation has the same material properties and type of analysis as that used in the finite element data run for the prism. The support conditions used to define the boundary conditions of the finite element discretisation were as follows:

a) At 350 mm from one end, the structure was restrained against translation in both the x and z directions, but free to translate in the y direction and free to rotate about the y axis.

b) At 350mm from the other end, the structure was restrained against translation in the z direction, and free to translate in both the x and y directions and free to rotate about the y axis.

There were two load cases.

The first type of load case was the application of a face load pressure on the bearing plate element area. During construction, the fill grout was placed in the pocket after the implementation of prestressing load, so that the fill grout was not subjected to the prestressing pressure. Therefore, several trial and error finite-element data runs for both no fill and concrete infill pocket models were carried out. Results showed that a load of one and half times

the experimental prestressing load magnitude was required for the concrete infill pocket model to produce acceptable results.

The second load case was the application of concentrated loads in the y direction at a distance of 350 mm from the beam/slab centre line elements. The loading cases should be the idealisation of experimental prestressed two point load structure. Several tendon material properties were implemented in order to achieve the optimum finite element simulation. The first model trial assumed the use of an initial strain bar element in 3 dimensions with non-linear material properties. All data run trials obtained results which were of unacceptable accuracy. This resulted from the fact that the brickwork element materials were behaving in compression as well as in tension and so the location of the neutral axis depth was constant. But, in brickwork as tension develops and cracking occurs the compressive strain above the neutral axis depth increases rapidly with the pressure and the neutral axis depth decreases until failure occurs.

5.1.3.2

In 1990, LUSAS version 9 introduced a plane stress concrete model. This model can be accommodated by semi-loof shell elements (QSL8) for shells as well as plate finite element analysis. The material models are capable of modeling a non-linear bi-axial concrete material. The main aim of the LUSAS plane stress concrete model is to simulate the non-linear response of reinforced concrete. The model can consider the following aspects:

a) The non-linear stress -strain relationship in compression as well as in tension.

b) The ability of the cracked section to carry tensile stress.

c) The ability to transfer shear through the cracked section.

The concrete is represented as an equivalent homogeneous continuum with uniformly distributed properties. The plane stress concrete model behaviour under load can numerically represent the distributed crack, strain-softening and crunching and an assumed material orthogonality.

The model dimensions and stress units were in millimetres and newtons respectively. The model length and width were 3000 and 1000 respectively and the model consisted of 290 elements. The discretisation was one of balance between computer time and result accuracy. The options selected were as follows:

The invocation of finer numerical integration rules for elements, fracture energy strain-softening, and strain-variable shear retention;
Continuation of the solution even if more than one negative pivot occurs;
Total Lagrangian geometric non-linearity;
The invocation of composite properties/assignments;
The suppression storage of shapes.

Brickwork was modelled as a bi-axial non-linear model and the material properties were assumed as follows:

Young's modulus	= 21000 N/MM^2
Poisson's ratio	= 0.15
compressive strength of brickwork	= 24.75 N/MM^2
shear retention factor	= 1.41
strain at peak compressive strength	= 0.025
softening factor	= 50

The concrete infill was modelled as a bi-axial non-linear model and the material properties were assumed as follows:

Young's modulus	= 22500N / MM^2
Poisson's Ratio	=0.25
compressive strength of grout	= 28 N/ MM^2
shear strength factor	= 1
tensile strength	= 2 N / MM^2
strain at peak compressive strength	= 0.003
softening factor	= 50

Tendon bars were modelled as incorporating non-linear isotropic hardening, and the material properties for the implicit backward Euler von Mises material model. These properties were assumed as follows:

Young's modulus	=210000 N / MM^2
initial uni-axial yield stress	= 400 N / MM^2
slope of the section of the uni-axial yield stress against effective plastic strain curve	= 0.0001 N / MM^2
limit of the effectiveness plastic strain up to which the section of the hardening curve is valid	= .012
number of straight line approximations to the hardening curve	= 1

The model elements consisted of 12 composite material layers. Composite material input was used to laminate a variety of materials together within a single element. Each element may have a composite property set up to 100 layers. The thickness of each layer is subjected to specifying layer stresses and the support conditions used to define the boundary conditions of the finite element discretisation were the same as those used on the previous (HX8) element model. Two types of load

case were used. The first type assumed the application of concentrated loads and moments on the bearing plate nodes area. The second type assumed the application of concentrated loads in the x direction on the nodes at a distance of 350 mm from the beam/slab centre line elements. These load cases represent the idealisation of the experimental prestressed two point loading on the structure. The data run was in non-linear analysis control, using 0.1, 0 and 0.001 as the convergence factors control for displacement norm, residual force norm and external work norm respectively.

5.1.4 Walls

A suitable model idealisation can offer a more sophisticated approach that allows the more complicated aspects of the behaviour of post-tensioned pocket walls to be investigated. The problem presented is the development of overlap prestressing forces in a complex bi-axial bending behaviour in which the wall spans vertically from the base whilst the brickwork panels span horizontally between the pockets. A three-dimension (QSL8) was idealised for post-tensioned wall analysis. Model dimensions and stress units were in millimetres and Newtons respectively. The model height, width and thickness were 1700, 1200 and 100 respectively and the model consisted of 154 elements. This discretisation was one of optimum balance between execution computer time and resultant accuracy. The options selected for the analysis were the same as those selected for the beam/slab analysis. Brickwork was modelled as a bi-axial non-linear model and the material properties were assumed as follows:

Young's Modulus	= 14000 N/MM^2
Poisson's Ratio	= 0.15
compressive strength of brickwork	= 19.50 N/MM^2

shear retention factor	= 1
tensile strength	= 1.87 N / MM^2
strain at peak compressive strength	= 0.0046
softening factor	= 50

The fill grout and tendon bars have the same material properties as for the beam/slab data run. The model elements consisted of 12 composite material layers. The structure discretisation was idealised as earth retaining walls subjected to a triangular pressure distribution. Therefore, the loading arrangement for analysing the six retaining walls with variable areas of steel is as shown in Fig. 4.8. There were two types of load case. Firstly the application of concentrated loads and moments on the bearing plate node area. Secondly, the application of pressure load (FLD) in a triangular arrangement in the z direction. At the base of the model, the structure was restrained against translation and rotation in all global directions. The data run was in non-linear analysis control and values of 0.1, 0 and 0.002 were assumed for the convergence factor control for displacement norm, residual force norm and external work norm respectively.

5.2 DIRECT ANALYSIS

5.2.1 General

The main characteristic of any structural member is its actual strength. This strength must be large enough to resist with some margin, any load which may act on it during the life of the structure. Therefore, the design of masonry was based on an elastic analysis in accordance with C.P. 111, 1970. The design of the section for the actual applied loads in compression (masonry) and in tension (steel) assumed linear elastic behaviour. But,the Codes of Practice are now based on a "limit state"

approach for the design of reinforced and prestressed masonry (B.S. 5628: part 2: 1985). The Code of Practice BS 5628: Part 2 makes the following recommendations:-

Firstly design for the ultimate limit state

1 - Bending

When analysing a cross-section to determine the design moment of resistance, M_d, the following assumptions should be made:

a) Plane sections remain plane when considering the strain distribution in the masonry in compression.

b) The distribution of stress is uniform over the whole compression zone and does not exceed: f_k/γ_{mm}.

where

f_k is the characteristic compressive strength of masonry

γ_{mm} is the partial safety factor for the compressive strength of masonry.

c) The maximum strain at the outermost compression fibre is 0.0035.

d) The tensile strength of the masonry can be ignored.

e) Plane section remains plane when considering the strain in bonded tendons and any other reinforcement, whether in tension or in compression.

f) Stresses in bonded tendons, whether initially tensioned or untensioned, and in any other reinforcement are derived from the appropriate stress-strain curve. A typical stress-strain curve is shown in figure 5 of the Code .

g) The stresses in unbonded tendons in post tensioned members do not exceed the value derived from figure 6 in the code.

h) The effective depth, d, to unbonded tendons is determined by taking full account of the freedom of the tendons to move.

2. Axial Loading

Prestressed masonry elements subjected to axial or vertical loading with a resultant eccentricity not exceeding 0.05 times the thickness of the wall should be designed in accordance with Clause 24 of the Code. The design axial load resistance of tension members should be taken as being equal to the design axial load of the prestressing tendon and any other reinforcement, making no allowance for any tensile strength of the masonry.

3. Shear

For prestressed sections, the shear stress v, due to design loads at any cross-section in a member may be calculated using the following equation:

$$v = \frac{V}{b\, d_c}$$

When v exceeds fv/γ_{mv}, where γ_{mv} is the partial safety factor for shear strength of masonry, shear reinforcement should be provided as described in clause 22.5.1 of the code.

Secondly, Design for the serviceability limit state.

1. The compressive strength of the masonry at transfer should be at least 2.5 times the compressive stress induced by the prestressing forces, for approximately uniform distribution of prestress, or 2.0 times this stress for approximately triangular distribution of prestress.
2. The compressive stress in the masonry after all losses have occurred should not exceed:
   (a) $0.33f_k$, for approximately uniform distribution of prestress;

(b) $0.4f_k$ for approximately triangular distribution of prestress;

where f_k is the characteristic compressive strength of masonry.

3. Where the area of concrete infill represents more than 10% of the section under consideration, an elastic analysis should be undertaken using the transformed area calculated from the values of elastic modulus given in Clause 19.1.7 (see also Clause 16.1.2) of the Code.

4. The deflection of members should be calculated following the recommendations of clause 16.2.2.1.

5.2.2 Flexural Strength

Pedreschi and Sinha have carried out experimental tests on post-tensioned brickwork beams, where they proved that the experimental ultimate moment can be closely predicted by theoretical moments derived from a simplified cubic parabolic stress/strain relationship for the brickwork. (Pedreschi, R.F. and Sinha, B.P., 1982).

The section of the post tensioned beams and retaining walls tested were all rectangular, using only prestressed reinforcement. Therefore, it is more reasonable to illustrate the stress distribution in the compression zone by stress block factors as shown in Fig 5.1.

λ_1 is the ratio of the stress distribution to the enclosing rectangle. λ_1, multiplied by the compressive stress at the extreme fibre gives the compression zone average stress.

λ_2 is the depth factor between the extreme fibre and the neutral axis.

λ_3 is the ratio between the ultimate compressive stress at failure to the compressive strength obtained from uniaxial tests.

At equilibrium

$$C = T_s$$

$$\therefore \quad \lambda_1 f_m b n = A_{ps} f_{su} \qquad (1)$$

There are three types of strain:

i) ε_{se} is the total strain in the prestressing steel due to the effective prestress forces after losses.

ii) $\beta\varepsilon_{me}$ is the total strain on the brickwork at tendon level due to the prestressing load and overlap prestressing forces.

iii) ε_{ma} is the strain on the brickwork at tendon level due to the applied load.

The ultimate strain ε_{su} is given by:

$$\varepsilon_{su} = \varepsilon_{sa} + \varepsilon_{se} \qquad (2)$$

and the total strain due to the applied load is equal to

$$\varepsilon_{sa} = \varepsilon_{ma} + \beta\varepsilon_{me}$$

But $$\beta\varepsilon_{me} = \frac{\text{prestressing stresses at tendon level}}{E_m}$$

$$\varepsilon_{ma} = \varepsilon_m \left[\frac{d-n}{n}\right]$$

$$\therefore \quad \varepsilon_{su} = \varepsilon_m \left[\frac{d-n}{n}\right] + \beta\varepsilon_{me} + \varepsilon_{se} \qquad (3)$$

$$\therefore \quad n = \frac{\varepsilon_m d}{\varepsilon_{su} + \varepsilon_m - \beta\varepsilon_{me} - \varepsilon_{se}} \qquad (4)$$

From (1) and (4)

$$f_{su} = \frac{\lambda_1 f_m b d}{A_{ps}} \cdot \frac{\varepsilon_m}{\varepsilon_{su} + \varepsilon_m - \beta\varepsilon_{me} - \varepsilon_{se}}$$

The value of f_{su} and ε_{su} must satisfy the material stress-strain curve for the steel.

$$M_u = A_{ps}.f_{su} \left[d - \frac{\lambda_2 \varepsilon_m d}{\varepsilon_{su} + \varepsilon_m - \beta\varepsilon_{me} - \varepsilon_{se}} \right]$$

or,

$$M_u = A_{ps}.f_{su} \left[1 - \rho \frac{\lambda_2 f_{su}}{\lambda_1 f_m} \right] d$$

Using the idealised stress block shown in Fig. 5.1c as suggested by the British Code of Practice, the values of λ_1 and λ_2 are 1 and 0.5 respectively.

A balanced steel area ensures that all materials yield simultaneously. The presence of the prestress strain and the overlap prestressing forces produce complications. Therefore, replacing ε_{su} and f_{su} with ε_{sy} and f_{sy} respectively, the balanced steel area is given as:

$$\rho_B = \frac{\varepsilon_m}{\varepsilon_m + \varepsilon_{sy} - (\beta\varepsilon_{me} + \varepsilon_{se})} \cdot \frac{\lambda_1 f_m}{f_{sy}}$$

(experimental results from tests on walls recommend $\beta \simeq 2$)

5.2.3 Shear Strength

A gradual flexural failure with warning that permits remedial measures is preferable to a sudden shear failure with unexpected collapse. Only a limited amount of research has been carried out on the shear strength of

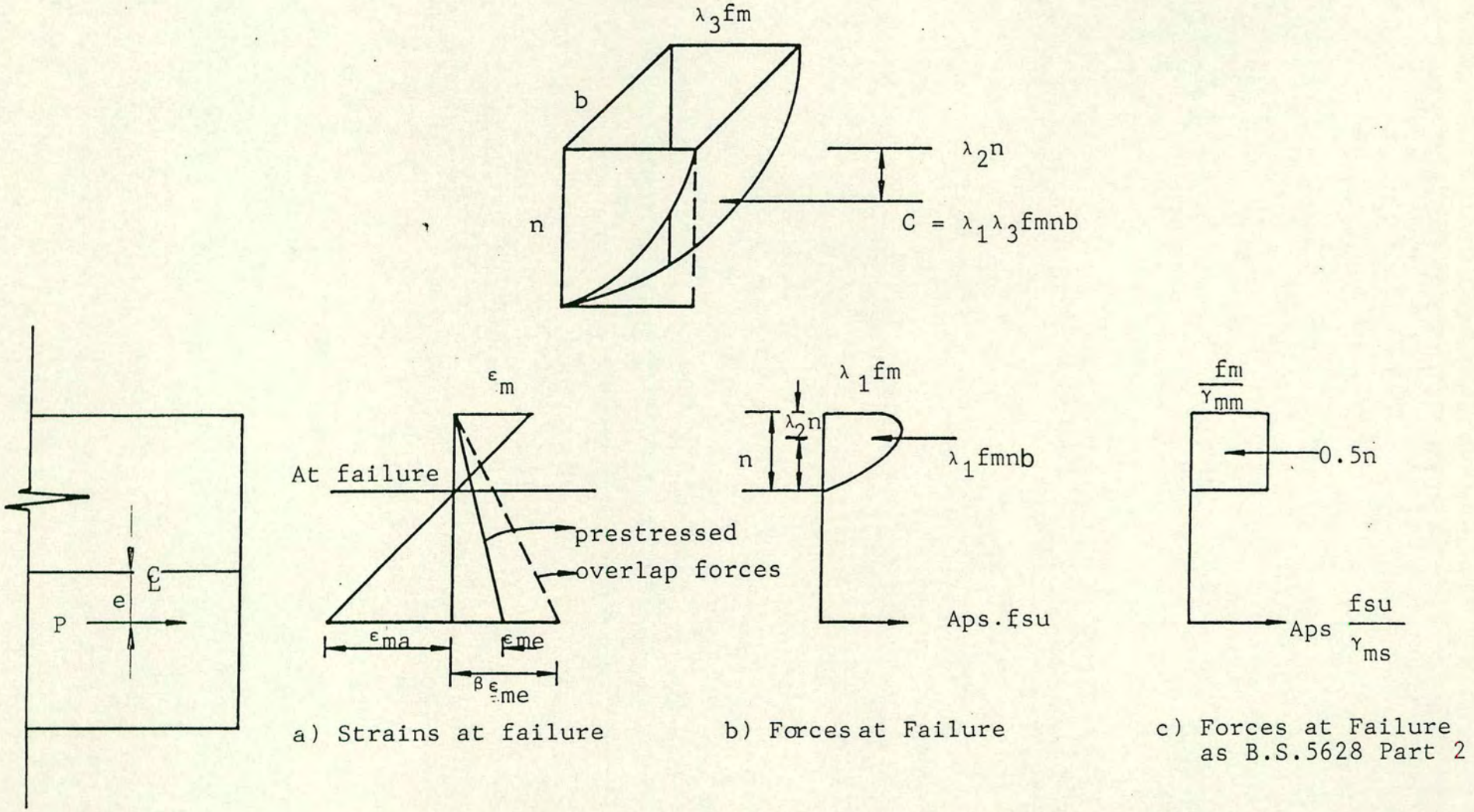

Figure 5.1 Conditions at failure in a prestressed brickwork wall

prestressed brickwork structures. Suter, Hendry and Sinha have shown that the shear strength of reinforced brickwork increases with decreasing shear span/effective depth ratio and increasing steel area (Suter and Hendry, 1975; Sinha, 1982). Pedreschi and Uduehi have carried out extensive tests on prestressed brickwork beams. (Pedreschi, 1983; Uduehi, 1989). Both authors have found that the shear strength of prestressed brickwork beams without shear reinforcement can be determined by the plastic theory as developed for reinforced concrete. The use of plastic theory assumes that the material exhibits a degree of ductility. Brickwork is not a ductile material, therefore an empirical factor, υ, called the effectiveness factor was introduced experimentally and applied to the compressive strength of the material. The ultimate load may be found by agreement between results obtained from lower bound and upper bound solutions. The upper bound assumes a failure mechanism. Then, equating the internal and external work done, the lower bound assumes a statically admissible stress distribution, and the corresponding load can be calculated. The proposed method is described in greater detail by the authors elsewhere. Roumani and Philpps have predicted a cracked shear formula for T- and I- sections based on the maximum tensile principal stress (Roumani, 1985; Phipps, 1986).

$$Vcr = \frac{Ib}{Ad_c}\sqrt{(f^2_{tf} + f_p f_{tf})}$$

where $0.25 < f_{tf} = (2.25 - a/d) < 1.25 N/mm^2$

and f_p = average compressive stress to prestress.

The authors assumed failure had occurred when cracks penetrated the compression flange.

$$Vu = \frac{Ib}{Ad_c}\sqrt{(f^2_{tf} + f_{pu}\, f_{tf})}$$

where $f_p < f_{pu} = (2.5f_p - f^2p) < 2f_p$

In prestressed brickwork walls, there are some factors which greatly reduce the intensity of the diagonal tensile stress. The first is the combination of the longitudinal compressive stresses caused by prestressing and the overlapping prestressing forces with the cross-section vertical shear stress. The second is where the bed joint runs perpendicular to the direction of the induced compressive stress. The majority of earth retaining structures (with triangular pressure distribution) are lightly reinforced and therefore subjected to flexural failure. All experimental results indicate a ductile flexural failure .

Test results show that the formula developed by B.S. 5628: Part 2 to predict the maximum shear strength for post-tensioned retaining walls is conservative.

5.3 YIELD LINE ANALYSIS

5.3.1 General

Post-tensioned brickwork pocket type retaining walls have a complex bi-axial bending behaviour in which the wall spans vertically from the base whilst the brickwork panels span horizontally between the pockets. Pocket type retaining walls contain several panels of brickwork spanning between pockets. Yield line analysis was employed to study the behaviour of the unreinforced panels spanning between the pockets. Haseltine and Moore stated that yield line analysis was the basis for the design of uniformly loaded brickwork panels to B.S.5628: Part 1 (Baker,

L.R., 1981). Baker, Tellett and Sinha have each stated that the yield line approach over-estimates the lateral wall strength (Baker, 1981; Tellett, 1984; Sinha, 1978). Sinha proposed a simplified method for the design based on fracture lines taking into account both strength and stiffness orthotropies (Sinha, 1978). Extending this argument, it was thought that yield line analysis could also be applied to the analysis of continuous brickwork panels subjected to in-plane prestressing forces and an out of plane hydrostatic pressure, i.e. "A triangular pressure distribution". Yield line theory is based on an ultimate load analysis. Two types of wall panels were considered. Firstly, the interior panels which arch between the pockets since the neighbouring panel provides a buttressing resistance. Secondly, the exterior panels which have a free end movement which provides the end pocket with sufficient in-plane stiffness to resist the arching forces (Tellett, 1984). The yield line conditions, governed by the yield line pattern for the panels, were assumed to be the following:-

a) Yield lines end at panel's boundary "wall pockets".

b) Yield lines are straight.

c) Yield lines produced pass through the intersection of the axes of rotation of adjacent panel elements.

Therefore, the boundary conditions' "axes" for the panels were assumed to be the following:-

a) For the interior panels, fixity at three sides and free at the top.

b) For the exterior panels, simple supports along three sides and free along the top.

The method of solution used is the equilibrium method which is described in greater detail elsewhere (Jones, L.L., 1965). The proposed method is

based on a study of the equilibrium of each element into which the panel is divided by the yield line. By equating the internal and the external moments and resolving the vertical forces, the equilibrium equation can be obtained. Along any yield line there are twisting moments and shear forces as well as the bending moments. Therefore, several alternative yield line patterns must be studied in order to find the most critical collapse mechanism. The most difficult task was deciding the values of the parameters μ and i especially under the influence of the prestressing forces and buttressing resistance on the unreinforced brickwork panels. A computer program was written to deal with the large number of iterative operations required to obtain the maximum moment that will cause panel failure. The program procedure is explained in the following steps:

1. The main program takes the following parameters as input: α, μ, ω and L.
2. The main program calls C root to calculate β from which moment 1E is calculated.
3. The main program calls EQ2E to calculate a_1, a_2, and a_3, the constants of the specified quadratic equation.
4. The main program calls quad to calculate the real roots of the quadratic equations and outputs the corresponding moments.
5. Steps 3 and 4 are repeated two more times for EQ3E and EQ4E.
6. Steps 2, 3, 4 and 5 are repeated for the interior panel equations.

5.3.2 Interior Panels

$$P = \frac{\omega h L}{14}$$

L = Panel Length

P = Load/unit length

ω = hydrostatic pressure (N/unit area/h)

Case 1 when $e > B_4$

A rectangular wall section, analysed in the orthotropical direction; simply supported on one side and fixed on the other two sides and subjected to hydrostatic pressure. If symmetry is assumed the unknown dimension βL determines the necessary pattern, therefore, two equilibrium equations are required.

Buttressing resistance and prestressing forces between the pockets can cause an even yield line mesh, therefore the nodel forces should be considered.

m_{be} is the bending moment

m_{te} is the twisting moment

Q_{Ab} is the nodel force acting in the angle ϕ at the free edge.

According to Jones(1961):

$$Qe = \pm (m_{be} \cot \phi + m_{te})$$

$$\therefore \quad Q_{Ab} = -(m_{be} \cot \phi + m_{te})$$

where $\cot \phi = -\beta/\alpha$ as shown in Fig. 5.2.

$$\therefore \quad Q_{Bb} = + (m_{be} \cot \phi + mt_e)$$

AND

$$m_b = \sum_{i=1}^{n} m_i \cos^2 \phi_i$$

$$m_t = \sum_{i=1}^{n} m_i \sin \phi_i \cos \phi_i$$

$$\therefore \quad m_{be} = m \cos^2 \frac{\pi}{2} + \mu m \cos^2 0 = \mu m$$

$$\therefore \quad m_{te} = m \sin \frac{\pi}{2} \cos \frac{\pi}{2} + \mu m \sin 0 \cos 0 = 0$$

If these values are substituted in the equation for Q_{Ab} we get

$$Q_{Ab} = - (\mu m) (-\frac{\beta}{\alpha}) = \frac{\beta \mu m}{\alpha}$$

AND $$Q_{Bb} = -\frac{\beta \mu m}{\alpha}$$

For area B and C

By taking moments about a f.

$$m\alpha L + im\alpha L - \beta \mu m/\alpha \times \beta L = P \times .82\beta L \times \frac{.82\beta L}{2}$$

$$+ 2P \times .485\beta L \times \frac{.485\beta}{2} + 4P \times .15\beta L \times \frac{.15\beta L}{2}$$

$$\therefore \quad m_1 = \frac{.616P\beta^2 L}{\alpha(1 + i)} - \frac{.616P\alpha L}{\mu}$$

For Area A

By taking moment about fG

$$2\mu m\beta L + 2\mu m\beta/\alpha \times \alpha L = P(L - 1.64\beta L)(.82\alpha L) +$$

$$2P(L-.97\beta L)(.485\alpha L + 4P(L-.3\beta L)(.15\alpha L)$$

$$\therefore \qquad m_2 = \frac{P\alpha L(2.39-2.46\beta)}{4\mu\beta}$$

when $m_1 = m_2$ we get

$$M_u = \frac{PL\alpha(2.39-2.46\beta)}{4\mu\beta} \qquad (11)$$

where $\beta = \sqrt[3]{\frac{2\alpha^2}{\mu}}$

CASE II when $B_4 > e > B_3$

This pattern, is also assumed to be symmetrical. Two equilibrium equations are required and these can be obtained by taking moments about a f for the equilibrium of element B, and about f9 for the equilibrium of element A. The nodal forces at e are all zero since the three yield lines are governed by the same mesh, and the nodal forces at e are both zero since m_{te} is zero and because the yield line meets the free edge at 90^o.

By taking moments about axis a f for the equilibrium of element B.

$$m\alpha L + im\alpha L = P \times \frac{.41L}{\beta} \times \frac{.41L}{2\beta} + 2P \times \frac{.2425L}{\beta} \times \frac{.2425L}{2\beta} + 4P \times \frac{.075L}{\beta} \times \frac{.075L}{2\beta}$$

$$m(\alpha L + i\alpha L) = .0841P\ L2/\beta 2 + .0588P\ L^2/\beta 2 + .0113P\ L^2/\beta 2$$

$$\therefore \qquad m_1 = \frac{.1542PL}{\beta^2\alpha(1+i)}$$

For Area A

$$\mu mL = P(L - .82L/\beta)(.82\alpha L) + 2P(L-.485L/\beta)(.485\alpha L)$$

$$+ 4P(L - .15L/\beta)(.15\alpha L)$$

$$\therefore \quad m_2 = \frac{P\alpha L}{\mu}\left[2.39 - \frac{1.233}{\beta}\right]$$

when $m_1 = m_2$ we get

$$m_u = \frac{P\alpha L}{\mu}\left[2.39 - \frac{1.233}{\beta}\right] \qquad (21)$$

where $\left[\frac{31\alpha^2}{\mu}\right]\beta^2 - \left[\frac{16\alpha^2}{\mu}\right]\beta - 1 = 0$

Case III when $B_3 > e > B_2$

For Area B

$$m\alpha L + im\alpha L = P(L/2)(L/4) + 2P\left[\frac{.2425L}{\beta}\right] x \frac{.2425L}{2\beta} + 4P \times \frac{.075L}{\beta} \times \frac{.075L}{2\beta}$$

$$\therefore \quad m(\alpha L + i\alpha L) = PL^2/8 + .0588PL^2/\beta 2 + .0113\, PL^2/\beta^2$$

$$\therefore \quad m_1 = \frac{.125PL + .07PL/\beta^2}{\alpha(1+i)}$$

For Area A

$$\mu mL = 2P(L - .485L/\beta)(.485\alpha L) + 4P(L- .15L/\beta)(.15\alpha L)$$

$$\therefore \qquad m_2 = \frac{P\alpha L(1.579-.561/\beta)}{\mu}$$

when $m_1 = m_2$ we get

$$m_u = \frac{PL\alpha\left[1.579 - \frac{.561}{\beta}\right]}{\mu} \qquad (3I)$$

where $$\left[1.79 - \frac{45.11\alpha^2}{\mu}\right]\beta^2 + \left[\frac{16\alpha^2}{\mu}\right]\beta + 1 = 0$$

Case IV when $B_2 > e > B_1$

For Area B

$$m\alpha L + im\alpha L = P(L/2)(L/4) + 2P(L/2)(L/4) + 4P \times \frac{.075L}{\beta} \times \frac{.075L}{2\beta}$$

$$\therefore \qquad m_1 = \frac{PL}{\alpha(1+i)}\left[.375 + \frac{.01125}{\beta^2}\right]$$

For Area A

$$\mu mL = 4P(L - .15L/\beta) \times .15\alpha L$$

$$m_2 = \frac{.51P\alpha L}{\mu\beta}$$

When $m_1 = m_2$ we get

$$m_u = \frac{PL}{2\alpha}\left[.375 + \frac{.01125}{\beta^2}\right] \qquad (4I)$$

where $(33.57)\beta^2 - \left[\frac{91\alpha^2}{\mu}\right]\beta + 1 = 0$

Exterior Panels

Case 1 when e > B_4

A rectangular wall section, analysed in an orthotropical direction, simply supported along three directions and free along the top. If symmetry is assumed the unknown dimension βL determines the necessary pattern, therefore two equilibrium equations are required.

Buttressing resistance and prestressing forces between the pockets can cause an even yield line mesh, therefore, the nodal forces should be considered.

$$Q_{Ab} = -Q_{Bb} = \mu m \, \beta/\alpha$$

For Area B

If moments are taken about a f for element B

$$m\alpha L - \mu m \, \beta/\alpha \times \beta L = P \times .82 \, \beta L \times$$

$$\frac{.82\beta L}{2} + 2P \times .485\beta L \times \frac{.485\beta L}{2} + 4P \times .15\beta L \times \frac{.15\beta L}{2}$$

$$\therefore \quad m_1 = \frac{.616P\beta^2 L}{\alpha} - \frac{.616PL\alpha}{\mu}$$

For Area A

$$2\mu m\beta L + 2\mu m\beta/_{\alpha} \times \alpha L = P(L - 1.64\beta L) \times .82\alpha L + 2P(L - .97\beta L) \times .485\alpha L + 4P(L - .3\beta L) \times .15\alpha L$$

$$\therefore \quad m_2 = \frac{P\alpha L(2.39 - 2.46\beta)}{4\mu\beta}$$

When $m_1 = m_2$ we get

$$m_u = \frac{P\alpha L(2.39 - 2.46\beta)}{4\mu\beta} \qquad (1E)$$

where $\beta = \sqrt[3]{\frac{\alpha^2}{\mu}}$

Case II when $\beta_4 > e > \beta_3$

If symmetry is assumed, two equilibrium equations are required. The nodal forces at e are all zero since the three yield lines are governed by the same mesh, and the nodal forces at e are both zero since m_{te} is zero and because the yield line meets the free edge at 90^o.

For Area B

$$m\alpha L = P \times \frac{.41L}{\beta} \times \frac{.41L}{2\beta} + 2P \times \frac{.2425L}{\beta} \times \frac{.2425L}{2\beta} + 4P \times \frac{.075L}{\beta} \times \frac{.075L}{2\beta}$$

$$\therefore \quad m_1 = \frac{.1542PL}{\beta^2\alpha}$$

For Area A

$$\mu mL = P(L - .82L/\beta)(.82\alpha L) + 2P(L - .485L/\beta) \times .485\alpha L + 4P(L - .15L/\beta)(.15\alpha L)$$

$$\therefore \quad m_2 = \frac{p\alpha L}{\mu}\left[2.39 - \frac{1.233}{\beta}\right]$$

when $m_1 = m_2$

$$\therefore \quad M_u = \frac{PL\alpha}{\mu}\left[2.39 - \frac{1.233}{\beta}\right] \qquad (2E)$$

where $\left[\frac{15.50\alpha^2}{\mu}\right]\beta^2 - \left[\frac{8\alpha^2}{\mu}\right]\beta - 1 = 0$

Case III when $\beta_3 > e > \beta_2$

For Area B

$$m\alpha L = P(L/2)(L/4) + 2P\left[\frac{.2425L}{\beta}\right] \times \left[\frac{.2425L}{2\beta}\right] + 4P \times \frac{.075L}{\beta} \times \frac{.075L}{2\beta}$$

$$\therefore \quad m_1 = \frac{PL}{\alpha}\left[.125 + \frac{.07}{\beta^2}\right]$$

For Area A

$$\mu mL = 2P(L - .485L/\beta)(.485\alpha L) + 4P(L - .15L/\beta) \times .15\alpha L$$

$$\therefore \quad m_2 = \frac{PL\alpha}{\mu}\left[1.579 - \frac{.561}{\beta}\right]$$

when $m_1 = m_2$

$$\therefore \quad M_u = \frac{PL\alpha}{\mu}\left[1.579 - \frac{.561}{\beta}\right] \qquad (3E)$$

where $\left[1.79 - \frac{22.56\alpha^2}{\mu}\right]\beta^2 + \left[\frac{8\alpha^2}{\mu}\right]\beta + 1 = 0$

Case IV when $\beta_2 > e > \beta_1$

For Area B

$$m\alpha L = P(L/2)(L/4) + 2P(L/2)(L/4) + 4P \times \frac{.075L}{\beta} \times \frac{.075L}{2\beta}$$

$$m_1 = \frac{PL}{\alpha}\left[.375 + \frac{.01125}{\beta^2}\right]$$

For Area A

$$\mu mL = 4P(L - .15L/\beta) \times .15\alpha L$$

$$m_2 = \frac{.51P\alpha L}{\mu\beta}$$

when $m_1 = m_2$ we get

$$M_u = \frac{PL}{\alpha}\left[.375 + \frac{.01125}{\beta^2}\right] \qquad (4E)$$

where $(33.33)\beta^2 - \left[\frac{45.33\alpha^2}{\mu}\right]\beta + 1 = 0$

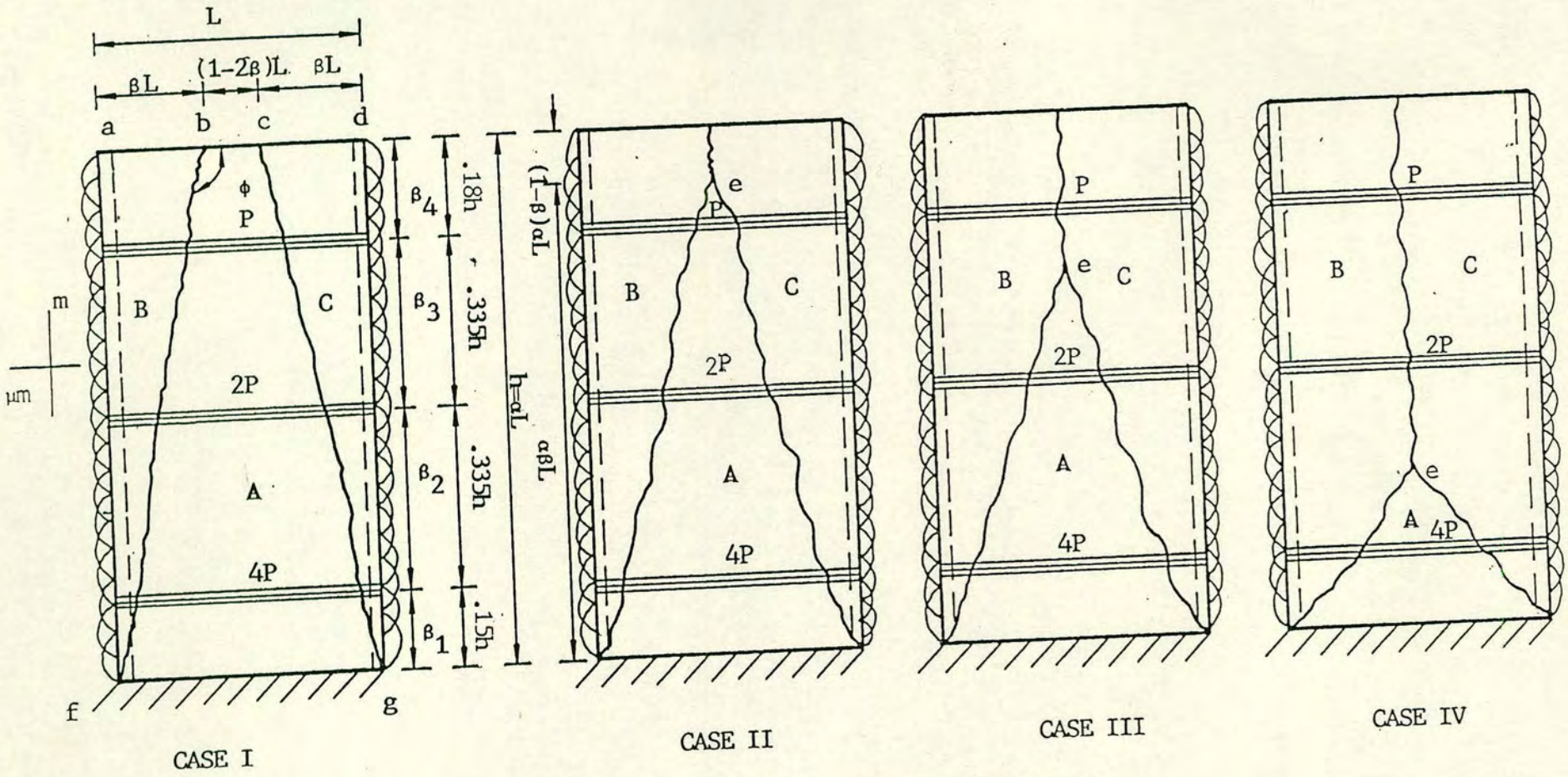

Figure 5.2 Interior Panels

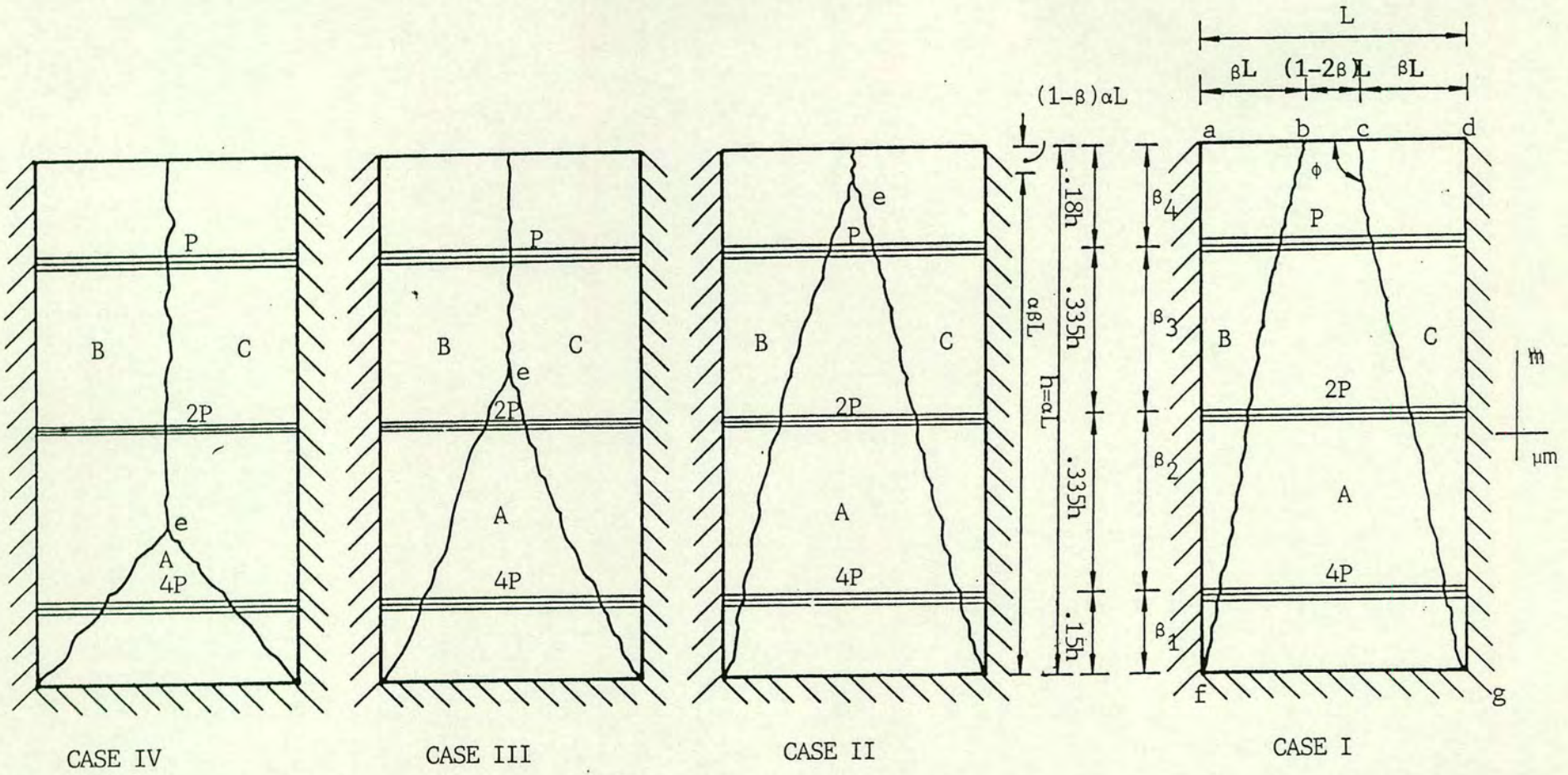

Figure 5.3 Exterior Panels

CHAPTER 6

EXPERIMENTAL RESULTS AND COMPARISON WITH THEORY

6.1 PRISMS

6.1.1 General

A post tensioned pocket-type retaining wall is a vertical retaining structure with pockets formed in the brickwork at a specified spacing along the cross-section as shown in Fig. 6.1.1. Prestressing anchorages are at an eccentric location equal to (t/6) from the centre line of the wall. The concrete infill is placed in the pockets after the prestressing load has been applied and the overlap dispersion forces are set. Under excessive loading, the state of stress at a certain part of the wall will be a combination of axial compression and bi-axial tension. The bi-axial tension is a result of the differential lateral strain between the mortar and the brick and may cause tensile failure. Therefore, it is necessary to study the behaviour of pocket-type masonry under direct stresses and estimate the dispersion angle under the bearing plate. The application of direct stresses over confined areas of masonry has been under study for some time. Several factors are of importance in determining the compressive strength and behaviour of the masonry. A considerable amount of experimental and theoretical work has been carried out on a range of masonry types using a variety of materials and testing procedures, and is reported elsewhere. (Page, A.W. et al., 1987; Malek, M.H., 1987; Ali, S., 1987; Rutherford, D.J., 1968; Page, A.W. and Hendry, A.W., 1988; Page, A.W. and Shrive, N.G., 1990; Arora, S.K., 1986; and Hendry, A.W., 1990).

The work carried out in this research project concentrates on studying the effect of a vertical concentrated eccentric load on open and concrete infill pocket brick masonry.

Six prisms were tested, three open pockets and three concrete infill, each prism consisting of six courses of brick. The prism dimensions were 215 x 550 x 440 mm. The formed pockets in the prisms and the bearing plate dimensions were 110 x 120 x 440 mm and 140 x 320 x 30 mm respectively. The loads were located at an eccentricity of (t/6) from the centre line of the cross-section and applied in convenient steps up to the cracking stage. Thereafter, the load was increased at a rate of 1 N/mm^2 per minute up to failure. For each prism, the strain was measured at approximately sixty positions using a mechanical dial gauge for at least five increments of loading as shown in Fig. 4.1. Three extra prisms, consisting of six courses, were loaded axially so that the cross-section was subjected to a uniformly distributed compressive load. The compressive strength and modulus of elasticity were calculated from the test results. Applying these results to the theoretical analysis, it was possible to predict the behaviour of pocket masonry up to failure and estimate approximately the load dispersion angle under the bearing plate for an eccentric concentrated load. The LUSAS computer package was used to analyse the behaviour of the concrete infill and no fill brickwork pocket prisms. The analysis was applied to three dimensional elements, each element consisting of 8 nodes and 24 degrees of freedom with three translations at each node.

6.1.2 Compressive Strength and Failure Mechanism

The compressive strength of masonry has been under investigation for a considerable period of time. When a concentrated load is applied to

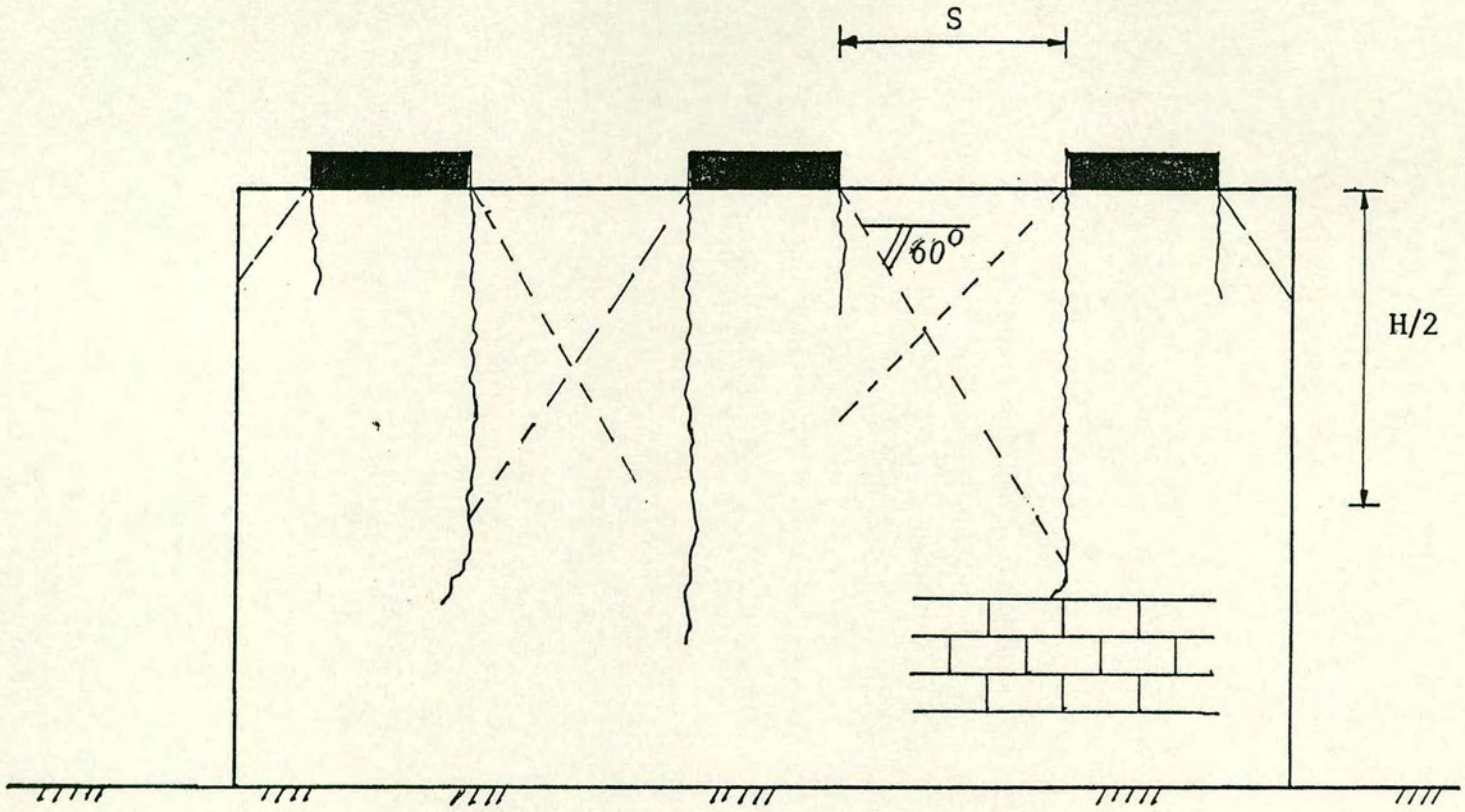

Figure 6.1.1 Failure of pocket type brick masonry subjected to vertical concentrated eccentric load

masonry, the compressive resistance of the masonry immediately under the load is greater than the (normal) compressive strength of the masonry under uniform loading. This phenomenon occurs due to a high local triaxial compressive stress state which is developed in this region, whereas at a zone further away from the load bearing plate the stress state changes to one of vertical compression and bi-axial tension. Since masonry is weak in tension, this zone will be critical and cracking will develop over the height of the specimen (Page et al, 1987; Page and Hendry, 1988).

In all, three open pocket prisms, i.e. pockets formed in the brickwork with no concrete infill, were tested . The contact stress under the bearing plate was considerably greater than the compressive strength of the prisms that were tested axially, as shown in Table 6.1 In all the open pocket prisms, high local triaxial compressive stresses were developed in the region directly beneath the bearing plate (see Figs. 6.1.4, 5). The area directly under the bearing plate was significantly influenced by planes of weakness due to the fact that masonry bearing strength depends on the degree of restraint supplied to the local highly stressed region by the surrounding material. All three prisms exhibited similar failure characteristics. Cracks first occurred at the corner edge of the pocket directly beneath the bearing plate. This crack commenced at a load of between 50 and 60 percent of the corresponding ultimate value. As the load was increased, the normal to the plane crack progressed into the courses beneath the direction of the mortar joints in a line normal with the loading plate. Further down the specimen, the stress state changed to one of vertical compression and bi-axial tension. Since masonry is weak in tension, after excessive load the transverse tensile stress became critical, a vertical crack developed over the full height of

the specimen until the specimen crushed. It was clear that the failure mode was directly influenced by the load dispersion under the bearing plate. The mode of failure was fundamentally different from solid masonry under concentrated load so that theories and design methods suitable for concentrated loads acting on solid masonry may not apply to open pocket masonry.

All the finite element transverse stress distribution results were in good agreement with the experimental results as shown in Figs. 6.1.4,5 . However, it can be seen that the finite element transverse stress distribution results were in smaller than the experimental results for the open pocket prisms. Both sets of results, however have similar slope gradient. This is perhaps due to the difficulty in obtaining experimental readings using a Demec mechanical dial gauge at the centre line under the bearing plate within the presence of an open pocket. The final vertical strain reading was taken at 70 per cent of the corresponding ultimate load. No horizontal strain measurements were taken after the cracking load.

In the concrete infill pocket prisms, the contact stress under the bearing plate was considerably higher than the compressive strength of axially loaded prisms. However, the total failure load was much less. This phenomenon occurs due to the following reasons:

i) The unloaded section of the prism restrains the lateral expansion of the area immediately under the bearing plate.

ii) In the area immediately under the bearing plate there are two different types of material, brickwork and concrete infill. Differences in values of deflection and Poisson's ratio results in the following :-

a) Under excessive load, the concrete infill acts as an in-plane solid concrete column dispersing the load under the bearing plate.

b) The area directly under the bearing plate is significantly influenced by the prism behaviour. Planes of weakness are caused by the fact that under excessive load, the infill grout and brickwork are partially apart. The masonry bearing strength depends on the degree of restraint supplied to the local highly stressed region by the surrounding material.

In all the concrete infill pocket prisms, high local triaxial compressive stresses were developed in the region directly beneath the bearing plate as shown in Fig. 6.1.7 . In the zone which is in line with the edge of the loading plate, however, where the tensile stress and shear stress are both a maximum, the state of stress changed to one of vertical compression and bi-axial tension. At loads between 60 and 75% of the corresponding ultimate value, a crack commenced and propagated vertically through the bricks and joints towards the loading plate before extending towards the specimen base where failure occurred. The crack in the concrete infill was observed much later than the crack in the brickwork zone, and was in line with the edge of the loading plate. This phenomenon occurred due to the following :-

i) At a zone which was several courses beneath the bearing plate cracks mainly occurred in the concrete infill near the centre of the prisms. In this case, the shear stress was zero and transverse tensile stresses controlled the whole cracking process.

ii) At a zone which was several courses down and in line with the edge of the bearing plate in the brickwork, the cracks occurred

away from the centre of the prism. In this case, transverse tensile stresses and the shear stress influenced the cracking process.

iii) The brickwork was weaker than the concrete at the zone where the tensile stress and shear stresss were a maximum. This is because the brick is only sufficiently strong to resist the axial compression, but bi-lateral tension, resulting from differential strain between the mortar and the brick and sometimes referred to as "bursting" stress, has caused a premature failure in the brittle brick.

It was clear that the mode of failure was comparable to solid masonry under concentrated load. Therefore, the theories and design methods applicable to concentrated loads on solid masonry may apply to concrete infill pocket masonry.

The finite element simulation results were in good agreement with the experimental results as shown in Fig. 6.1.7. The material model used was capable of predicting the initial cracking load, the ultimate load and the failure pattern with reasonable accuracy only in the two-dimensional analysis. A non-linear analysis for the behaviour of the prisms was made using an iterative incremental data run. Brickwork and grout material were modelled separately with provision for non-linear deformation characteristics. The deformation characteristics were determined from tests on individual mortar specimens and axially loaded six courses prisms as explained in section 5.1.2.

6.1.3 Stress Distribution

The in-plane prestressed anchorages in the pockets can cause overlap prestressed forces in the area beneath the loading plate. The stress

Prism	Type	Brick Strength N/mm^2	Mortar Strength N/mm^2 $1:\frac{1}{4}:3$	Grout Strength N/mm^2 $3:2\frac{1}{2}:2$	a/d Ratio	f_{crack}	$f_{bearing}$	$f_{uniaxial}$	Average N/mm^2	Ultimate Strain
1	6 course uniaxial loading	100	26	-	1.25	12.68	-	30.87	30	0.0025
2	6 course uniaxial loading	100	24	-	1.25	16.91	-	31.29		0.0027
3	6 course uniaxial loading	100	26	-	1.25	13.53	-	27.91		0.0025
4	6 course no fill t/6 loading	100	23	-	1.25	17.86	25.85	-	*32.86	0.0023
5	6 course no fill t/6 loading	100	25	-	1.25	11.16	22.84	-		0.0021
6	6 course no fill t/6 loading	100	24	-	1.25	11.16	20.85	-		0.0022
7	6 course concrete infill t/6 loading	100	27	26	1.25	17.86	30	-	31.88	0.0027
8	6 course concrete infill t/6 loading	100	24	28	1.25	24.55	33.50	-		0.0024
9	6 course concrete infill t/6 loading	100	25	29	1.25	17.86	32.14	-		0.0022

* Net Area

Table 6.1 Compressive Strength of Brickwork Prisms

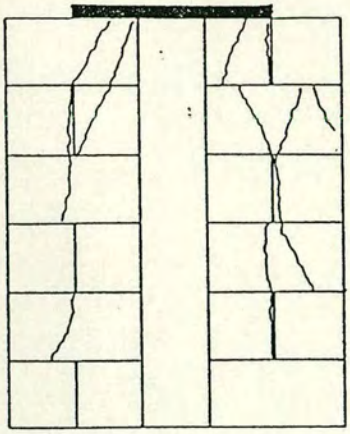

Crack @ 800kN
Failure @ 1158kN

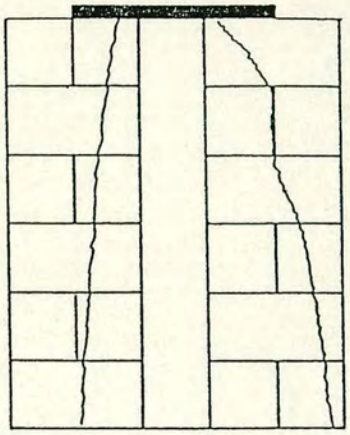

Crack @ 800kN
Failure @ 1345kN

Crack @ 500kN
Failure @ 1023kN

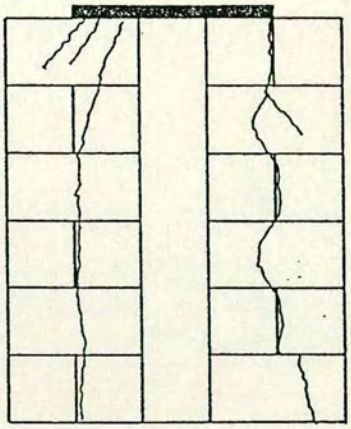

Crack @ 1100kN
Failure @ 1500kN

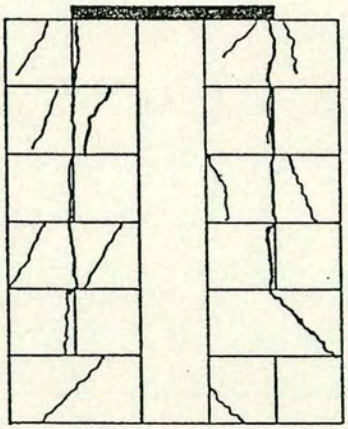

Crack @ 500kN
Failure @ 934kN

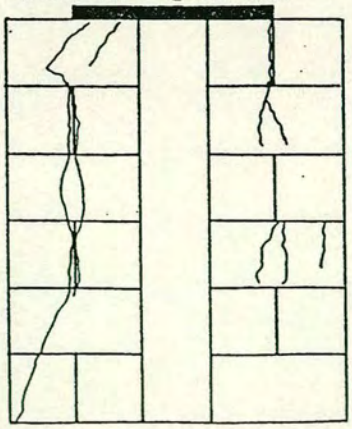

Open Pocket Prisms

Crack @ 800kN
Failure @ 1440kN

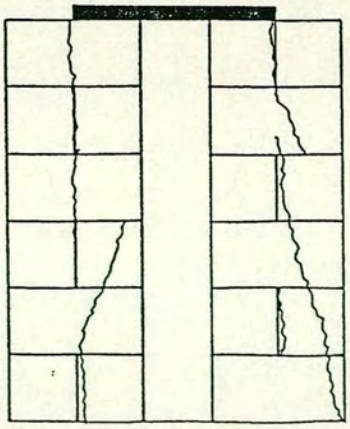

Concrete Infill Pocket Prisms

Figure 6.1.2 Failure of prisms subjected to vertical concentrated eccentric load

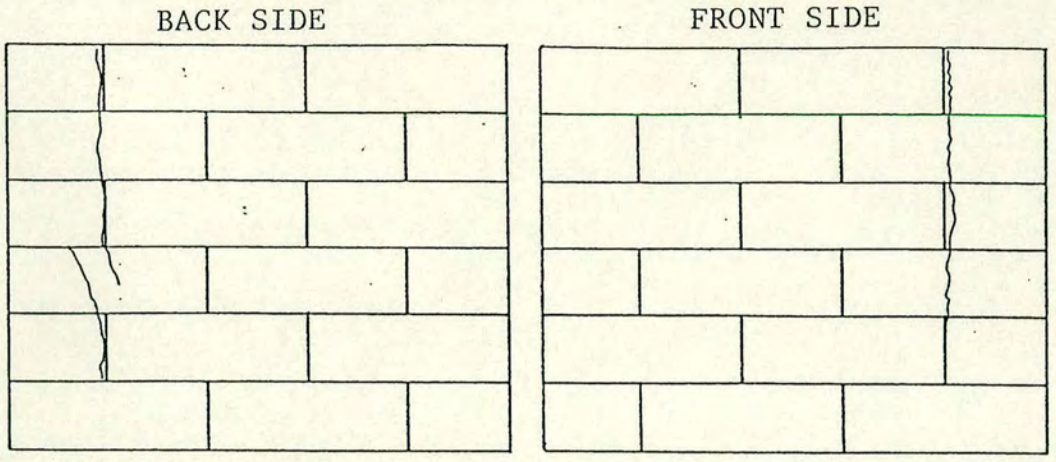

Crack @ 1500kN
Failure @ 3650kN

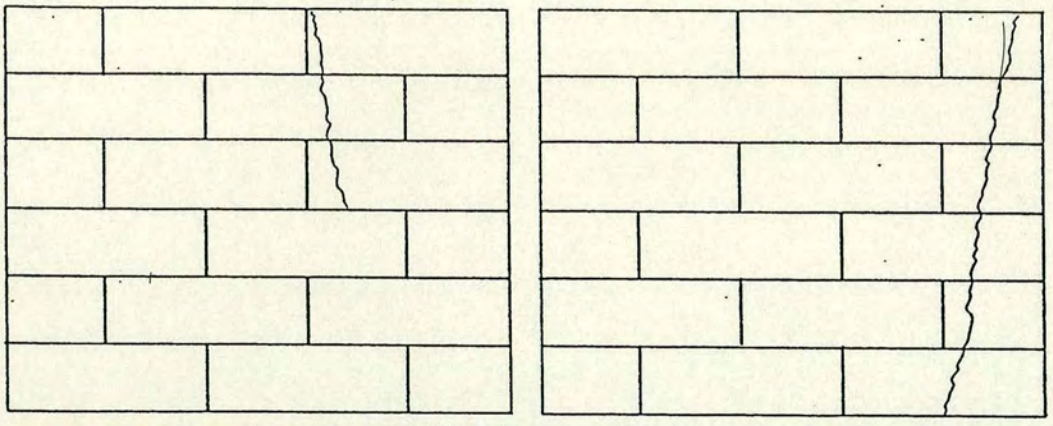

Crack @ 2000kN
Failure @ 3700kN

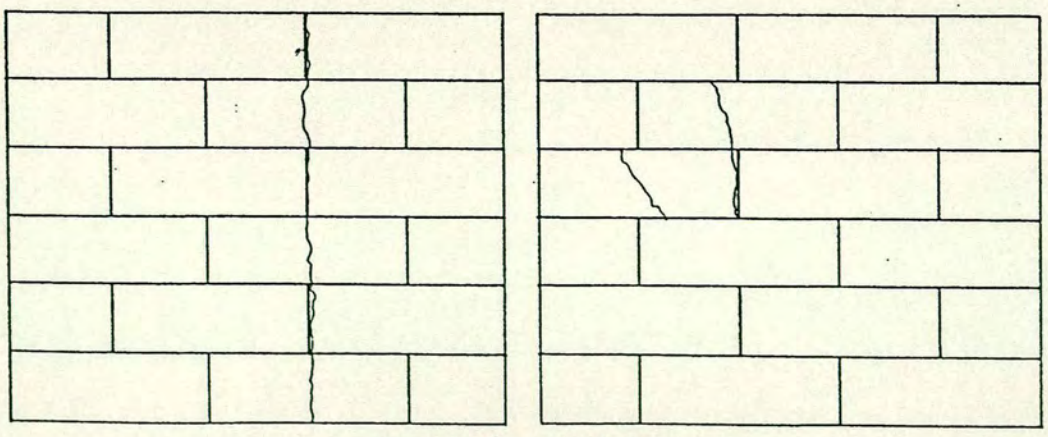

Crack @ 1600kN
Failure @ 3300kN

Figure 6.1.3 Failure of Solid Prisms subjected to Axial Load

condition will be one of vertical compression and bi-axial tension. If the load becomes excessive this zone of tensile stress will be critical. Vertical splitting of the wall will commence in an area several courses down in line with the edge of the bearing plate where the tensile stresss and shear stress are a maximum. The main objective of this work is to study the stress distribution of the concentrated force and the dispersion angle under the bearing plate and so predict a minimum value for the spacing of the wall pockets.

Most experimental and analytical studies to-date have been concerned with stress distributions caused by uniform vertical compression. In 1986, Arora carried out an experimental and theoretical study of the load dispersion in masonry walls subjected to a concentrated load (Arora, 1986). The research work was mainly concentrated on the performance of masonry walls under concentrated load. Several tests were made on 1.4 m high walls, constructed of both brick and block materials, and subjected to concentrated loads of varying magnitude, configuration and position. He concluded that the dispersion angle varied between 60^{o} and 80^{o} from the horizontal. In 1986 and 1987, both Malek and Ali respectively reported on the stress distributions in masonry under concentrated load.These results are given elsewhere (Malek, 1987; Ali, 1987). In 1990, Page and Shrive reported on the behaviour of face-shell bedded hollow concrete masonry subjected to in-plane concentrated loads. A total of 45 wallettes were subjected to either concentric or eccentric concentrated loads using various sizes of loading plates. The work concluded that the dispersion of the load from the bearing plate through the bond beam to the masonry below was approximately 30^{o} to the vertical or 60^{o} to the horizontal for one-course bond beams and 25^{o} to the vertical or 75^{o} to the horizontal for two-course beams.

In all six prisms, the strains were measured for a minimum of five increments of loading at approximately sixty locations using a mechanical dial gauge. After cracking, the load was increased at an approximate rate of 1.0 N/mm^2 per minute up to failure. The non-linear finite element analysis utilised data on the deformation characteristics and compressive strength obtained from tests on individual grout and mortar specimens and axially loaded solid brickwork six course prisms.

At each increment of loading, the stresses in the x and y directions were calculated. The load dispersion under the bearing plate was assumed to be a line joining the points of zero vertical stress. The respective dispersion angles under the bearing plate for open and concrete infill pocket prisms were 60 and 63 degrees to the horizontal experimentally and 57 and 61 degrees to the horizontal theoretically as shown in Figs. 6.1.8-11. These figures show that the experimental values of the vertical stress distribution were higher than the applied concentrated stress given by the bearing plate area. This is because the experimental vertical strain measurements were effected by the possible strain gradient. The finite element analysis predicted the dispersed load under the bearing plate for open and concrete infill pocket prisms with reasonable accuracy compared to the experimental results. From this theoretical and the experimental study the following was concluded:

1. The dispersion angle under the bearing plate for eccentric concentrated loading is at an angle of approximately 60^o to the horizontal.
2. The critical overlap forces zone is in line with the edge of the loading plate at a point where the tensile stress and shear stress are a maximum.

3. The minimum spacing between the pockets in post-tensioned brickwork retaining walls should be limited to $H/3$, where the panel length equals the distance between the centre lines of the formed pockets.

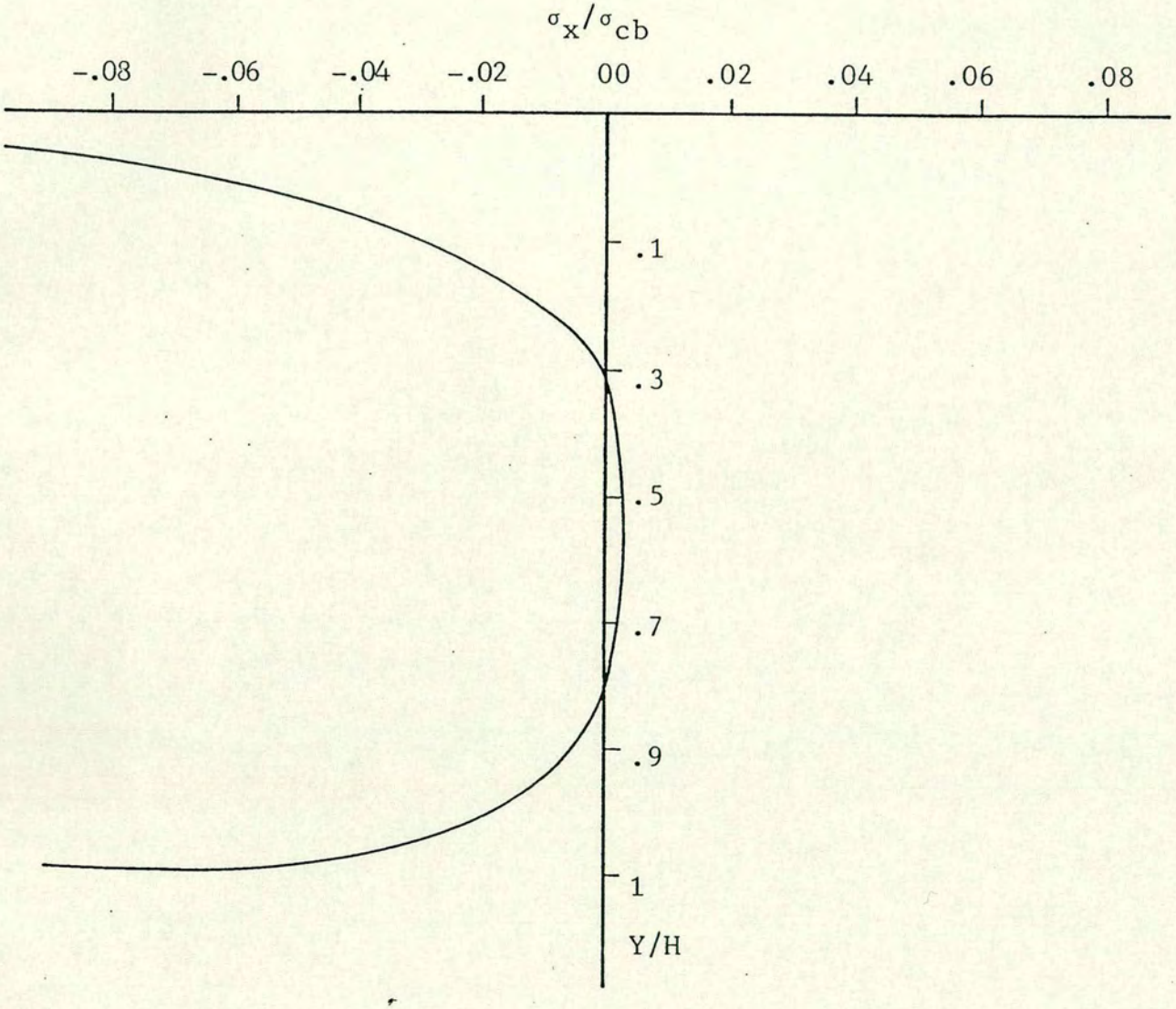

Figure 6.1.4 Transverse Stress Distribution
Elasto-plastic finite element analysis
(open pocket prisms)

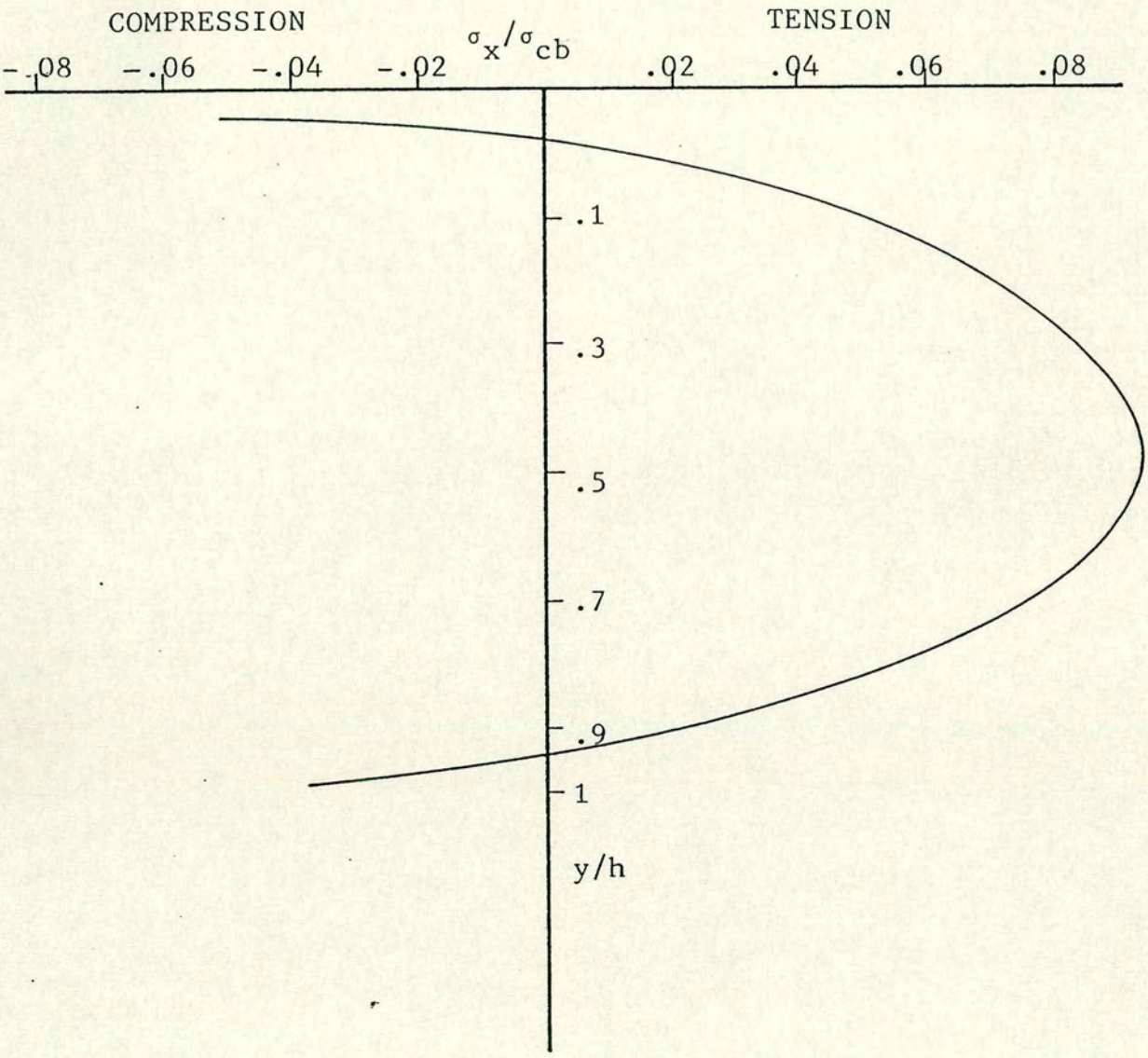

Figure 6.1.5 EXP. Transverse Stress Distribution
(Open pocket prisms)

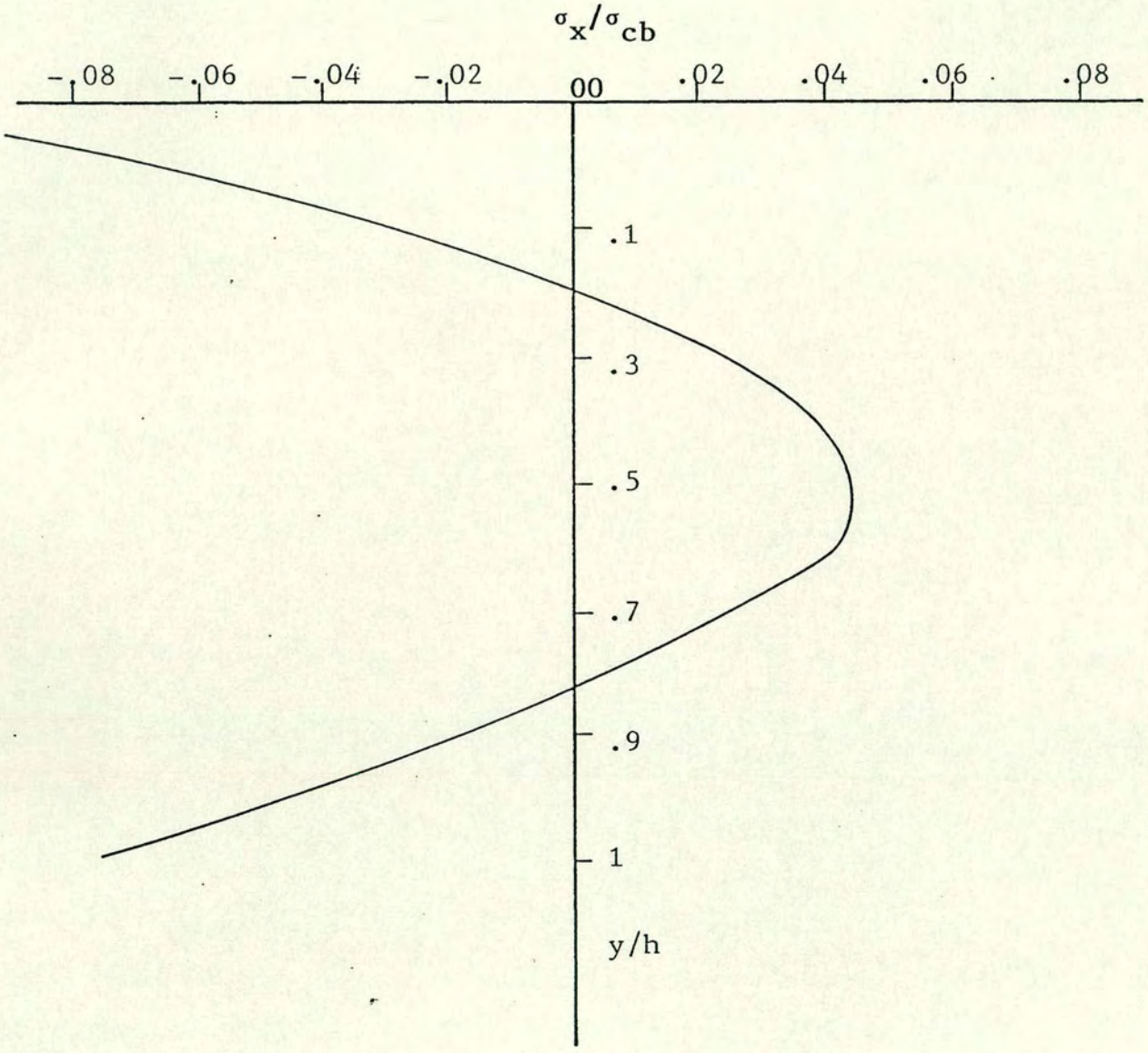

Figure 6.1.6 Transverse Stress Distribution
Elasto-plastic finite element analysis
(concrete infill pocket prisms)

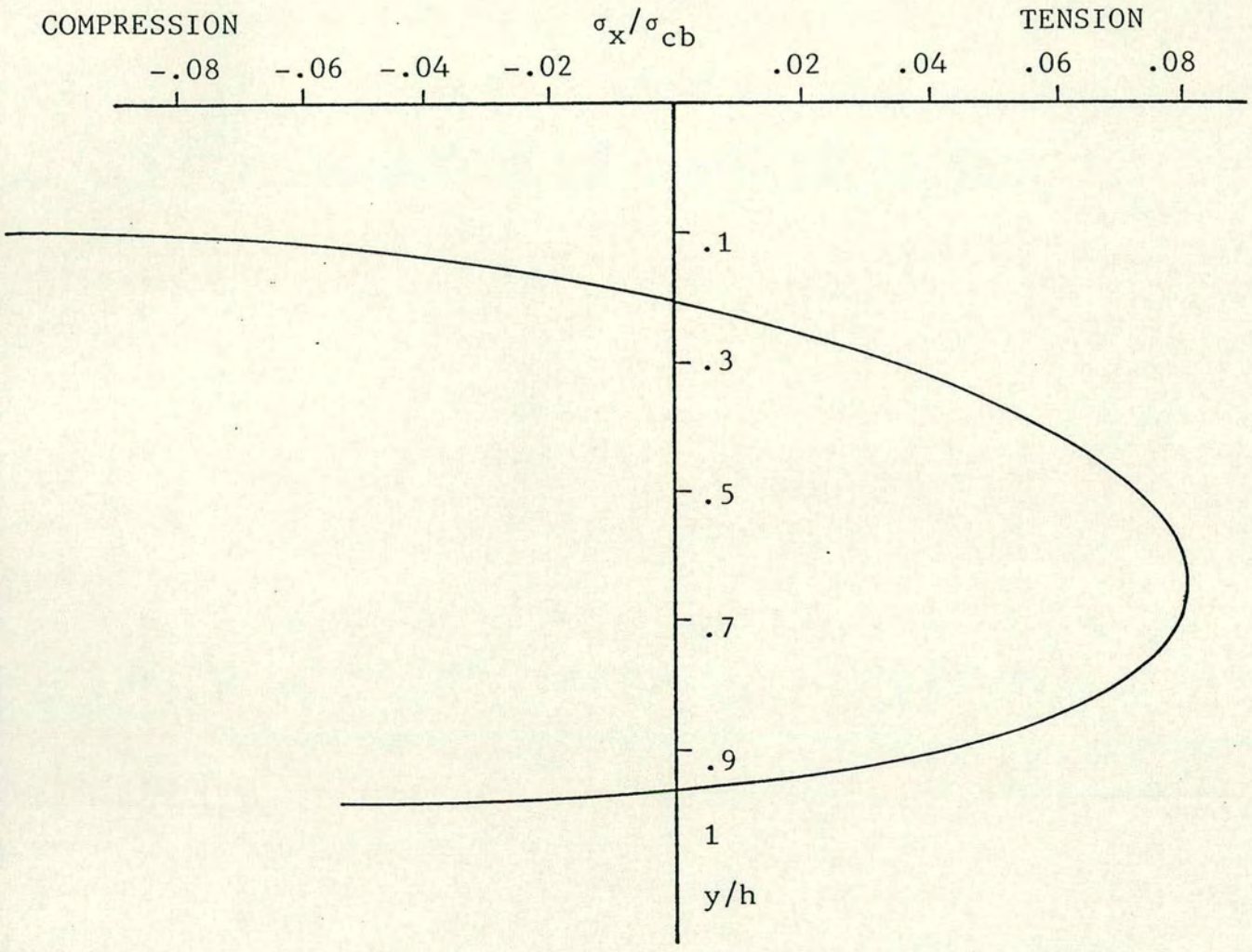

Figure 6.1.7 Exp. Transverse Stress Distribution
(concrete infill pocket prisms)

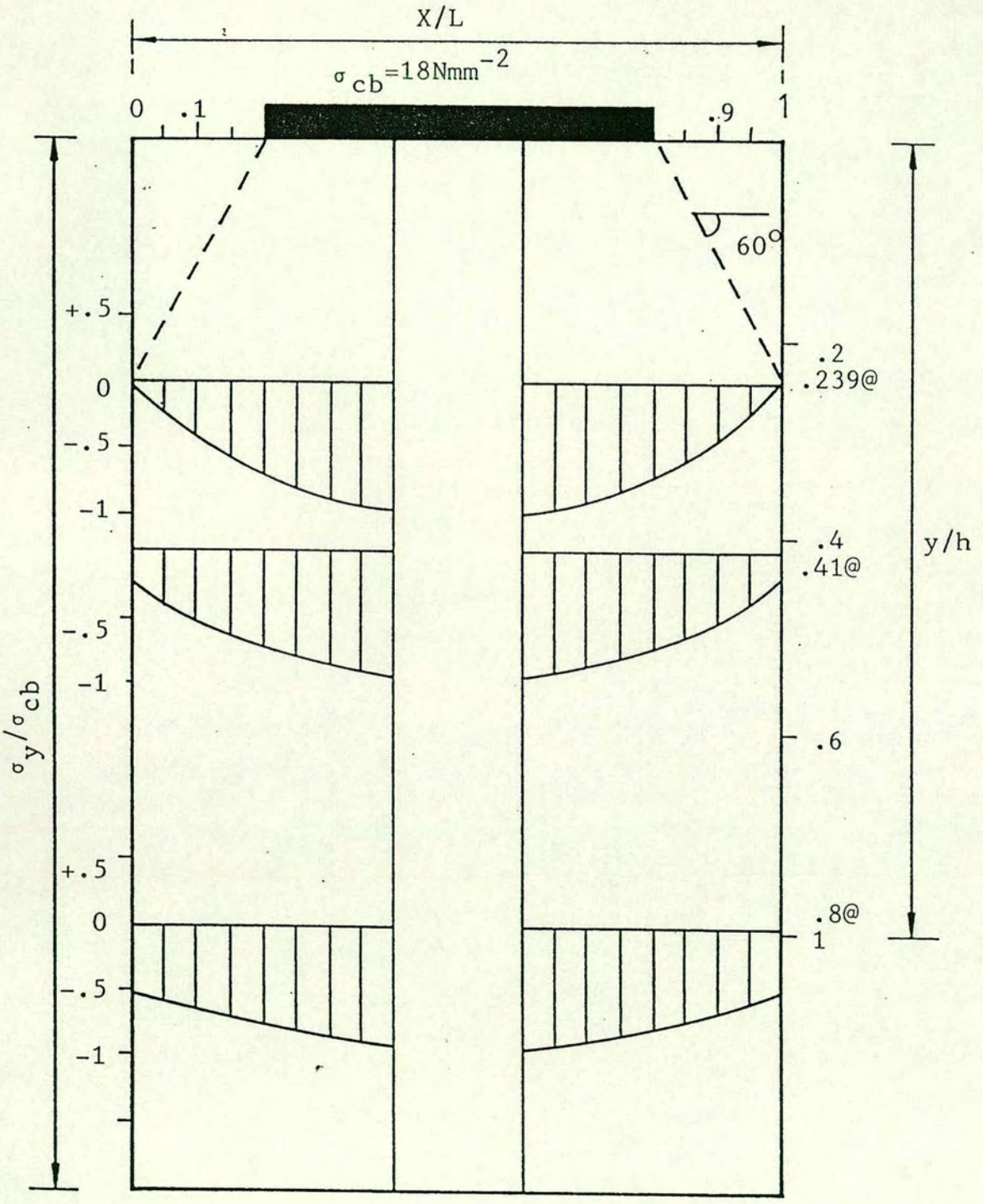

Figure 6.1.8 Experimental vertical stress distribution (open pocket prisms)

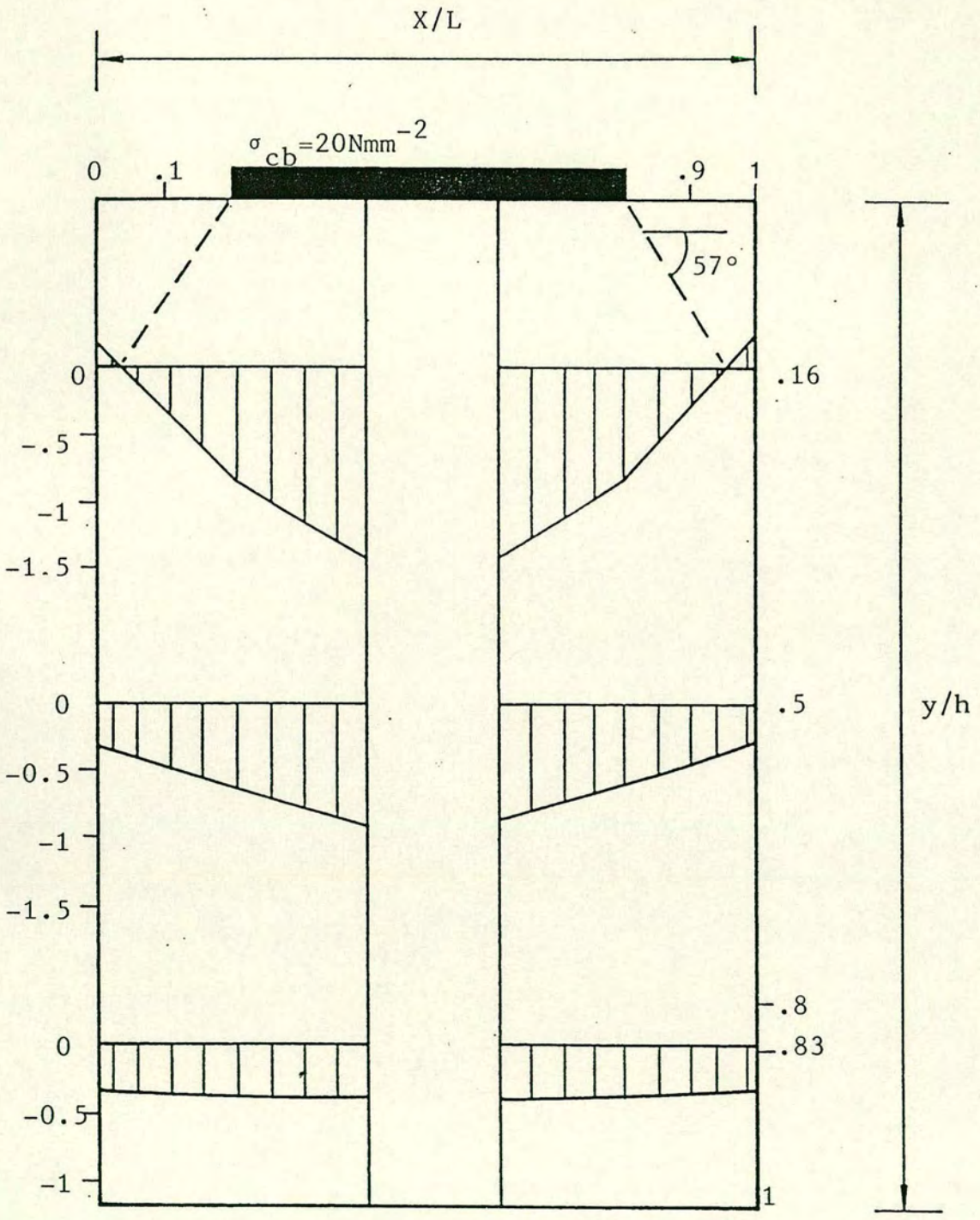

Figure 6.1.9 Elasto-Plastic Finite Element Analysis
(open pocket prisms)

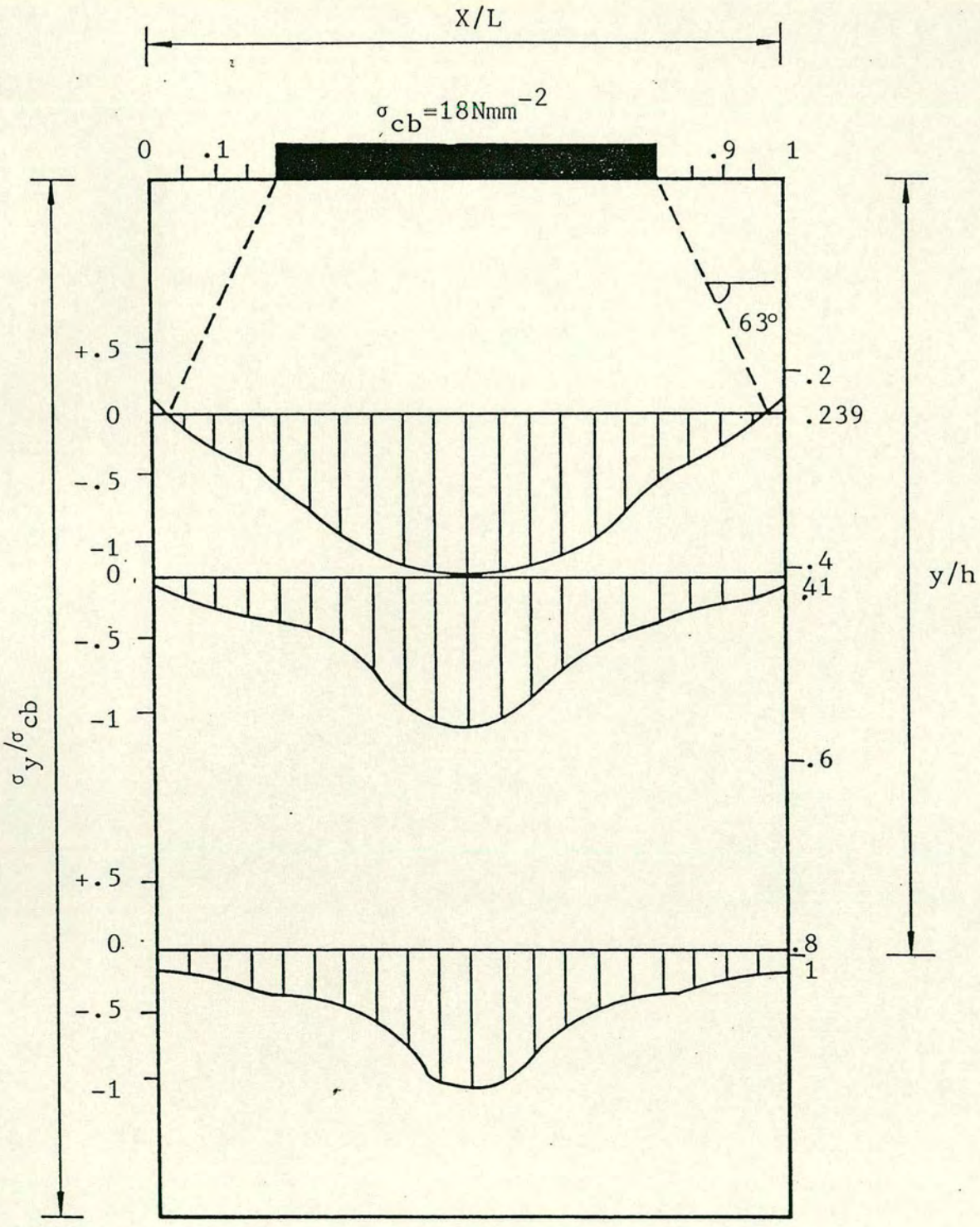

Figure 6.1.10 Experimental vertical stress distribution (concrete infill pocket prisms)

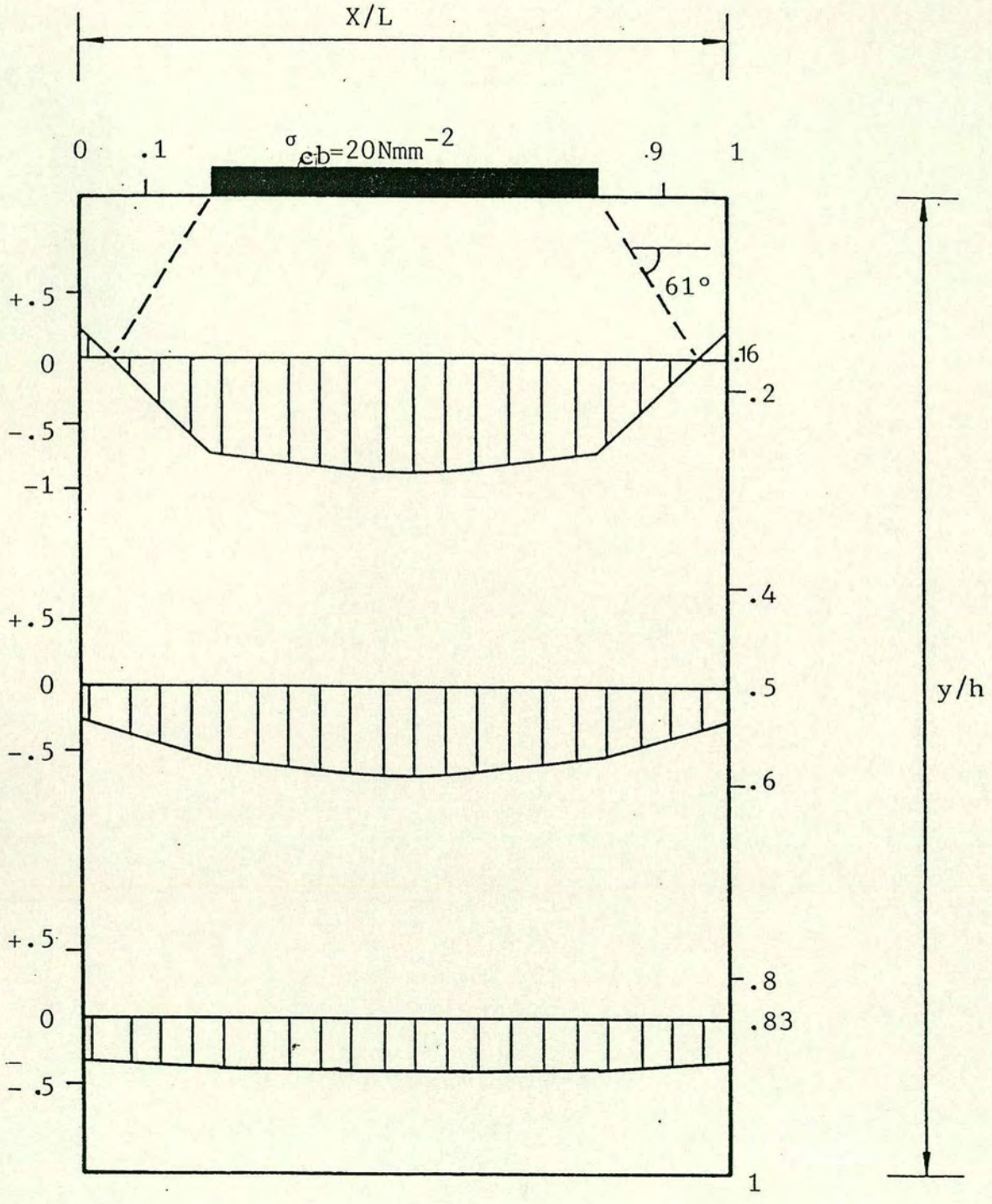

Figure 6.1.11 Elasto-plastic finite element analysis (concrete infill pocket prisms)

Figure 6.1.12 Typical failure mode and crack pattern for open pocket prisms

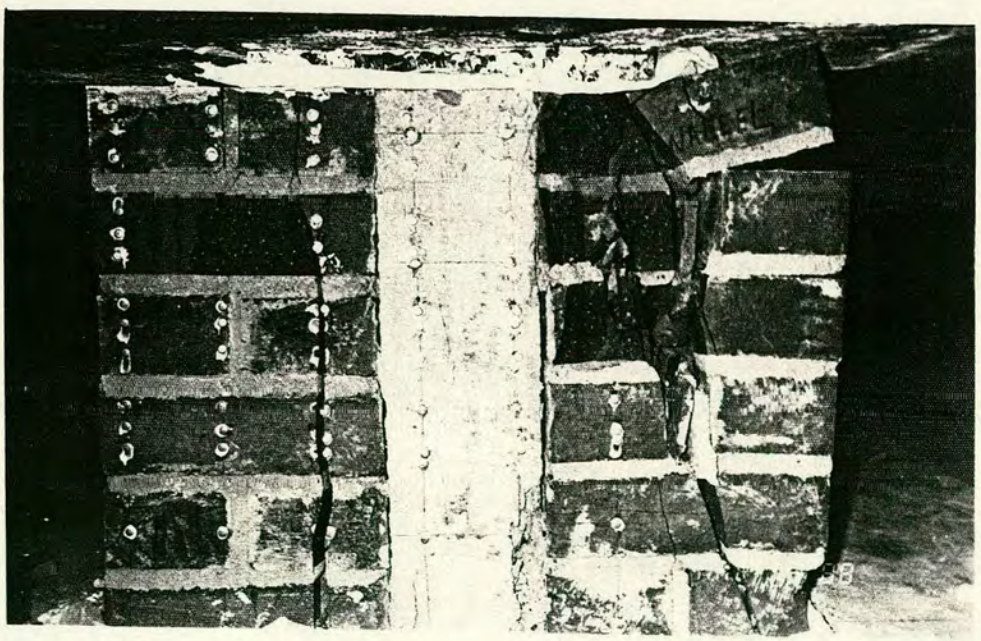

Figure 6.1.13 Typical failure mode and crack pattern for concrete infill pocket prisms

Figure 6.1.14 Typical failure mode and crack pattern for solid six course prism under axial loading

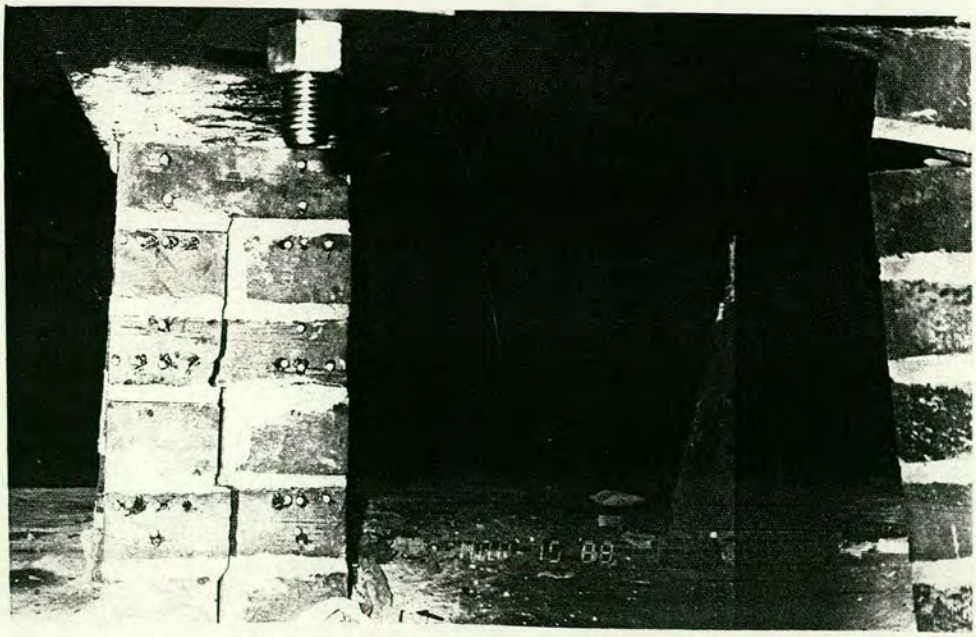

6.1.4 Summary and Conclusions

Overlap prestressing forces in post-tensioned pocket type brickwork retaining walls can cause vertical splitting of the wall due to the development of lateral tension. Six prisms were tested, three open pockets and three concrete infill, each consisting of six courses of brick. The strains in each prism were measured at approximately sixty positions using a mechanical dial gauge for at least five increments of loading. Testing was carried out on no fill pocket and concrete infill pocket prisms under eccentric concentrated load because during construction pouring the concrete infill into the wall pockets takes place after the prestressing load has been applied so that the overlap dispersed forces were already set. The experimental and theoretical analyses utilised the deformation characteristics and compressive strengths obtained from tests on individual grout and mortar specimens and three solid brickwork six course prisms subjected to a uniformly distributed compressive load. A 3-dimensional isoparametric solid element (HX8) was idealised for the open pocket and concrete infill pocket prisms, the model consisting of 96 elements. This discretisation was based on a balance between execution computer time and resultant accuracy. The analysis was applied to three dimensional isoparametric solid elements, each element consisting of 8 nodes and 24 degrees of freedom, with three translations at each node. The concrete infill and brickwork were modelled as elasto-plastic von Mises yield surface models. The geometrically and materially non-linear finite element analysis was capable of predicting the dispersed load under the bearing plate, the initial cracking load and the structural behaviour up to failure. The simulations were reasonably accurate in comparison with the experimental results. The following conclusions can be summarised from the theoretical and the experimental analyses:-

1. The failure mode for open pocket prisms was fundamentally different from that for solid masonry subjected to a concentrated load. Therefore, the theories and design methods applicable to concentrated loading on solid masonry may not apply to open pocket brick masonry.
2. The failure mode for concrete infill pocket prisms was similar to that for solid masonry subjected to concentrated load, so that the theories and design methods applicable to concentrated loading on solid masonry may apply to concrete infill pocket brick masonry.
3. The dispersion angle under the bearing plate, for eccentric concentrated loading on open pocket and concrete infill brick masonry is at approximately 60 degrees to the horizontal.
4. The minimum spacing between pockets in prestressed brickwork retaining walls should be limited to $H/3$ where the panel length equals the distance between the centre lines of the formed pockets.
5. A standard package, LUSAS, can be used successfully to simulate the behaviour of brickwork masonry structures subjected to an eccentric concentrated load. It is capable of predicting the initial cracking load and the structural behaviour up to failure. Experience with the package, serviceability and implementation is a requisite to achieving results of acceptable accuracy.

6.2 Beams

6.2.1 General

Brickwork walls may be built in several ways to produce a satisfactory bond and the type of bond used may be important from an architectural or historic point of view. Brickwork retaining walls are usually constructed without the need for external finishing. The commercial

brickwork wall bonds which require consideration are shown in Fig. 6.2.1

These bonds vary in appearance, producing characteristic 'textures' in the wall surface. A particular bond may be selected for its surface pattern rather than for its strength properties. The two bonds most commonly used for walls are English bond and Flemish bond. The type of bond selected for this project was conditioned by the following factors:-

i) Effective utilisation of as many bricks as possible in the cross-section.

ii) Construction Workability.

iii) Grouting Control.

iv) Architectural features.

v) Cost consideration.

Eight brickwork beams were fabricated and tested in the laboratory. The beams were tested using a two point loading arrangement applicable to a retaining wall situation as shown in Fig. 4.3 as it provides a region of a maximum shear and maximum moment at a certain point as well as a region of constant moment thus isolating flexure within this region. The region of constant moment provides data on pure flexural behaviour of the beam. This arrangement can provide information on the behaviour of post-tensioned brickwork pocket type slabs.

The load was applied in increments of about 7% of the expected ultimate load. The beams were loaded until the applied load was just less than that calculated to produce a flexural crack. The beams were then totally unloaded whereupon a 95% recovery of deflection was acheived. The beams were then reloaded to a stage where the crack width was approximately 0.20 mm, and then the beams were totally unloaded. The

recovery of deflection on unloading after cracking was 90% and the cracks closed completely. The beams were then reloaded up to ultimate failure. Measurements of deflection and cracking were recorded at each increment of loading.

The nominal descriptions and dimensions of the beams were as follows:-

i) Two beams, B_1 and B_2, were fabricated using Flemish bond. Alternative header and stretcher bricks in each course and the most common traditional bond were used. Although not as strong as English bond, Flemish bond was considered visually more satisfactory Fig. 4.4. The beams were built horizontally so that the joints run parallel to the direction of the prestressing load following the procedure used in previous studies. It was therefore possible to compare the performance of walls built using Flemish bond with those using English bond. The nominal dimensions of the beams were 215 x 365 x 6200 mm, with an average weight of 1.4 kN/m.

ii) Two beams, B_3 and B_4, were fabricated using English bond. This bond incorporates both headers and stretchers arranged with a header placed centrally over each stretcher in the course below in order to achieve a bond and minimise the number of straight joints Fig. 6.2.4 . The bond layers were therefore entirely free from straight joints. This type of bond is often found on early brick structures of the Tudor period.

Beams B_3 to B_8 were built standing vertically so that the bed joints run perpendicular to the direction of the induced prestressing load, as this arrangment is applicable to retaining wall situations in which they were built standing vertically. The nominal dimensions

of these beams were 215 x 110 x 3000 mm with an average weight of 1.8kN/m.

iii) Two beams, B_5 and B_6, were fabricated using Flemish garden bond with one header to three or five stretchers in each course. This bond is designed to minimise the number of headers in each layer, thus simplifying the task of selecting headers of uniform length. Where the headers pass through the thickness of the wall, a fair face can be obtained only with great difficulty Fig. 6.2.3.

iv) Two beams, B_7 and B_8 were fabricated using English garden bond with one course of headers to three or five courses of stretchers. This bond is sometimes used to improve the face appearance by the introduction of snap headers Fig. 6.2.5.

In this thesis, an experimental and theoretical study has been carried out to study the influences of bonding patterns of brickwork on the performance of the beams. The beams were analysed for the following parameters:-

(1) Ultimate moment.
(2) Steel strain and moment relationship.
(3) Top fibre strain and moment relationship.
(4) Moment-curvature.
(5) Load-deflection.
(6) Cracking moment, width and spacing.
(7) Neutral axis depth and moment relationship.
(8) Failure mechanism.

The theoretical investigation was carried out using a stress block analysis, a direct method of analysis and a finite element analysis. The

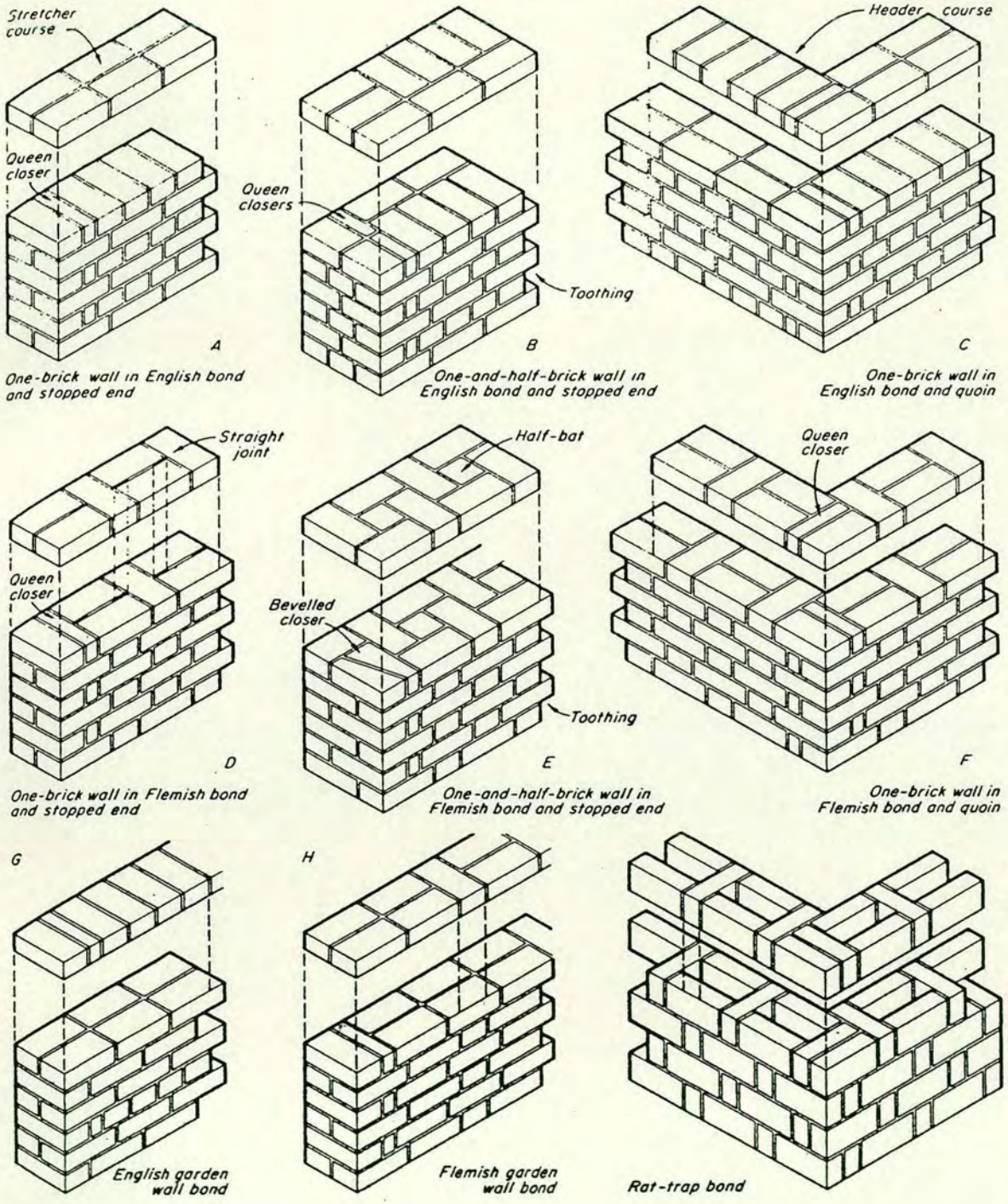

Figure 6.2.1 Types of Wall Bonds

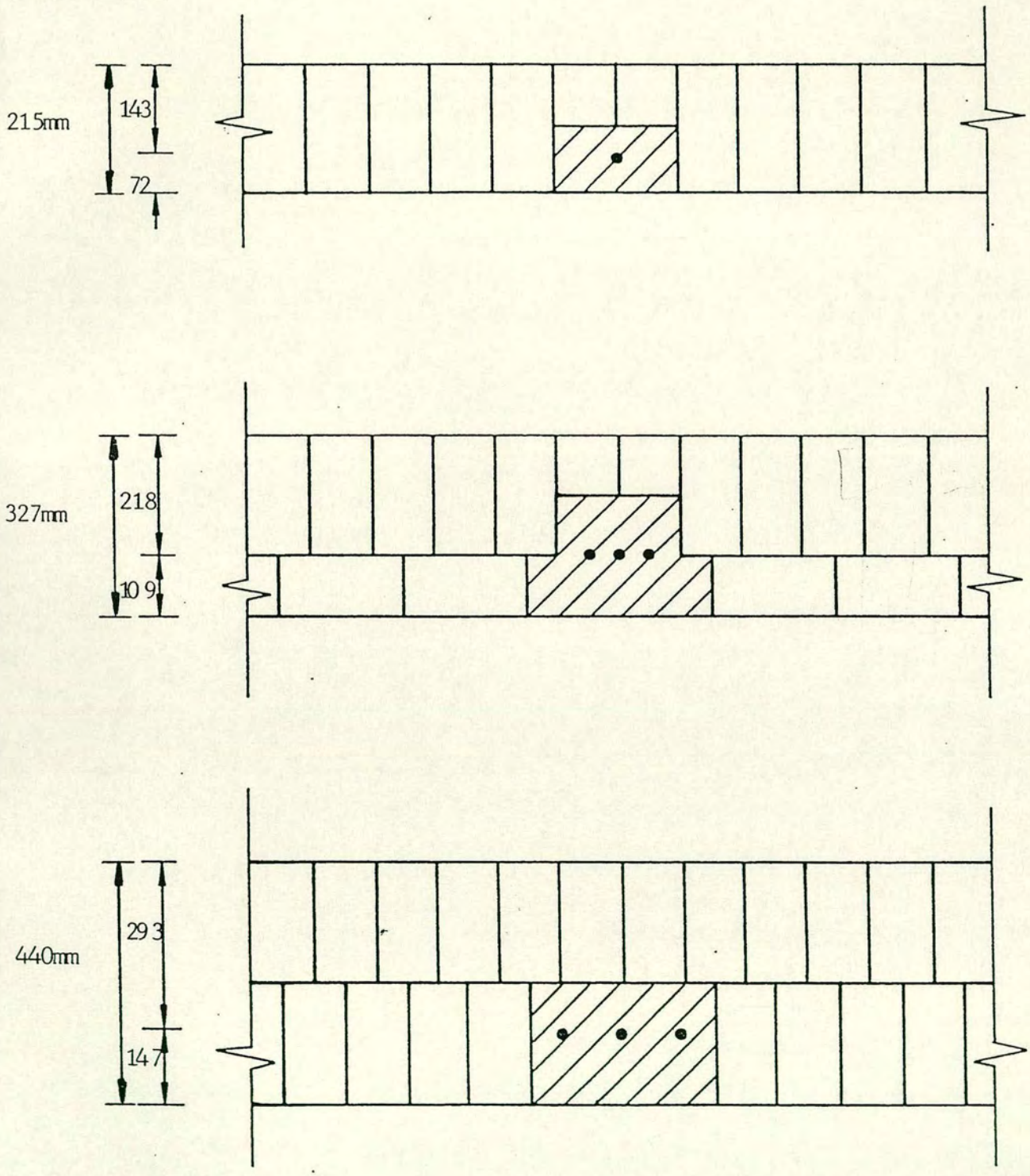

Figure 6.2.2 Types of pocket retaining walls

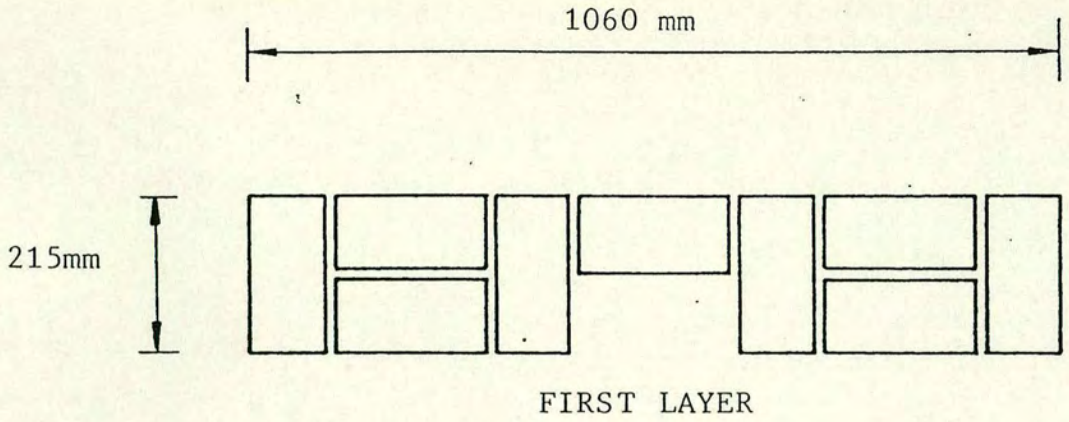

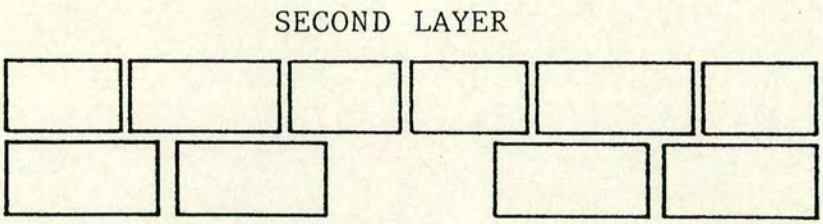

Figure 6.2.3 Flemish Garden bond beams cross-sections (B5-B6)
(constructed in vertical position)

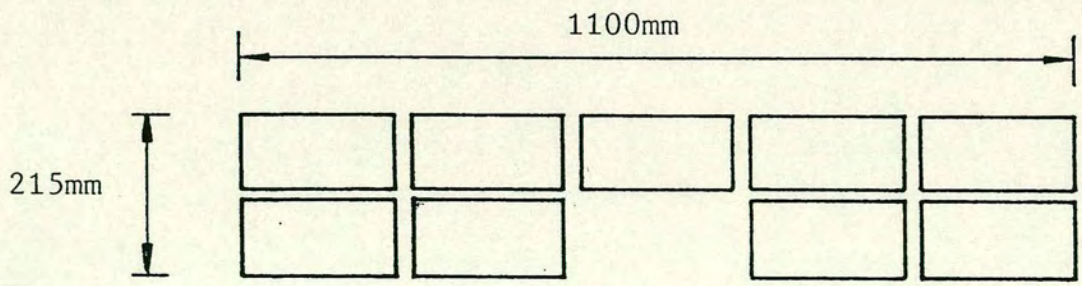

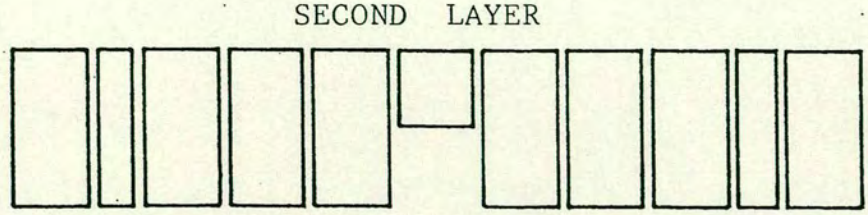

Figure 6.2.4 English bond beams cross-sections (B3-B4)
(constructed in vertical position)

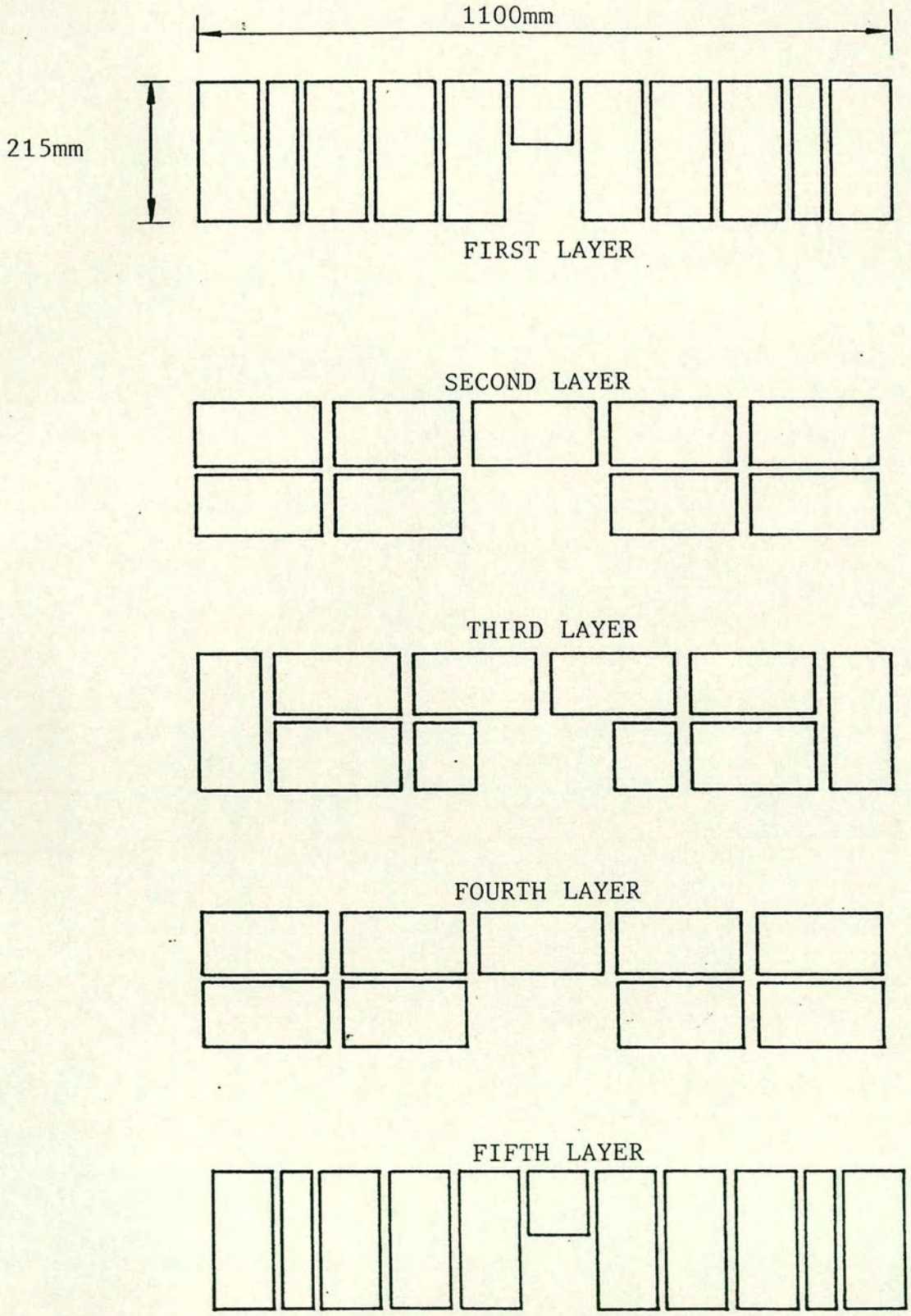

Figure 6.2.5 English Garden bond beams cross-sections (B7-B8)
(constructed in vertical position)

stress block analysis was based on the derivation of the theoretical moment assuming a simplified cubic parabolic stress/strain relationship for brickwork in the compression zone. The direct method of analysis was originally used for prestressed concrete and lately for prestressed brickwork beams (Pedreschi, 1983). This method utilises the actual stress/strain relationships of the composite material for prestressed brickwork beams to predict the moment-curvature relationship from the prestressing stage to ultimate load (see Appendix C). The finite element analysis was carried out using a model consisting of 290 elements. The discretisation achieved a balance between execution computer time and resultant accuracy. The geometrical and material three dimensional non-linear analysis model was accommodated by semiloof shell elements. The material model is capable of modelling a non-linear bi-axial concrete material. The material model was used for both the concrete infill and the brickwork beam.

6.2.2 Ultimate Moment

Due to the application of an eccentric prestress, the beam section was subjected to axial stress and a hogging moment. When the service load was applied, decompression of the prestressing force occurred, tensile stresses developed and flexural cracking took place. A crack progressed up through the section until failure occurred. Table 6.2 gives details of the material properties, effective prestressing force and the experimental ultimate moment of the beams . Finite element and direct method analyses were based on deformation characteristics and values of compressive strength obtained from tests on individual grout specimen, mortar specimen and five single course prisms. According to B.S. 5628, the method used was based on values of the characteristic compressive strength from the code and a brickwork compressive strain of 0.0035.

The reinforcement properties were obtained from the idealised stress/strain relationship for reinforcement shown in Fig. 3.5.

Pedreschi used English bond brickwork beams, the properties of which are given in Table 6.3 and are similar to the properties of the author's Flemish Bond beams, B_1 and B_2. Both types of beam sections were built horizontally, so that the joints run parallel to the direction of the prestressing load. It is therefore possible to compare the effect of bond on the beam's behaviour. The average experimental ultimate moment for the English bond beams is 57.87 kNm ; the average experimental ultimate moment for the Flemish bond beams,(B_1 and B_2) is 41.56kNm; that is approximately 30% difference between the two types of beam. Comparing the predicted ultimate moment for B_1 and B_2 using the Direct method, (i.e. B.S. 5628 when $\alpha_{mm} = 1$, and $\alpha_{ms} = 1$ also when $\alpha_{mm} = 2$ and $\alpha_{ms} = 1.15$, B.S.5628 using the author's prisms when $\alpha_{mm} = 1$ and $\alpha_{ms} = 1$ also when $\alpha_{mm} = 2$ and $\alpha_{ms} = 1.15$) with the experimental results; the predicted ultimate moments were 20% greater, 27% greater, 0%, 25% greater and 12% less than the experimental average ultimate moment respectively. On the basis of the experimental results, the flexural strength of the Flemish bond beam was less than that of the English bond beam when the beam bed joints runs parallel to the direction of the induced compressive stress.

In the case of beams B_3 - B_8, where the bed joint runs perpendicular to the direction of the induced compressive stress, Table 6.4 shows that the ultimate moments of the (B_3 - B_8) English, Flemish Garden and English Garden bond beams are all of the same magnitude. Also, these experimental moments compare satisfactorily with the ultimate moments predicted by both the direct method and the finite element analysis. The

Beam	Type	Brick Strength N/mm^2	Mortar Strength N/mm^2	Grout Strength N/mm^2	Span m	a/d Ratio	% Steel	Effective Prestress kN	Ultimate Moment kNm	Shear Stress N/mm^2	Failure Mode
1	Flemish Bond	100	27.60	27.50	6.20	11.17	0.274	134	46.33	0.32	Tension
2	Flemish Bond	100	26.80	29.50	6.20	11.17	0.274	134	36.79	0.26	Tension
3	English Bond	100	24.60	20.00	2300	5.60	0.183	240	52	0.41	Tension
4	English Bond	100	22.70	22.40	2300	5.60	0.183	240	66.4	0.59	Tension
5	Flemish Garden	100	25.20	29.90	2300	5.60	0.19	240	69.60	0.53	Tension
6	Flemish Garden	100	21.90	26.50	2300	5.60	0.19	240	68	0.50	Tension
7	English Garden	100	30.55	28.0	2300	5.60	0.183	240	72	0.57	Tension
8	English Garden	100	26.00	27.50	23000	5.60	0.183	240	68	0.54	Tension

Table 6.2 Summary of Experimental Results

Beam	Type	Brick Strength N/mm^2	Mortar Strength N/mm^2	Grout Strength N/mm^2	Span m	a/d Ratio	% Steel	Effective Prestress kN	Ultimate Moment kNm	Shear Stress N/mm^2	Failure Mode	Work Done
B1	English	88	15.80	17.80	6.20	11.21	0.274	133	52.9	0.440	Tension	Pedreschi
B2	English	88	15.80	17.80	6.20	11.21	0.274	115	56.4	0.428	Shear	Pedreschi
B3	English	88	15.80	6.20	6.20	11.21	0.274	133	61.50	0.476	Tension	Pedreschi
B4	English	88	20.80	6.20	6.20	11.21	0.274	144	58.40	0.448	Tension	Pedreschi
B5	English	88	20.80	6.20	6.20	11.21	0.274	133	59.20	0.454	Tension	Pedreschi
B6	English	88	16.60	6.20	6.20	11.21	0.274	152	58.8	0.451	Tension	Pedreschi
1	Flemish Bond	100	27.60	27.50	6.20	11.17	0.274	134	46.33	0.32	Tension	Own
2	Flemish Bond	100	26.80	29.50	6.20	11.17	0.274	134	36.79	0.26	Tension	Own

Table 6.3 Comparison with Pedreschi's Results

Beam	Type	Exp.	Ave.	F.E.	Exp./Theo.	Direct Method	Exp./Theo.	$\gamma_{mm}=1.0$ $\gamma_{ms}=1.0$	Exp./code	$\gamma_{mm}=2.0$ $\gamma_{ms}=1.15$	Exp./code	$\gamma_{mm}=1.0$ $\gamma_{ms}=1.0$	Exp./code	$\gamma_{mm}=2.0$ $\gamma_{ms}=1.15$	Exp./code
1	Flemish Bond	46.33	41.56	-	-	51.67	0.80	56.87	0.73	41.51	1	54.78	0.76	37.25	1.12
2	Flemish Bond	36.79													
3	English Bond	52.0	66.40	64	1.04	63.49	1.05	59.36	1.12	48.52	1.37	59.0	1.13	46.70	1.42
4	English Bond	66.40													
5	Flemish Garden Bond	69.60	68.80	64	1.08	63.49	1.08	59.36	1.16	48.52	1.42	59.0	1.17	46.70	1.47
6	English Garden Bond	68.0													
7	English Garden Bond	72	70	64	1.1	63.49	1.1	59.36	1.18	48.52	1.44	59.0	1.19	46.70	1.50
8	English Garden Bond	68													

Table 6.4 Ultimate Moment kNm

B.S. 5628 approach, however, predicted lower ultimate moment values than the experimental results. The ratio of experimental moments to code predicted moments varied from 1 to 1.5, so that applying the safety factors from the code results in increases in the percentage ratio. For design purposes it is advantageous to have a ratio greater than 1.0. In all the cases the magnitude of variance was convenient.

6.2.3 Relationship between Steel Strain and Moment

The experimental relationship between the steel strain and the moment is given in Fig 6.2.7 , where the strain values given are the strains in the steel resulting from the application of the live load. Within the region of constant moment, the strains were measured manually using a "Demec" gauge. After cracking, the strains were measured in the prestressing tendons using highly sensitive electrical strain gauges. In all the beams, cracking commenced at a load of between 30 and 40 per cent of the yield load. During formation of the crack, the total strain increased up to the yield point. Fig 6.2.6 shows that the Flemish bond beams, B_1 and B_2 achieved higher strains in relation to the applied moment than the English bond beams, as noted by Pedreschi. This is due to the higher compressive strength of the English bond beams and the development of cracking in the Flemish bond beams at an earlier stage.

Fig 6.2.7 shows that the English bond beams, B_3 and B_4, acheived higher strain values in relation to moment than the English Garden bond beams, B_5 and B_6, and the Flemish Garden bond beams, B_7 and B_8. The three curves of steel strain plotted against moment show similar characteristics, namely an initial linear relationship then a more rapid increase in the slope tending towards a direction parallel to the x-

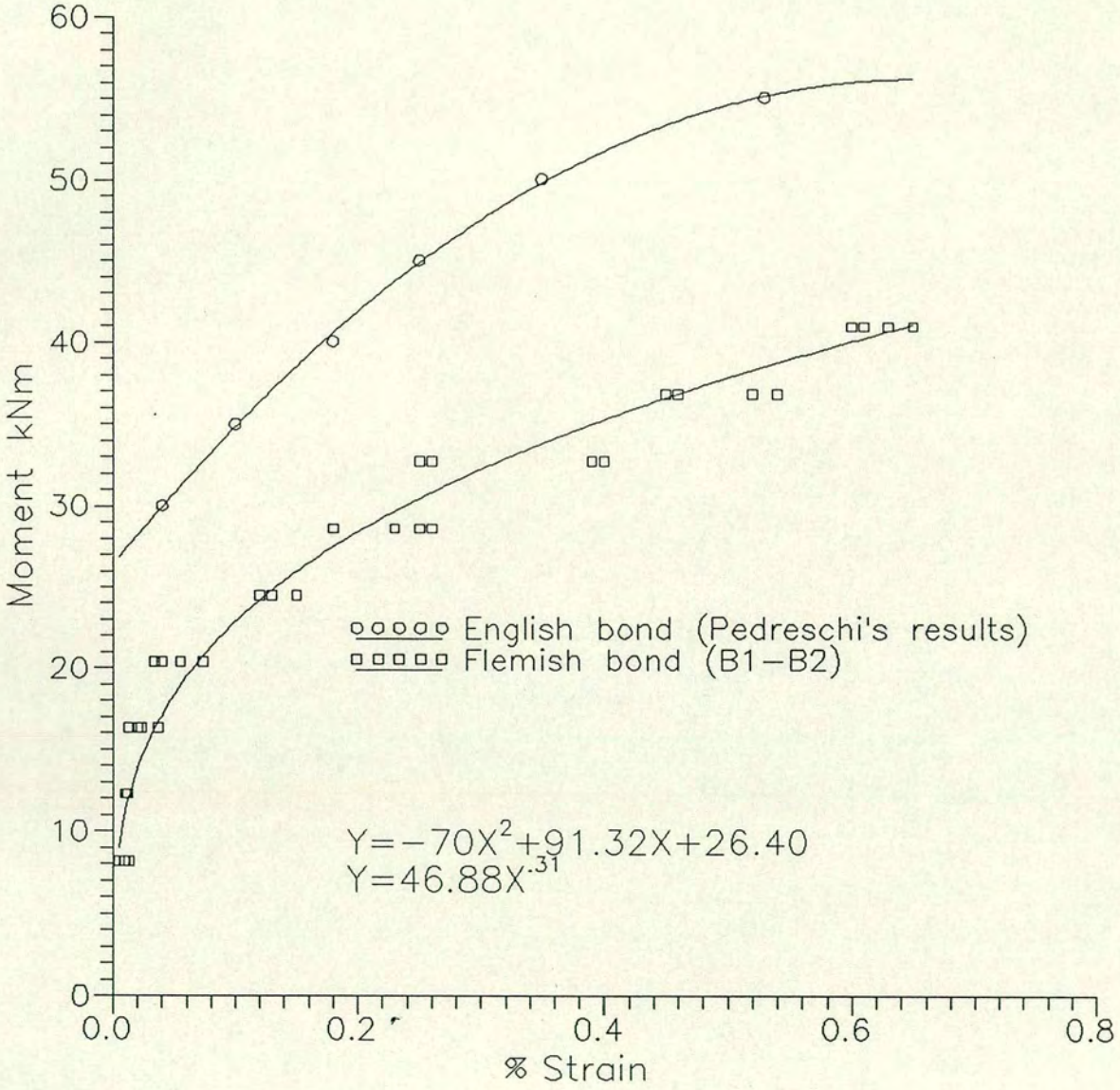

Steel strain – moment relationship.

Figure 6–2–6

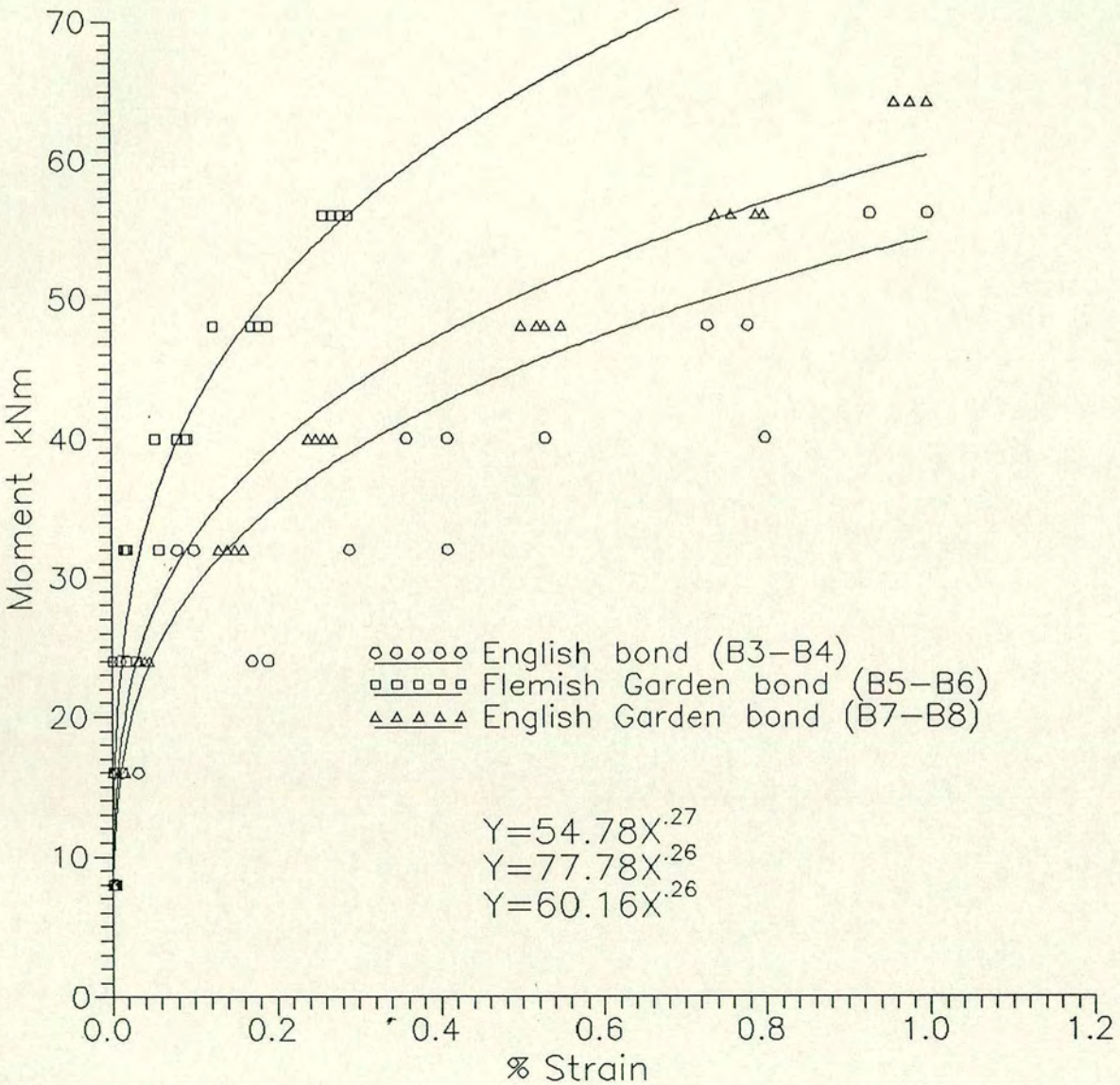

Steel strain – moment relationship

Figure 6–2–7

axis. The strain in the steel was therefore near to the yield point and all the beams exhibited a pure flexural tensile failure.

6.2.4

Relationship Between Top Fibre Strain and Moment

Figs. 6.2.8,9 give details of the experimental compressive strains in the top fibres in relation to the applied moment, measured in the constant moment zone of the beams. The compressive strains in all the beams increased uniformly with load up to cracking, with an increase of slope of the curve towards failure. Fig 6.2.8 showsthat the Flemish bond beams, B_1 and B_2, acheived higher compressive strains in relation to applied moment than the English bond beams, as found by Pedreschi. This is due to the development of cracks which cause loss of prestress in the Flemish bond beams at an early stage.

Fig 6.2.8 showsthat for beams B_1 and B_2, the average compressive strain at failure is 0.0031. Therefore, the average compressive strain for the Flemish bond beams, B_1 and B_2, where the bed joint runs parallel to the direction of the induced compressive stress, is in close agreement with the corresponding value derived for the axially loaded single course prisms, i.e., 0.0035.

Fig 6.2.9 showsthat the English bond beams B_3 and B_4 attain higher compressive strains, relative to applied moment, than the English Garden bond beams, B_5 and B_6, and the Flemish Garden bond beams, B_7 and B_8. The English bond beams and English Garden bond beams showed similar characteristics, with initial elastic behaviour up to cracking, then a rapid increase in slope of curve towards the horizontal.

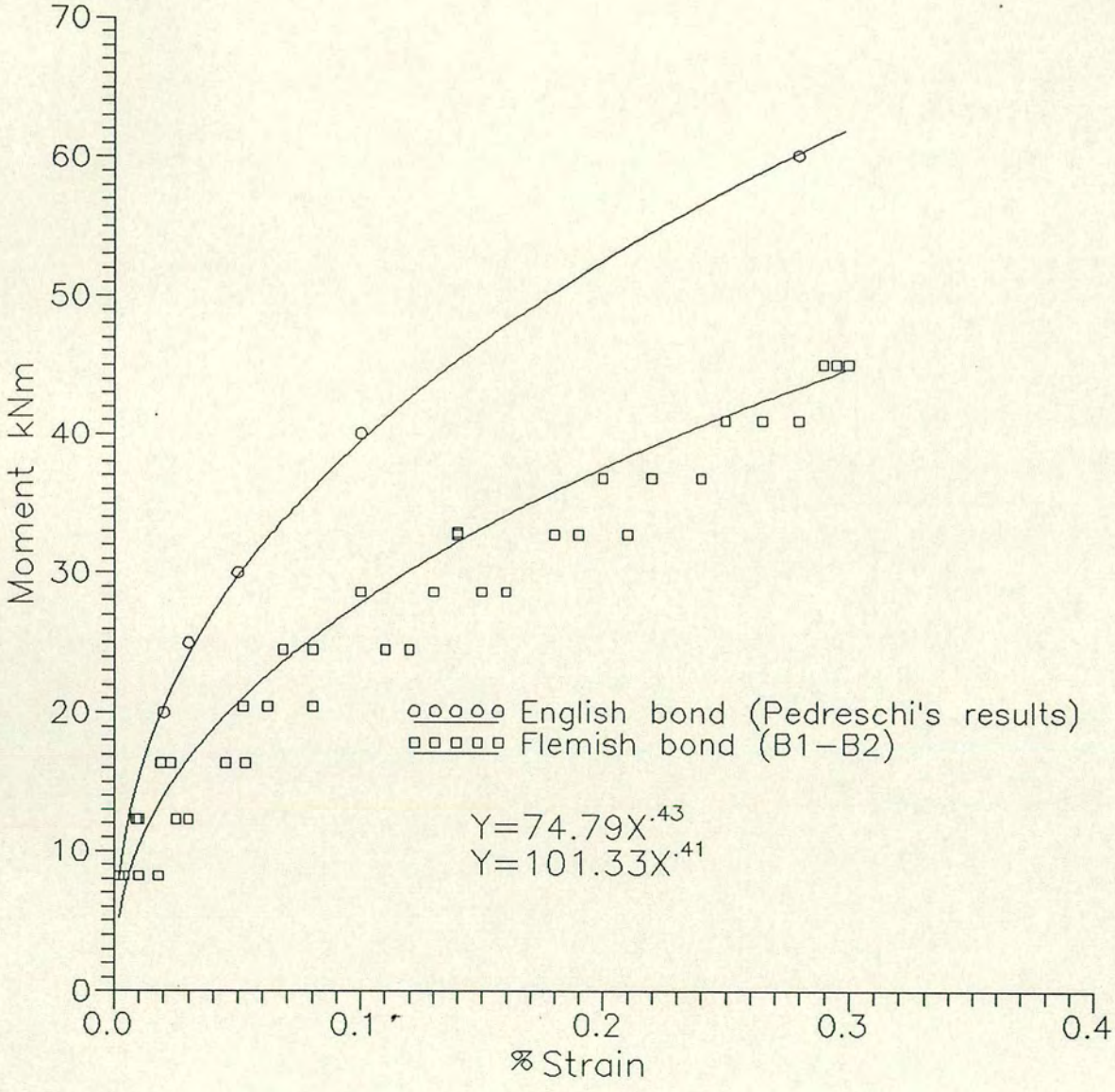

Top fibre strain – moment relationship.

Figure 6–2–8

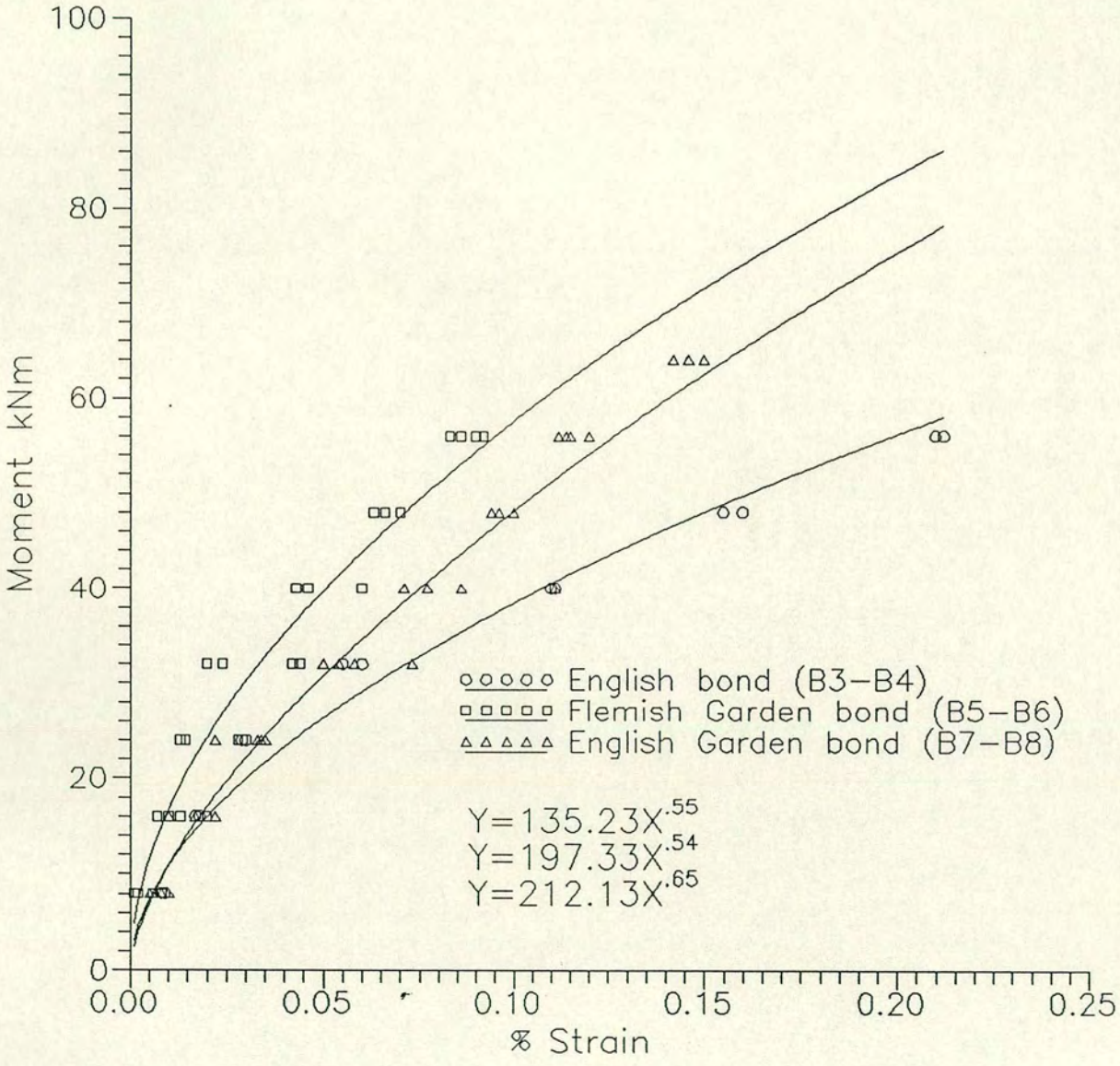

Top fibre strain – moment relationship.

Figure 6–2–9

6.2.5 Relationship between Curvature and Moment

The experimental moment-curvature relationship was obtained from the slope of the brickwork strain distribution at a given load. The strain was measured manually using "Demec" points over the middle region of the constant moment zone up to cracking, after which the compressive strain was measured manually and the strain in the prestressing tendons was measured by highly sensitive electric strain gauges. The applied load was measured by load cells connected to a pen-chart recorder. The moment-curvature relationship was obtained experimentally using the following equation:

$$\phi_{av} = \frac{\varepsilon_1 + \varepsilon_{sam}}{d}$$

In all cases, the moment-curvature curves exhibited three phases corresponding to uncracked, cracked with steel in the elastic range, and cracked with steel yielding. The curves were initially linear up to the cracking moment, after which the curvature increased more rapidly for the same increase in moment. Thus, prior to cracking the beam was stiff and behaved elastically, while after cracking the beam's stiffness started to reduce rapidly allowing the curvature to increase rapidly whilst the stress in the tendons was still within the elastic range. When the steel started yielding, however, the curvature increased very rapidly resulting in a ductile failure. All the beams were under reinforced and exhibited a similar type of behaviour. Where structures exhibit compression and shear failure, the moment-curvature relationship does not enter the third phase.

The experimental and theoretical values of curvature were in good agreement. The stress/strain relationship based on tests on single course prisms predicted a slightly greater curvature than from the results obtained from single course prisms by Pedreschi.

The moment-curvature relationship obtained from the finite element analysis slightly overestimated the curvature of the English bond beams B_3 and B_4, and slightly underestimated the curvature of the English Garden bond beams, B_7 and B_8 and the Flemish Garden bond beams, B_5 and B_6. The results from the finite element analysis were in closer agreement with the experimental values of curvature than those from the direct method of analysis. However, the theoretical and experimental ultimate moments were in good agreement. The accurate simulation provided by the finite element analysis is due to the material model, which assumes that cracking occurs when one or both of the principal stresses is in violation of the cracking criterion defined by the tensile failure. Although these cracks are assumed fixed throughout the remainder of the analysis, they may open and close in response to load reversals. After cracking, the neutral axis depth reduces enabling the section to maintain the same moment. The stresses in the steel continue to increase so that the compressive strain will increase causing the neutral axis depth to further decrease up to section failure. This assumption must have a considerable affect on the accuracy of the finite element results.

Figs 6.2.10,11 show that the English Bond beams, B_1 and B_2 have larger curvatures in relation to applied moment than the English Bond Beams tested by Pedreschi. This clearly shows that the English Bond beam is much stiffer than the Flemish Bond beam when the cross-section

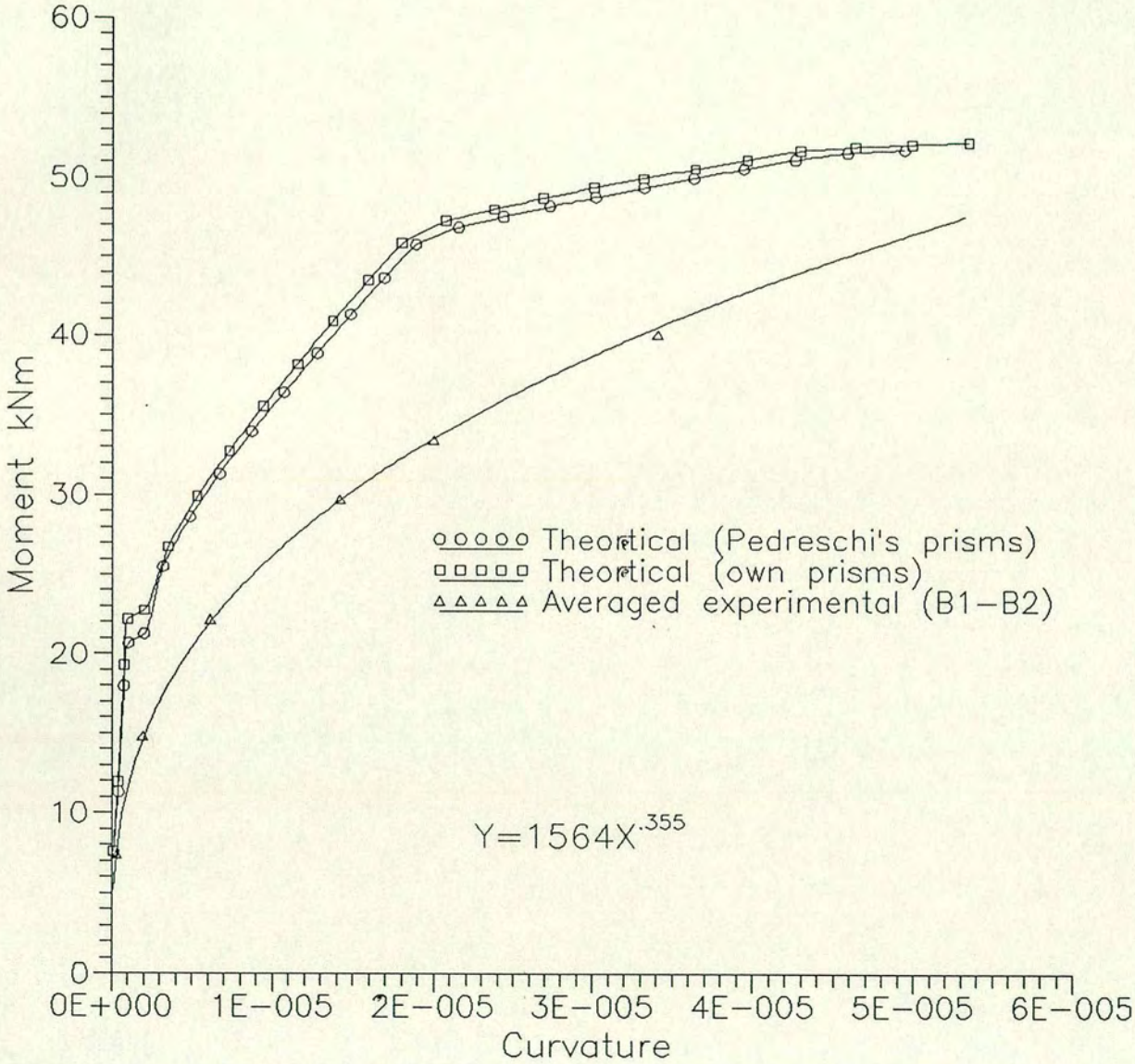

Curvature – average moment relationship for Flemish bond beams (B1–B2).

Figure 6–2–10

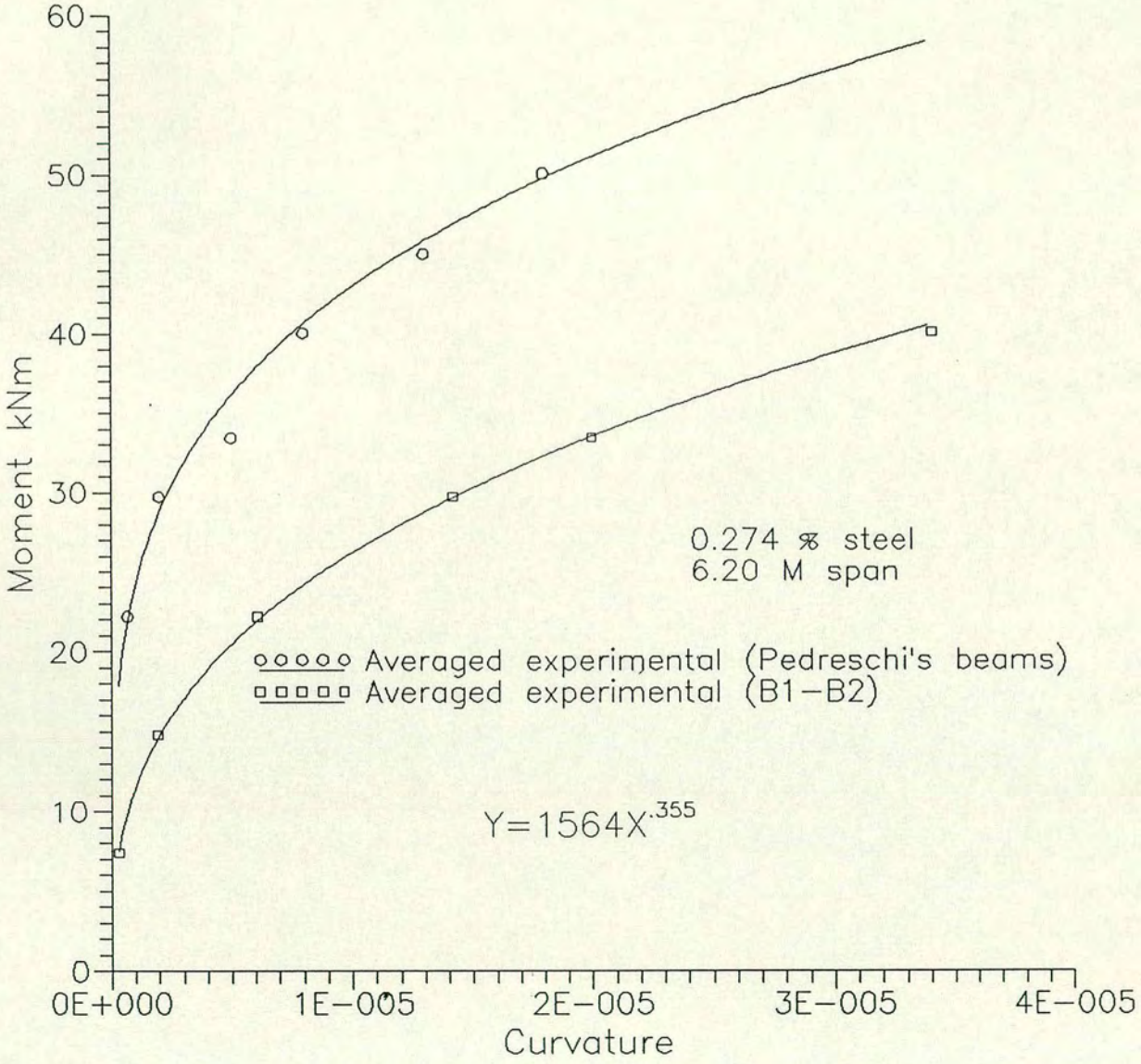

Curvature – average moment relationship for English and Flemish bond beams.

Figure 6-2-11

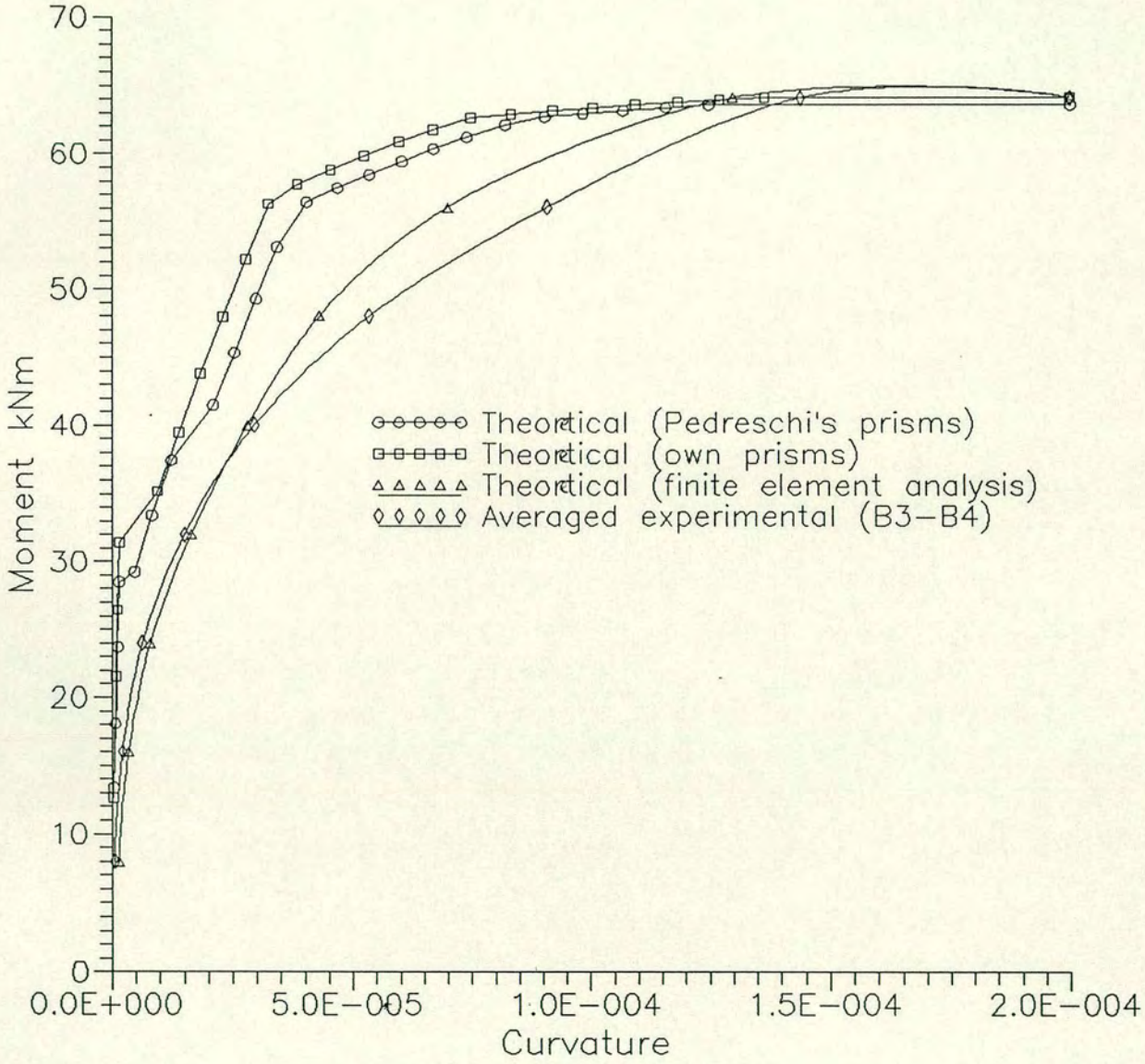

Curvature – average moment relationship for English bond beams/slabs (B3–B4).

Figure 6–2–12

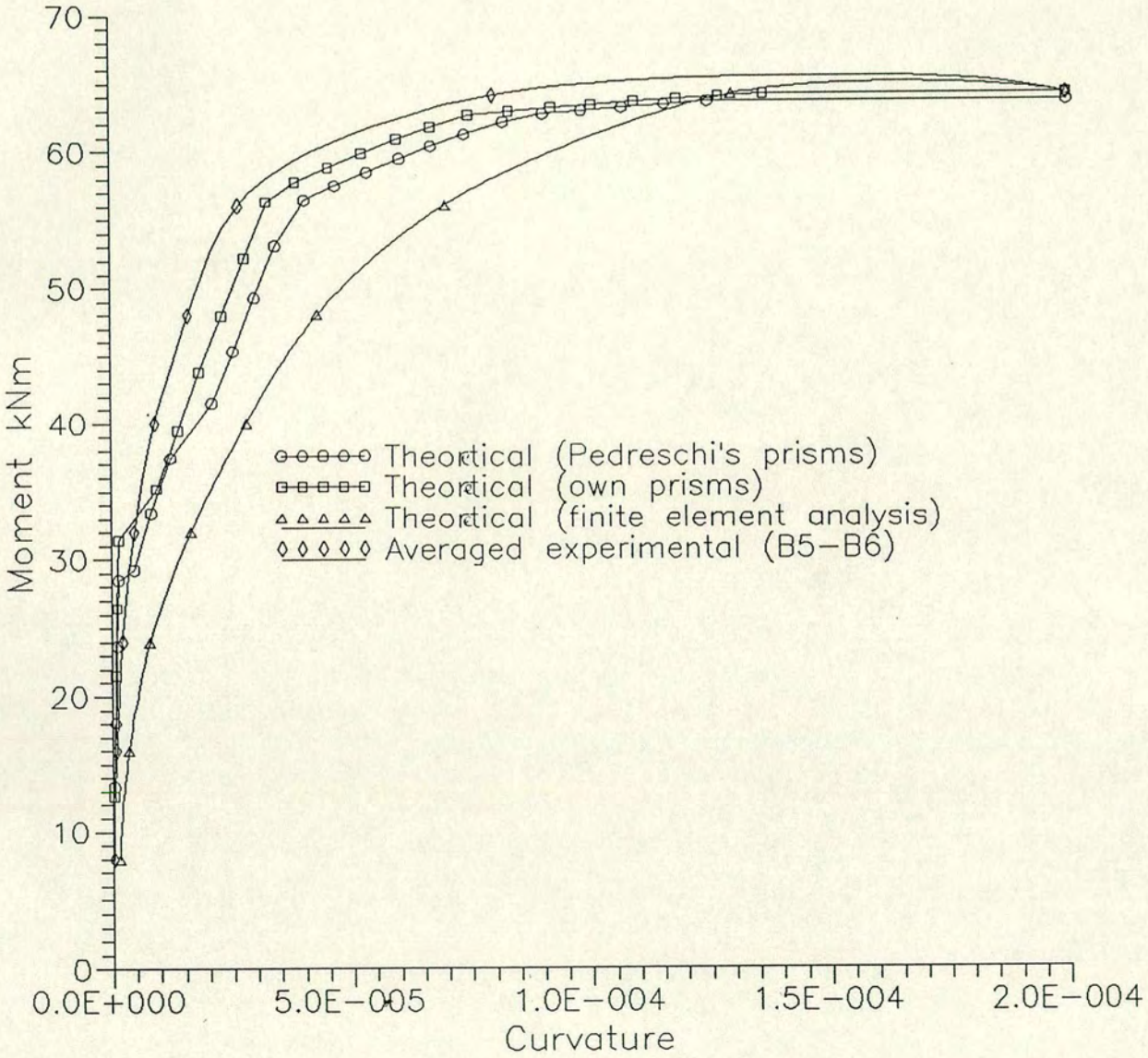

Curvature – average moment relationship for Flemish Garden bond beams/slabs (B5–B6).

Figure 6–2–13

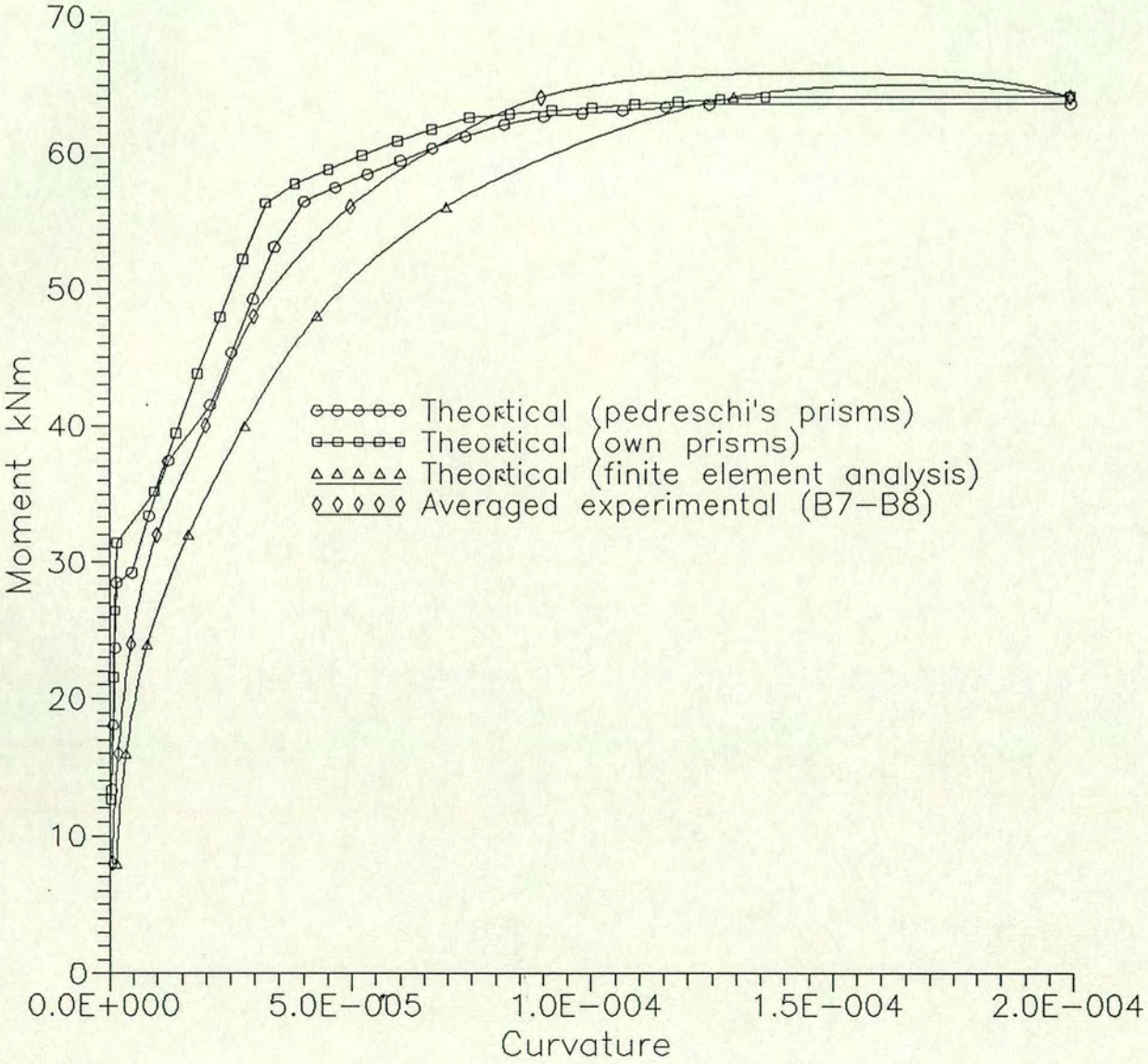

Curvature – average moment relationship for English Garden bond beams/slabs (B7–B8)

Figure 6–2–14

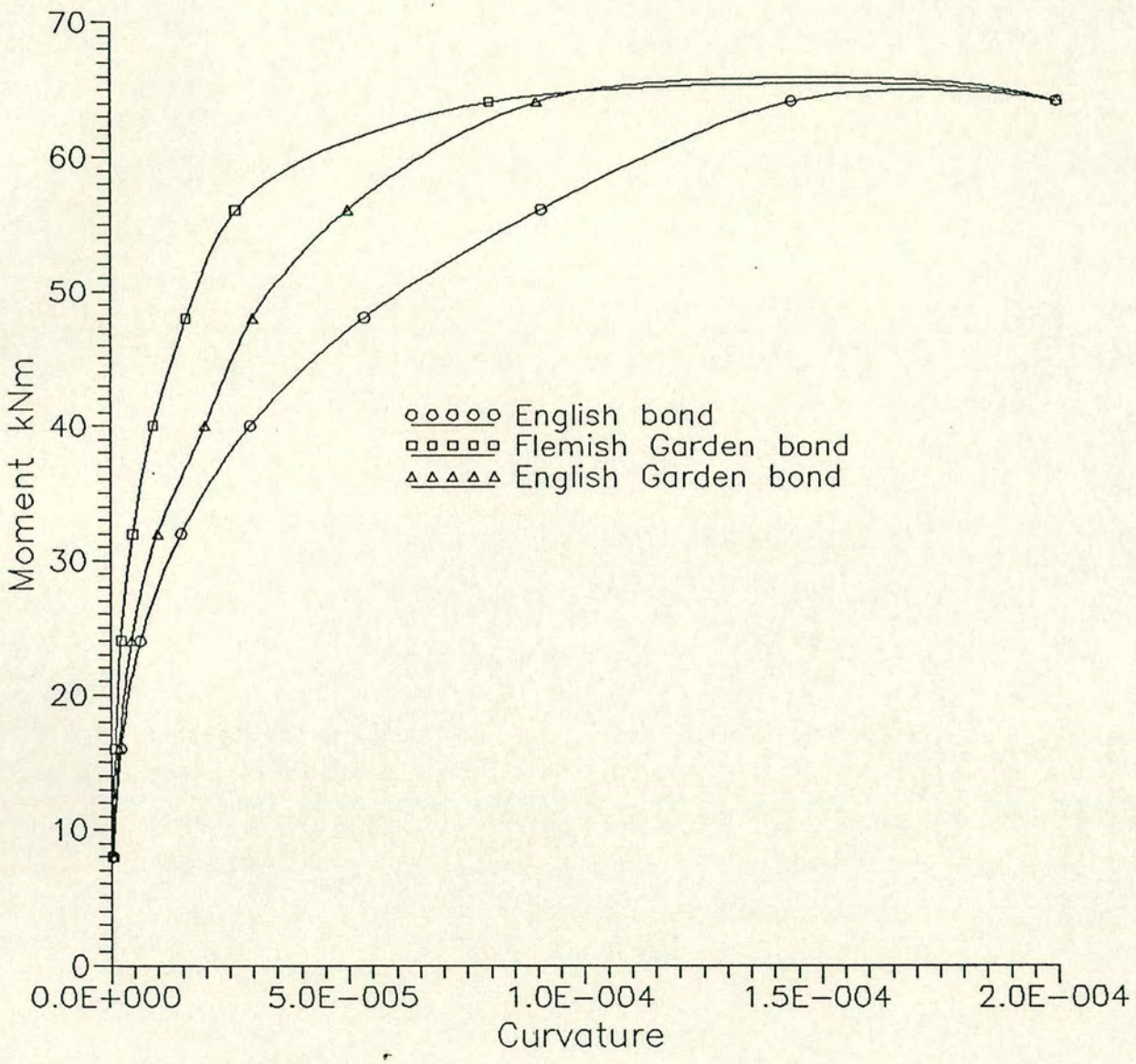

Curvature – average moment relationship for English, Flemish Garden and English Garden bond beams/slabs.

Figure 6–2–15

is built horizontally producing joints running parallel to the direction of the induced compressive stress.

Figs 6.2.12–15 show that the beams B_3 to B_8, i.e. English Bond, English Garden and Flemish Garden, all have similar curvature relationships and that the predicted curvatures correlated well with the experimental results.

6.2.6 Relationship between Load and Deflection

The main advantage of prestressing masonry walls is the improvement in its ultimate strength and performance under serviceability conditions. Excessive deflection produces cracks in the wall, and these crack widths must be kept within prescribed limits to prevent damage and maintain effective cover to the reinforcement. The serviceability limit state of deflection aims to ensure that deflection does not effect the appearance or efficiency of the structure. B.S. 5628 recommends that the final deflection of all elements should not exceed length/125 for cantilevers or span/250 for all other elements. The calculation for deflection under working load, i.e. no cracking, can be based on a standard strength of materials approach. However, when cracking occurs the neutral axis depth decreases and the structure weakens so that the deflection calculation is more complicated. In this chapter, two methods were used to predict this deflection. The first method involves calculating the moment-curvature relationship; the deflection can then be determined by a double integration of the curvature along the span. This method is used most often for reinforced and prestressed concrete structures (Ghali and Neville, 1971). In 1983, Pedreschi applied the method to prestressed brickwork beams using a computer program to calculate the deflections. The program was based on the finite difference method

which employs all the sequence of calculations for the large amount of iterative and matrix operations (Pedreschi, 1983). The second method is based on a finite element approach. The non-linear behaviour of reinforced and prestressed concrete beams can be effectively modelled by the use of finite element techniques. In this research, the LUSAS plane stress concrete model was used to reproduce features of the materially and geometrically non-linear response of prestressed beams. The beams were considered to be in a state of plane stress and so that the failure surface is subjected to bi-axial stresses. Cracking was assumed to occur when one, or both of the principal stresses are in violation of the cracking criterion defined by a tensile failure. In masonry, this type of approach can be misleading. Brick is orthotropic and mortar is isotropic, therefore brickwork acts with a non-linear highly anisotropic material behaviour and cracking and is more liable to form at intervals which coincide with the mortar joints. The modelling of this behaviour is very complicated and can only be done through comprehensive and detailed theoretical and experimental investigation. The deflections were calculated in both methods using the stress/strain relationships obtained from tests on single course prisms. Figs 6.2.18-20 show that the finite element results underestimated the load-deflection relationship in comparison with values obtained using the direct method or from the experimental results. This is because the finite element load-deflection relationships were based mainly on the displacement of the structure from the stiffness analysis for a given force, while the direct method load-deflection relationships were derived from the moment-curvature results which were based on the gradient of the line between points in the compression zone only.

In beams B_1 to B_8, the load-deflection relationship was linear over the elastic range up to the point of cracking after which the deflection increased rapidly with the curve tending towards the horizontal. The elastic portions of the curve were in all cases of similar gradient because prior to cracking all beam's sections had the same stiffness. After cracking, all the beam sections had reduced stiffnesses resulting in rapid increases in deflection with no corresponding increase in load As expected, the Flemish Bond beams, B_1 and B_2 exhibited a higher load-deflection curvature relationship than the English bond beams, as found by Pedreschi and as shown in Fig 6.2.17 . Fig 6.2.16 showsthat the direct method analysis in conjunction with the single course prism results gave results which were more compatible with those from the experimental load-deflection relationship.

Figs6.2.18-20 indicates that the predicted load-deflection relationships based on finite element analysis change about the third phase of the experimental load-deflection relationships. Fig 6.2.21 showsthat the English Garden bond and the English bond beams have relatively larger curvature than the Flemish Garden Bond beams. This is probably due to the bonding effect at the compression zone. All the beams have the same characteristics for the load-deflection relationship up to the cracking stage. Beyond cracking, the plot of strain against depth of beam was no longer linear, as the strains below the neutral axis in the tensile zone increased rapidly. In all cases, a distinct three phase load-deflection relationship exists Fig6.2.21 corresponding to uncracked, cracked with steel still in the elastic range and cracked with the steel yielding.

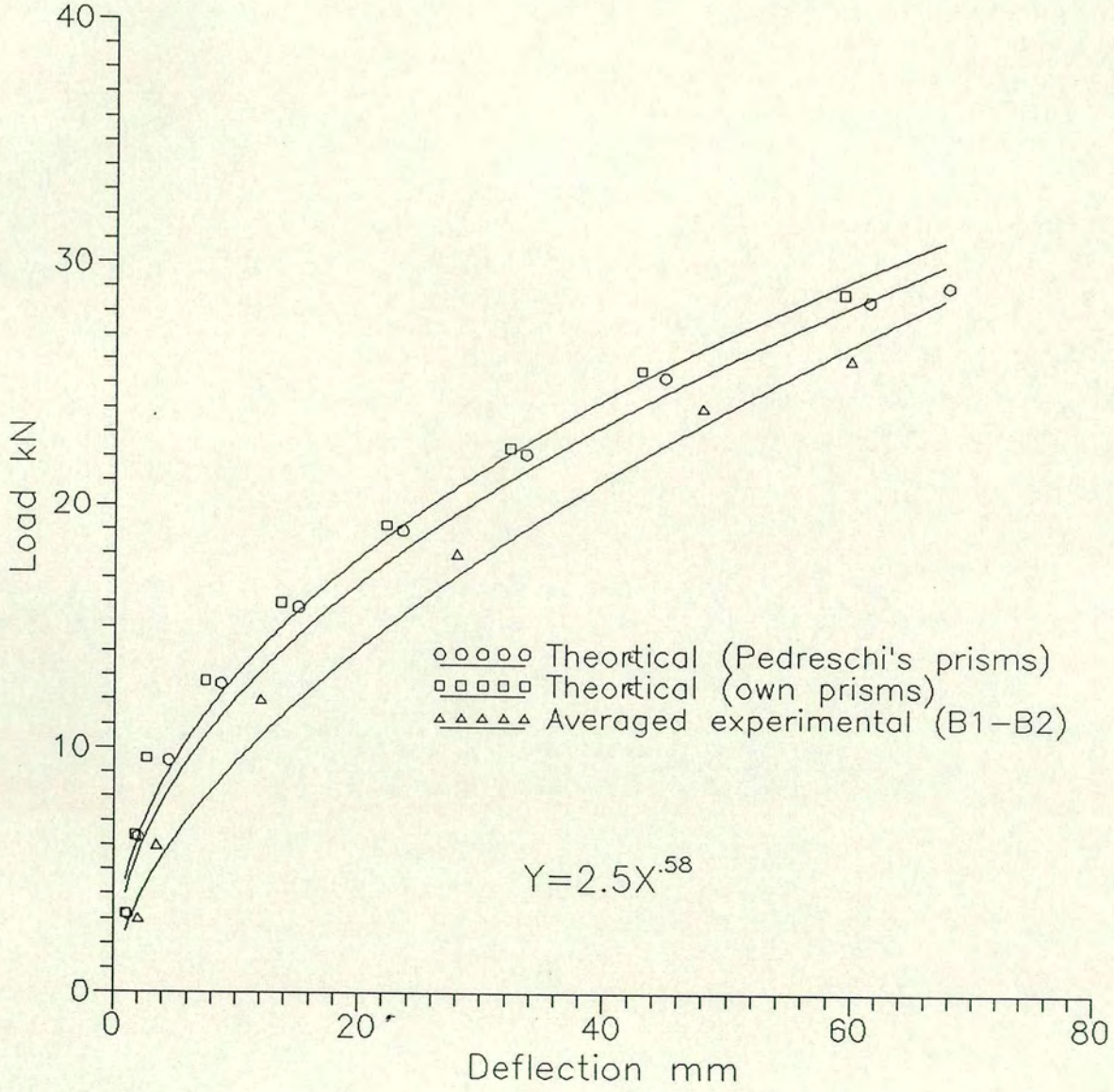

Deflection – total applied load relationship for Flemish bond beams (B1–B2).

Figure 6–2–16

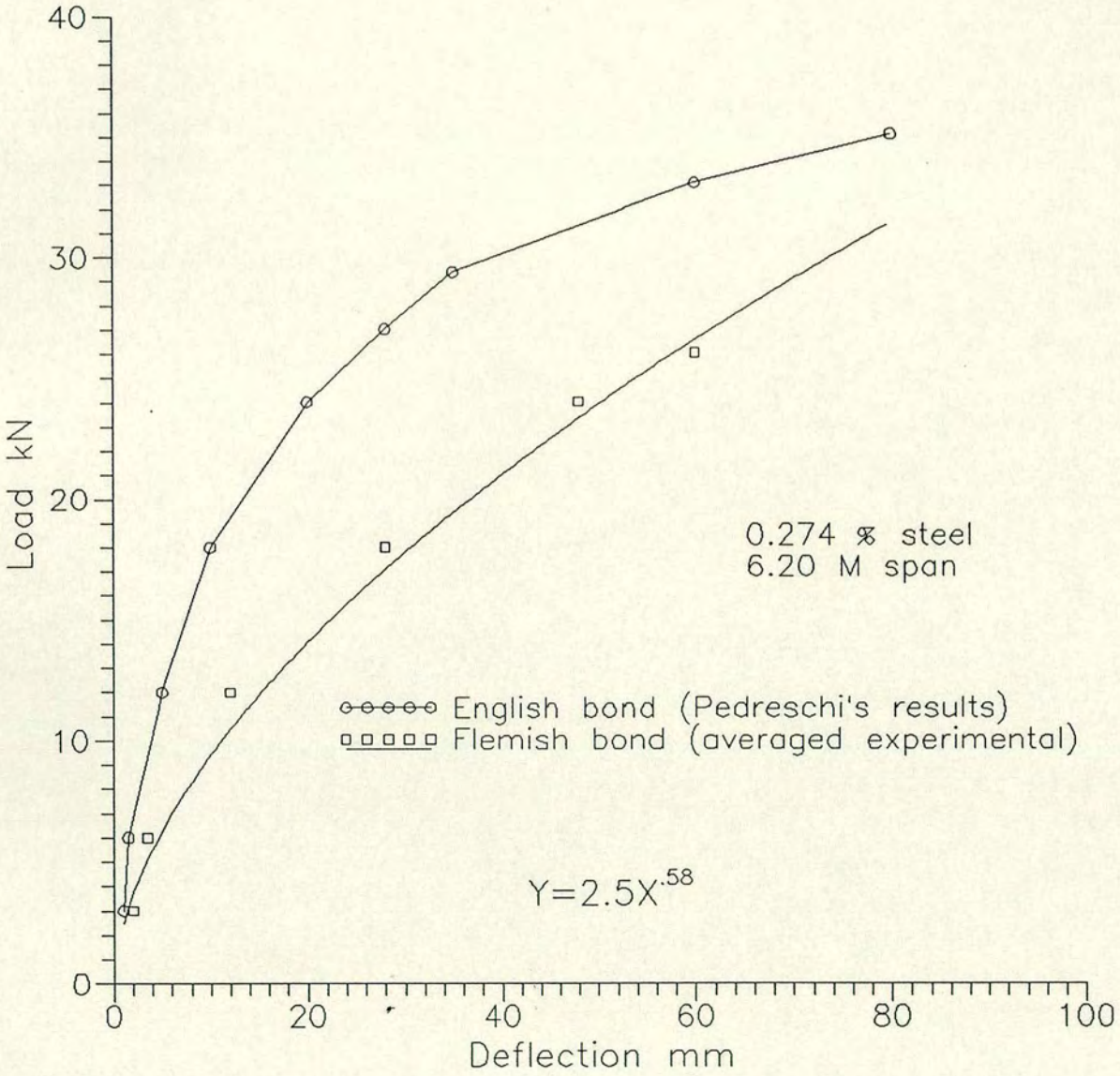

Deflection – total applied load relationship for English and Flemish bond beams.

Figure 6–2–17

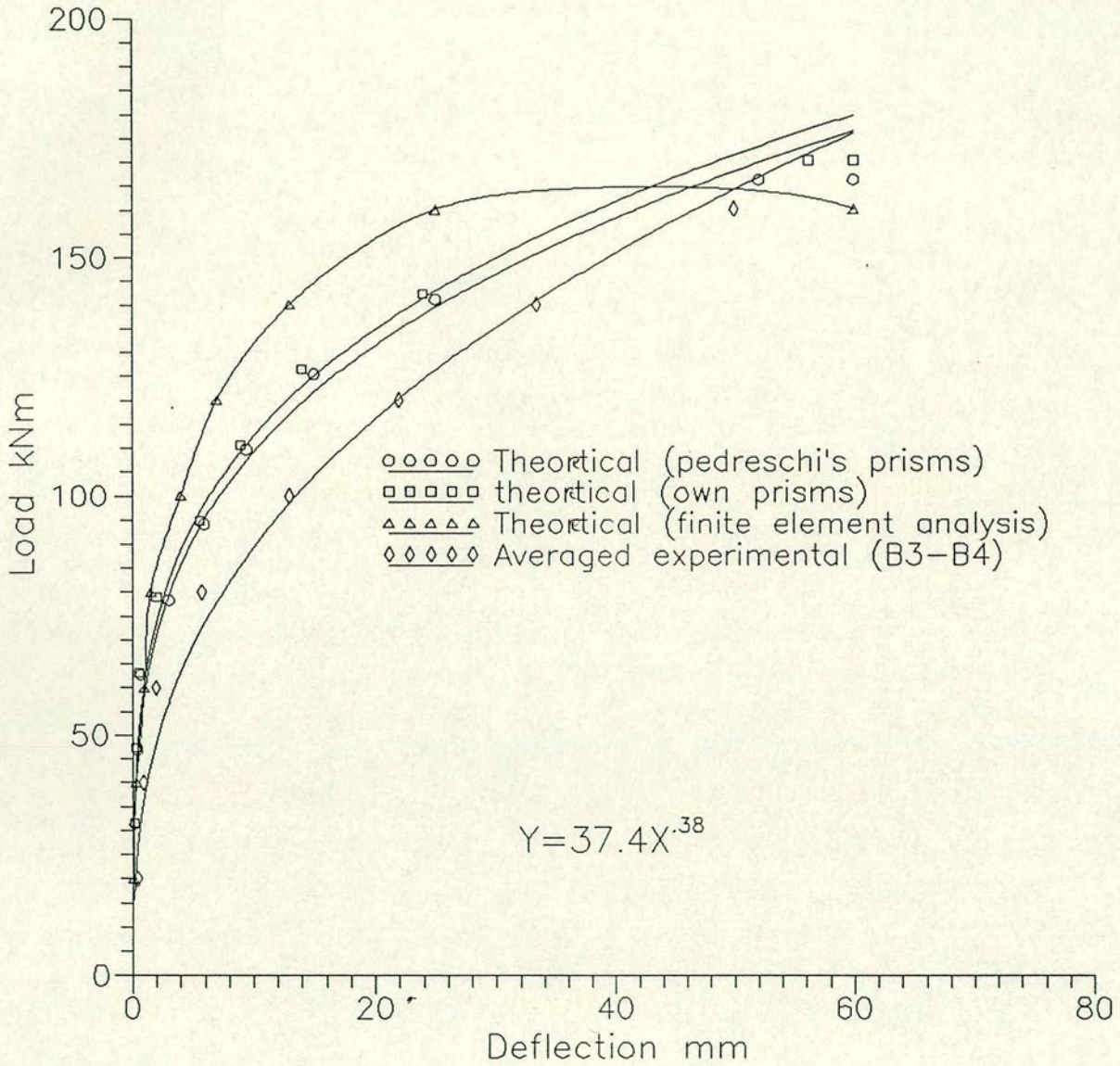

Deflection – total applied load relationship for English bond beams/slabs (B3–B4).

Figure 6–2–18

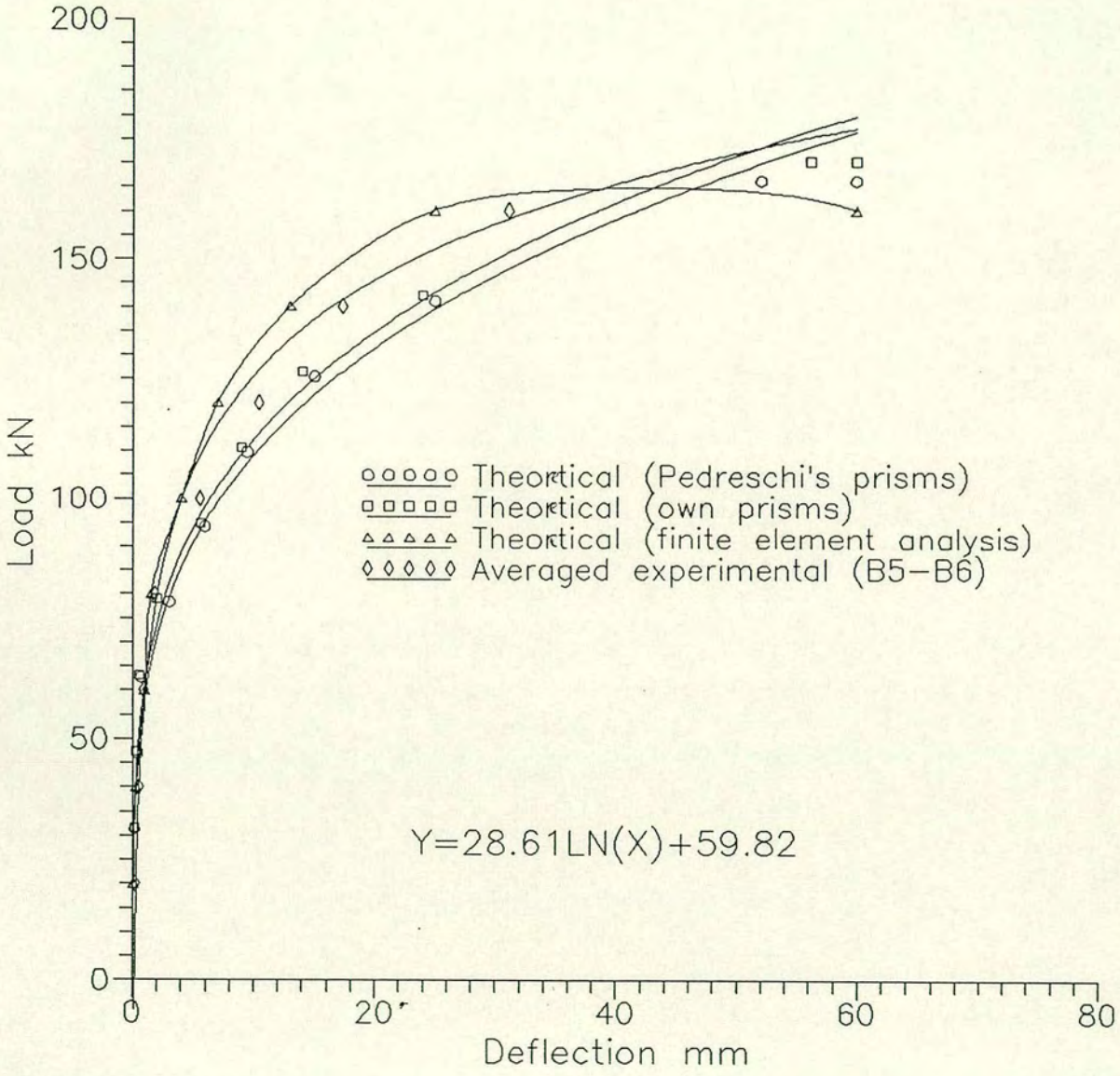

Deflection – total applied load relationship for Flemish Garden bond beams/slabs (B5–B6).

Figure 6–2–19

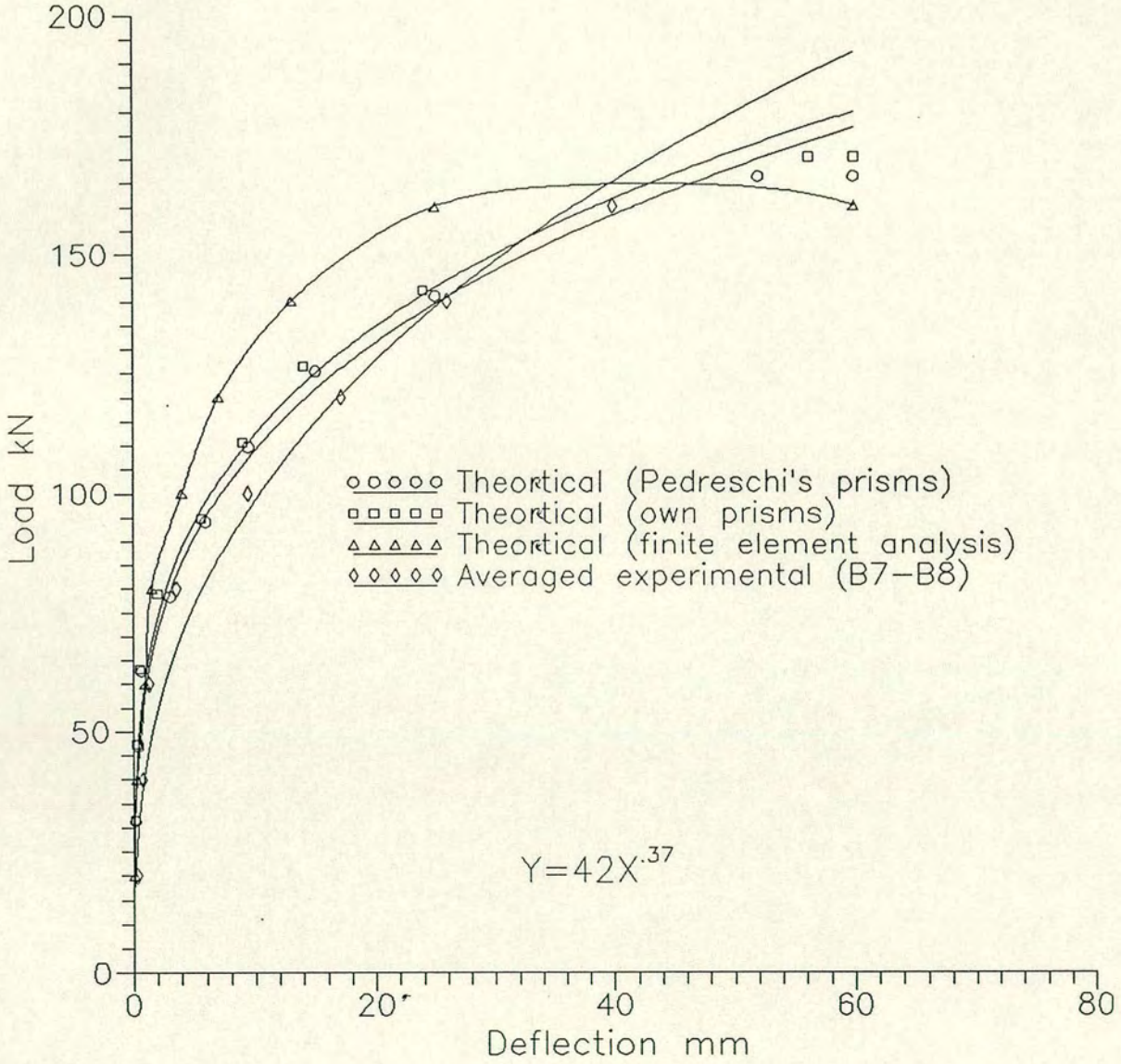

Deflection – total applied load relationship for English Garden bond beams/slabs (B7–B8).

Figure 6–2–20

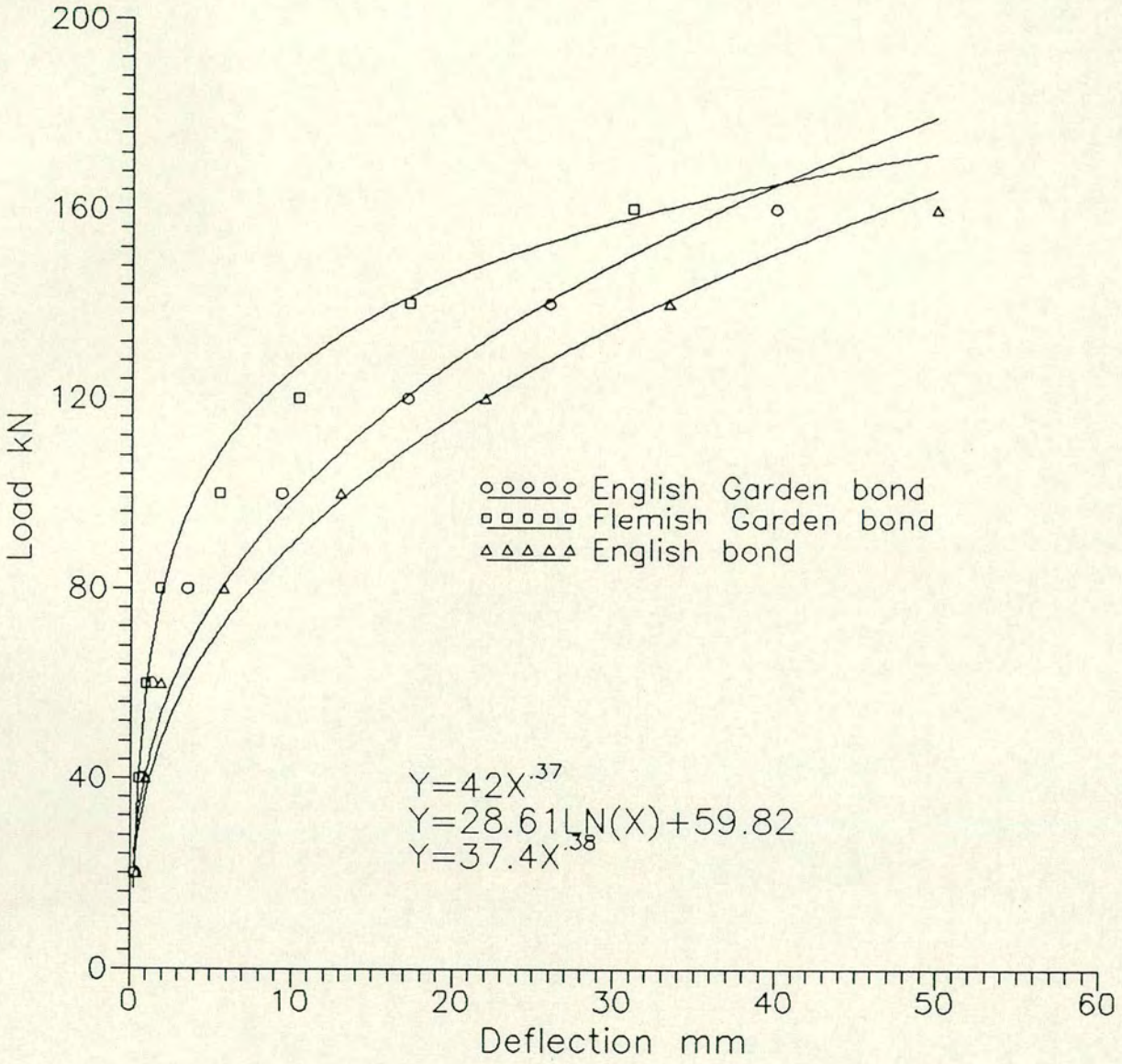

Deflection – total applied load relationship for English, Flemish Garden and English Garden bond beams/slabs.

Figure 6–2–21

6.2.7 Relationship between Neutral Axis Depth and Load

Fig 6.2.22 shows the relationship between load and neutral axis depth. It can be seen that the the neutral axis depth relative to load relationship for the Flemish bond beams is less than for the English bond beams (Pedreschi's results). On application of the eccentric prestress load, the compressive strain decreased in the lower sections and increased in the upper sections of the beam. As tension developed and cracking commenced, the neutral axis depth moved upward, the compressive strains above the neutral axis increased rapidly with load and the neutral axis depth decreased further. Fig 6.2.22 showsthat the English bond beams develop larger tensile forces than Flemish bond beams, and as a result require a larger neutral axis depth in order to develop compressive forces of a similar magnitude. Therefore, English bond beams have a beneficial neutral axis depth with load relationship compared to Flemish bond beams when the beam bed joint runs parallel to the direction of the induced compressive stress.

Fig 6.2.23 shows that the Flemish garden bond beams have a dominant neutral axis depth against load relationship compared to the English and English Garden bond beams when the beam bed joints run perpendicular to the direction of the induced compressive stress.

6.2.8 Cracking Moments

Cracking is a major problem in the design of masonry structures. Cracking can be developed from a variety of reasons which include bending stress, shrinkage, creep and fatigue load. Brickwork is very weak in tension, cracks must be kept within control at all costs. The penetration of corrosive elements to the main reinforcement disrupts the steel-concrete matrix and affects the integrity of the composite material.

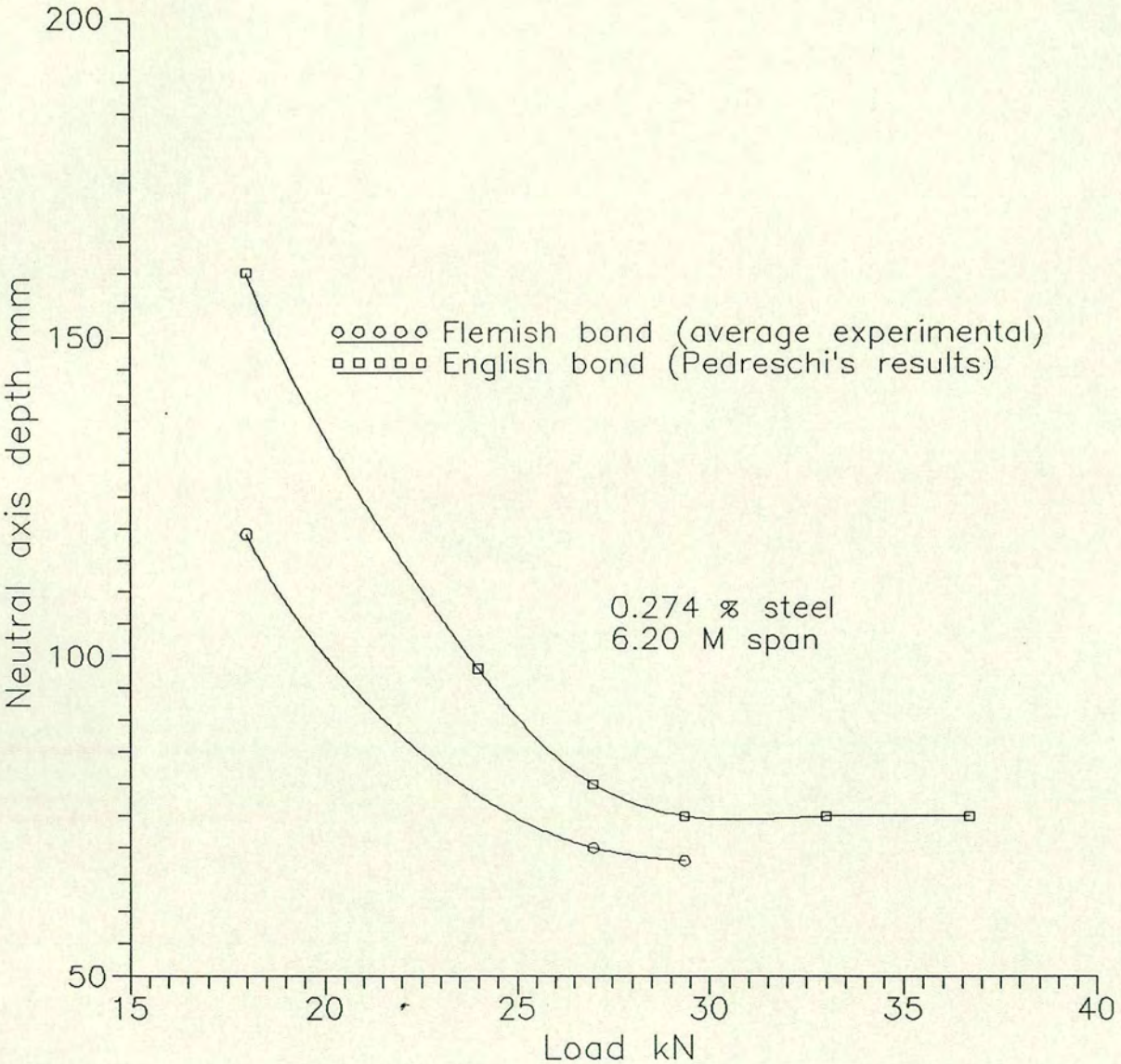

Neutral axis depth – load relationship for English and Flemish bond beams.

Figure 6–2–22

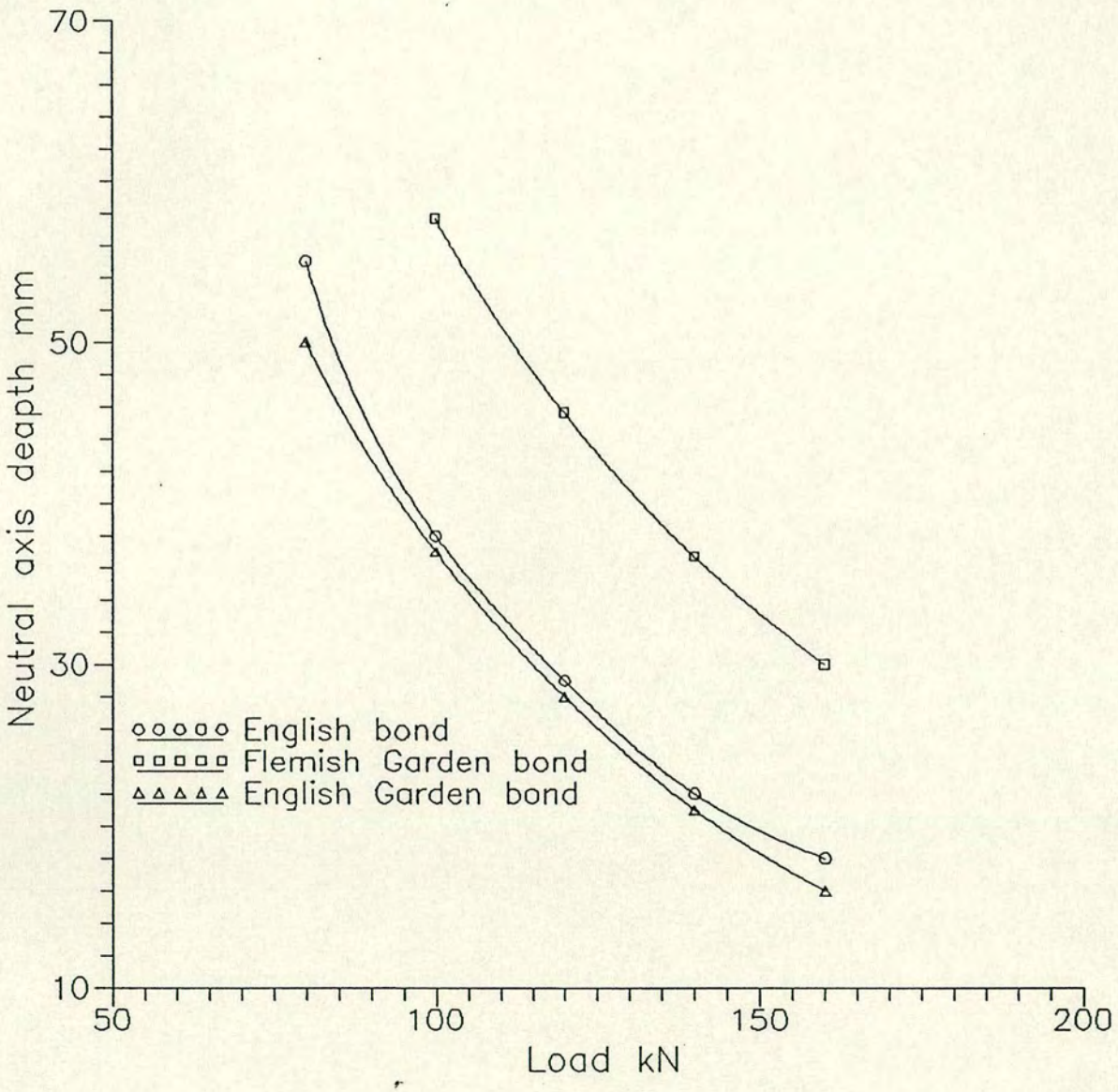

Neutral axis depth – load relationship for English, Flemish Garden and English Garden bond beams/slabs.

Figure 6–2–23

C.P.110 limited the permissible crack width to between 0.1 and 0.3 mm, depending on the nature of the environment (C.P.110, 1972). B.S.8110, Part 2, limits the crack width to a maximum of 0.1 mm for severe environments and a value of 0.2 mm in all other environments (B.S.8110, 1985). It is very important for the beam or the wall to have an adequate factor of safety against collapse. In prestressed brickwork structures there are three classes of structure which determine the working load. Class one structures, in which no tensile stresses are allowed under working load, can be considered as a conservative design. In Class two structures tensile stresses are allowed but no cracking is permitted under working load. In Class three structures, cracks up to a maximum of 0.2 mm are allowed under working load. The factor of safety of the structure is adversely affected by the working load values, so that when the working load of a prestressed brickwork structure is increased, the design factor of safety is decreased.

All the beams were adequately designed against shear to ensure that the full flexural capacity was reached. Deflections were within code allowable limits when cracking was allowed under working load (B.S.5628). If the beams were designed as class one members then from Table 6.6 it can be seen that the average ratio of M_{ult}/M_{C1} = 3.34 - 3.60. For class two beams the design working load decreases to between 2.3 and 3. Under this working load, tension is allowed to develop up to the maximum flexural tensile strength of the brickwork. But, if cracks are allowed up to a maximum width of 0.2 mm, the safety factor drops to between 1.85 and 1.92. Therefore, the performance of class three beams has a safety factor of between 1.85 and 1.92.

Table 6.5 shows that average experimental cracking moment for beams B_1 and B_2(Flemish bond) was smaller than the values predicted by the elastic and direct methods of analysis. The experimental cracking moments of beams B_3-B_8 were in good agreement with the values predicted by the finite element analysis. But, the values predicted by other methods underestimated the the experimental cracking moments. It was not possible, therefore to forecast experimentally the exact cracking load. Some times there were audible signs of cracking without any cracking being visible.

In this research, the crack width was predicted by the use of the average strain method (Desayl, 1975).

$$w = s_m \varepsilon_{sm} \qquad (1)$$

Experimentally, the crack widths were measured 5 mm from the bottom of the beam. Therefore, the predicted average strain was obtained from the average additional strain at the level of the strand, calculated using the stress/strain relationship obtained from tests on single course prisms (Pedreschi, 1983).

$$\varepsilon_{smb} = \left[\frac{d_1-n}{d-n}\right] \varepsilon_{sam} \qquad (2)$$

where d_1 = the distance from the top fibre of the beam to the crack level

Several researchers found that this method, with some limitations, was capable of reflecting the behaviour of prestressed brickwork beams even beyond yielding of the tensile reinforcement (Walker, 1987; Uduehi,

1989). Relationships were obtained experimentally using the strains in the prestressing strand, measured with electrical resistance gauges, and on the brickwork, measured with 'Demec' gauges. The average of the first two crack widths was measured using crack detection moving microscope. In all cases, the cracks were initiated at the brick/mortar interface rather than through the brick or mortar. The cracks mostly formed at multiples of the distance between the two adjacent joints and between the two point load in the region of constant moment.

Fig 6.2.24 showsthe experimental total moment-average crack width relationship for the Flemish bond beams, B_1 and B_2. The crack widths were plotted against the applied moment after cracking. The predicted crack widths slightly underestimated the experimental results, but showed better agreement in the later stages. Generally, the predicted crack widths were reasonably accurate in predicting the actual behaviour of the Flemish bond beams when the bed joints runs parallel to the direction of the induced compressive stress.

Figs 6.2.25 – 27 show that equation (1) provides an accurate prediction of crack widths in relationship to the applied moment after cracking for the Flemish Garden, English and English Garden beams, (B_3-B_8). The predicted crack widths were reasonably accurate in the earlier stages of cracking. This is due to the fact that only one crack usually formed at the cracking moment, and at that time the crack spacing was ignored in the predicted formula. The crack width relationship with moment was only related to the strain at this level along the total length of the beam minus the average strain prior to cracking. The strain differences were small and the ignored residual strain in the brickwork had a significant effect on the results. Fig 6.2.28 showsthat the

Flemish Garden bond beams have a smaller average crack width relative to applied moment after cracking than the English and English Garden Bond beams when the beam bed joints run perpendicular to the direction of the induced compressive stress.

6.2.9 Experimental Observations and Discussion

The aim of this part of the investigation was to study the effect of brickwork bonding on the flexural behaviour of post-tensioned brickwork beams. The two point loading arrangement allowed an easier understanding of the simply supported beam, slab and cantilever situation where shear force and bending moment are a maximum at the base (Fig.4,3).

In beams B_1 and B_2 (Flemish Bond), three pairs of 6 mm diameter mild steel rods were built into the beams during construction. The rods were placed through the perforations in the bricks for the full depth of the beams. These rods were provided to prevent tensile bursting forces under the anchorages. Several pairs of 6 mm diameter mild steel rods were placed as shear reinforcement on either side for the whole length of the beam (Fig. 6.2.31).

In the English bond, Flemish Garden bond and English Garden bond beams, (B_3-B_8), bursting and shear reinforcement was not included. All the beams were adequately designed against shear to ensure that the full flexural capacity was reached. All the beams failed primarily in flexure by yielding of the steel at the maximum moment zone. This type of failure was representative of under-reinforced structures.

Beam	Type	Experimental	Average	Elastic Method	Direct method use of Pedreschi Prisms	Direct method use of own Prisms	Non linear F.E.
1	Flemish Bond	16	16.50	23.01	20.68	22.20	-
2	Flemish Bond	17					
3	English Bond	22	24	20.70	19.15	19.90	25
4	English Bond	26					
5	Flemish Garden Bond	30	29	20.70	19.15	19.90	25
6	Flemish Garden Bond	28					
7	English Garden Bond	23	22	20.70	19.15	19.90	25
8	English Garden Bond	21					

Table 6.5 Cracking Moment kNM

Beam	Type	Predicted Ultimate Moment *Mu (kNM)	Working Load Moments			Mu	Mu	Mu
			Class 1 MCL2	Class 2 MCL2	Class 3 MCL3 .2mm	MC1	MC2	MC3
1	Flemish Bond	54.44	16.28	23.01	29.50	3.34	2.37	1.85
2	Flemish Bond							
3	English Bond	61.46	17.12	20.70	32	3.60	3	1.92
4	English Bond							
5	Flemish Garden Bond	61.46	17.12	20.70	32	3.60	3	1.92
6	Flemish Garden Bond							
7	English Garden Bond	61.46	17.12	20.70	32	3.60	3	1.92
8	English Garden Bond							

*Mu = Average of F.E., Direct Method, BS 5628 Alone and B.S. 5628 using Prisms Results.

Table 6.6 Serviceability Conditions

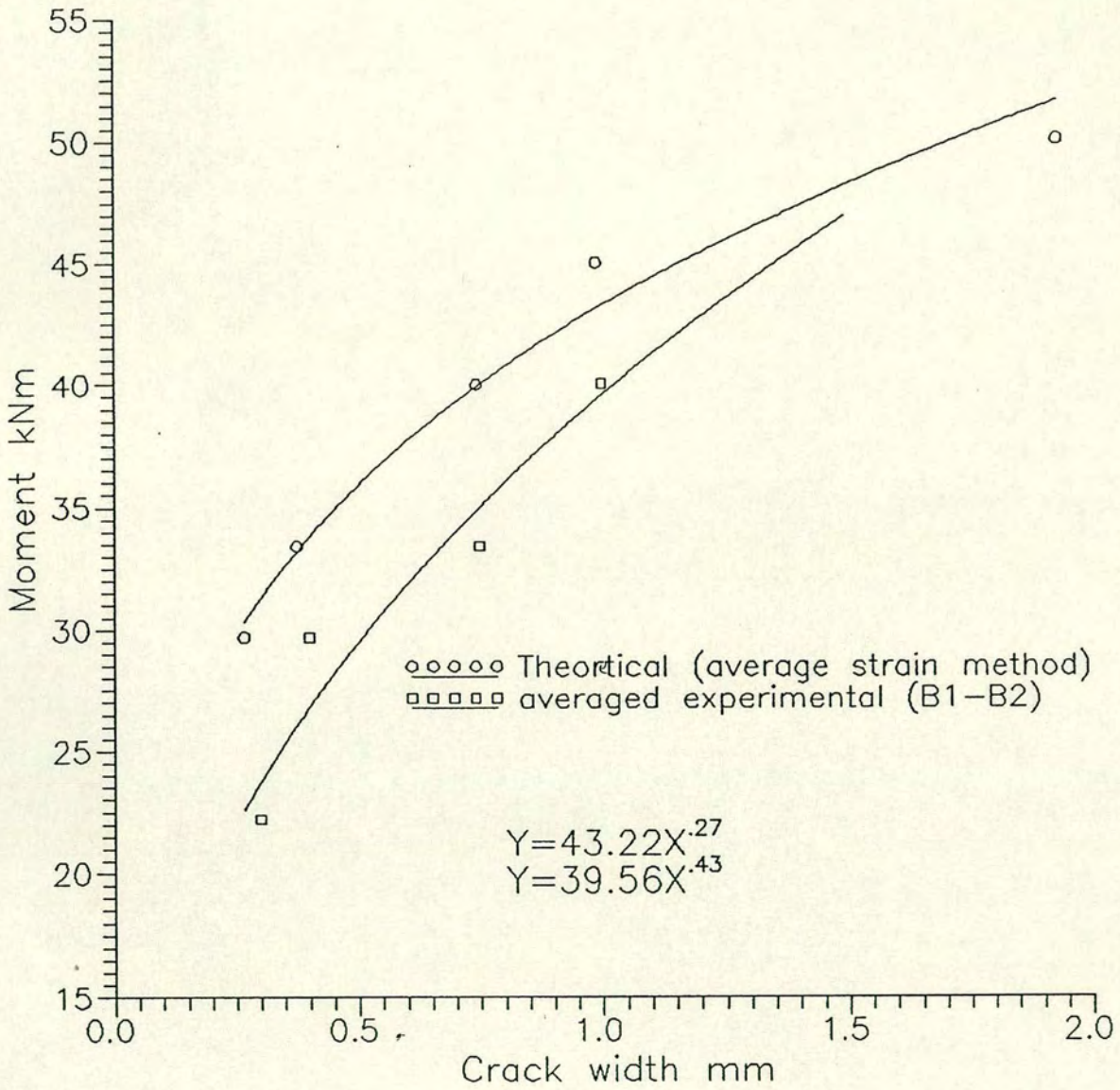

Comparison between predicted and experimental average crack width for flemish bond beams (B1–B2).

Figure 6–2–24

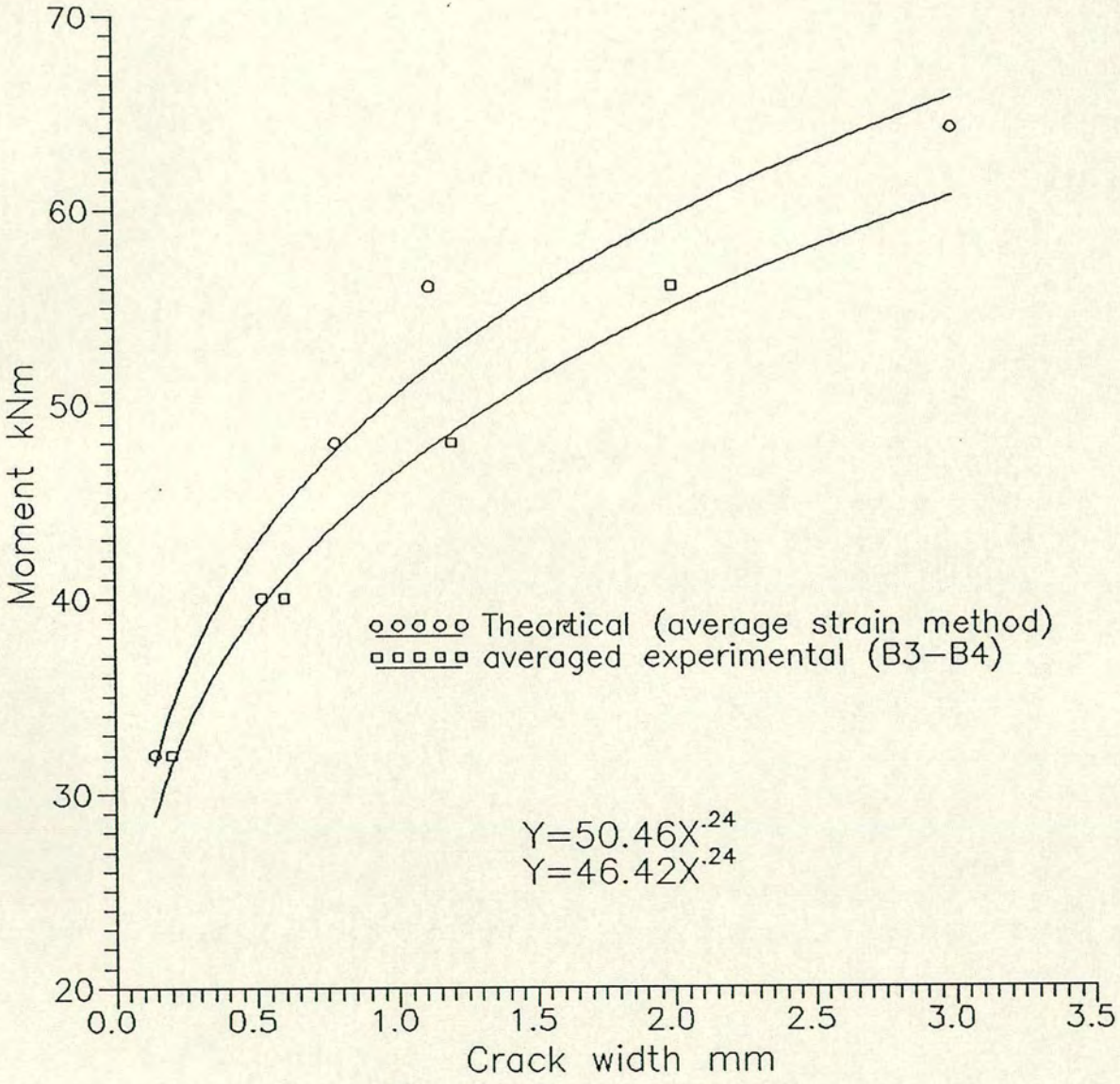

Comparison between predicted and experimental average crack width for English bond beams/slabs (B3–B4).

Figure 6–2–25

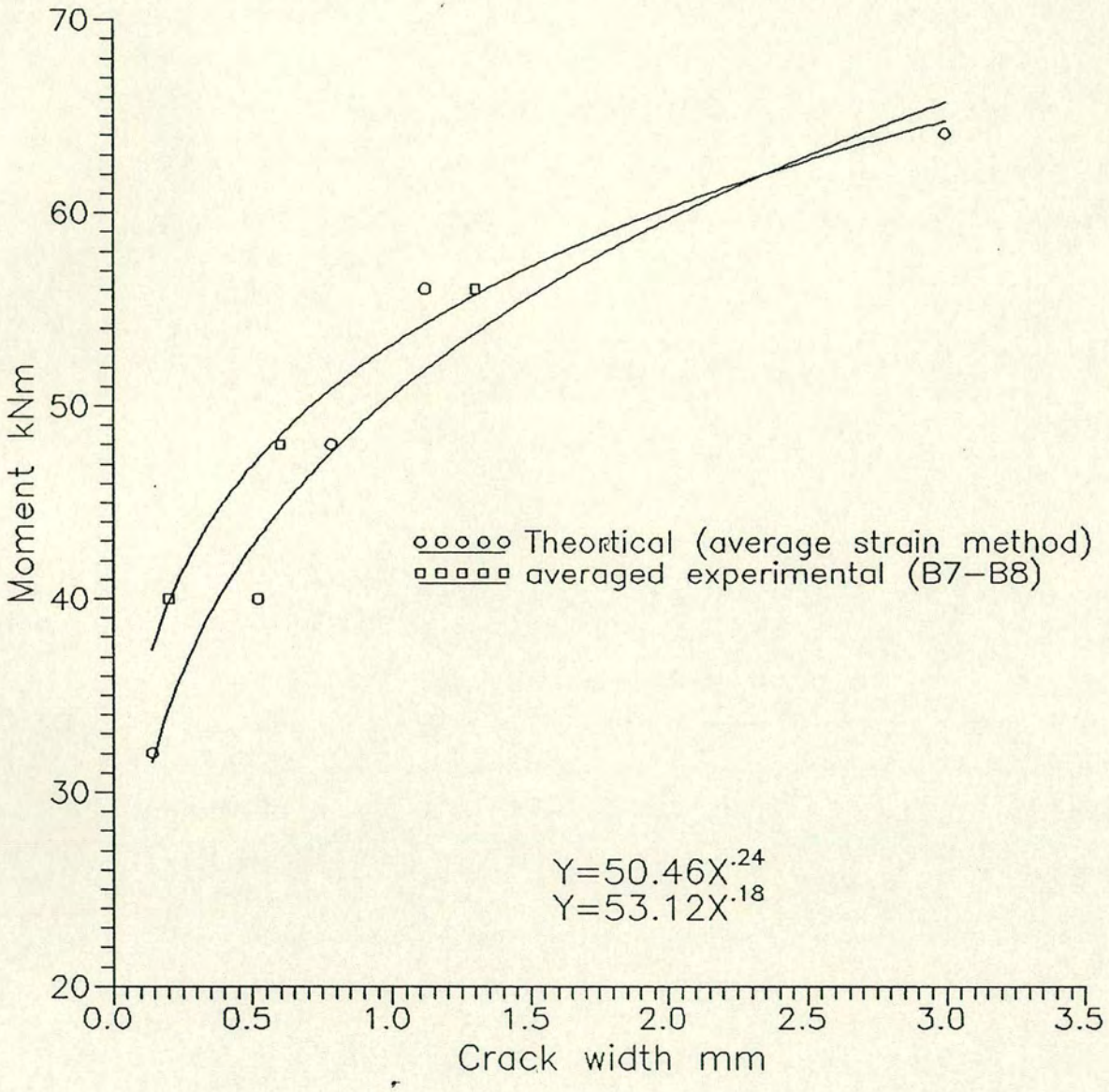

Comparison between predicted and experimental average crack width for English Garden bond beams/slabs (B7–B8).

Figure 6–2–26

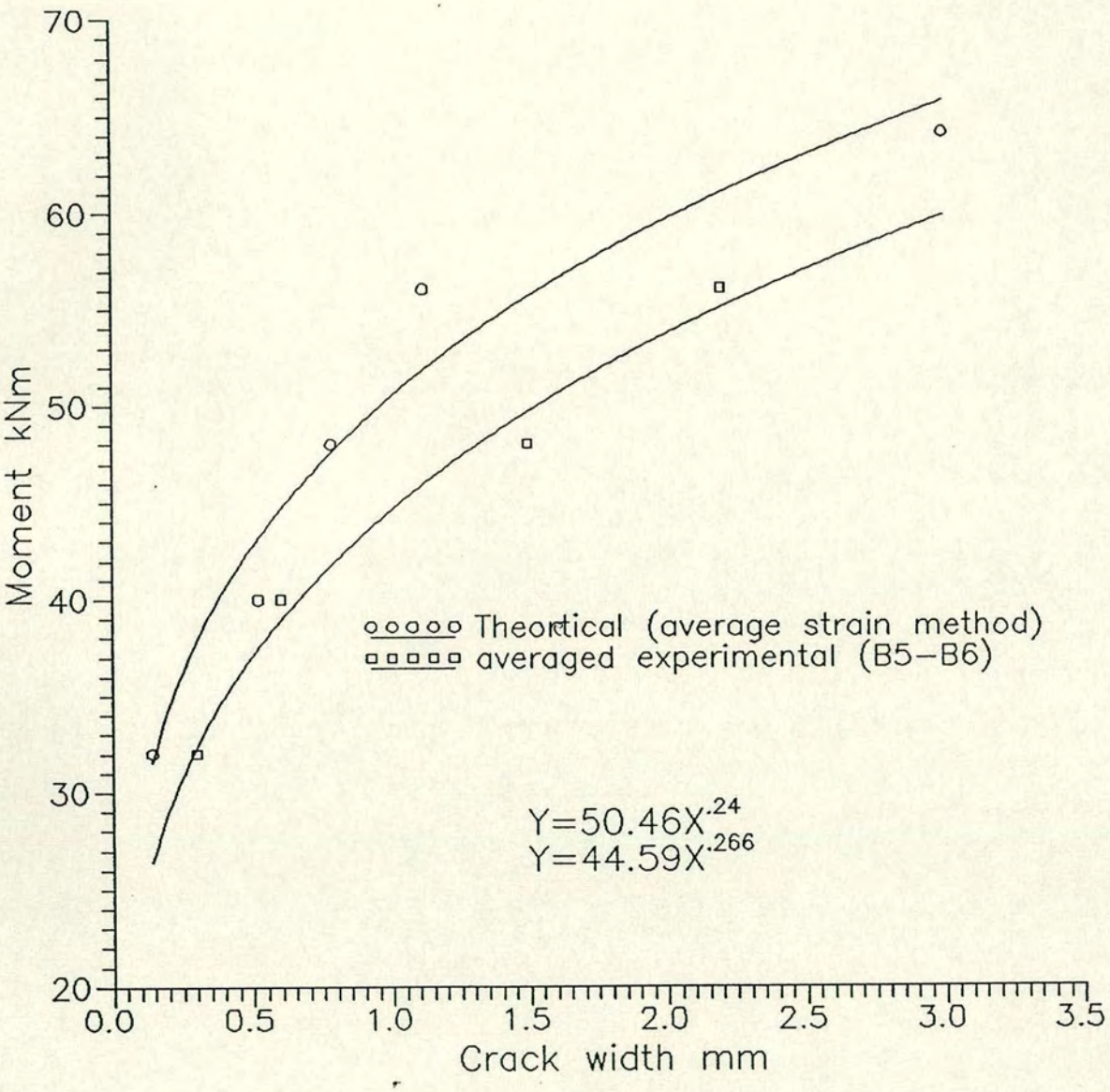

Comparison between predicted and experimental average crack width for Flemish Garden bond beams/slabs (B5–B6).

Figure 6–2–27

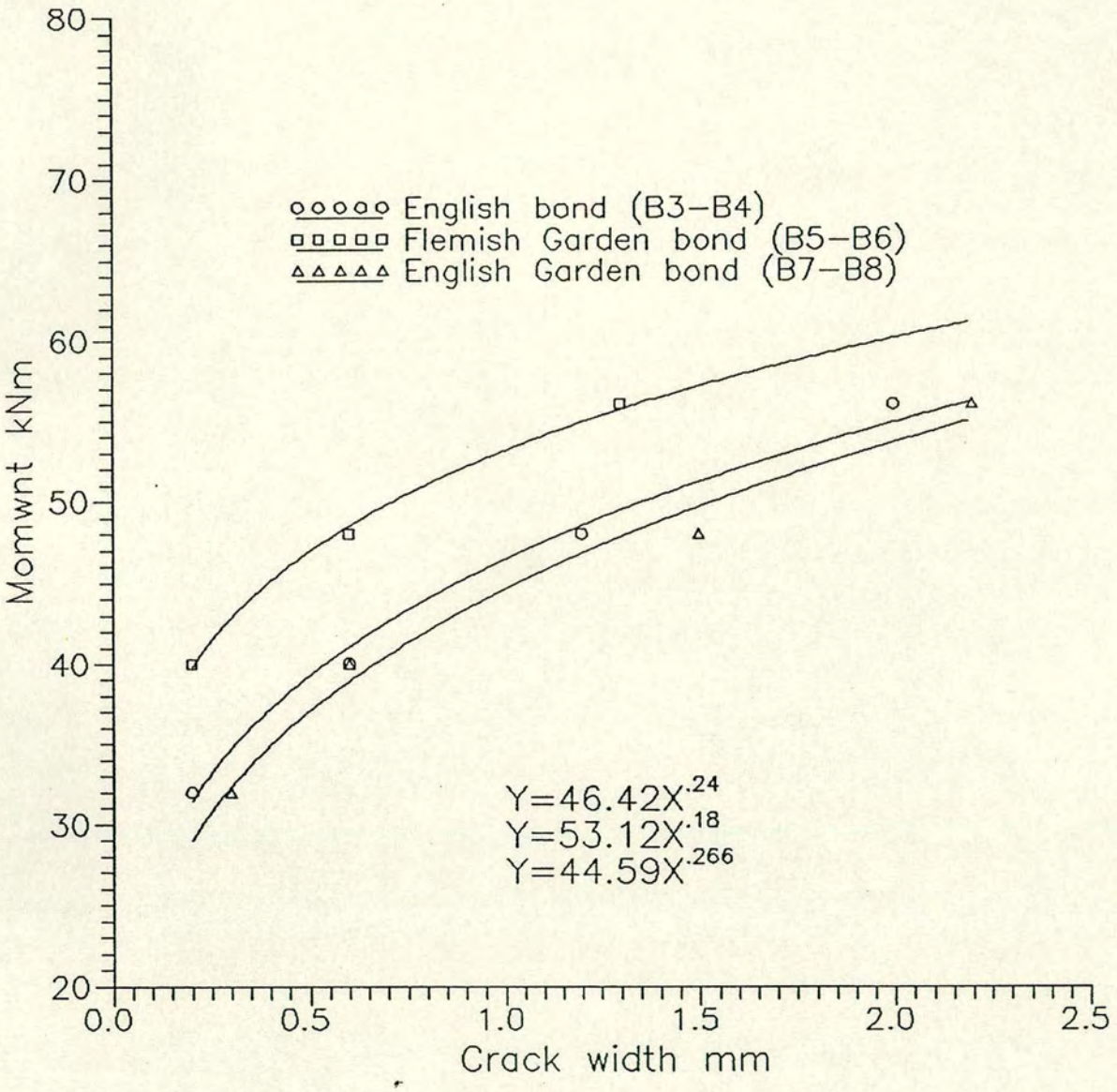

Crack width – moment relationship for English,flemish Garden and English garden bond beams/slabs.

Figure 6–2–28

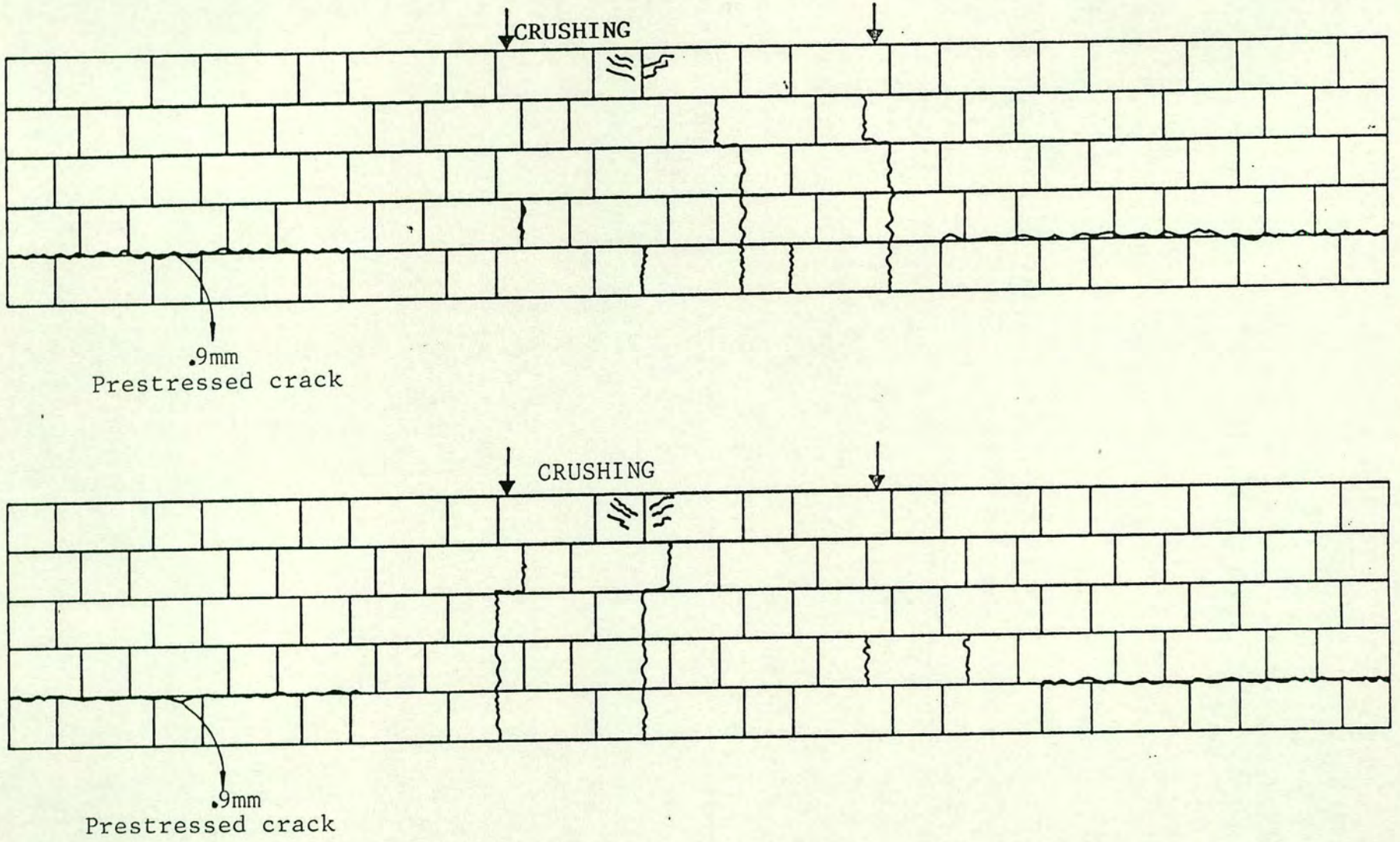

Figure 6.2.29 Crack Patterns for Flemish Bond Beams (B1-B2)

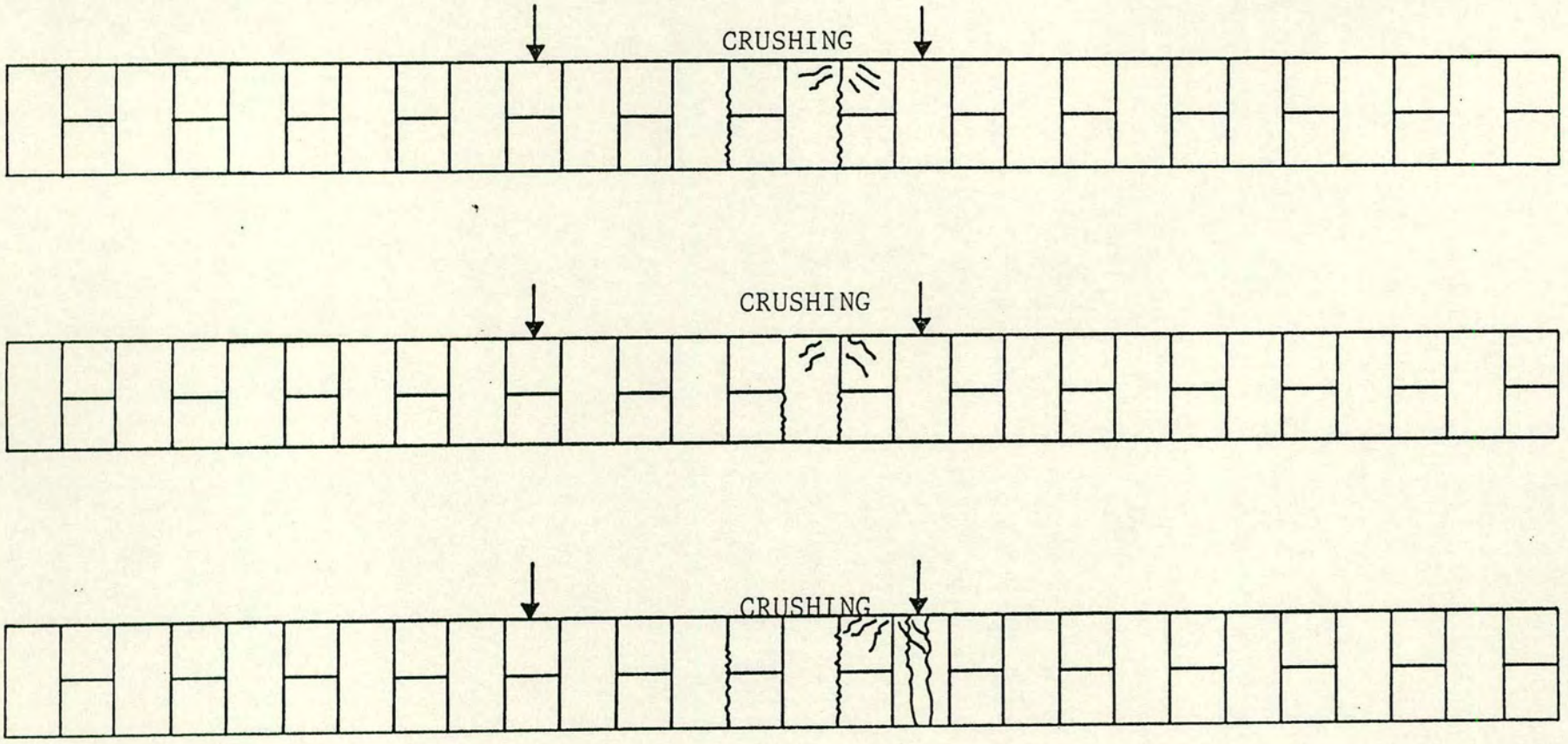

Figure 6.2.30 Typical Crack Patterns for English, Flemish Garden and Flemish Garden Beams/Slabs

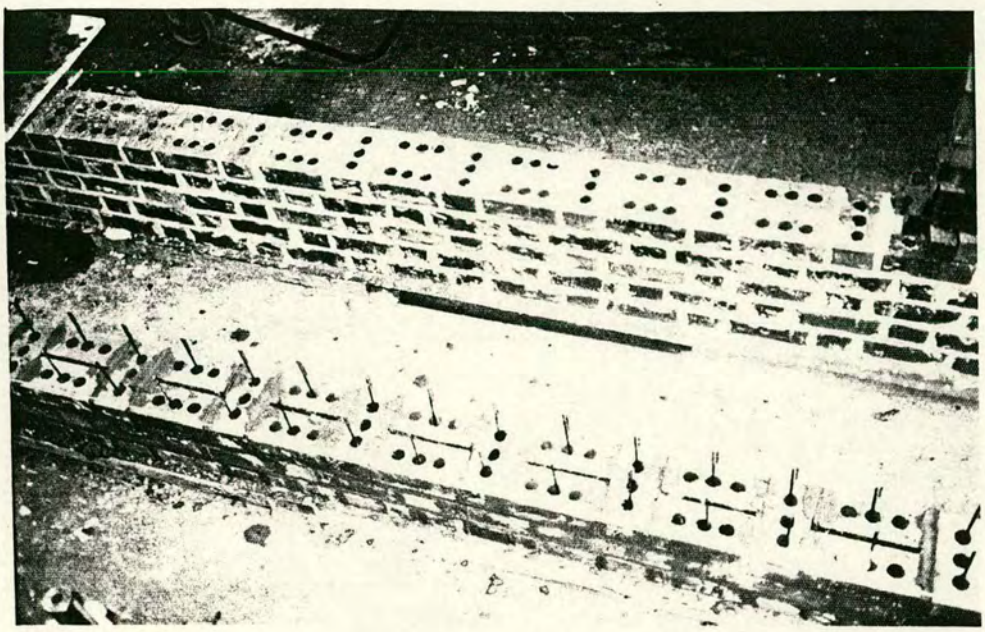

Figure 6.2.31 Flemish bond beams under construction (B1-B2)

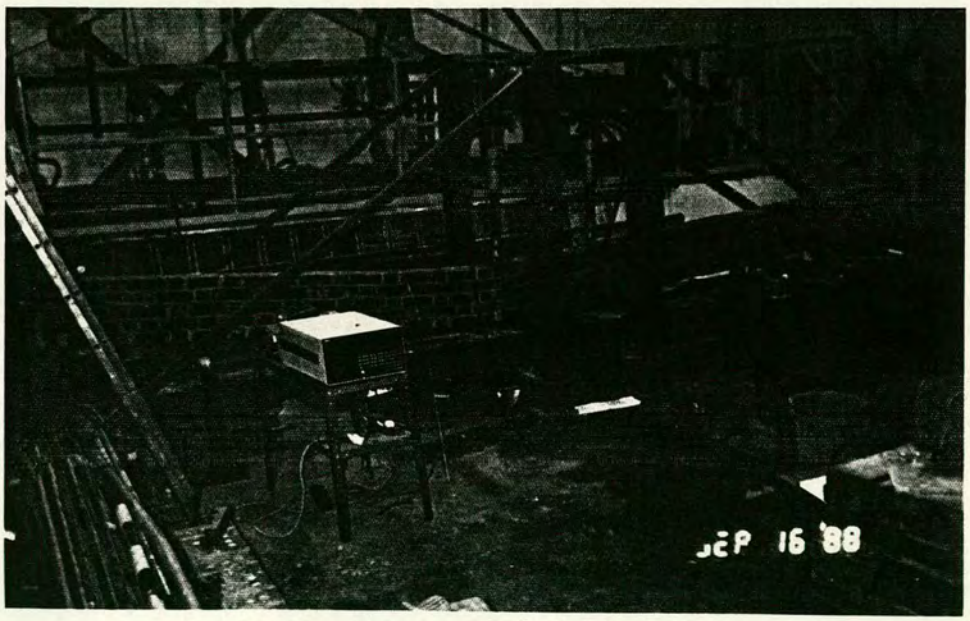

Figure 6.2.32 Typical failure of Flemish bond beams (B1-B2)

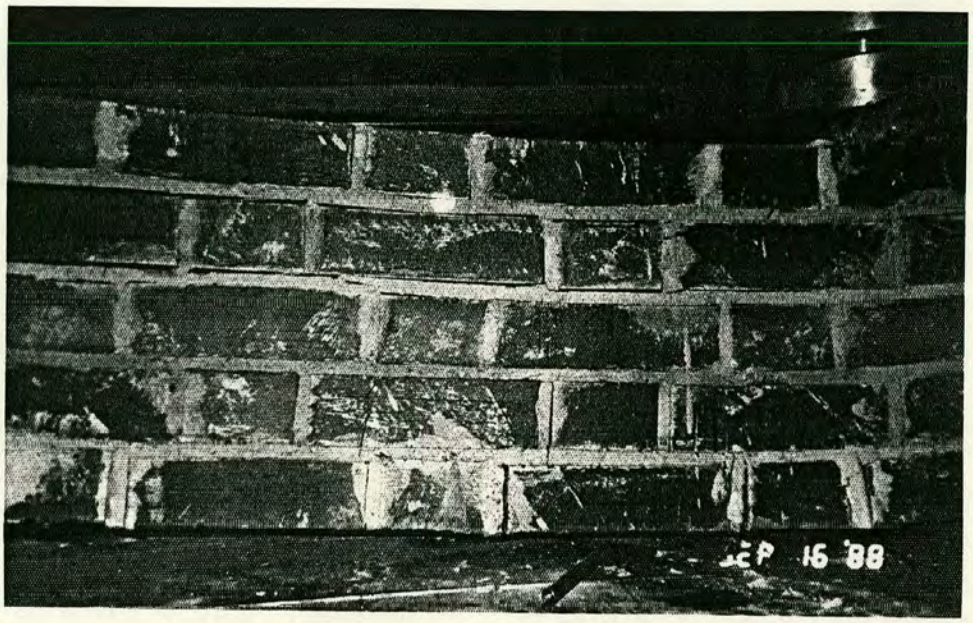

Figure 6.2.33 Typical failure mode and crack pattern for Flemish bond beams (B1-B2)

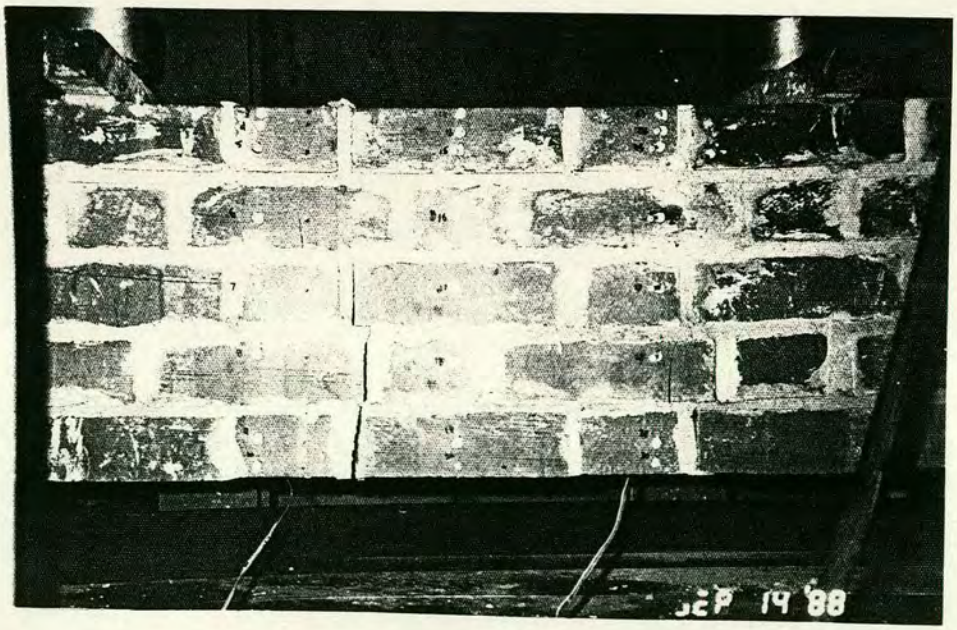

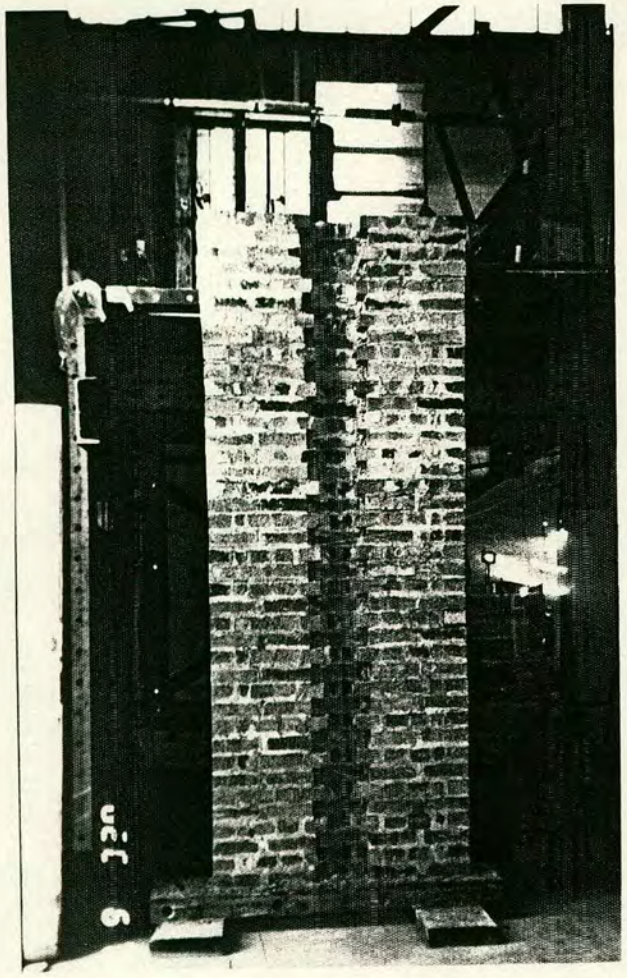

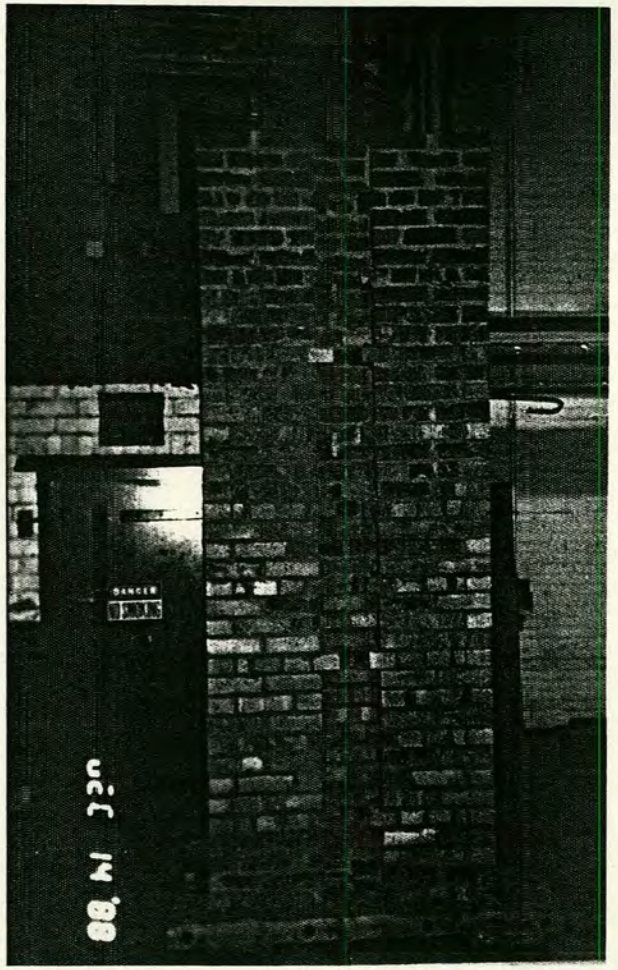

Figure 6.2.34 Beams/slabs after construction

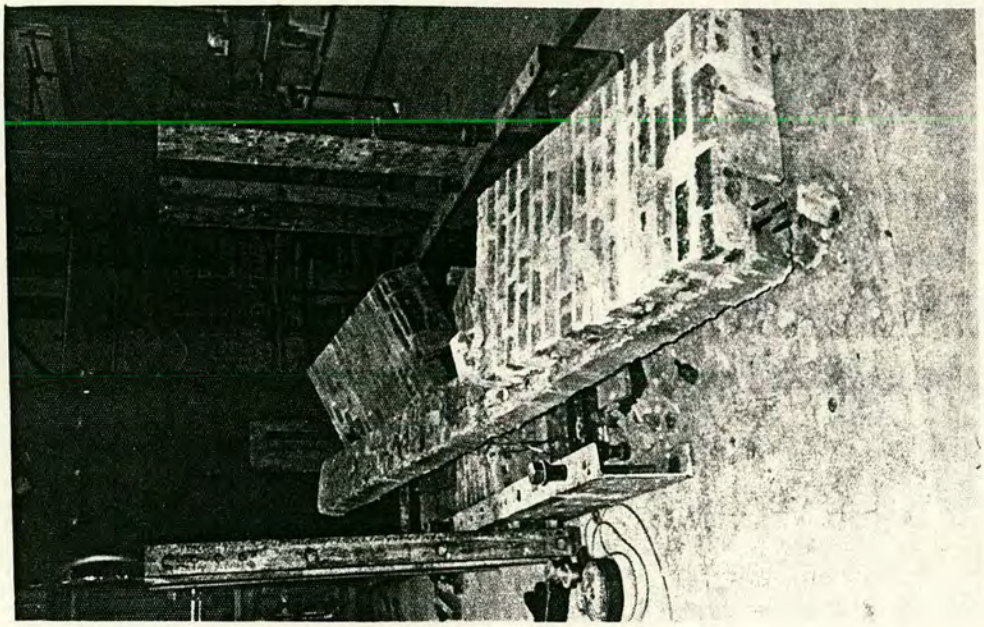

Figure 6.2.35 Typical failure mode of beams/slabs

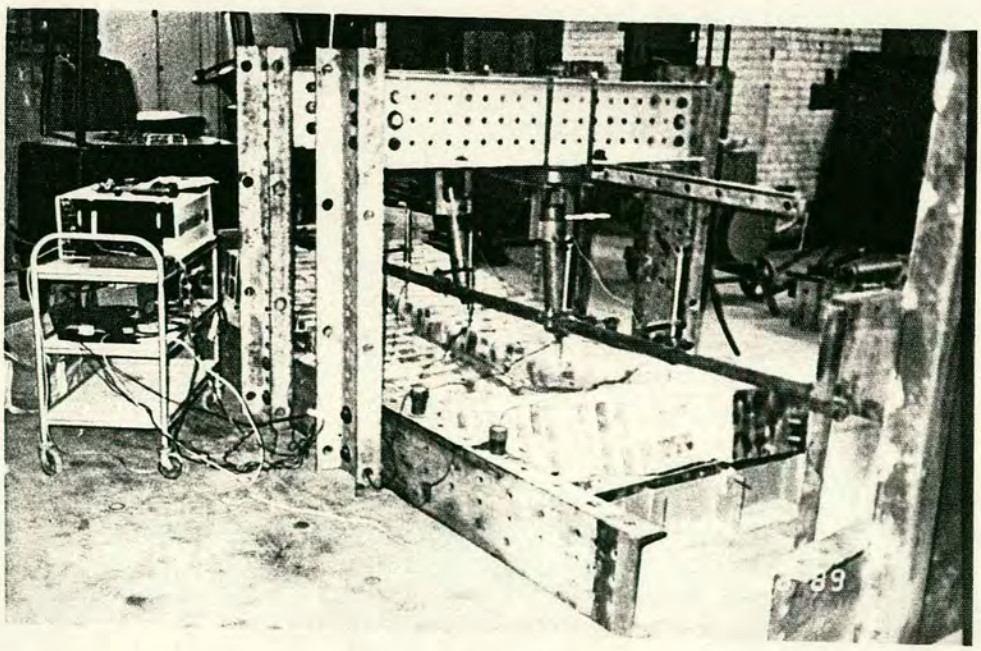

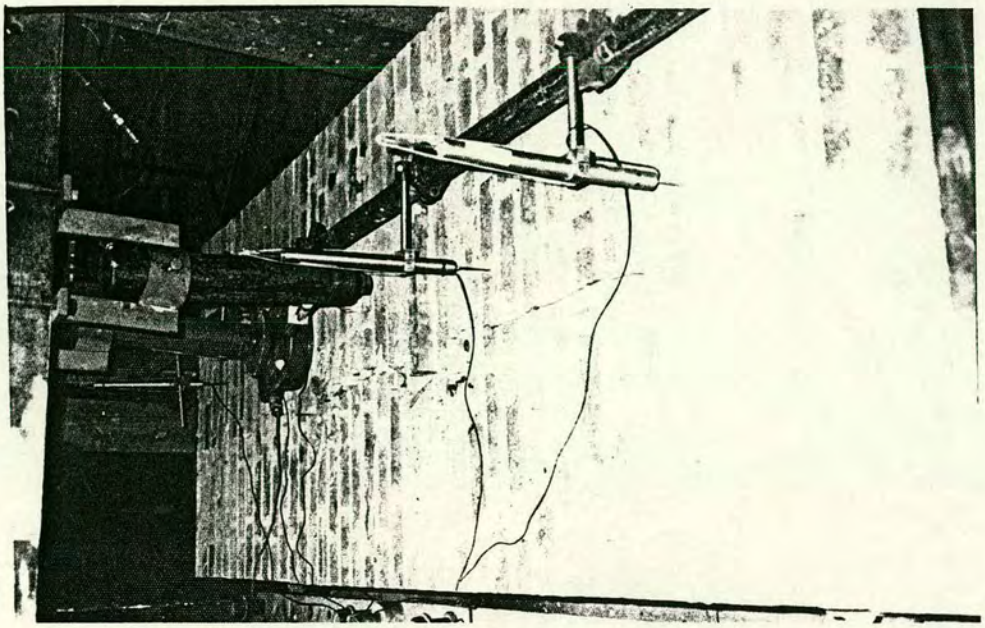

Figure 6.2.36 Typical failure mode and longitudinal crack along the pocket boundary for beams/slabs

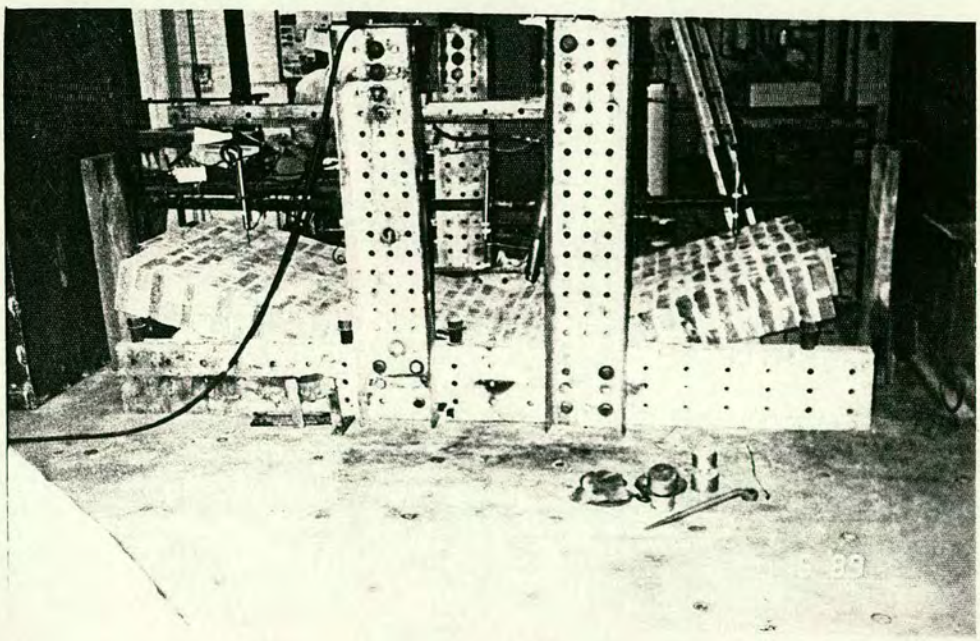

In the two Flemish bond beams, B_1 and B_2, slight hairline cracks in the bed joint near the soffit of the beam were noticed during the prestressing stage. The flexural cracks were initially propogated when the initial compression at the soffit had been neutralised and the flexural tensile strength of the brickwork exceeded. The flexural tensile strength is normally referred to as the modulus of rupture. The modulus of rupture was slightly affected by the type of bond especially when the bed joint ran perpendicular to the induced compressive stress. The tensile strength of individual brick and mortar is normally greater than that of the brickwork bonding where tensile failure usually occurs within the vertical brick/mortar joint interface. The bond strength varied from joint to joint and cracking occurred at the weaker joint first (poorly filled joints). The distribution of the crack spacing at the constant moment zone was influenced by the type of bonding. However, the crack spacing was mainly between one or two vertical joints Figs 6.2 • 29-30. At higher loads, cracks were propagated through the bricks to the uppermost bed joint where some cracks propogated diagonally towards the mid-section. At the maximum load, splitting occurred along the uppermost bed joints of the beams, at which time, the beams were no longer able to sustain further load and failure took place in a ductile mode. When the cracks reached the uppermost section of the beam, it became apparent that the uppermost part of the beam was carrying most of the compressive force in the section. Therefore, the compressive strength of single course prisms adequately represented the compressive strength of the prestressed brickwork beam. Prior to cracking, all the beams had adequate stiffness; after cracking, all the beams had a reduced stiffness causing a rapid increase in deflection with no corresponding increase in load.

The beams B_3 - B_8 failed secondarily due to cracking along the length of the upper section. The longitudinal crack initiated in the middle of the beams in the constant moment zone. At higher deflections, the crack propagated throughout the length of the beam. This type of failure was observed by Adekola, Barnard, Johnson, Sless and Reddy (Adekola, A.O., 1959; Barnard, P.R. and Johnson, R.P., 1965, Siess, C.P. et al, Reddy, V.M., 1968)., They all pointed out that the cause of failure was the transverse tensile stress along the length of the beam. Adekola concluded that 0.4% minimum transverse reinforcement in the concrete floor with adequate bond length was sufficient to prevent such a failure at working load. The author tested composite beams with a ratio of flange width to span equal to 0.40 and 0.187, and indicated that the correct choice of width to span ratio with respect to percentage of transverse reinforcement is required to prevent this type of failure. In this investigation, the development of the longitudinal cracks can be explained by the following two simultaneous actions :-

First, following excessive deflection, the post-tensioned pocket type brickwork beam can be considered as a composite structure, i.e. reinforced concrete and no fill brickwork beams, bonded together along their contact surfaces. Since the adhesion is weak, the two pieces separated and slid relative to each other . If the adhesive is effective, there are stresses acting which prevent this sliding or shearing. These horizontal stresses are the shear stresses which act separately in the plane along the bottom and sides of the pocket between the infill concrete and the brickwork beam. The same shear stresses occur in the horizontal plane in the infill concrete and in the brickwork beams, and differ in intensity according to their distance from the neutral axis.

Second, after separation of the concrete infill and the brickwork beam, as explained, the transverse tensile stresses in the brickwork, which are induced by the excessive deflection and the compressive stress perpendicular to the bed joint, initiate a crack at the "top" of the middle part of the beam which propagates through the structure until failure.

From experimental observations the longitudinal separation of the brickwork along the shear connection is not a serious problem. This is because the longitudinal crack only developed after the rapid increase in deflection, with no corresponding increase in load, and can therefore be considered as a secondary mode of failure.

6.2.10 Summary and Conclusions

The commercial bonds considered incorporated both headers and stretchers in the wall and were arranged with the header placed centrally over each stretcher in the course below to achieve a bond and minimise the number of straight joints. Two beams, B_1 and B_2 were fabricated using Flemish bond with the joints running parallel to the direction of the prestressing load. The results from tests on these beams could be compared with results from tests on the English bond beams.

Six beams, B_3 to B_8, were fabricated using English bond, Flemish Garden bond and English Garden bond. The sections were built standing vertically, consequently the bed joint runs perpendicular to the direction of the induced prestressing load. The aim of the test was to study the flexural behaviour of post-tensioned brickwork structures of variable bonds up to failure. All the beams were tested in a two point loading rig and simply supported on a pin and roller. Since the applied load is

primarily due to bending, the theory of beams and slabs can be applied to retaining walls where shear force and bending moment are greatest at the base. Three methods of analysis were considered, viz. stress block , direct method of analysis and finite element analysis. The direct analysis was based on the derivation of the theoretical moment from a simplified cubic parabolic stress/strain relationship for brickwork in the compression zone. The direct method of analysis had been previously used for prestressed concrete and more recently introduced to prestressed brickwork beams by Pedreschi (as shown in Appendix B). Finite element analysis was based on three dimensional geometrically and materially non-linear discretisation, consisting of 290 semiloof shell elements. The material model was capable of modelling a non-linear bi-axial concrete material. The results obtained from the analysis were then compared with those based on the Code of Practice, BS 5628, Part 2.

The conclusions from the theoretical and experimental analyses can be summarised as follows:

1. All the prestressed brickwork beams exhibited a ductile flexural mode of failure, caused by the steel yielding in the maximum moment zone, that is similar to an under reinforced concrete structure. The mode of failure is independent of the type of bond used in the beam.

2. The moment-curvature and the load-deflection relationships for all the prestressed brickwork beams exhibit a distinct three phase type of behaviour corresponding to uncracked, cracked with the steel still elastic and cracked with steel yielding.

3. The orientation of the bedjoint in the beam in relation to the induced prestressing load has an insignificant effect on the ultimate flexural strength of the beam.

4. The prestressed brickwork beams with Flemish bond, B_1 and B_2, where the bed joints run parallel to the direction of the induced prestressing load, achieved smaller flexural strengths and cracking moments, and exhibited greater deflections and curvatures than the English bond beams tested by Pedreschi.

5. The behaviour of prestressed brickwork beams with Flemish Garden bond, B_5 and B_6,where the bed joints running perpendicular to the direction of the induced prestressing load, acheived slightly larger flexural strengths and cracking moments, and smaller deflections and curvatures than the beams with English bond and English Garden bond.

6. The theoretical analysis, based on the deformation characteristics obtained from single course prisms tested in this project, predicted satisfactorally the general behaviour characteristics of all the beams.

7. The prestressed pocket brickwork beams, B_3 - B_8, all failed by secondary cracking along the pocket boundary. Shear reinforcement, in the form of rectangular links located across the pocket boundary, may have prevented the formation of a shear crack.

8. The results confirmed the practical application of prestressed brickwork slabs and retaining walls with various types of bond.

6.3 WALLS

6.3.1 General

The method normally used to investigate earth retaining walls assumes a triangular pressure distribution, so this was selected in the current programme to test the pocket walls which are generally 3 m high, and of uniform thickness with a pocket spacing of 1.0 m. Six half scale post-tensioned brickwork retaining walls were tested to examine the effect of varying the area of steel on the magnitudes of deflection, cracking and ultimate moment of the wall. The brickwork walls were built in English bond, and vertical pockets were formed around the reinforcement by omitting the whole or half bricks from the bond as shown in Fig. 4.6. A maximum of two pockets per wall were chosen to examine the possibility of the brickwork arching between the pockets or the wall splitting vertically due to the development of lateral tension from the overlap prestressing forces. The walls were fabricated vertically onto a steel base, whereas on site the retaining wall would be constructed on a reinforced concrete base. In the laboratory, the use of a steel base was more economic as it could be more easily repaired and reused after each test was completed. The steel base was more easily anchored to the strong floor and was designed to allow the location of the reinforcement to be varied. The displacements were measured using linear voltage displacement transducers with a maximum travel of 25 mm. The transducers were set at the mid height and top of the wall, and as the displacement at the top of the wall was greater than 25 mm, the transducers had to be moved several times during the test. An inclinometer was placed at the bottom of the wall to measure any

rotation of the wall. Seven horizontal jacks were mounted on three beams attached to the back of the strong wall at three levels up the wall. The jacks were mounted horizontally on a rigid steel reaction frame. A plastic bag filled with dental plaster was placed between the spreader beam and the wall to distribute the load evenly over the brickwork surface, as shown in Fig 6.3 . 29. The loading arrangement was chosen to give a combination of bending moment and shear force at the base of the wall similar to that produced by a triangular pressure distribution. The load was applied incrementally in ten or more stages up to total failure. At each increment of load, deflections and crack propagation were recorded.

All the walls failed in flexure due to either the reinforcement reaching its yield stress or the brickwork crushing Fig 6.3 . 32. There was no indication of any shear failure in any of the tests. Walls 1 and 2 failed due to the steel yielding, whilst walls 4, 5 and 6 failed by crushing of the brickwork. Wall 3 failed as a balanced section (i.e. both yielding and crushing occurred at the same time). There was no indication of any arching of the brickwork panels or vertical splitting of the wall between the pockets. Finite element analysis was adopted as the best theoretical method of simulating the complex bending behaviour of the prestressed brickwork structure in which the wall spans vertically from the base whilst the brickwork panels span horizontally between the pockets. The finite element analysis was modelled by discretisation consisting of 154 elements. The analysis was geometrically and materially non-linear, and based on three dimensional semiloof shell elements. The theoretical and experimental results showed that prestressing took advantage of the greater compressive strength of the material by applying a compressive force which increased the amount of applied lateral load required to

cause the deflection, cracking and ultimate moment of the wall and reduced the possibility of premature shear failure.

6.3.2 Ultimate Moment

The post-tensioned rods were located within the wall section at a distance not greater than h/6 from the centroid, where h is the overall depth, to avoid tensile stresses due to prestress. When the precompression caused by the prestress force at the soffit was neutralised, tensile stresses developed and flexural cracking took place. The experimental results for the ultimate moments and shear stresses at failure for all the walls tested are summarised in Table 6.8. In walls 1, 2 and 3, horizontal splitting of the bottom bed joints of the wall was observed at high levels of load towards failure. In walls 4, 5 and 6, splitting of the bed joint perpendicular to the direction of the compressive force occurred, followed by crushing of the brickwork in the compression zone. Using the strain measurements taken in the steel rods, it was possible to determine whether the strain in the steel exceeded the strain corresponding to the proof stress and hence the failure mode. It is of considerable practical interest to find the balanced section with respect to the overlap prestressing forces. The percentage of tensile reinforcement used in wall 4 was repeated in wall 6. Both walls exhibited a similar mode of failure. Wall 3 was designed as a balanced section, in which both materials, brickwork and steel reach their respective crushing & yield simultaneously, whereas wall 5 performed as a highly over-reinforced structure. From the test results, the following conclusions were drawn:

i) The minimum spacing of the pockets in post-tensioned brickwork retaining walls was confirmed as H/3 where the panel length is

considered as the distance between the centre line of the formed pockets.

ii) Arching of brickwork panels between pockets in post-tensioned brickwork retaining walls subjected to high lateral load does not occur.

iii) Vertical splitting of post-tensioned brickwork retaining walls due to the development of lateral tensile stresses between the pockets caused by the induced overlap prestressing forces does not occur. Table 6.8 compares the experimental ultimate moments with the predicted moments using finite element analysis, direct method of analysis and the recommendation of the draft code of practice, B.S.5628.

The moments predicted from the direct method of analysis generally underestimate the experimental results by 30%, whereas the ultimate moments, based on finite element analysis, average within 96% of the experimental results. This is because the finite element analysis takes into account the extra nominal strength gained by the development of the overlap prestressing forces. Fig. 6.3.1 shows the relationship between ultimate moment and percentage area of steel for all the experimental results. When the area of steel and prestress force increased the failure load also increased. Fig. 6.3.25 showsthe variation of the neutral axis depth with steel area. An increase in steel area in a fully prestressed brickwork retaining wall therefore increased the ultimate moment and the neutral axis depth, especially where the section is over-reinforced and the steel does not yield.

Wall	Brick Strength N/mm^2	Mortar Strength N/mm^2	Grout Strength N/mm^2	Span M	a/d ratio	% steel	Effective Prestress KN	Ultimate Moment kNM	Shear Stress N/mm^2	Failure Mode
1	36	28.65	25.00	1.70	4	0.10	34	13.88	0.31	Tension
2	36	25.90	31.60	1.70	4	0.151	51	15.87	0.36	Tension
3	36	28.50	30.20	1.70	4	0.201	68	23.80	0.54	Tension
4	36	28.15	22.20	1.70	4	0.251	85	27.77	0.63	Compression
5	36	28.70	28.80	1.70	4	0.302	102	31.73	0.72	Compression
6	36	28.20	28.70	1.70	4	0.251	85	25.78	0.58	Compression
-	-	-	-	-	-	-	-	-	-	-

Table 6.7 Summary of Experimental Results

		Theoretical				BS 5628 using own prisms			
Wall	Exp.	F.E.	$\frac{\text{exp.}}{\text{theory}}$	Direct Method	$\frac{\text{exp.}}{\text{theory}}$	$\gamma_{mm}=1.0$ $\gamma_{ms}=1.0$	$\frac{\text{exp.}}{\text{code}}$	$\gamma_{mm}=2.0$ $\gamma_{ms}=1.15$	$\frac{\text{exp.}}{\text{code}}$
1	13.88	14.50	0.96	8.08	1.72	8.36	1.67	6.88	2.0
2	17.85	18.64	0.96	11.66	1.53	12.20	1.46	9.12	1.96
3	23.80	24.50	0.97	15.02	1.59	15.80	1.51	10.92	2.18
4	27.77	28.50	0.97	17.88	1.55	18.55	1.51	12.60	2.20
5	31.73	32.50	0.98	20.45	1.55	20.96	1.51	14.08	2.25
6	25.78	28.50	0.91	17.88	1.44	18.44	1.40	12.60	2.0

Table 6.8 Ultimate Moment kNM

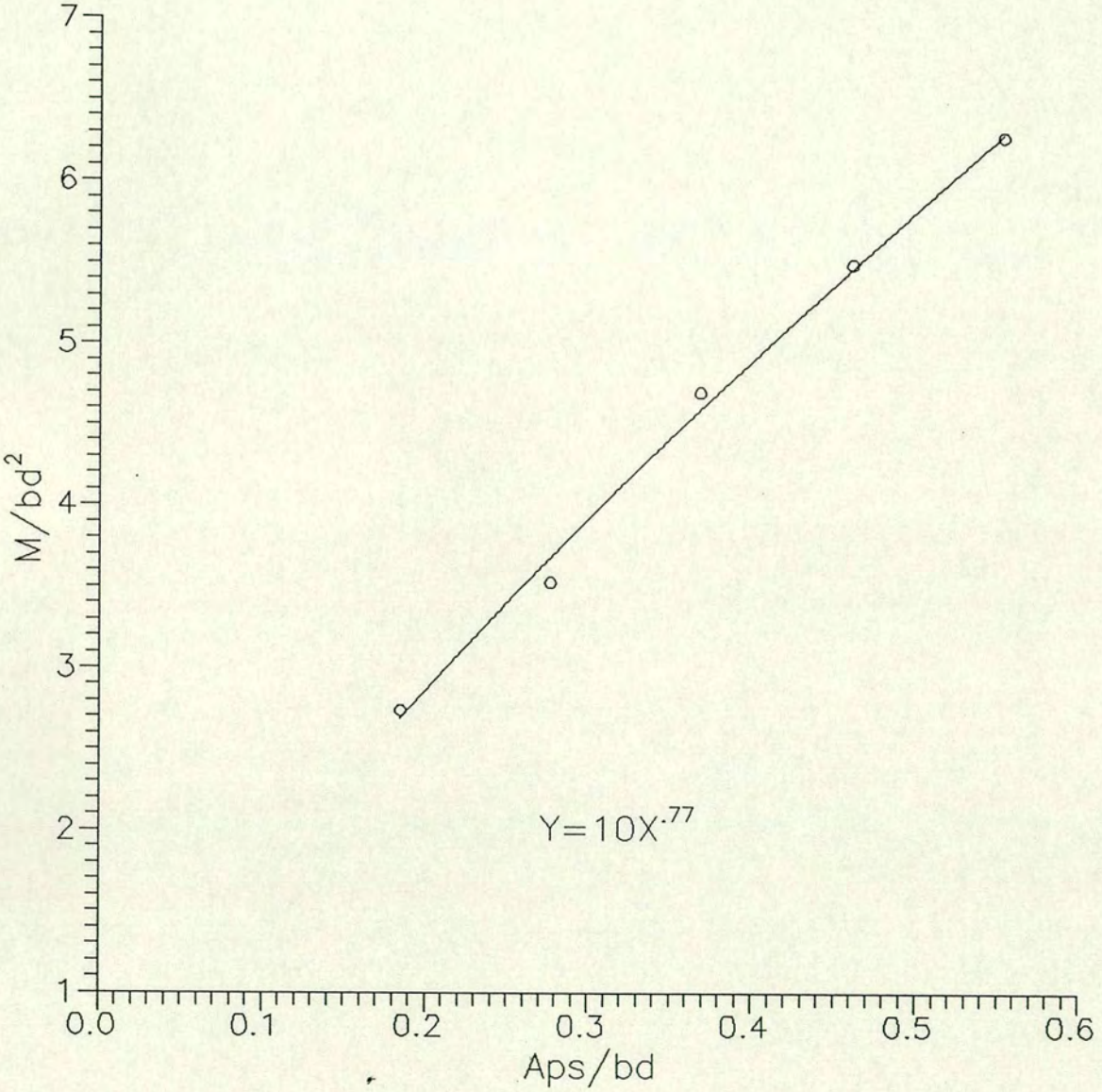

The effect of steel % on ultimate moment for wall1 to wall6.

Figure 6–3–1

6.3.3 Relationship between Steel Strain and Moment

The additional strain in the reinforcement was influenced greatly by the presence of cracking in the maximum moment zone. Figs. 6.3.2-6 show the experimental relationship between the moment and the additional strain in the strand. As cracks did not form at an early stage in wall 5, the relationship between moment and steel strain for this wall was not influenced by the presence of cracks. In the walls where flexural failure took place, the failure mode could be anticipated by comparing the values of strain measured with the proof stress. Figs. 6.3.2-6 show that in walls 1, 2 and 3 the strain in the steel was at the yield point, whereas in walls 4, 5 and 6 the strain in the steel was well below the yield point. This resulted from differences in the magnitude of the prestress forces and the percentage of steel in the walls.

In walls 1, 2 and 3, the slope of the curve for the steel strain beyond the proof stress became steeper in the direction of the x-axis. All the curves plotted of additional strain in the tensioned steel against moment show similar characteristics. Initially, a linear elastic relationship exists between the moment and the steel strain up to cracking, after which the strain increases more rapidly up to total failure.

6.3.4 Relationship between Top Fibre Strain and Moment

Figs 6.3.7-11 present the compressive strains measured in the top fibres in the maximum moment zone, i.e. the second layer to the base of the wall. The compressive strain in each wall was linear up to cracking so that the wall was behaving elastically. After cracking, the strain increased more rapidly with respect to the applied moment until failure occurred. In walls 4, 5 and 6, the strains were only measured up to a point prior to sudden crushing of the brickwork. In walls 1, 2 and 3, the

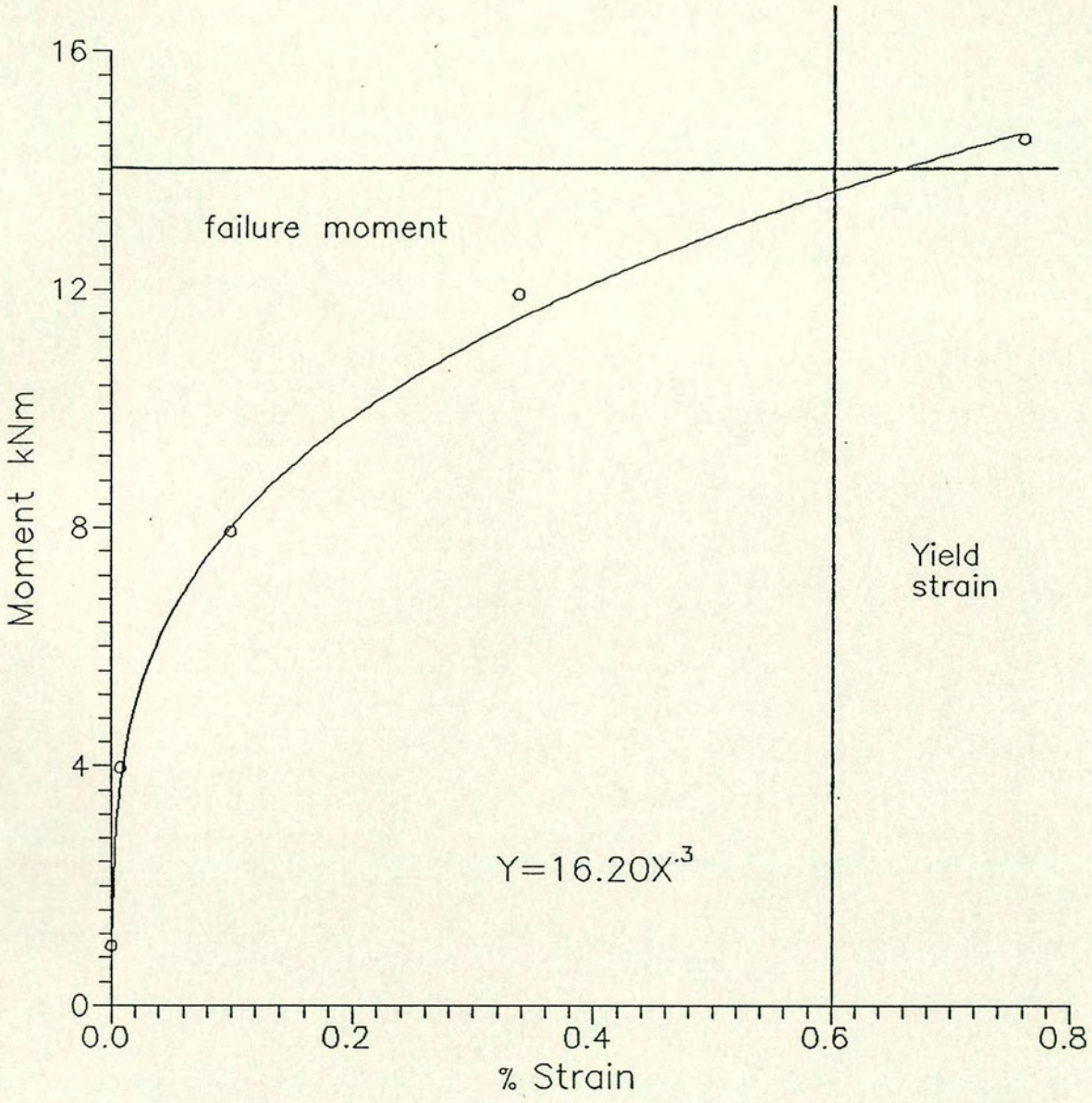

Steel strain – moment relationship for wall1.

Figure 6–3–2

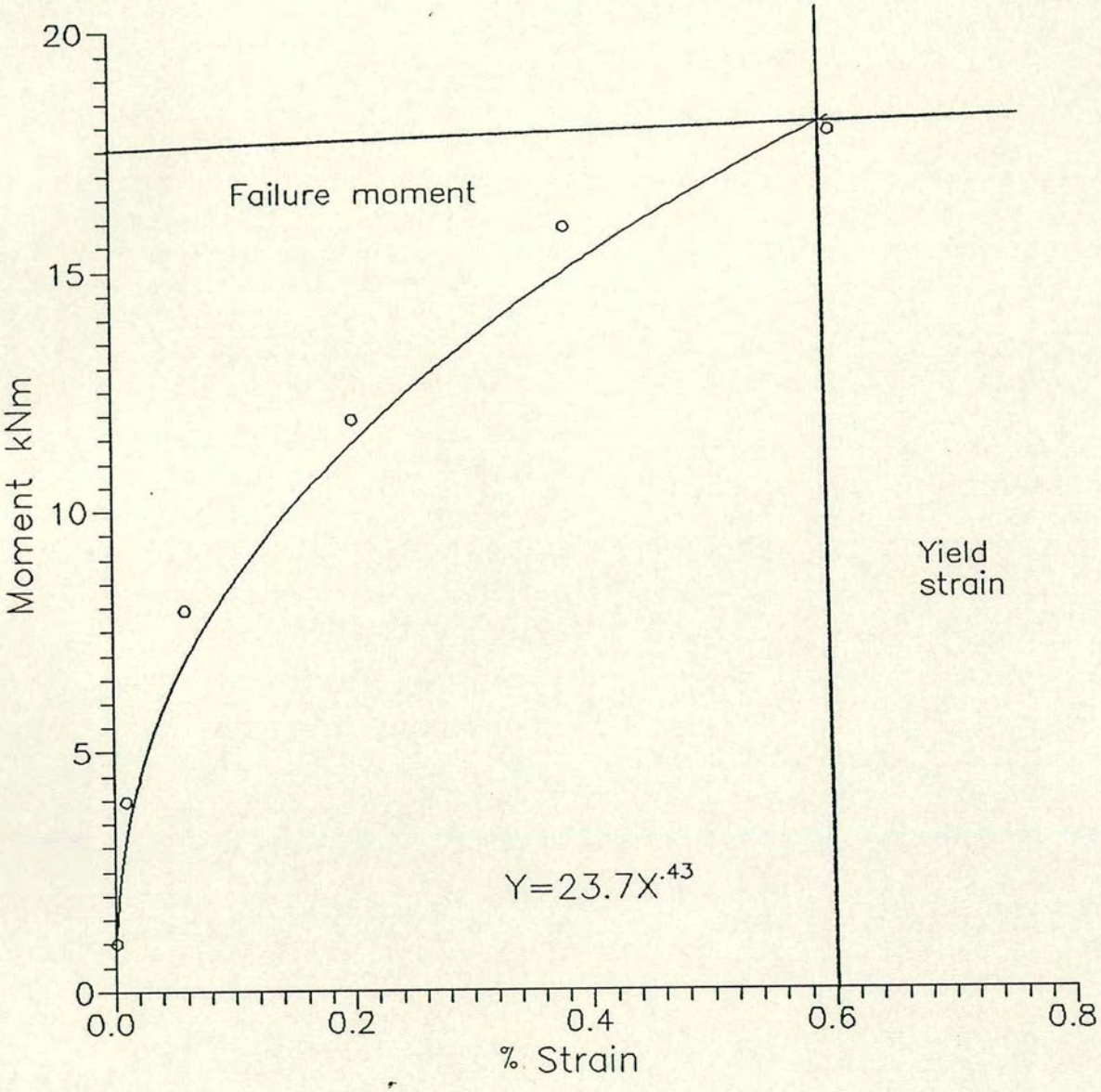

Steel strain – moment relationship for wall2.

Figure 6–3–3

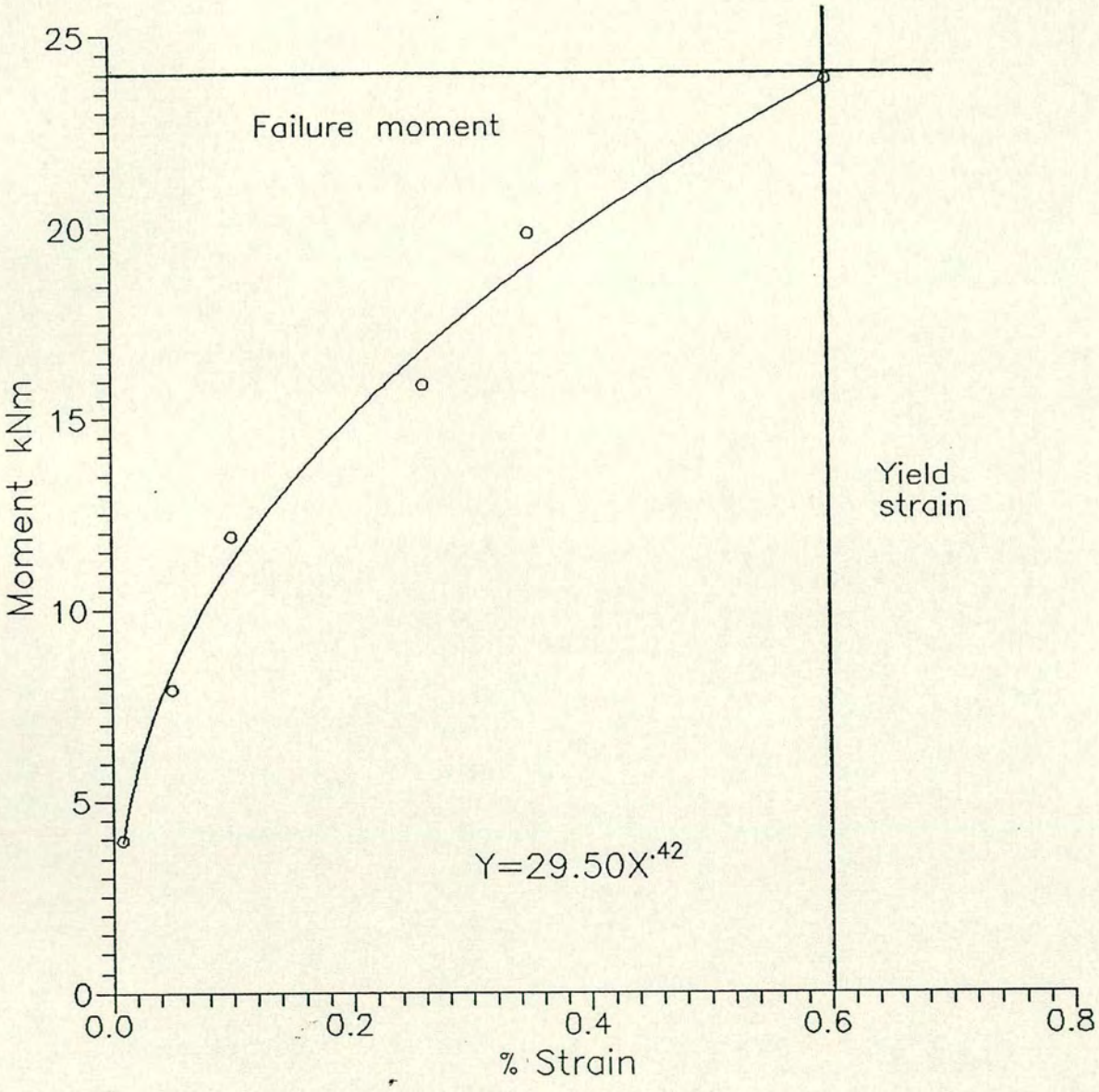

Steel strain – moment relationship for wall3.

Figure 6–3–4

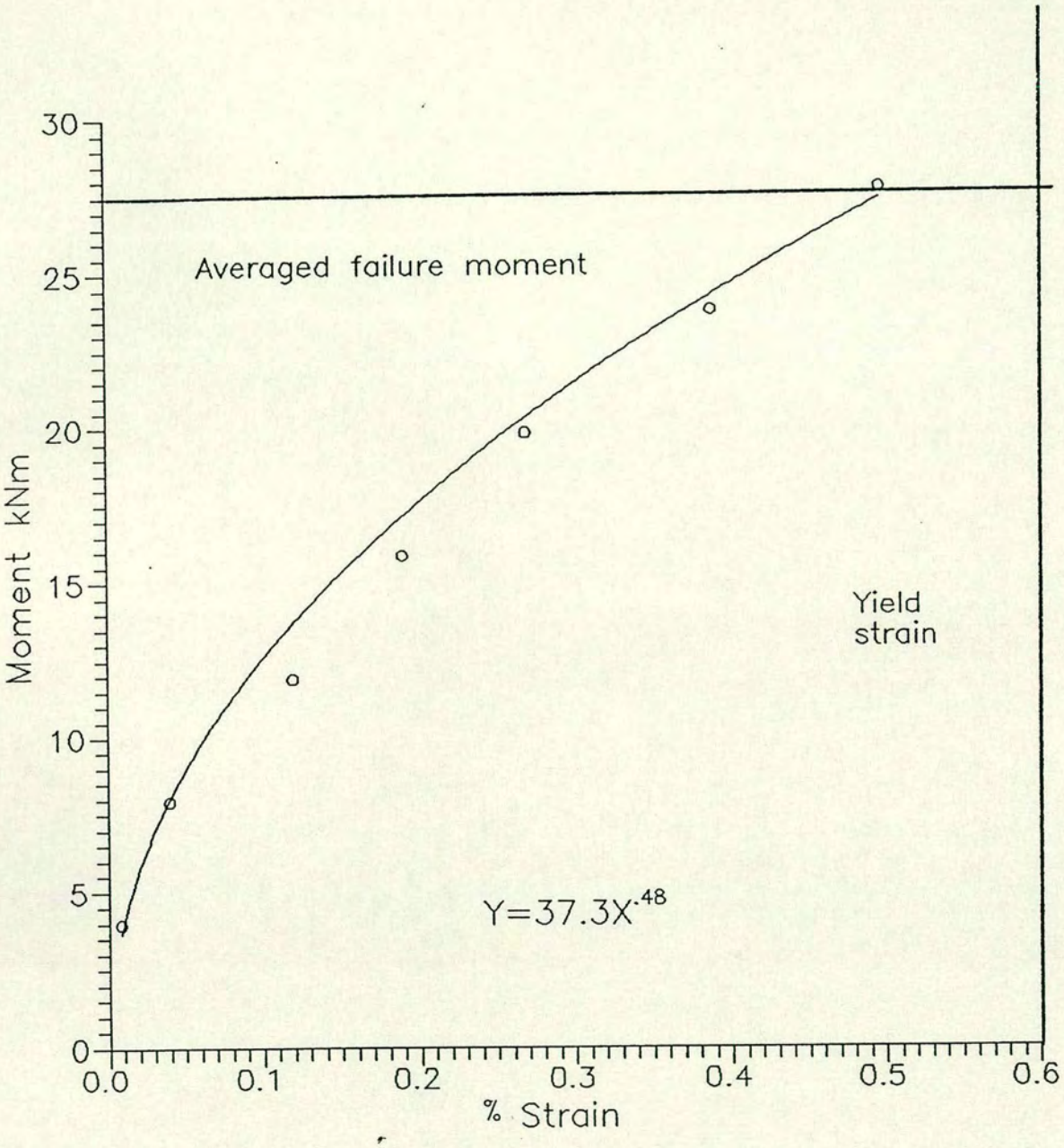

Steel strain – moment relationship for wall4 and wall6.

Figure 6–3–5

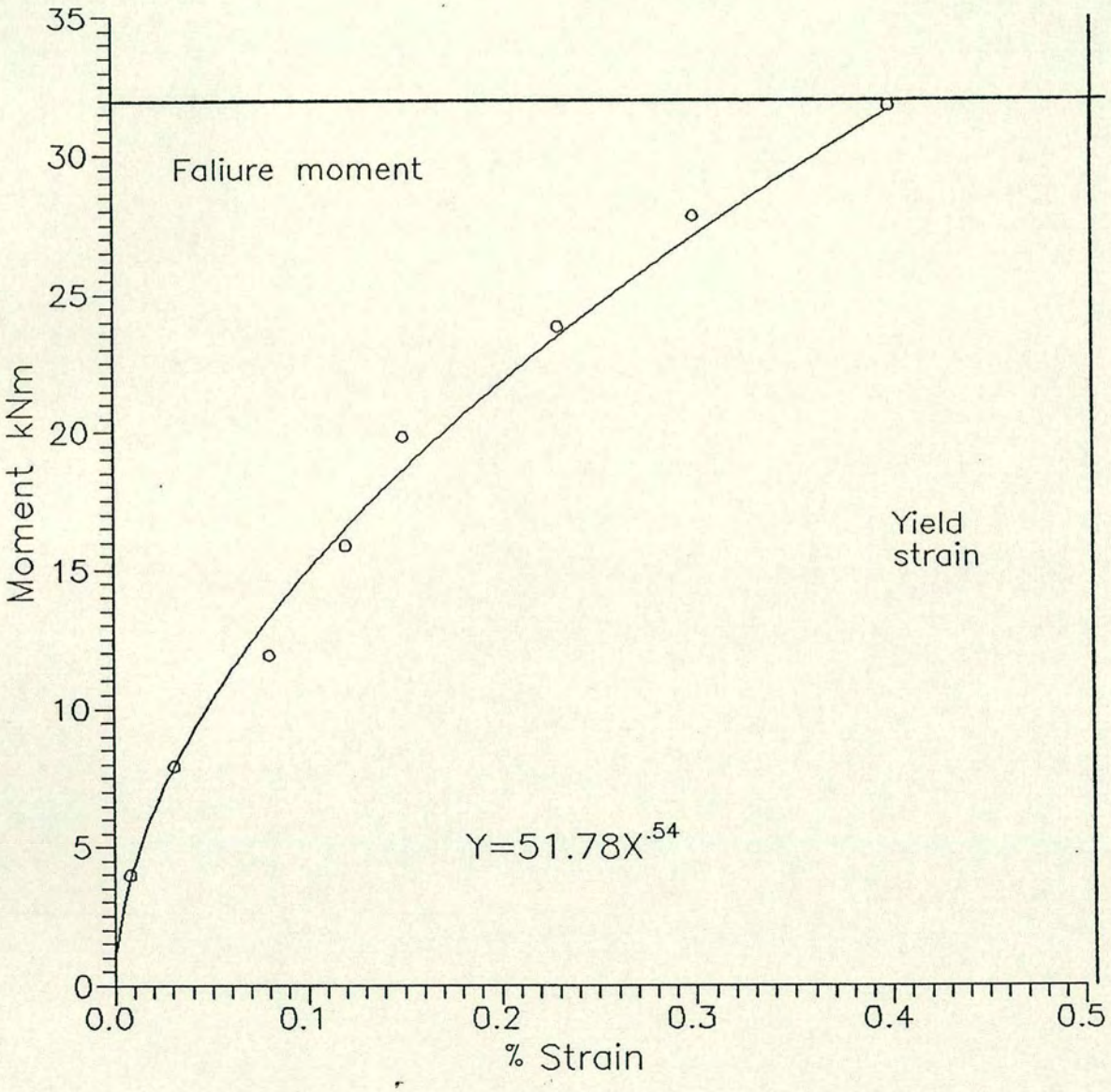

Steel strain – moment relationship for wall5.

Figure 6–3–6

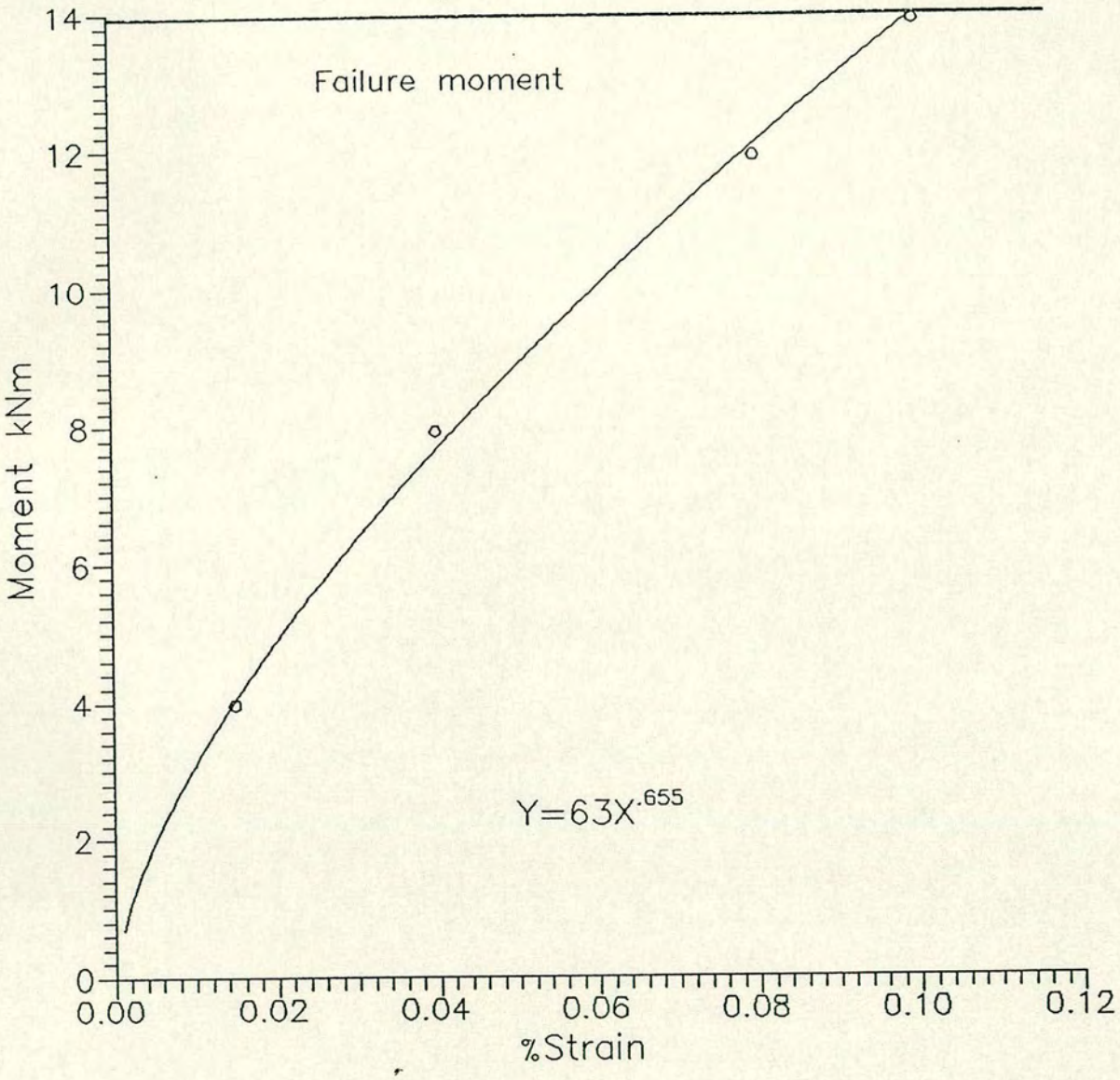

Top fibre strain – moment relationship for wall1.

Figure 6–3–7

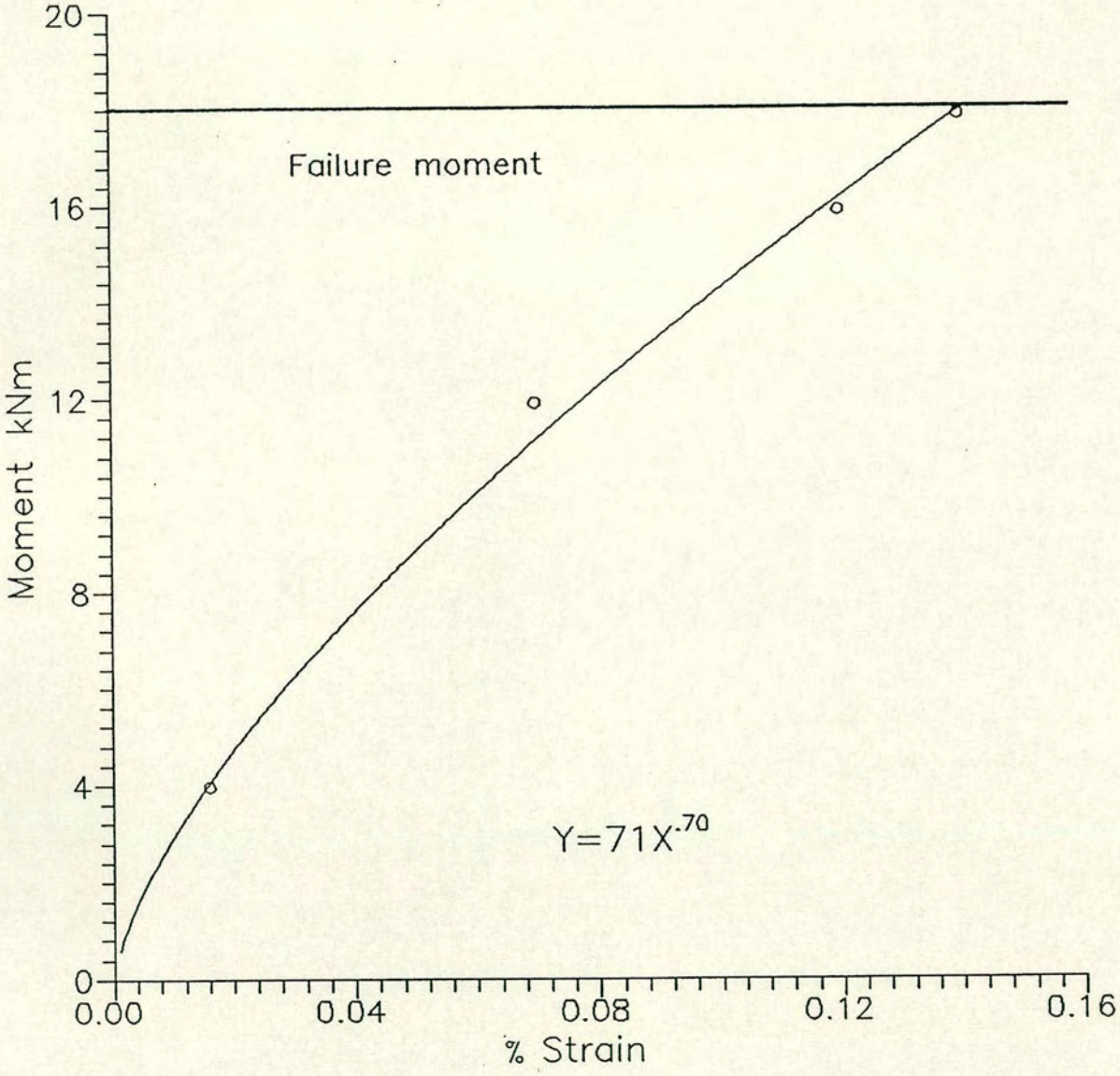

Top fibre strain – moment relationship for wall2.

Figure 6–3–8

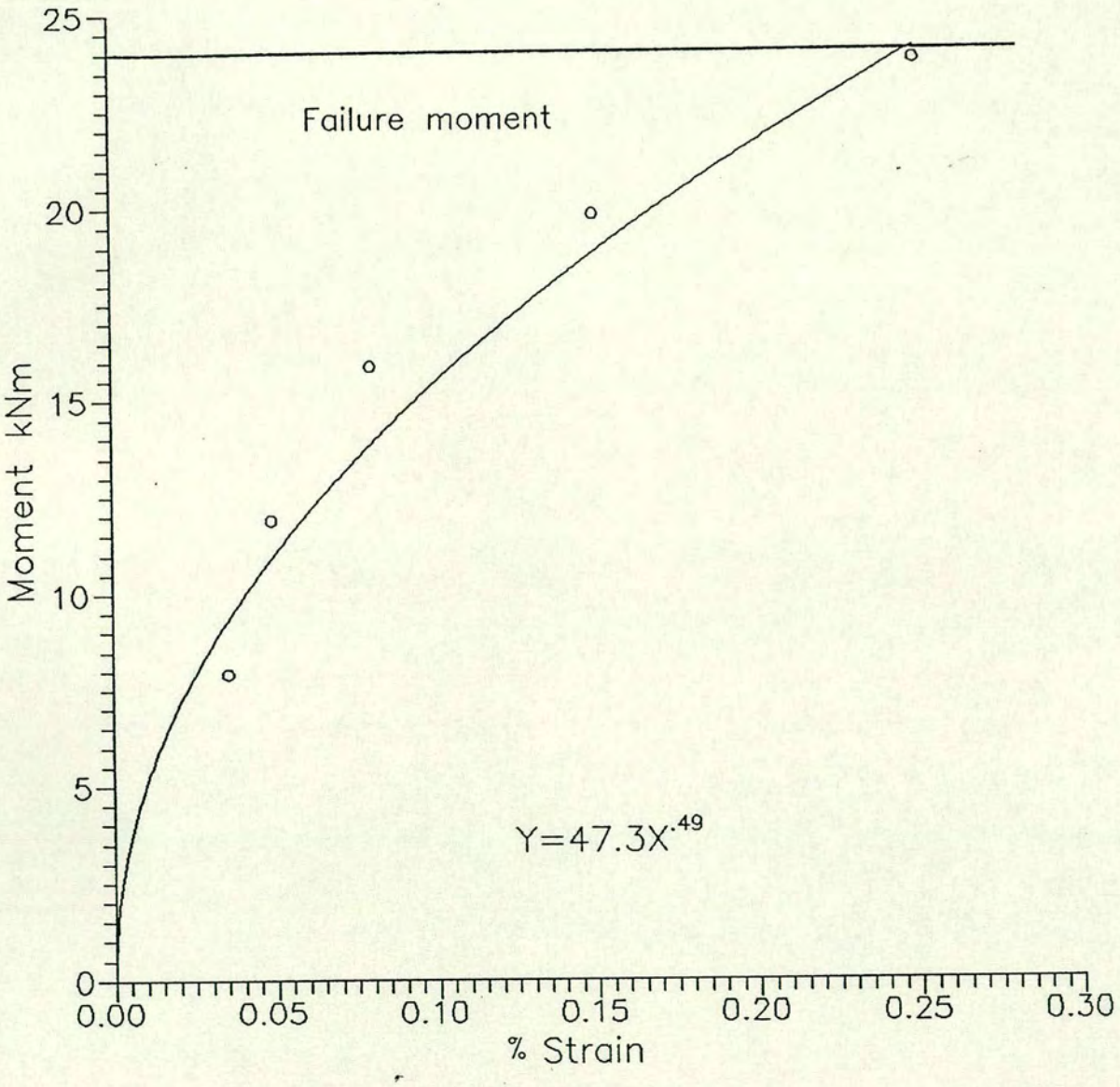

Top fibre strain – moment relationship for wall3.

Figure 6–3–9

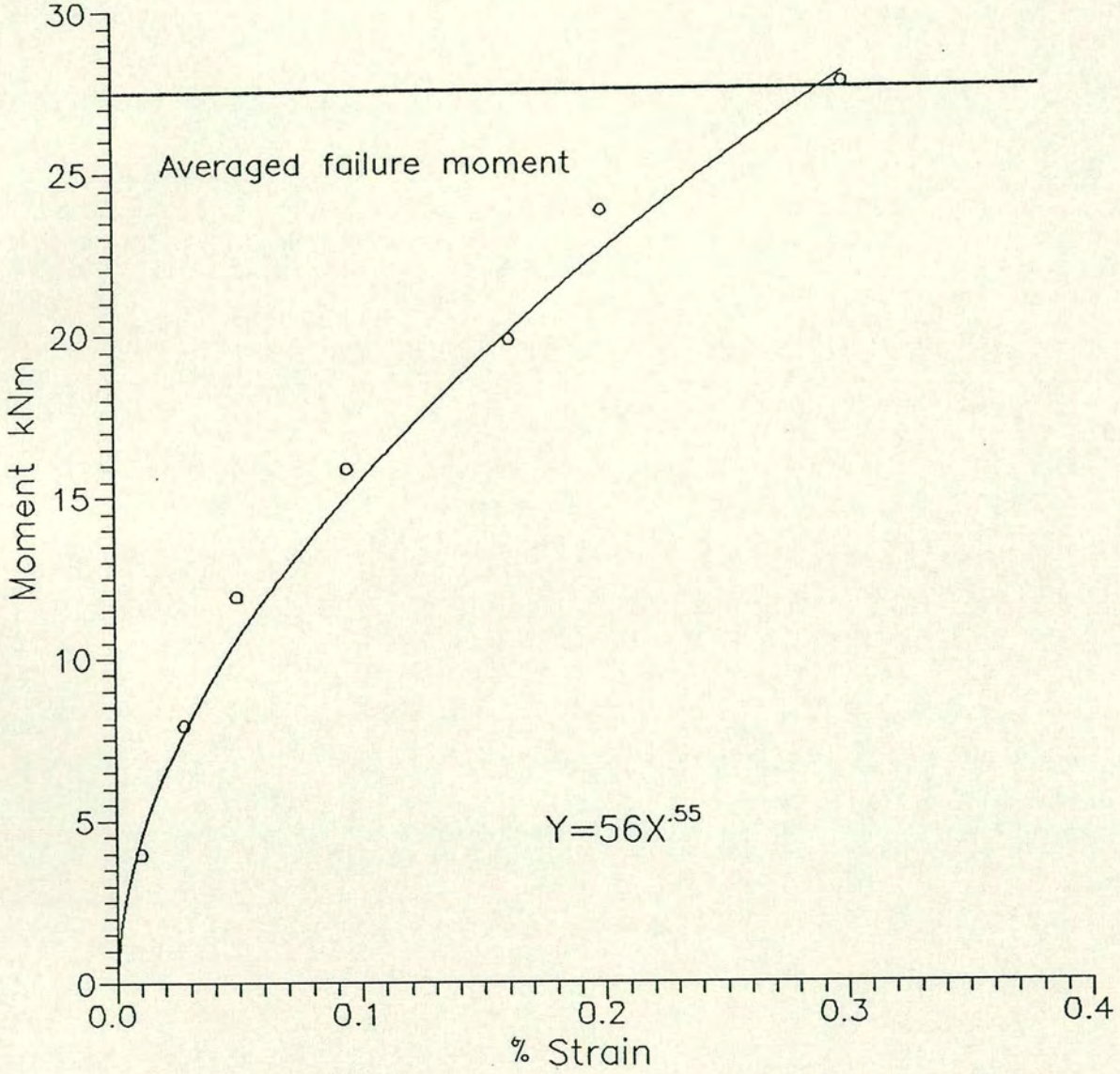

Top fibre strain – moment relationship for wall4 and wall6.

Figure 6–3–10

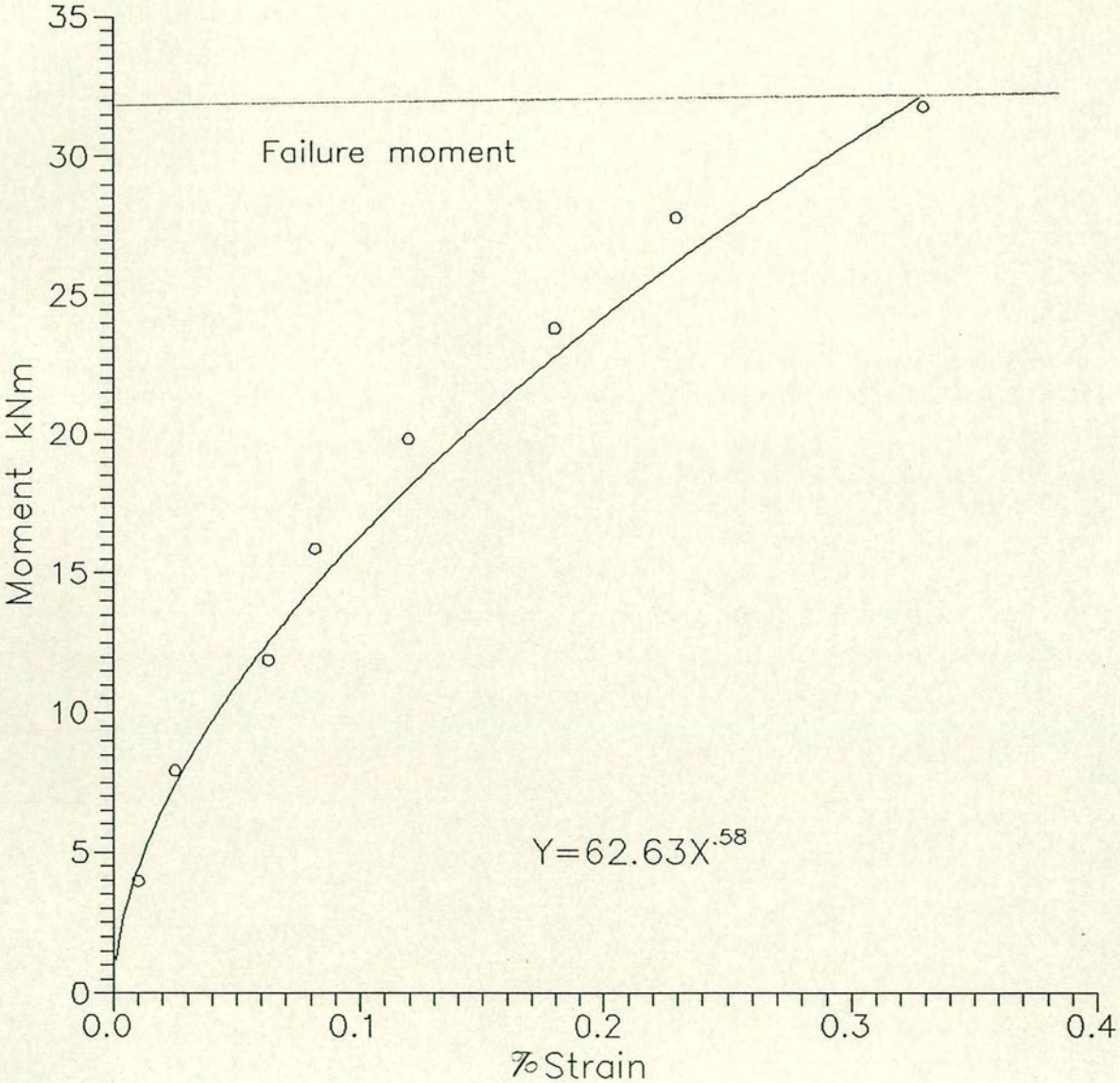

Top fibre strain – moment relationship for wall5.

Figure 6–3–11

strains were measured until yielding of the tensile reinforcement and total failure occurred. The ultimate compressive strain of the brickwork was obtained from the intersection of the curve representing the average experimental results with the horizontal line representing the averaged ultimate compressive strain, ε_m, and for walls 1, 2 and 3 was 0.001, 0.0016 and 0.0028 respectively. Wall 3 was therefore considered to be a balanced section, in which both materials reached their respective yield points simultaneously. The average value for the ultimate compressive strain for walls 4, 5 and 6 was 0.0038, which is in close agreement with the corresponding value derived from the axially loaded single course prisms, $\varepsilon_m = 0.0046$.

6.3.5 Relationship between Curvature and Moment

The moment-curvature relationships for the walls 1 to 6 are presented in Figs. 6.3.12-16 The experimental curvature was derived from strain measurements taken on the brickwork up to the cracking stage. After cracking, only the compressive strain was measured manually. The strain in the prestressing tendons was measured by highly sensitive electrical strain gauges. The curvature was obtained from the slope of the brickwork strain distribution curve for a given load. The average curvature for walls 1, 2 and 3 exhibited three phases corresponding to uncracked, cracked with steel in the elastic range, and cracked with steel yielding. Figs 6.3.15-16 show that the moment curvature relationship did not enter the third phase for walls 4, 5 and 6 .

Increases in steel area tend to prevent the moment-curvature curve from reaching the third phase. The curves were linear throughout the elastic range up to cracking, after which there was a rapid increase in curvature with no corresponding increase in moment, as a result of the reduced

stiffness. As expected, the initial value of curvature was negative due to the "camber" induced by the prestress. Fig/ 6.3.17 shows that an increase in the steel area and in the prestress force reduced the curvature for a given moment value, although the general characteristics of the walls were the same. This is because the tensile strength of the brickwork, prestressing forces and overlap prestressing forces were resisting the tensile forces caused by flexure. After cracking, the stresses in the steel increased in order to sustain the same moment, producing a decrease in the neutral axis depth. The magnitude of the prestressing force and the steel area influenced the moment at which cracking occurred. Therefore, walls with small pocket spacings, and therefore high overlap prestressing forces, will remain uncracked up to higher loads and consequently bend less than walls with larger pocket spacing but the same steel area. The finite element analysis underestimated the curvature at any given moment beyond the cracking stage. When cracking occurs, the plot of strains against depth of the wall section is no longer linear and the strains below the neutral axis in the tensile zone increased rapidly. The experimental results produce a slope of line from the compression zone only which results in a lower curvature value than that predicted by the finite element analysis. However, the experimental and theoretical moment-curvature relationships show similar characteristics and compatible values for the ultimate moment.

6.3.6 Relationship between Deflection and Load

Figs. 6.3.18-22 present the experimental and the predicted load-deflection relationships. The deflections were measured at the top level of the wall and at mid-span, 0.85 m from the support. The mid-span load-deflection relationship showed similar characteristics to the top of the wall load-deflection relationship with a total magnitude equal to $1/2$.

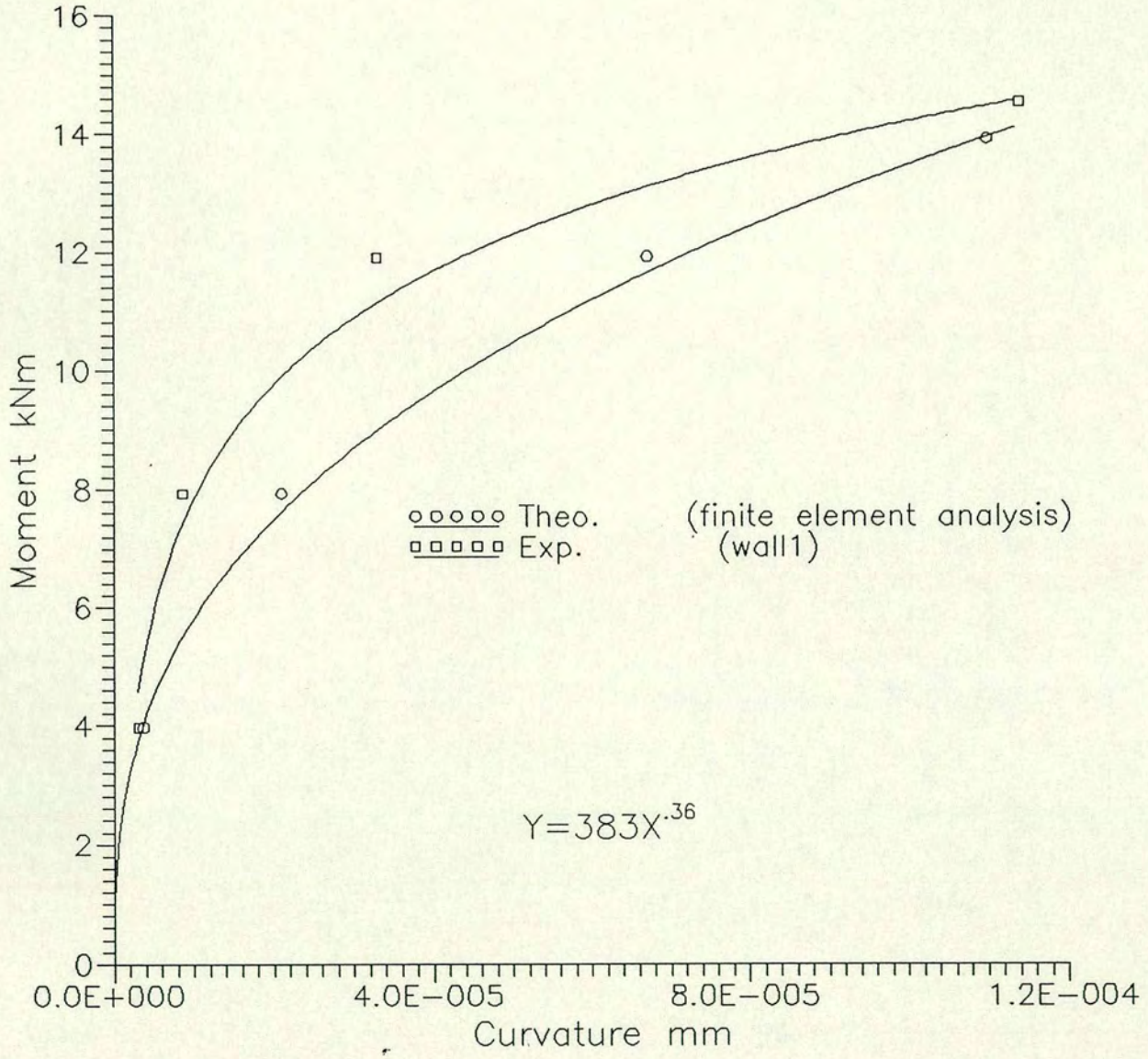

Curvature – moment relationship for wall1.

Figure 6-3-12

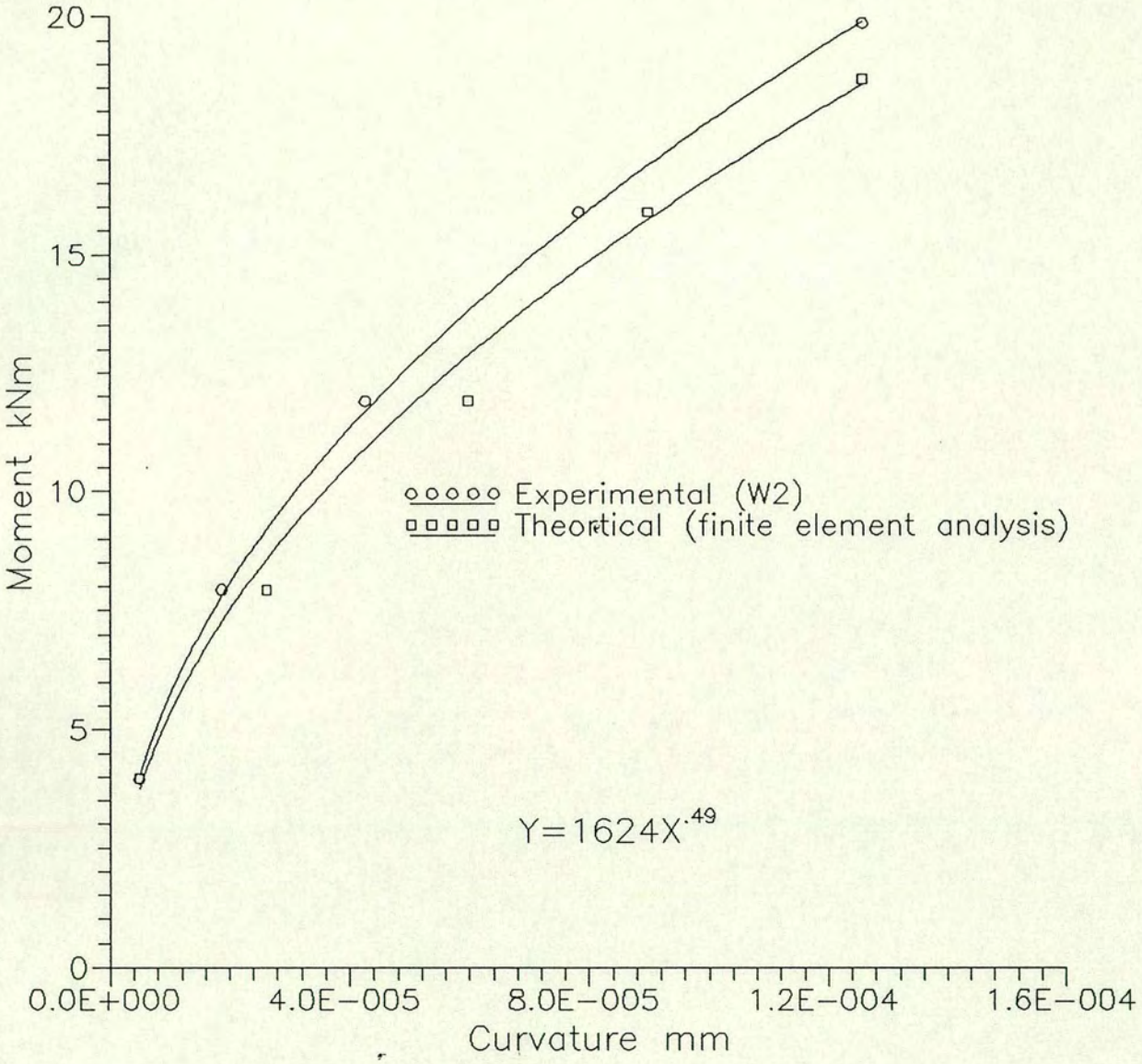

Curvature – moment relationship for wall2.

Figure 6–3–13

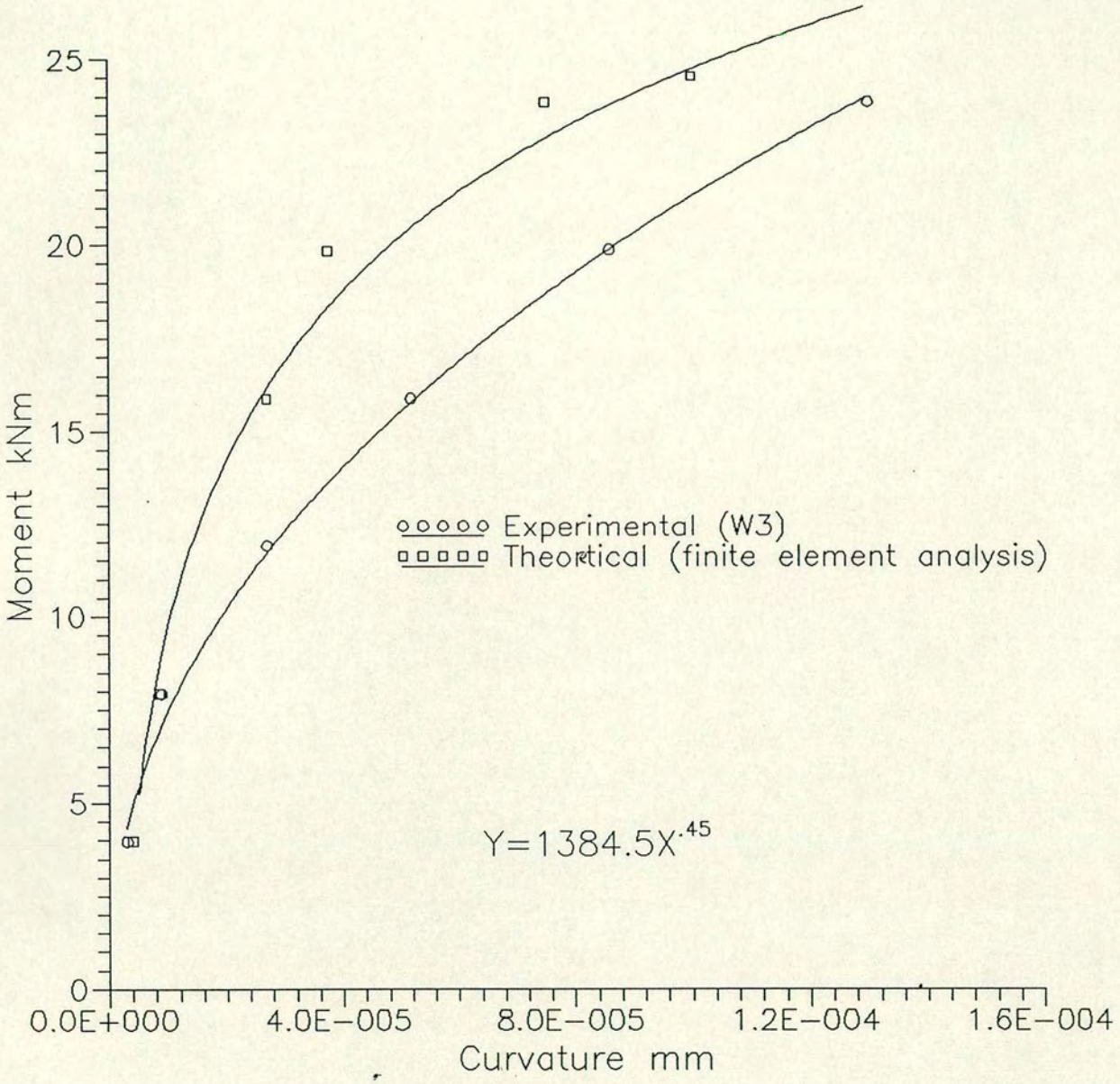

Curvature – moment relationship for wall3.

Figure 6–3–14

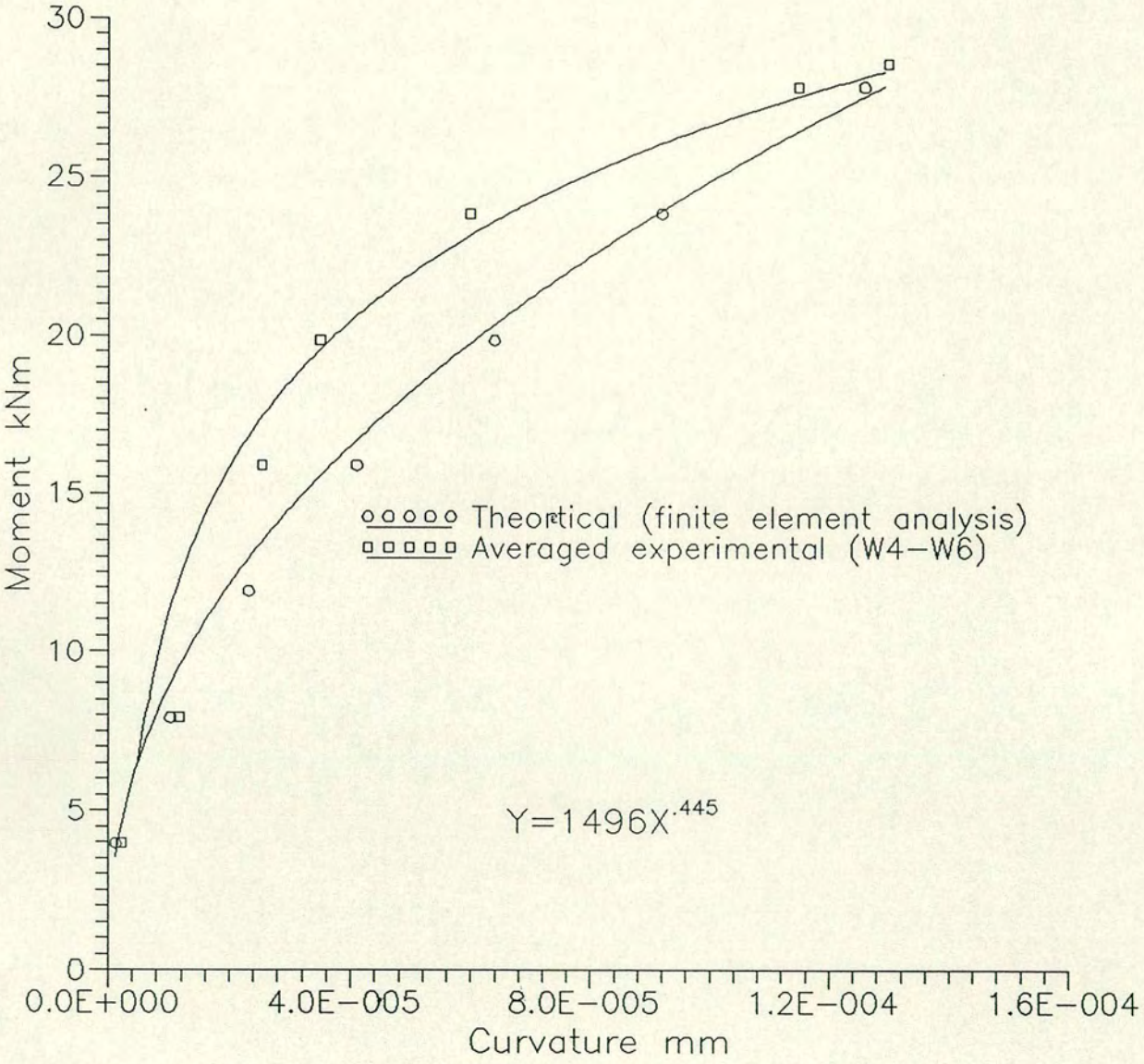

Curvature – average moment relationship for wall4 and wall6.

Figure 6–3–15

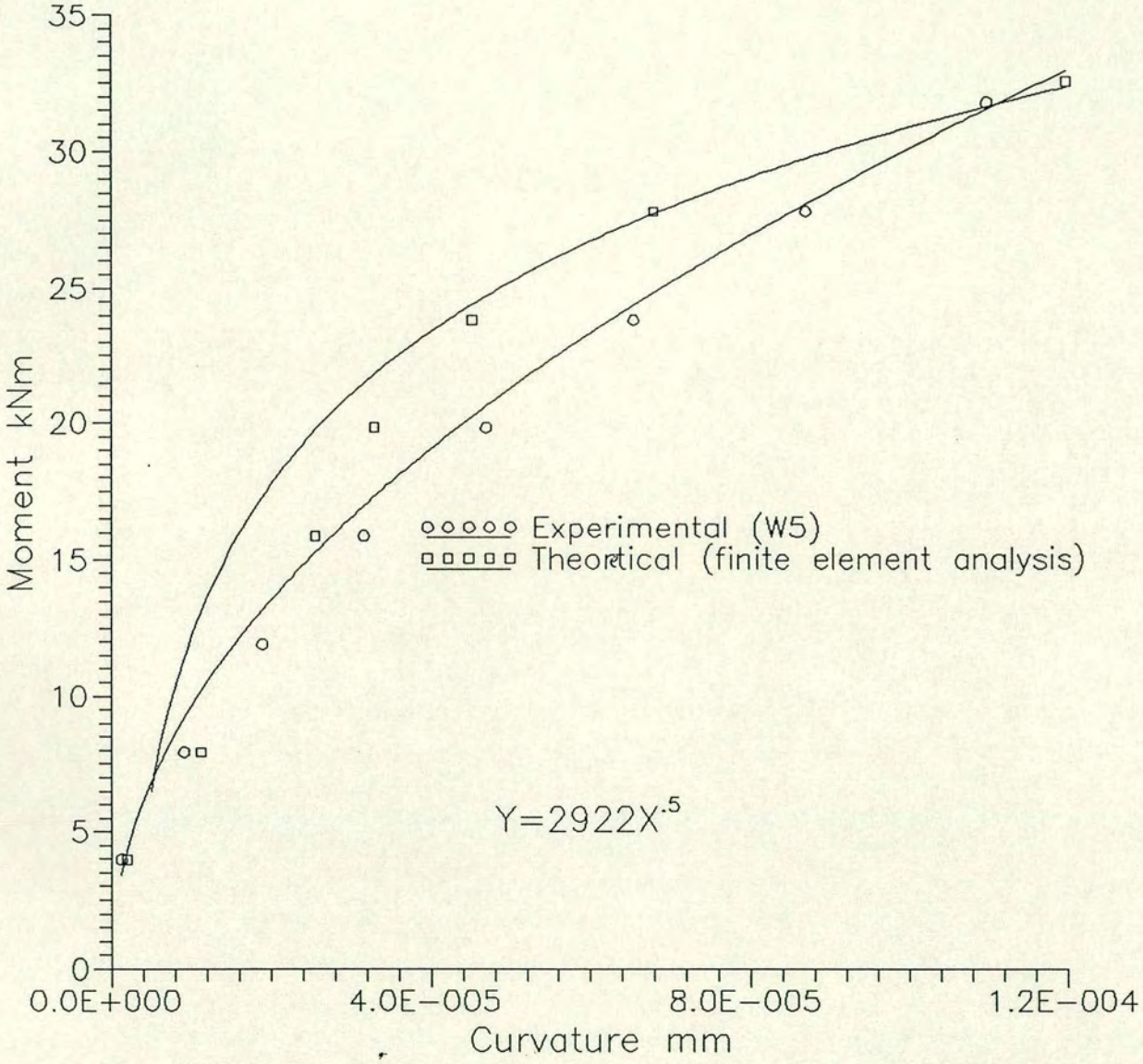

Curvature – moment relationship for wall5.

Figure 6–3–16

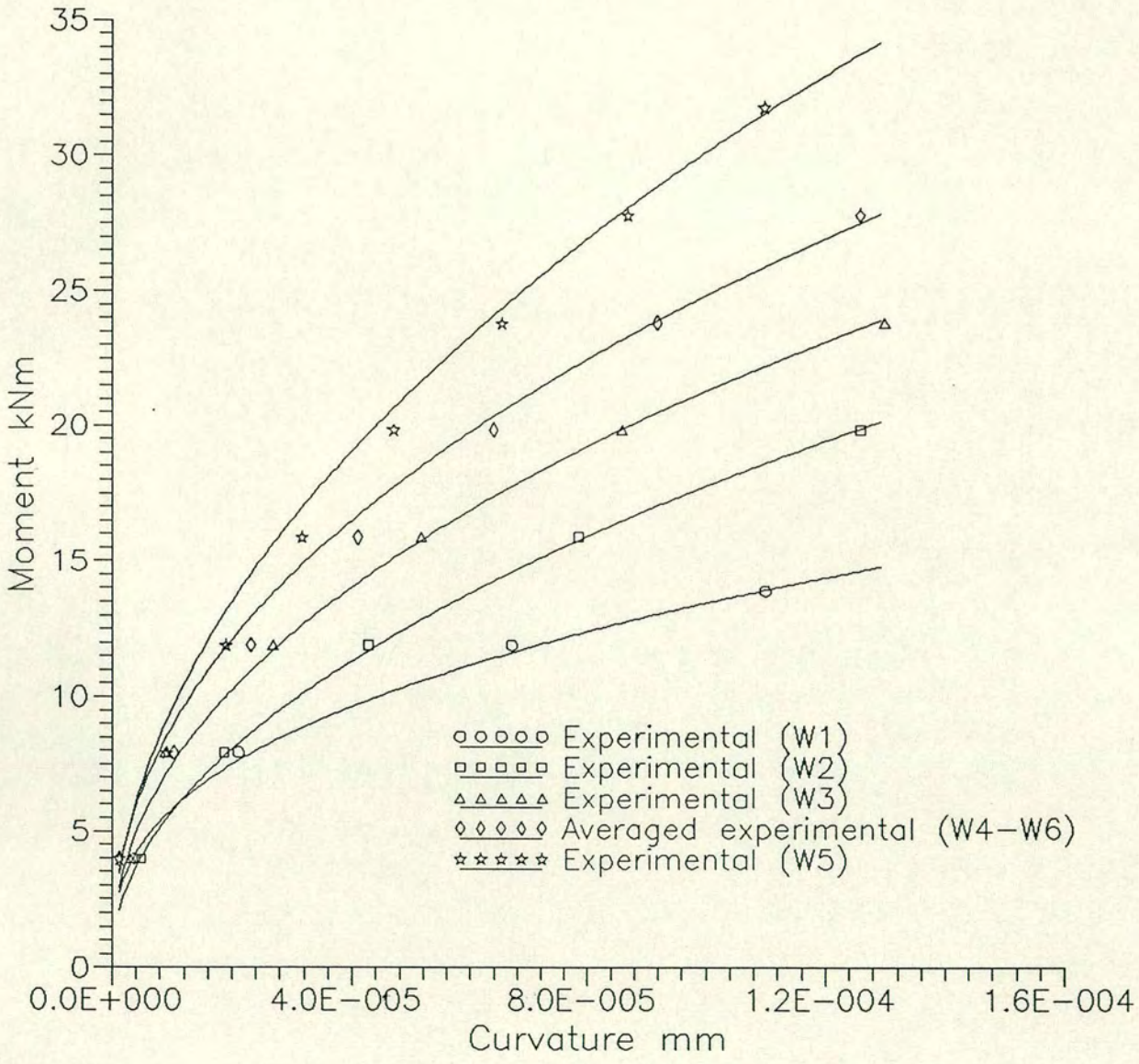

Curvature – moment relationship for wall1 to wall6.

Figure 6-3-17

Due difficulty in recording the self-weight deflection of the wall in the vertical standing position, the load-deflection curves commence at the origin and do not show the initial negative camber caused by the prestressing forces. The walls were loaded through two cycles. In the initial loading cycle, the applied load was that calculated by finite element analysis to produce a flexural crack. In the final cycle, the load applied to the walls was sufficient to cause failure. Deflections and magnitude of load were recorded at regular intervals. The percentage recovery of deflection on removal of the load exceeded 90%, and the cracks completely closed. The extent of the deflection recovery was mainly due to the elastic behaviour of the tensile reinforcement.

In all the tests, the load-deflection relationship was initially linear, and after cracking the deflection increased more rapidly with load due to the sudden reduction in wall stiffness. The behaviour of each wall was independent of the percentage area of steel up to the cracking stage, but after cracking the largest deflections occurred in the walls with the least area of steel and smallest prestressing forces. A decrease in steel area, prestressing force and overlap prestressing force produces an increase in stress in the reinforcement at the cracked section in order to sustain the same load. This causes an increase in the compressive strain and a reduction in the neutral axis depth which corresponds with an increase in deflection Fig. 6.3. 23.

The load-deflection relationships for walls 1, 2 and 3 indicated under-reinforced sections. Immediately after cracking there was a large increase in deflection due to the sudden reduction in stiffness, and after the steel yielded, excessive deflections developed with no corresponding increase in load until total failure occurred. The deflection curves

exhibited three phases corresponding to uncracked, cracked with steel in the elastic range, and cracked with steel yielding.

The experimental load-deflection relationships were compared with the deflections predicted by the finite element analysis. The predicted results slightly under-estimated the deflections obtained from the experimental deflection-load relationship up to failure. The predicted load-deflection curve was initially linear and in good agreement with the experimental results up to the point where cracking occurred, after which the experimental deflections increased more rapidly than the predicted results due mainly to the extra lateral pressure from the wall self-weight. The finite element deflection-load relationship results should therefore be modified to allow for the wall self-weight.

6.3.7 Relationship between Neutral Axis Depth and Load

Fig. 6.3.24 shows the experimental results for the variation in the neutral axis depth with load for each wall. The values of neutral axis depth were derived from the brickwork strain profiles measured on each wall at every load increment. Initially, the relationship indicated a rapid decrease in the neutral axis depth with increasing load. At higher loads, with the section cracking and the steel yielding, the curve started to level off towards a minimum value at which point failure of the section occurred. The magnitude of the neutral axis depth at failure was dependent upon the percentage of steel in the wall i.e. the larger the steel area the greater the neutral axis depth at failure. All the curves plotted for neutral axis depth against load show similar characteristics, namely a rapid decrease in the neutral axis depth with increased load. Therefore as tension developed and cracking commenced, the compressive strain above the neutral axis increased rapidly with load and further decrease in

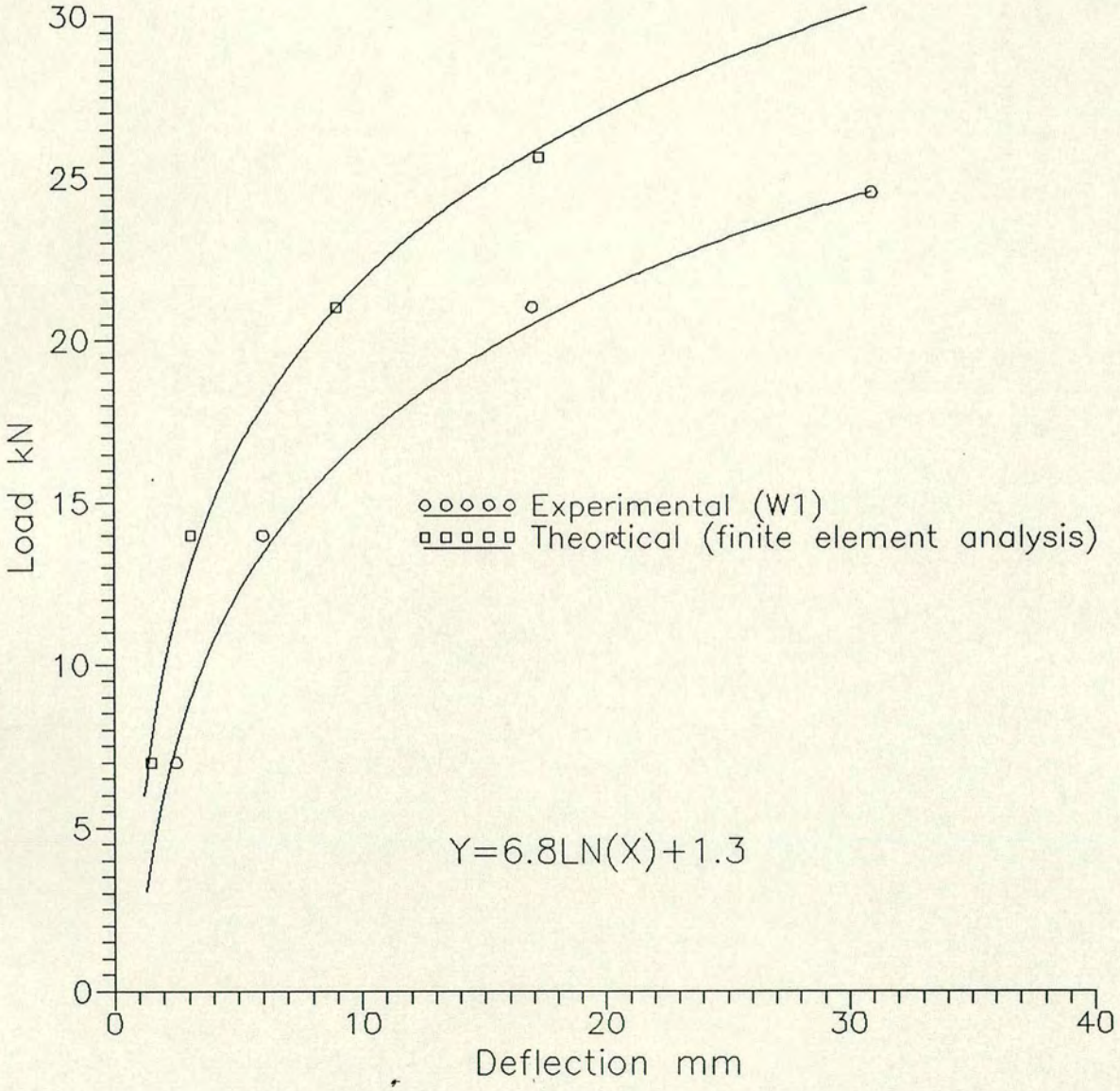

Deflection – total applied load relationship for wall1.

Figure 6–3–18

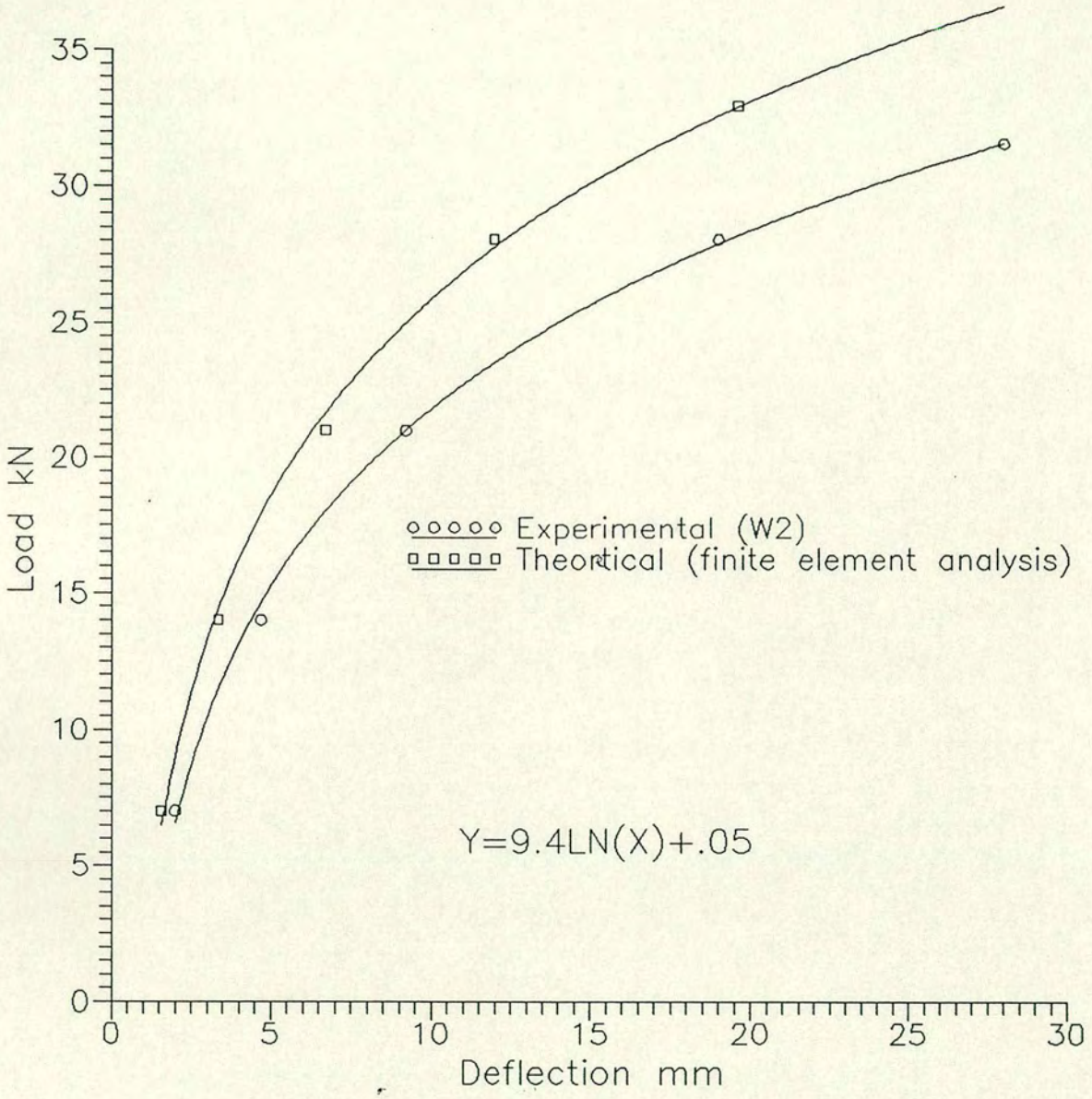

Deflection – total applied load relationship for wall2.

Figure 6–3–19

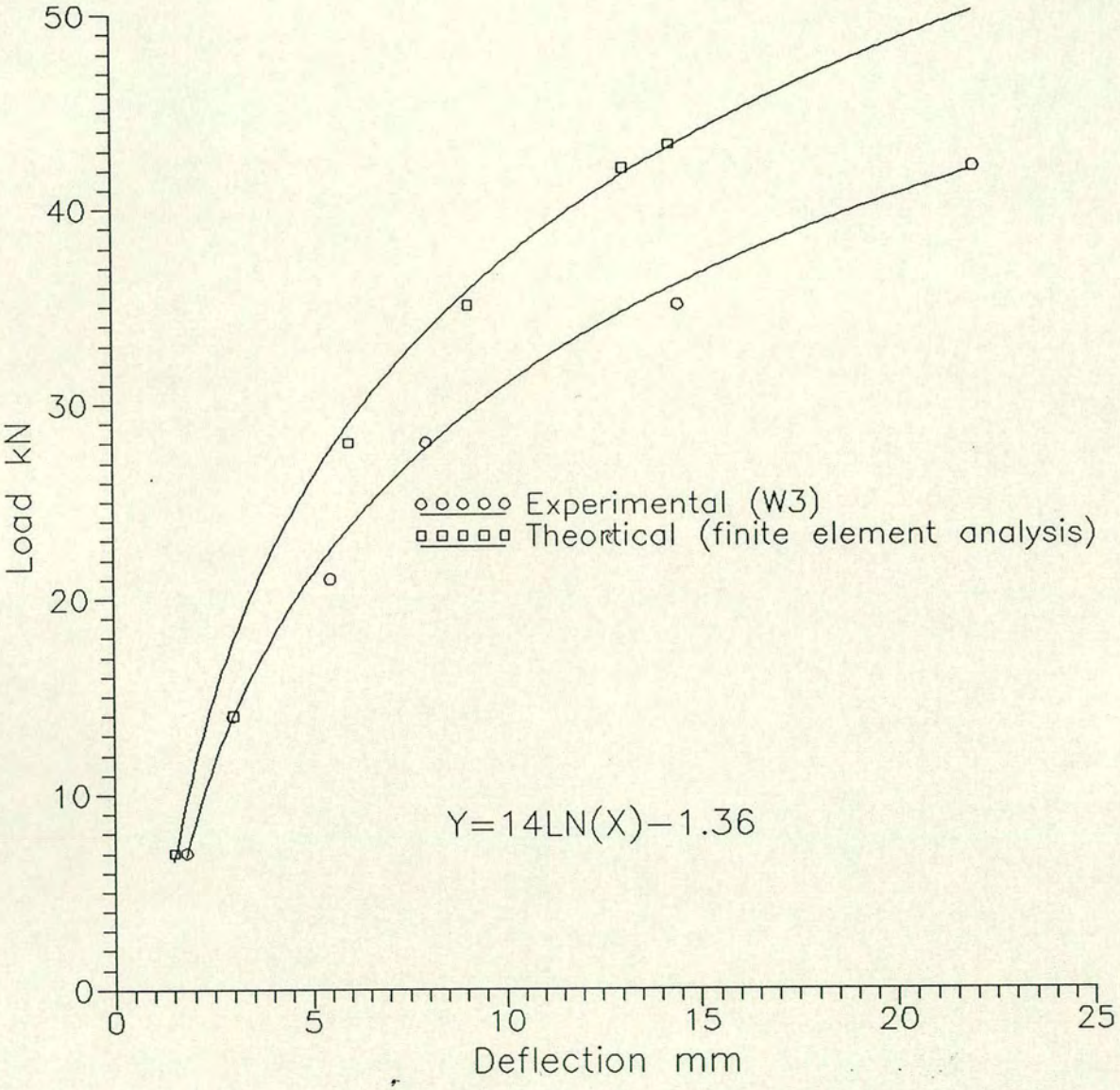

Deflection − total applied load relationship for wall3.

Figure 6−3−20

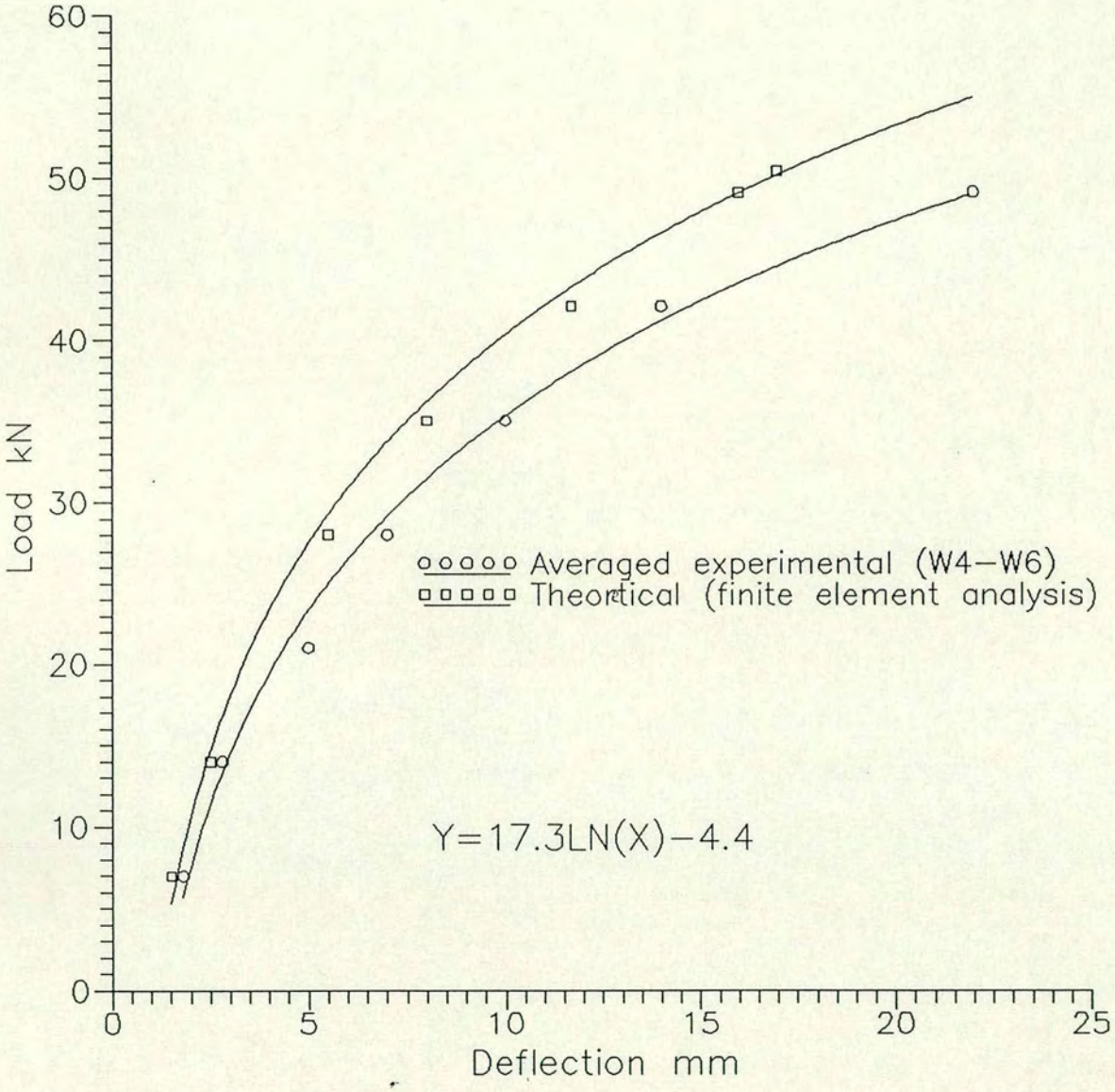

Deflection – total applied load relationship for wall4 and wall6.

Figure 6–3–21

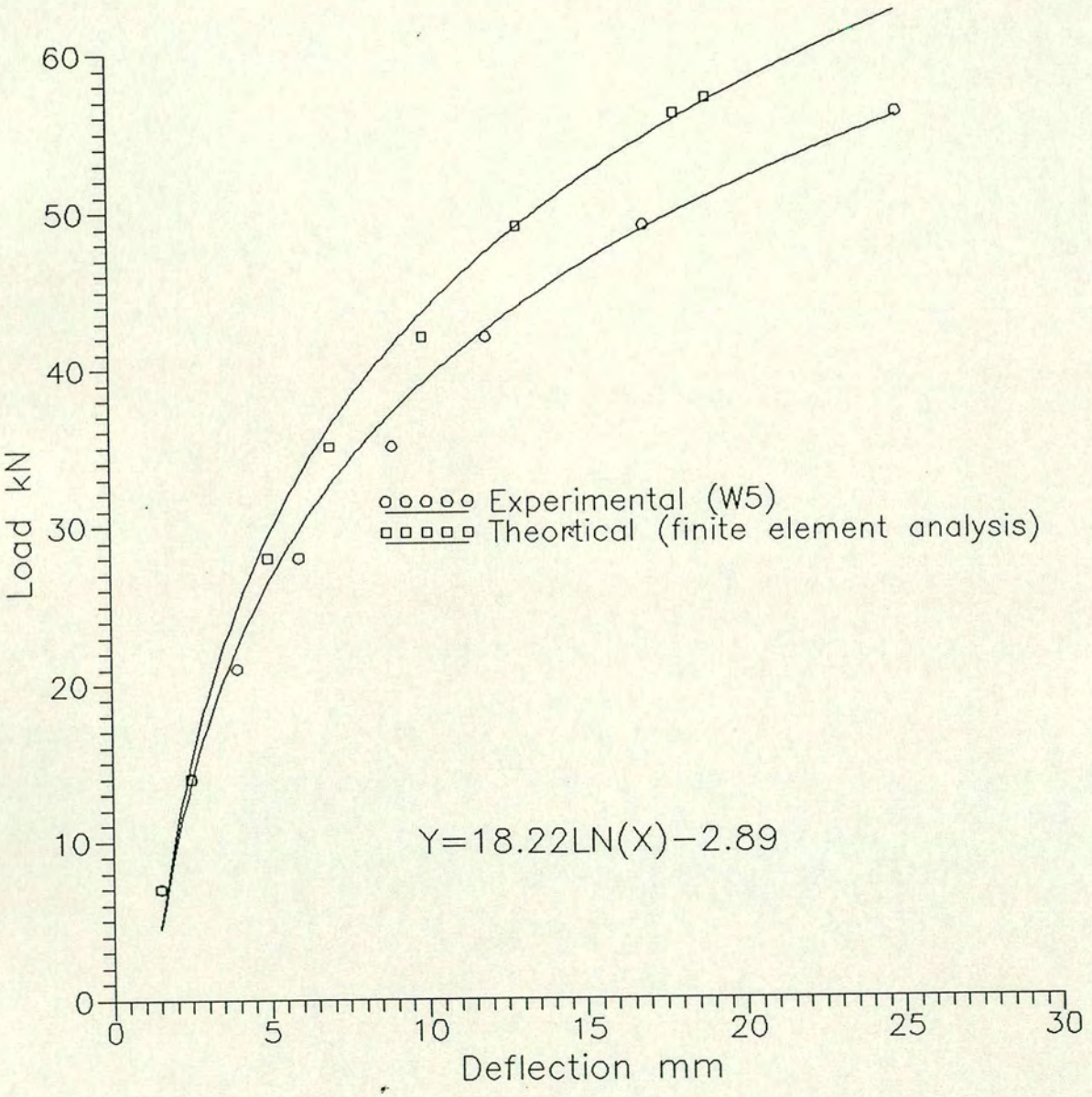

Deflection – total applied load relationship for wall5.

Figure 6–3–22

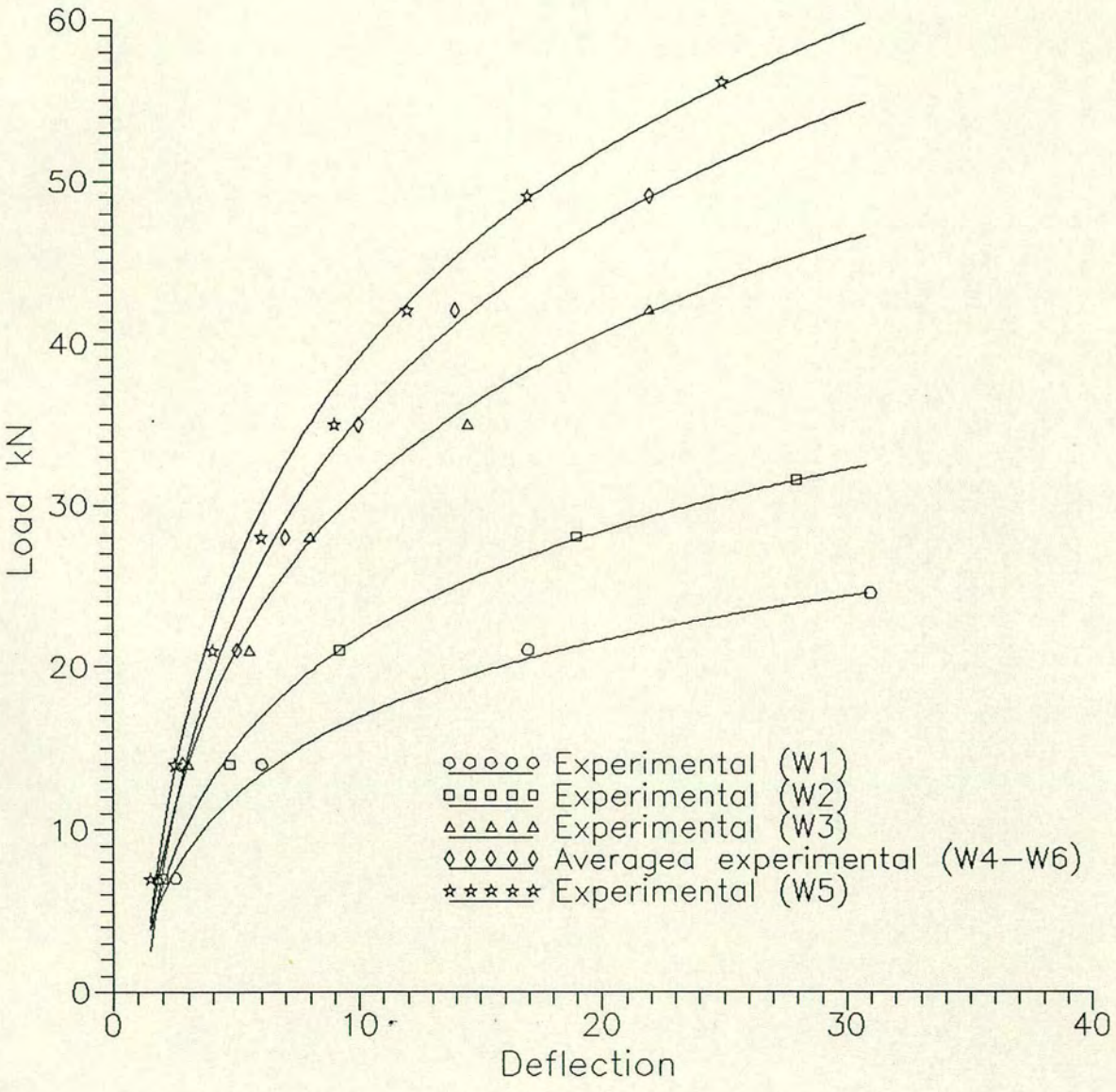

Deflection – total applied load relationship for wall1 to wall6.

Figure 6–3–23

the neutral axis depth. The deflection in Wall 5, with a larger area of steel and a greater prestressing force, levelled off at a greater neutral axis depth. Therefore, increasing the steel area and prestressing force permits larger tensile forces to develop, thereby producing a larger neutral axis depth to develop the corresponding compressive forces.

6.3.8 Cracking Moment

All the walls were designed for shear to ensure that the full flexural capacity was reached. Table 6.9 gives details of the experimental and predicted cracking moments of the walls. The under-reinforced walls, 1 and 2, and balanced section wall, 3, had similar crack patterns on the tension face. Initially, the cracks ran horizontally along the bed joints between the wall and the steel base. As the load increased several uneven cracks formed along the bed joints in an area higher up the wall.

The over-reinforced walls, 4, 5 and 6, had similar crack patterns on the tension face as outlined above. However, in the later stages with increased bending moments, crushing of the brickwork at the compression face took place in the form of a diagonal crack, indicating the presence of internal fracture. In general, all the cracks were formed at 35-45% of the ultimate load as flexural cracks at the final bed joint, where the bending moment and shear force are a maximum.

The predicted moments obtained from the elastic method and direct analysis method under-estimated the experimental results by 20-30%, whereas the cracking moment based on finite element analysis slightly over-estimated the experimental results.

In prestressed brickwork structures the working load is determined according to three different classes of structure. If the wall is designed

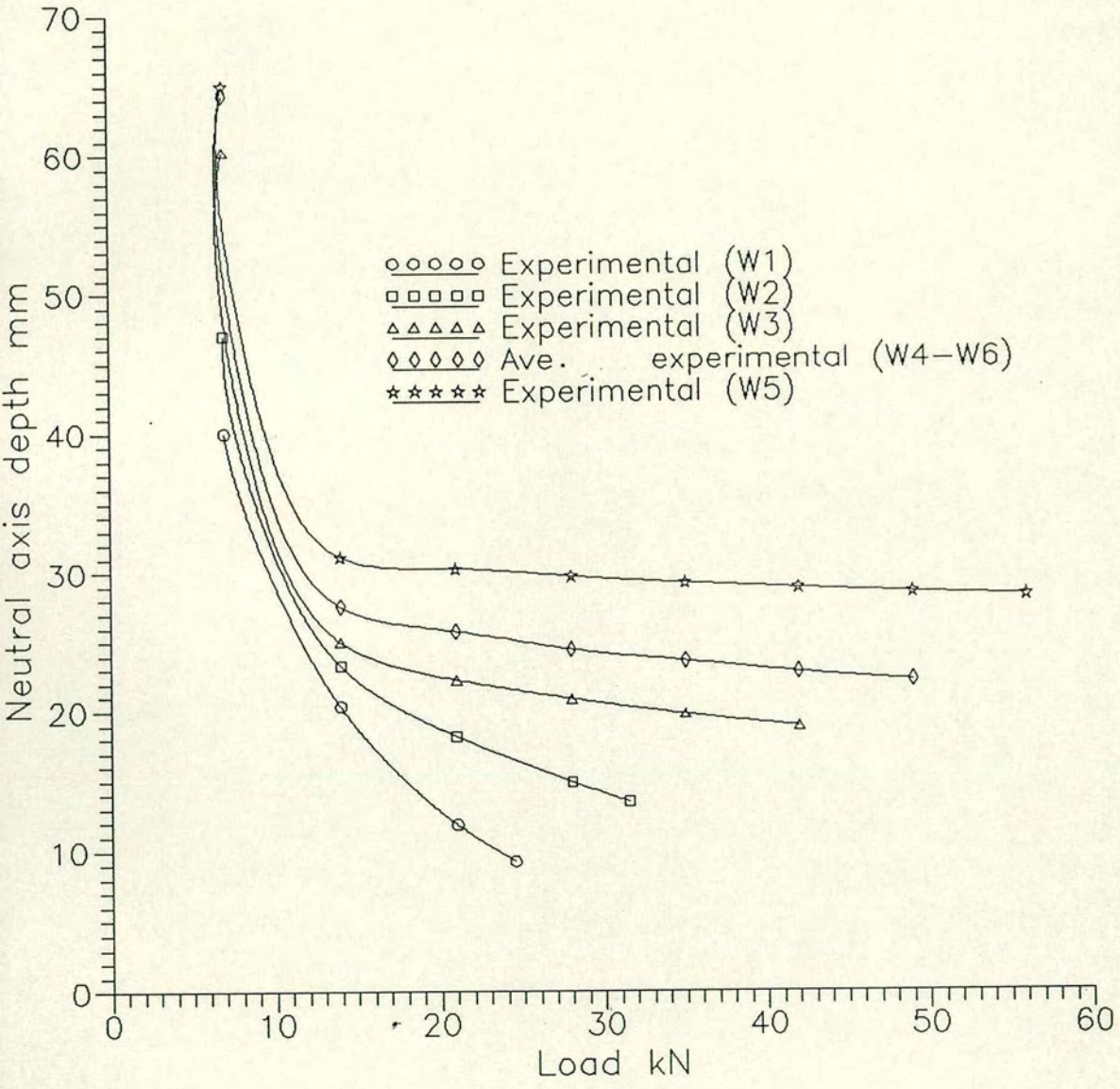

Neutral axis depth – load relationship for wall1 to wall6.

Figure 6–3–24

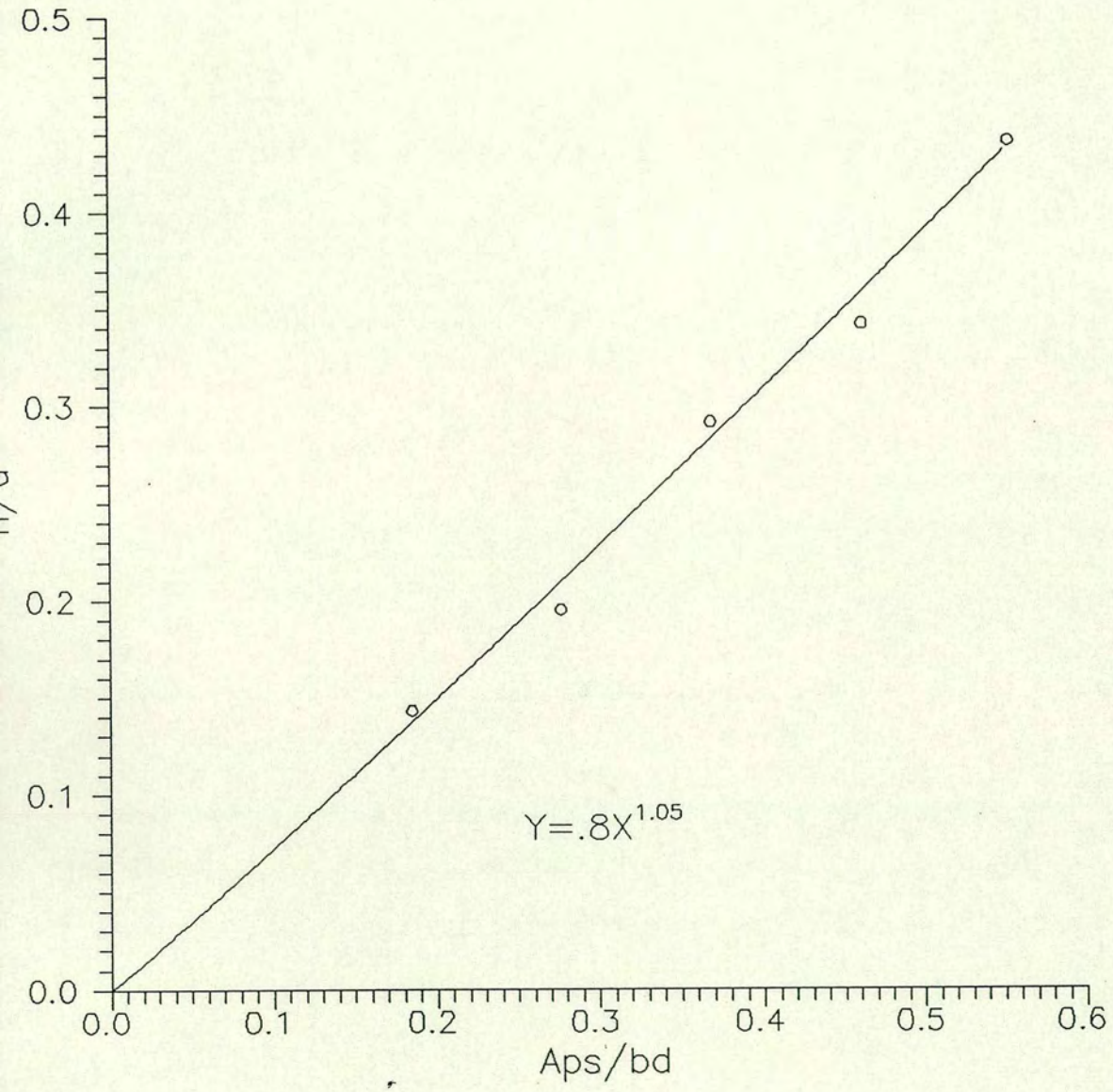

The effect of steel % on neutral axis depth for wall1 to wall6.

Figure 6-3-25

as a Class 1 structure then Table 6.10 shows that the average ratio of m_{ult}/m_{c1} = 13.80; for Class Two walls, tensile stresses but not cracking is permitted under working load and the ratio decreases to 5.31; and for Class 3, where cracks up to a maximum width of 0.2mm are allowed under working load, the safety factor drops to 1.80.

For economical reasons, it is not profitable to design the wall for a factor of safety above tow . The cracks are more likely to form at intervals which coincide with the mortar joints, though not necessarily at every brick/mortar interface. In the walls tested, the maximum crack width was located most often at the base of the wall which suggests that if suitable cover were provided for the steel area at the base of the wall, the post-tensioned brickwork retaining wall would be a more efficient structure. Fig. 6.3.26 shows the experimental relationships between moment and average crack width. The crack widths were taken as the average width of the first two cracks formed and were measured using crack detection moving microscope along the final bed joint at the base of the wall.

Since it is important to consider cracking at failure, the experimental and predicted crack widths were analysed up to ultimate moment. The characteristics of the moment-average crack width relationship for each wall was similar. As shown in Fig. 6.3.26, the experimental relationship was initially linear. After the steel yielded, the crack width increased and the neutral axis depth decreased more rapidly up to failure, as the curve tended towards being parallel to the x-axis.

The predicted results based on finite element analysis under-estimated the crack widths and moments, whereas the cracking moments were in

close agreement. The predicted results based on the direct method over-estimated the experimental results, as the direct method did not consider the effect of the overlap prestressing forces on the wall's nominal strength.

Increasing the area of steel, and therefore the prestressing forces and overlap prestressing forces, caused a decrease in the average crack width. The decrease in crack width was due to the increase in the stiffness of the wall section necessary to sustain a corresponding moment and crack width in the section with the smaller steel area. The spacing between the pockets should be decreased.

6.3.9 Experimental Observations and Discussion

Post-tensioned pocket-type brickwork retaining walls contain tendons which are concentrated in pockets formed in the brickwork at regular intervals along the loaded face. As the wall is to function as a retaining structure, the direction of the masonry bed joint must be perpendicular to that studied by previous researchers (Pedreschi, 1983; Uduehi, 1989).
Six half-scale walls were constructed with two pockets per wall to study the effect of the percentage steel area, prestressing and overlap prestressing forces on the performance of the wall under lateral hydrostatic pressure. The spacing between the pockets was chosen as H/3 to examine the possibility of the brickwork arching or vertical splitting of the wall occurring due to the development of lateral tension caused by excessive prestressing and overlap prestressing forces.

For the initial loading cycle, the load was applied up to 35-45% of the failure load at which stage flexural cracks had just occurred. In the second cycle, the load was re-applied up to failure. On removal of the initial load, the recovery of deflection was greater than 90%, and any

Wall	% Steel	Prestress Force	Experimental	Elastic Method	Direct Method	Non linear F.E. Analysis
1	0.10	34	4.95	2.70	3	5.50
2	0.151	51	7.90	3.42	3.95	9.50
3	0.201	68	8.90	4.20	4.94	11.50
4	0.251	85	10.87	4.90	5.87	12.00
5	0.302	102	11.67	5.60	6.58	13.50
6	0.251	85	11.00	4.90	5.87	12.00

Figure 6.9 Cracking Moment kNM

Wall	% Steel	Prestress Force	Predicted Ultimate Moment *Mu (kNM)	Working Load Moments			Mu	Mu	Mu
				Class 1 MCL2	Class 2 MCL2	Class 3 MCL3 .2mm	MC1	MC2	MC3
1	0.10	34	14.50	1.44	2.70	7.20	10.10	5.37	2.70
2	0.151	51	18.65	2.16	3.42	10.50	8.63	5.45	1.78
3	0.201	68	24.50	2.88	4.2	13.40	8.51	3.60	1.83
4	0.251	85	28.50	3.60	4.90	16.50	7.92	5.82	1.73
5	0.302	102	32.50	4.32	5.60	18.70	7.52	5.80	1.74
6	0.251	85	28.50	3.6	4.90	16.50	7.92	5.82	1.73

*Mu = Finite Element Analysis

Table 6.10 Serviceability Conditions

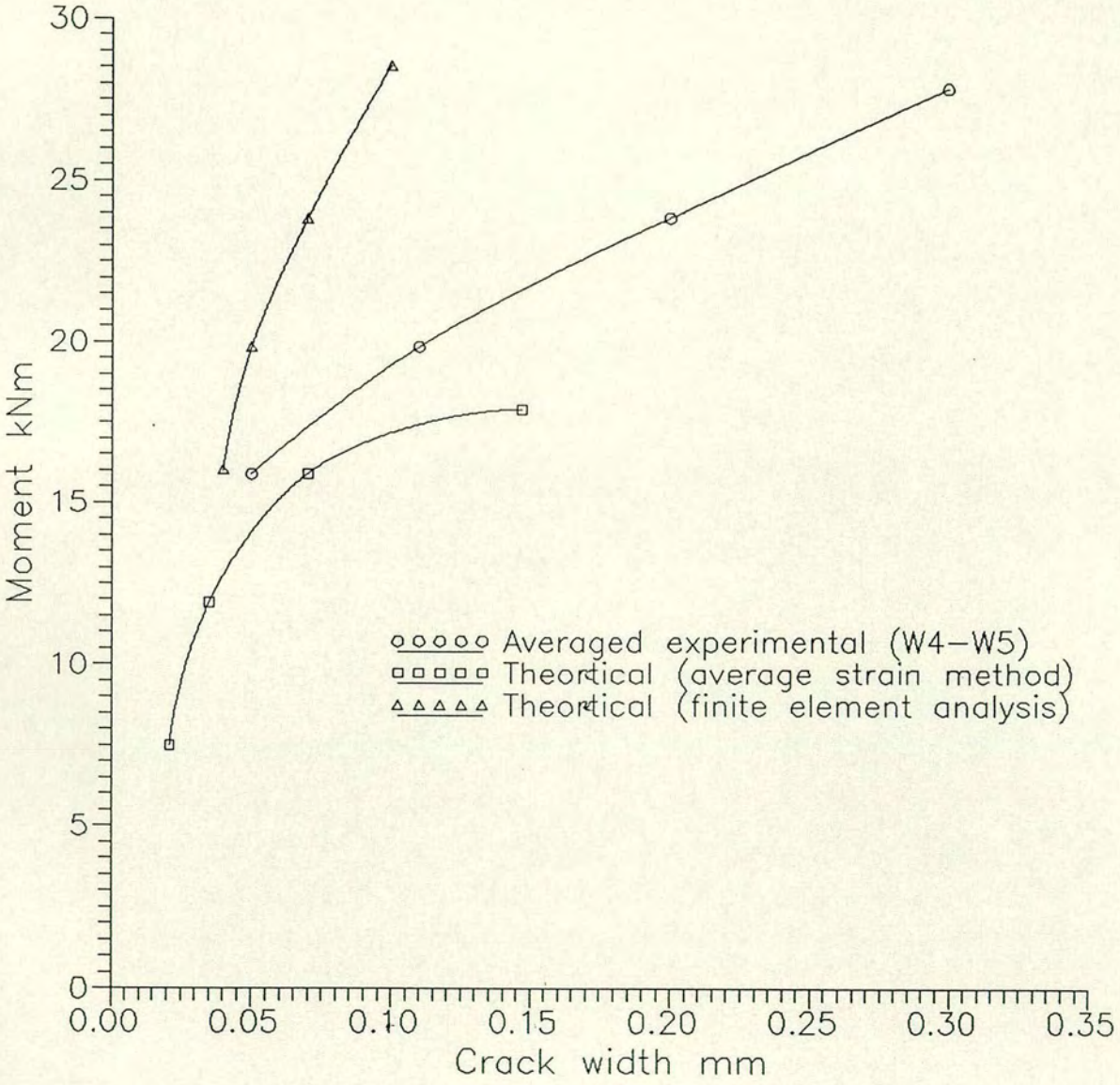

Comparison between predicted and experimental average crack width for wall4 and wall6.

Figure 6–3–26

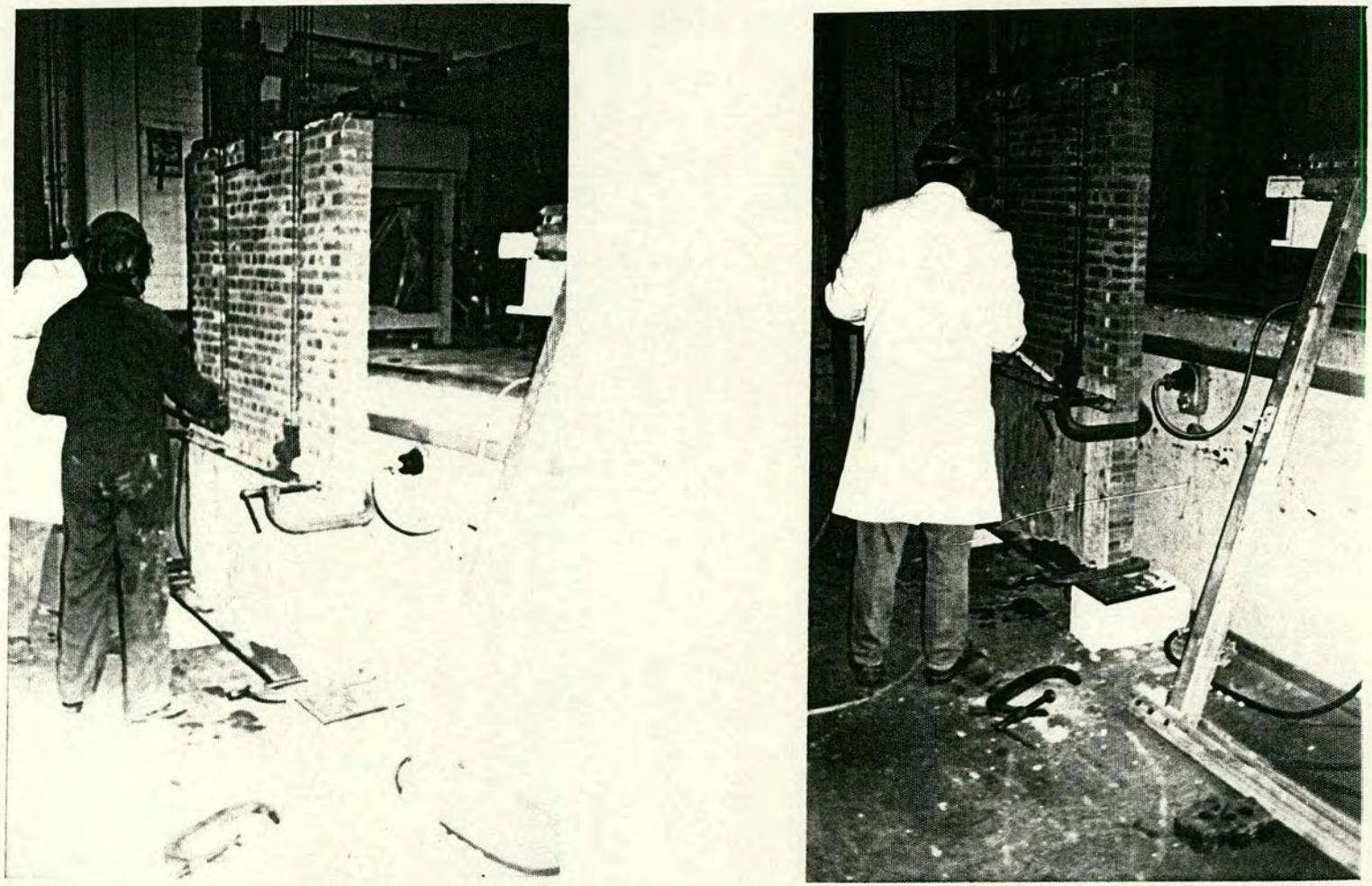

Figure 6.3.27 General view of walls at grouting stage

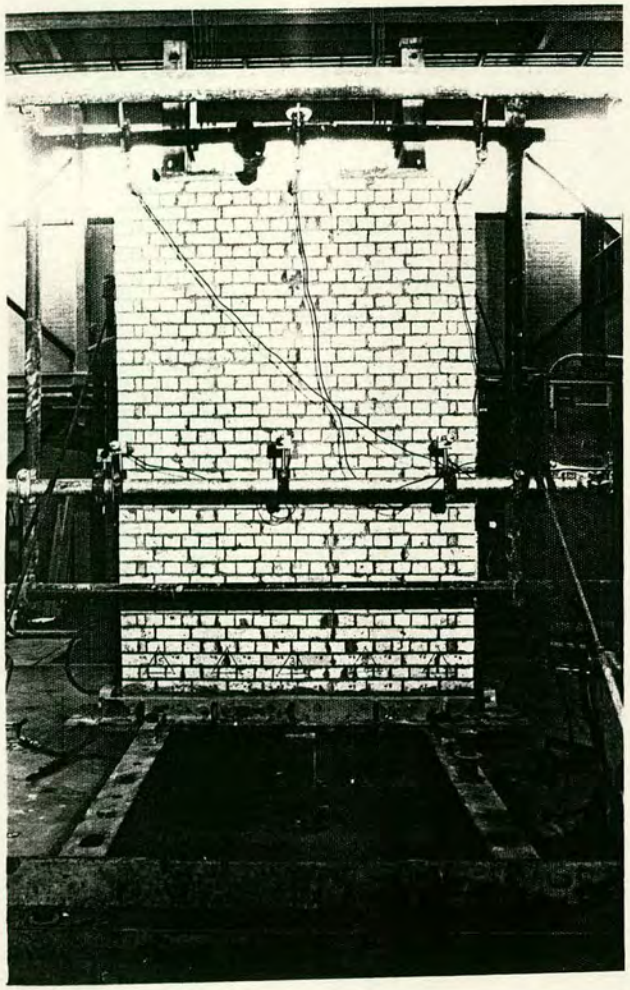

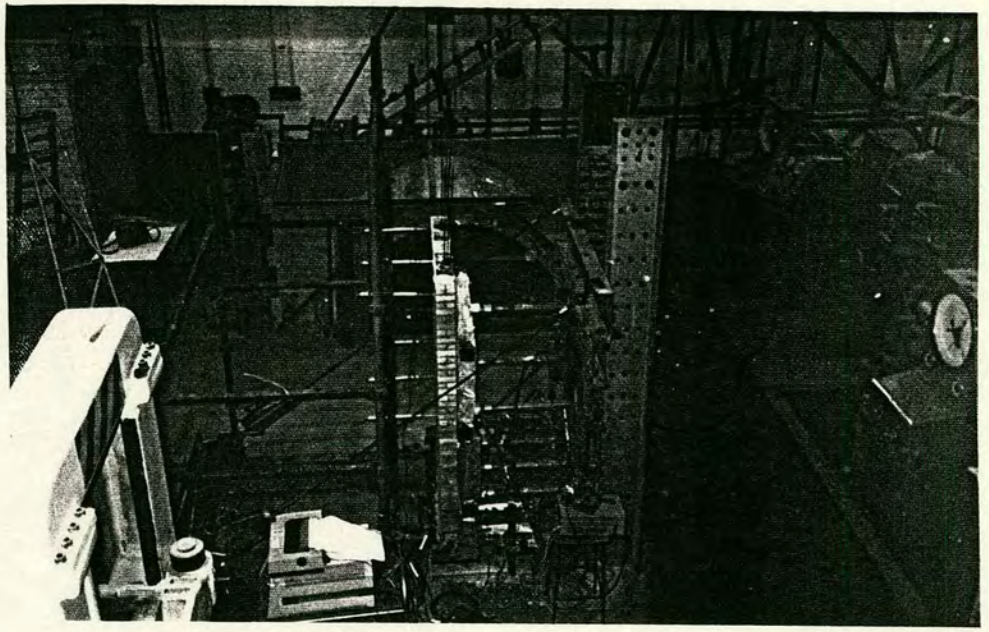

Figure 6.3.28 General view of walls loading arrangement

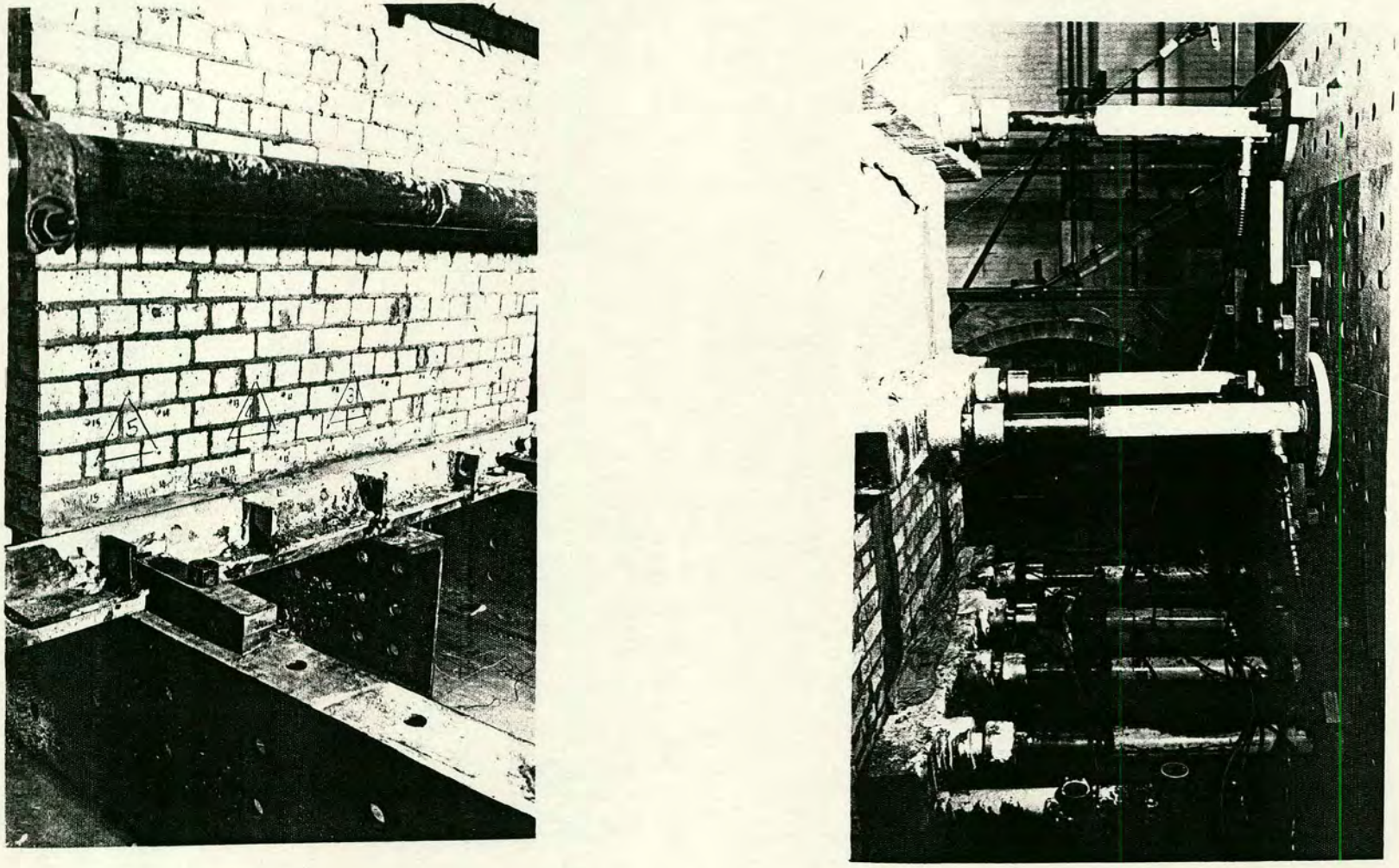

Figure 6.3.29 General view of walls loading arrangement and base plate.

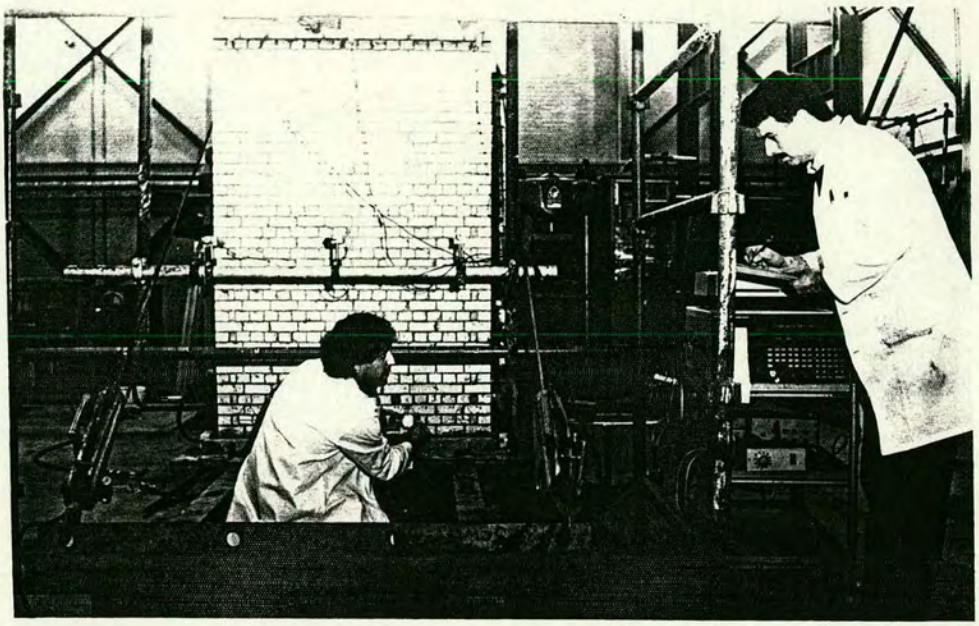

Figure 6.3.31 General view of walls during testing

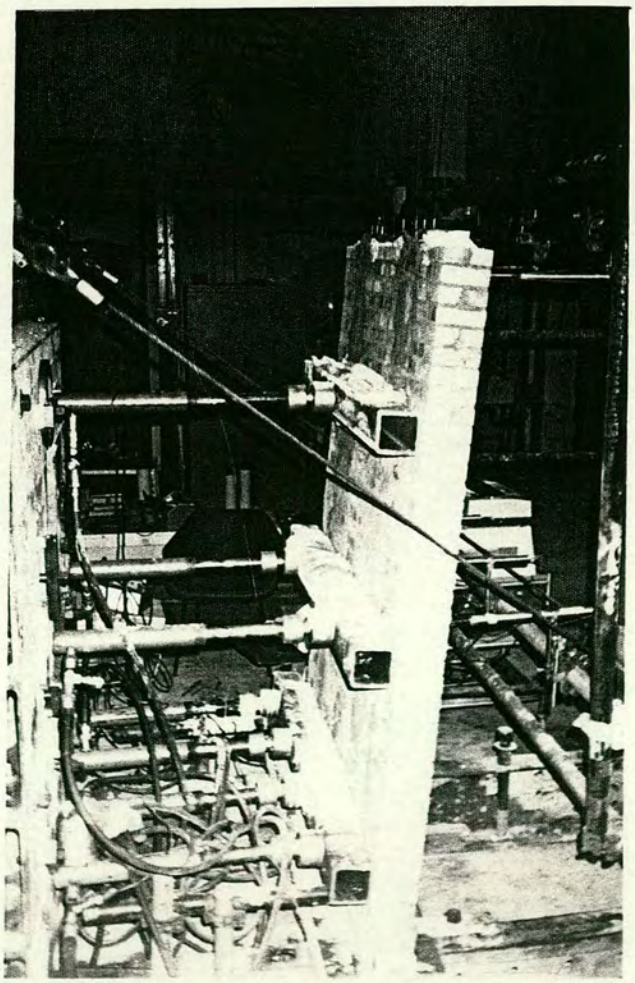

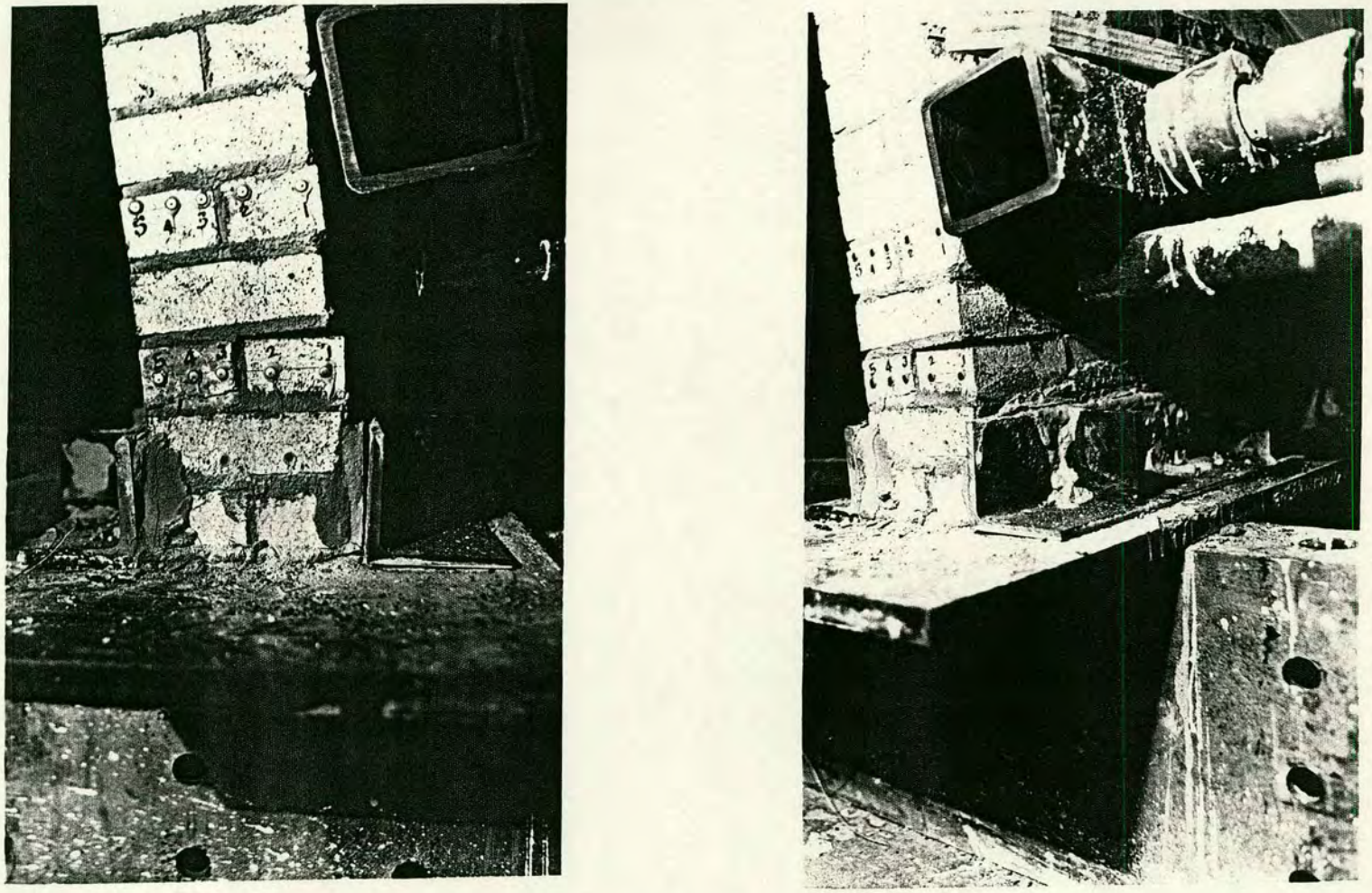

Figure 6.3.32 Typical failure mode and crushing of the brickwork at the base for over reinforced walls.

cracks completely closed. All the walls exhibited a ductile flexure mode of failure due, either to the reinforcement reaching its yield stress, or to the brickwork crushing. There were no signs of shear failure or the development of longitudinal cracks along the pocket boundary in any of the tests. There was no indication that arching of the brickwork panels or vertical splitting of the wall between the pockets had occurred especially with wall 5,the highly over-reinforced section.

Designing for shear to the draft code recommendations was found to be very conservative, primarily because the characteristic shear strength was too low and the partial safety factor for shear was high. Finite element analysis marginally predicted the wall behaviour more accurately than the direct method of analysis. The code recommendations predicted the strength of the over-reinforced section less accurately than the under-reinforced section, perhaps due to the extra nominal wall strength gained as a result of the overlap prestressing forces and the performance of the wall as a homogeneous cantilever. The code should therefore acknowledge these features.

On the other hand, the predicted balance condition, using the stress block analysis in section 5.2.2, showed good agreement with the experimental results. The cracks in general were initiated along the final bed joint at the base on the tension face. As the load increased, the under-reinforced walls, 1, 2 and 3, experienced yielding of the reinforcement which resulted in large increases in strain for small increases in load and caused the neutral axis depth to decrease until total failure occurred. This flexural tension failure was associated with excessive deflections and crack propogation. The over-reinforced walls 4, 5 and 6, exhibited similar failure modes, but at a later load stage a

sudden and brittle compression failure of the wall occurred. The flexural compression failure was associated with excessive deflections and crack propogation until total failure occurred. None of the walls experienced vertical cracking on the compression face nor any horizontal cracks, except in the first and second courses on the tension face. Therefore, the percentage of steel area and the prestressing and overlap prestressing forces have a considerable influence on the flexural strength, shear strength and failure mode of post-tensioned brickwork retaining walls.

6.3.10 Summary and Conclusions

The aim of this study was to investigate the behaviour of post-tensioned brickwork retaining walls. Six half-scale brickwork walls were fabricated vertically on top of a steel base. The walls were built using English bond with two pockets formed in the brickwork at regular intervals along the loaded face. The loading arrangement was chosen to produce bending moments and shear forces at the base of the wall similar to that produced by a triangular pressure distribution. The area of steel, and consequently the prestressing force, were varied and their effect on the magnitudes of the deflections, cracking characteristics and ultimate moment studied. The observed relationships were then compared with those obtained from theoretical analyses.

The following conclusions can be summarised below:-

1. Increasing the steel area, and consequently the prestressing force, in the wall produces corresponding increases in flexural strength and shear strength, and reductions in cracking, curvature and deflection.

2. The moment-curvature and load-deflection relationships for walls with small percentage areas of steel, exhibit a distinct three phase behaviour pattern corresponding to uncracked, cracked with steel in the elastic range, and cracked with steel yielding.
3. Increasing the steel area tends to eliminate the third phase of the moment-curvature and load-deflection relationships.
4. All the walls exhibited a ductile flexural mode of failure due either to the reinforcement reaching its yield stress or to the brickwork crushing. There was no indication that arching of the brickwork panels or vertical tensile splitting of the wall between the pockets occurred.
5. Experimental results indicated that a post-tensioned brickwork retaining wall was unlikely to fail in shear, even when heavily reinforced.
6. The most effective spacing of the pockets in post-tensioned brickwork retaining wall is H/3, where the panel length is the distance between the centre line of the formed pockets.
7. Finite element analysis provides results which show closer agreement with the experimental results than those based on the direct method of analysis or on the BS.5628 recommended stress block. This is because the finite element analysis method acknowledges the effect on nominal strength of the overlap prestressing forces and the performance of the wall as a homogeneous cantilever.
8. The balanced area of steel, predicted by the stress block analysis in section 5.2.2, was in good agreement with the value found experimentally.

CHAPTER 7

PARAMETRIC STUDY

7.1 General

The design of post-tensioned brickwork retaining walls involves the consideration of several factors. In this chapter, a programme of analysis was carried out to examine the effects of the following factors:

(i) pocket spacing,

(ii) slenderness and

(iii) percentage area of steel

on the performance of the wall.

The direct method, yield line method and non-linear finite element analysis were employed to carry out a parametric study into the behaviour of prestressed pocket-type brickwork retaining walls. Results obtained from the direct method were compared with those from the finite element analysis. The analysis equations are given in Appendix C. As referred to in previous chapters, the results from the finite element analysis showed good agreement with the experimental results because the analysis acknowledged the nominal strength gained by the overlap prestressing forces and the behaviour of the wall as a homogeneous cantilever. The results shown in Table 7.1 are qualitative rather than quantitative since the analysis is a numerical procedure and therefore did not take account out of plane shear stress. This factor may have little, or no, effect on the final result since out of plane shear failure was not observed in any of the tests. The finite element discretisation selected for the analysis was similar to that developed for the wall analysis outlined in Section 5.1.4. The brickwork was modelled as a bi-axial non-linear model, using the following material properties:

1.	Young's Modulus	= 21000 N/mm^2
2.	Poisson's Ratio	= 0.15
3.	Compressive strength for brickwork	= 30 N/mm^2
4.	Shear retention factor	= 1
5.	Tensile strength	= 1.5N/mm^2
6.	Softening factor	= 50

The geometric and non-linear material properties were based on deformation charactersitics obtained from tests on individual grout specimens, mortar specimens and single course prisms. The model elements consisted of 10 composite material layers. At the base of the model, the structure was restrained against translation and rotation in all global directions. At one end of the discretisation, the model nodes were restrained against translation in the x direction and against rotation about the y axis. This arrangement was modelled only in half the structure due to symmetry. The data run was in non-linear control. The convergence factor controls for displacement norm, residual force norm and external work norm were 0.1, 0 and 0.001 respectively.

Yield line analysis was used to analyse the unreinforced panels spanning between the pockets and off the base. The assumptions and equations used for the loading conditions were as outlined in section 5.3. The material strengths, shown above, were chosen to be representative of those most likely to be used in practice. The results obtained from this method were compatible with those given by the finite element method. Yield line analysis applied to the wall tests usually gives conservative results (Cajdert, 1980).

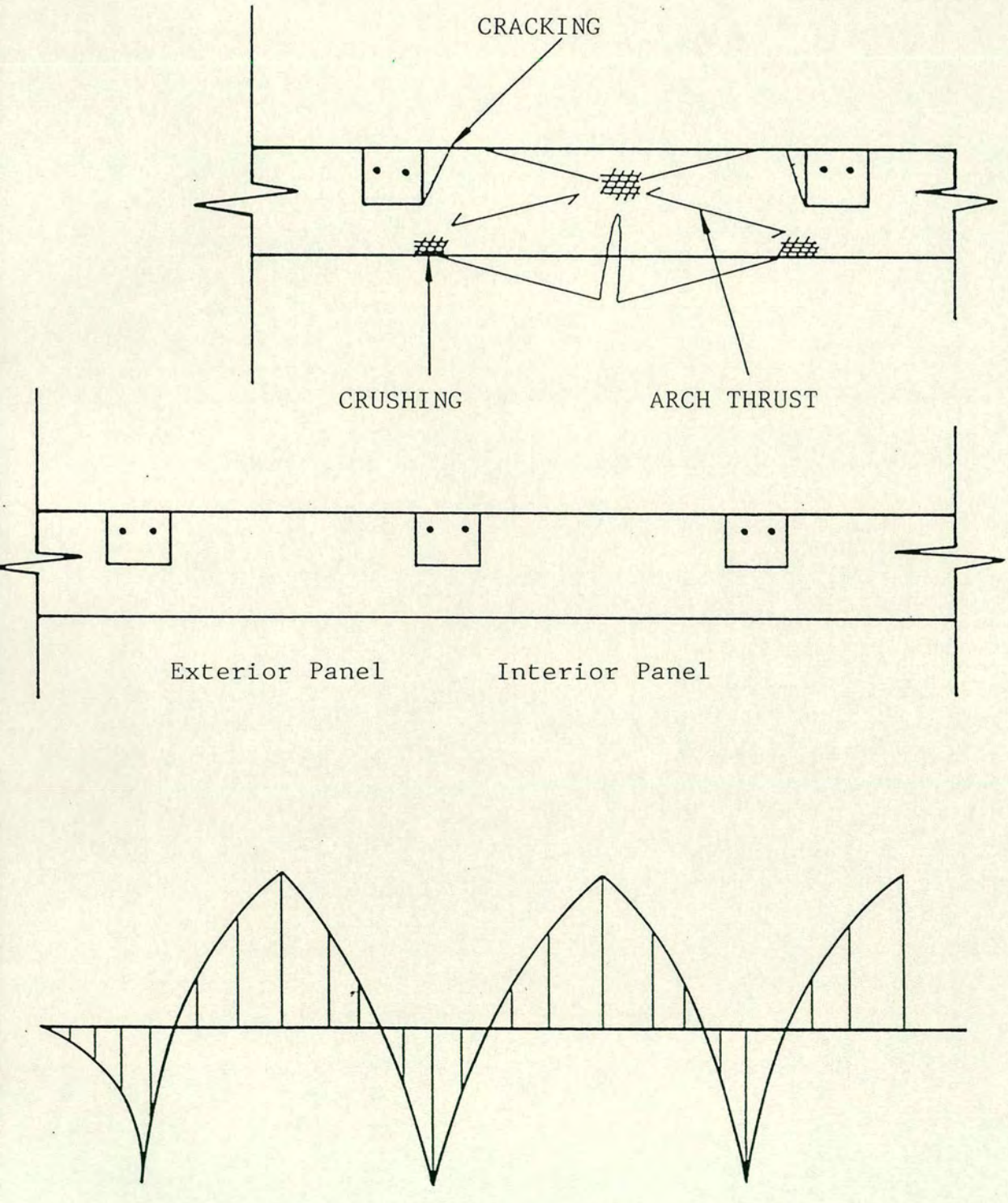

Figure 7.1 Arching Action

7.2 Results

Due to a lack of knowledge regarding the behaviour of laterally loaded masonry walls, the lateral load capacity could not be determined analytically (Satti, 1972). This statement was made because a direct analytical solution at that time gave no consideration to the nominal gain in strength produced by the wall behaving as a homogeneous structure.

Table 7.1 shows the results of a parametric study of 39 different types of wall. The study involved the use of the direct method, yield line method and finite element analysis. For each wall, the percentage area of steel was calculated to represent an under-reinforced structure. To determine the minimum aspect ratio, the analysis considered three types of wall height and three types of panel thickness. The programme selected the most common current techniques used in the construction of pocket walls. From the results shown it can be seen that the principal advantage of the finite element analysis, compared to the direct method, is that it investigates bi-axial bending produced by the wall spanning vertically from the base whilst the brickwork panels span horizontally between the pockets. It is therefore a quick and economic way of investigating in areas where full scale tests are necessary. It must be admitted that the parametric investigation and its results are more qualitative than quantitative in nature, even though in the previous chapter it has been shown that the results obtained from a finite element analysis of pocket-type structures were in good agreement with the experimental results. However, it was not possible to undertake an extensive experimental study because of the costs involved.

All the walls failed either in flexure by yielding of the steel, by crushing of the brickwork or by panel failure. There was no indication that arching of the panels took place. A balanced failure was achieved when the

tensile stress in the steel, the compressive strength of the brickwork and the bending strength of the panel spanning in both the vertical and horizontal directions reach their critical values simultaneously. The results from both the experimental and parametric studies showed clearly that the walls behaved as ductile structural elements.

The British Standard presently assumes that masonry is a brittle material and has adopted a factor of safety which may be unnecessarily large. The ACI Building Code has adopted a value of $0.45f_m$ as the allowable compressive strength. From experimental and theoretical wall results, in the author's opinion, these assumptions are extremely conservative Table 6.9.

It was observed during the data run that several of the element joints on the tension face of the wall had opened up substantially prior to failure. This can be explained by the fact that the tensile steel bars were fully bonded throughout. As the steel yields the length of the bars increase causing cracking in the joints on the tension face of the wall. Since the major weakness in brickwork retaining walls is the discontinuity introduced by the mortar joints, the analysis confirms that post-tensioning increases the tensile and flexural strength of the wall. It was observed both experimentally and theoretically that on removal of the load, even up to ultimate load, the panels regained their original shape. Post-tensioned brickwork retaining walls may be better suited to repeated or cyclic loading. Comparing the moments predicted from the direct method of analysis with those obtained from the finite element analysis, it can be seen that the moments from the direct method are 20-30% less than those from the finite element method. This is because the latter method allows for the effects of the overlap prestressing forces and the

behaviour of the wall as a homogeneous cantilever on the strength of the wall.

Figs 7.2-11 give details of the parametric study results predicted by the finite element analysis. The figures provide an efficient method of predicting the percentage area of steel and the ultimate moment for a specific value of aspect ratio. The figures also show reducing the aspect ratio value will decrease the percentage area of steel and increase the ultimate moment value required for failure of the panel. The panel failure predicted by the yield line approach gives a slightly conservative result compared to the finite element method.

The experimental evidence supported the assumption that masonry walls, subjected to lateral load, exhibit ductile properties, thus justifying the use of yield line theory. The main difficulty in using yield line analysis in the parametric study is deciding the values of "μ" and "i", when considering the influence of the prestressing forces and the buttressing resistance of unreinforced brickwork panels. The self-weight of the wall is negligible compared to the pre-compressive forces resulting from the applied prestressing load. "μ" is the rotational ratio i.e. the ratio of the flexure strength of the panel when failure is parallel to the bed joint to that when failure is perpendicular to the bed joints. "i" is the model of the boundary conditions for the interior and exterior panels as explained in the section 7.3. A computer program was developed to find a value of "μ" which was applicable to the various aspect ratios and ultimate moment relationships. For specified values of α, μ, ω and L, the Fortran program carried out a large number of analyses using equilibrium equations and output for the possible failure moments.

Figs 7.12-16 present the predicted results from the theory of yield line analysis, as outlined in section 5.3.2. The figure provides an efficient method of predicting the ultimate moment of a wall for specific values of aspect ratio, wall height and thickness. Variations in aspect ratio and ultimate moment relationship with respect to "μ" have been plotted and it can be seen that adopting a value of $\mu = 0.5$ gives results which are in closer argreement with the finite element results.

The parametric study clearly indicates that, for post-tensioned brickwork retaining walls, the effective width of the interior and exterior panels should be taken as h/3, with an aspect ratio greater than 1.15, where the panel length equals the distance between the centre lines of the formed pockets, and irrespective of the slenderness of the wall. It can also be concluded that any increase in the aspect ratio corresponds to significant increases in flexure strength and shear strength, and decreases in crack propagation and deflection. Post-tensioned brickwork retaining walls should be analysed using non-linear finite element techniques, and for highly reinforced structures, reinforcement should be provided in the form of rectangular links located across the pockets to prevent the following:

1. Vertical splitting of the wall due to the development of lateral tension from the prestressing forces and overlap prestressing forces.
2. Shear failure caused by the development of cracking along the pocket boundary.

Deflections under elastic conditions were small and can be assumed to be less than most Code serviceability requirements.

7.3 Wall Panels

Pocket-type retaining walls are usually built with the pockets formed in the brickwork at regular intervals along the loaded face. As adjacent panels provide buttressing, the interior panel may resist further lateral load by acting as a flat dome. Under excessive prestressing forces and lateral pressure, the interior panels might be expected to arch between the pockets. This would not occur in the exterior panel pockets, however, since the end pockets have sufficient in-plane stiffness to resist the arching forces. For various conditions, such as wall slenderness and percentage area of steel, the parametric study, using finite element analysis, predicted the following results:-

1. The behaviour of the wall panels up to failure.
2. "i" - the boundary conditions for the interior and exterior panels.

The boundary conditions, "i", is an important factor in the yield line analysis equilibrium equations, as outlined in section 5.3.2. Yield line analysis predicted the panel strength only, while the finite element analysis could be applied to the overall behaviour of the panel up to failure. Finite element analysis essentially ignores the fact that the lateral strength of the panel is influenced by the bond between the mortar and the brickwork. On the other hand, Hendry and Satti advised the use of $1:\frac{1}{4}:3$ mortar for brickwork walls where the flexural tensile strength is critical. In this case, the brickwork panel fails either by breaking two bricks and two vertical joints, or by a combination of loss of bond and splitting of one brick. Further full scale tests are required to confirm this result. The parametric study analysis, however, using finite element analysis has suggested the following types of failure:

1. Walls with an aspect ratio greater than 1.15:

   Failure resulted from cracking, propogated at the soffit of the wall horizontally along the base, when the flexural tensile strength was exceeded. for walls with high percentage areas of steel, cracking was propogated at the centroid of the section in the form of a diagonal slope, as a result of combined bending and shear. As the load increased several cracks formed along the bed joints at approximately equal heights up the wall.

2. Walls with an aspect ratio smaller than 1.15:

   These mostly failed in the yield line pattern.

3. Walls with a very small aspect ratio:

   These failed in the yield line pattern at one end pocket, and horizontally at 0.33 times the span height above the base at the other end pocket.

The collapse mode in Cases 1 and 3 are inconsistent with those assumed in the equilibrium equations in section 5.3. This is because yield line analysis does not consider the stresses initiated by the wall due to flexure about the base. In the finite element analysis, the stresses, deflection and cracking at the base of the wall were taken into account to counterbalance the area of contact. Finite element modelling of the wall indicated that the flexural stiffness of the panels in horizontal bending was about 25 - 40% of the flexural stiffness in vertical bending for walls with aspect ratios greater than 1.15. The flexural stiffness of the panels in horizontal and vertical bending was dependent upon the extent of the cracking in the cross-section. The extent of the cracking in

the vertical direction was controlled by the presence of diagonal lines of cracks due to the complex bi-axial bending behaviour of the wall spanning vertically from the base whilst the brickwork panel spans horizontally between the pockets. However, the panels exhibited considerable additional lateral capacity beyond initial cracking as a result of the in-plane thrust developed by the prestressing and arching forces of the panel. As described by Rumani and Phipps (1988), flexural cracking in unbonded beams causes the prestressing force in the tendons to increase with increase in applied load. This increase in tendon force is the same at all sections, the flexural cracking effectively transforming the beam into a tied arch. Along with prestressing load, the assumption that the wall is homogeneous increased the vertical moment of resistance of the panel but did not effect the horizontal moment of resistance.

The result from the analysis for the interior panels showed that only a relatively small lateral displacement developed at the pocket boundary prior to collapse. The largest relative displacement occurred midway between the pockets at the lower part of the wall and is associated with triangular load distribution. The deflection of the exterior panel formed in-plane forces causing an in-plane lateral displacement of the end pockets which was counteracted by in-plane arching forces produced by the in-plane prestressing forces. As a result, the exterior panels were only slightly weaker than the interior panels for all values of wall slenderness. The analysis indicated that both panels collapsed simultaneously. From these results it was concluded that, for walls with an aspect ratio smaller than 1.15, the interior panel acted as if it were fixed at the pocket whereas the exterior panel acted as if it were simply supported.

Analysis No.	Height mm	Aspect Ratio α	Panel Thickness mm	Effective Depth mm	Steel Area mm^2	Steel % $\frac{As}{bd}$	Direct Method		Finite Element Analysis				Yield Line Analysis	
							Mc KNM	Mu kNM	Mc kNM	Mu kNM	D Top	Failure Mode	Mp kNM	Failure Mode
1	2200	2.2	215	143	288	0.20	31.30	63.25	45	92	8	C+T	5	None
2	2200	1.6	215	143	360	0.18	40.40	79.71	56.50	109	15	C+T	11	None
3	2200	1.2	215	143	432	0.17	49.30	96.11	65	127	13	C	21	None
4	2200	1	215	143	432	0.14	53	97.69	70	138	12	C+T	30	None
5	2200	0.85	215	143	504	0.136	75	110	74	141	10	C+T	40	Panel
6	2200	0.70	215	143	432	0.10	62	99.78	77	160	8	T	58	Panel
7	2200	0.65	215	143	432	0.09	65.80	100.18	77	141	8	P	-	-
8	2200	0.85	215	143	432	0.117	58	99	77	141	9	P	-	-
9	3000	3	215	143	288	0.20	31.30	63.25	52.50	112	15	C	3.2	None
10	3000	2.15	215	143	360	0.18	40.40	79.71	63	130	14	T+C	7.4	None
11	3000	1.7	215	143	432	0.17	49.30	96.11	70	140	13	T	12	None
12	3000	1.4	215	143	432	0.141	53	97.69	77	150	13	T	19	None
13	3000	1.15	215	143	432	0.116	58	99	80.50	165	16	T	29	None
14	3000	1	215	143	432	0.10	62	99.78	-	122.50	-	P	-	-
15	3000	0.9	215	143	432	0.09	65.8	100.18	-	70	-	P	-	-
16	4500	4	215	143	288	0.18	31.30	63.25	50	100	12.5	T	1.6	None
17	4500	3	215	143	360	0.17	40.40	79.71	60	115	17	T	3.3	None
18	4500	2.4	215	143	432	0.16	49.30	96.11	79	130	33	T	5.9	None
19	4500	2	215	143	432	0.134	53	97.69	85	140	40	T	9.1	None

Table 7.1 Details and Results of Parametric Study

Analysis No.	Height mm	Aspect Ratio α	Panel Thickness mm	Effective Depth mm	Steel Area mm^2	Steel % $\frac{As}{bd}$	Direct Method		Finite Element Analysis				Yield Line Analysis	
							Mc KNM	Mu kNM	Mc kNM	Mu kNM	D Top	Failure Mode	Mp kNM	Failure Mode
20	4500	1.7	215	143	432	0.114	58	99	105	155	45	T	14	None
21	4500	1.5	215	143	432	0.10	62	99.78	105	163	51	T	18	None
22	4500	1.3	215	143	432	0.09	65.8	100.18	105	170	55	T	24	None
23	3000	3	330	220	360	0.164	53	114.2	87.50	192.50	5	T	5.5	None
24	3000	2.15	330	220	432	0.14	75.20	138.73	105	220	5	T	12	None
25	3000	1.7	330	220	504	0.13	93.98	163	157.5	235	15	T	21	None
26	3000	1.4	330	220	648	0.14	117.96	210.85	164.5	250	13	T	31	None
27	3000	1.15	330	220	720	0.126	137	232.72	164.5	270	10	T	47	None
28	3000	1	330	220	720	0.11	146	235.4	-	140	-	P	-	-
29	3000	0.9	330	220	720	0.098	157	237.53	-	140	-	P	-	-
30	3000	0.8	330	220	720	0.087	154	238.17	-	122.5	-	P	-	-
31	3000	0.7	330	220	720	0.076	162	238.9	-	87.5	-	P	-	-
32	3000	2.15	440	293	648	0.16	137	267.18	245	400	6.50	T	23	None
33	3000	1.7	440	293	720	0.139	178	300.27	227.50	445	6.40	T	39	None
34	3000	1.4	440	293	864	0.138	206	360.59	245	490	6	T	61	None
35	3000	1.15	440	293	864	0.113	229	365.47	262.5	525	10.5	T	91	None
36	3000	1	440	293	864	0.098	242	369.62	262.5	550	12.5	T	120	None
37	3000	0.9	440	293	864	0.089	241	371.2	245	590	15	T	150	Panel
38	3000	0.8	440	293	864	0.079	272	372.5	-	280	17	P	-	-
39	3000	0.7	440	293	864	0.069	270	373.52	-	280	21	P	-	-

Table 7.1 Details and Results of Parametric Study

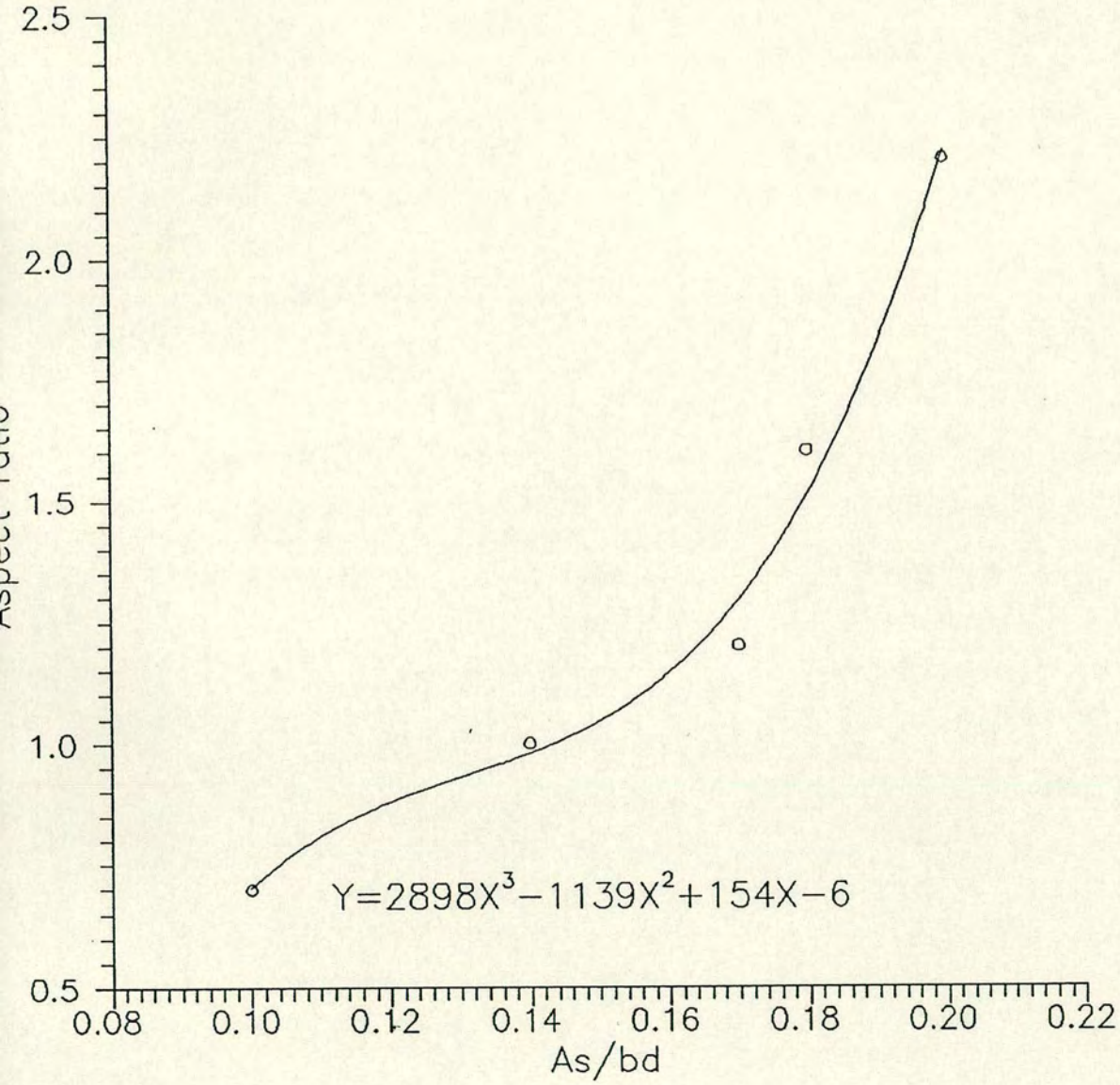

Aspect ratio – steel % relationship for walls (H=2200 & h=215).

Figure 7–2

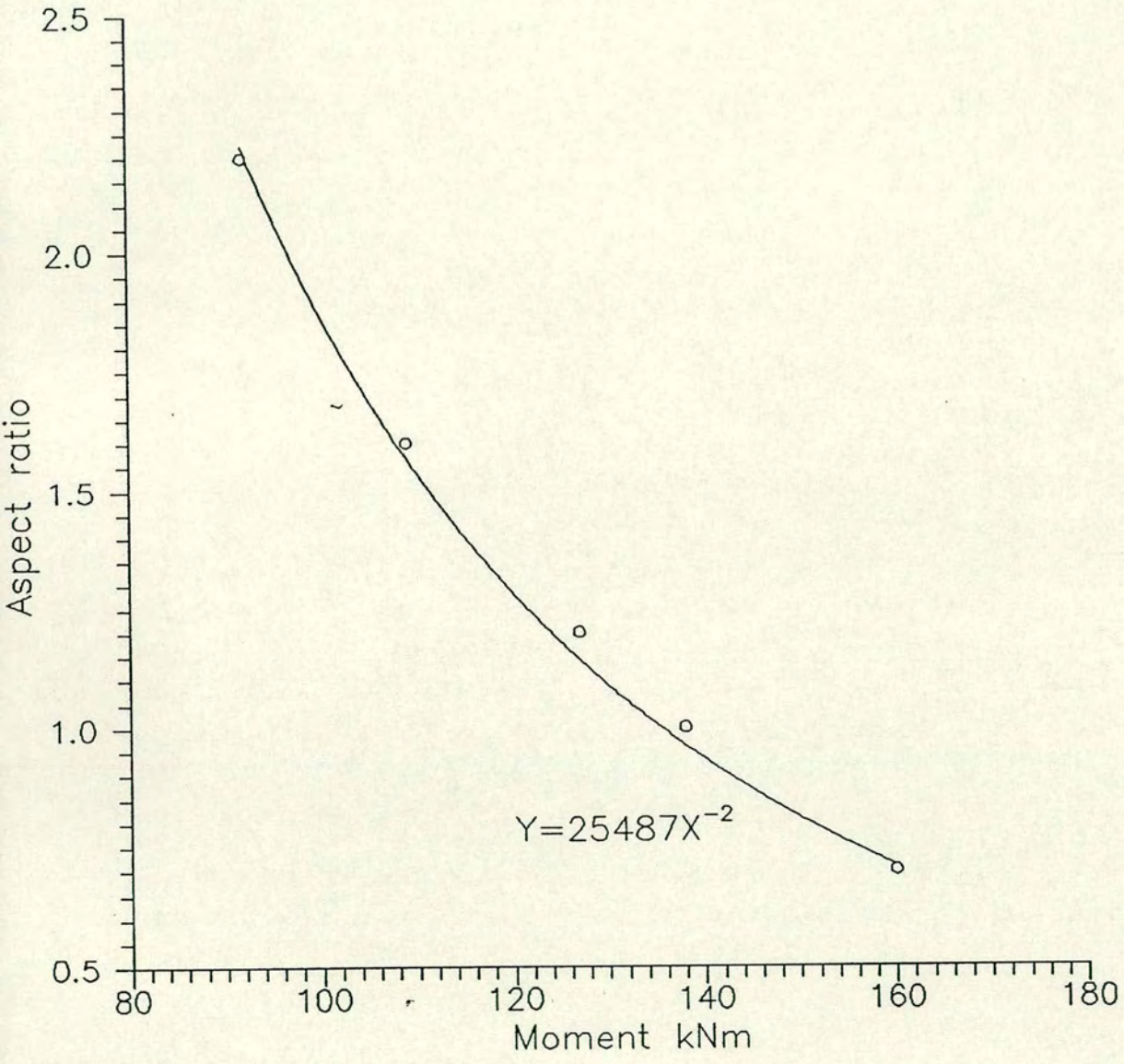

Aspect ratio – ultimate moment relationship for walls (H=2200 & h=215).

Figure 7–3

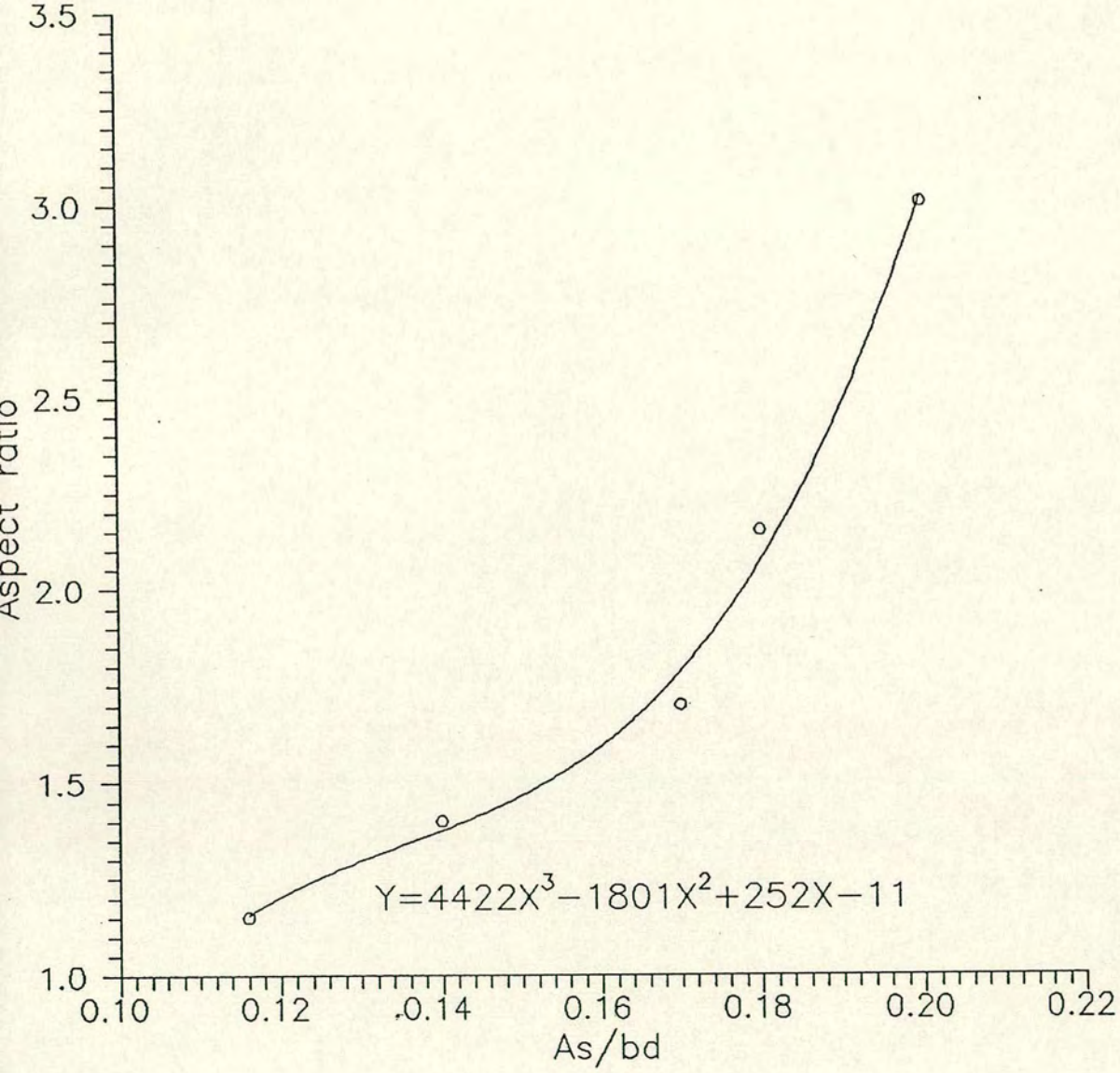

Aspect ratio – steel % relationship for walls (H=3000 & h=215).

Figure 7–4

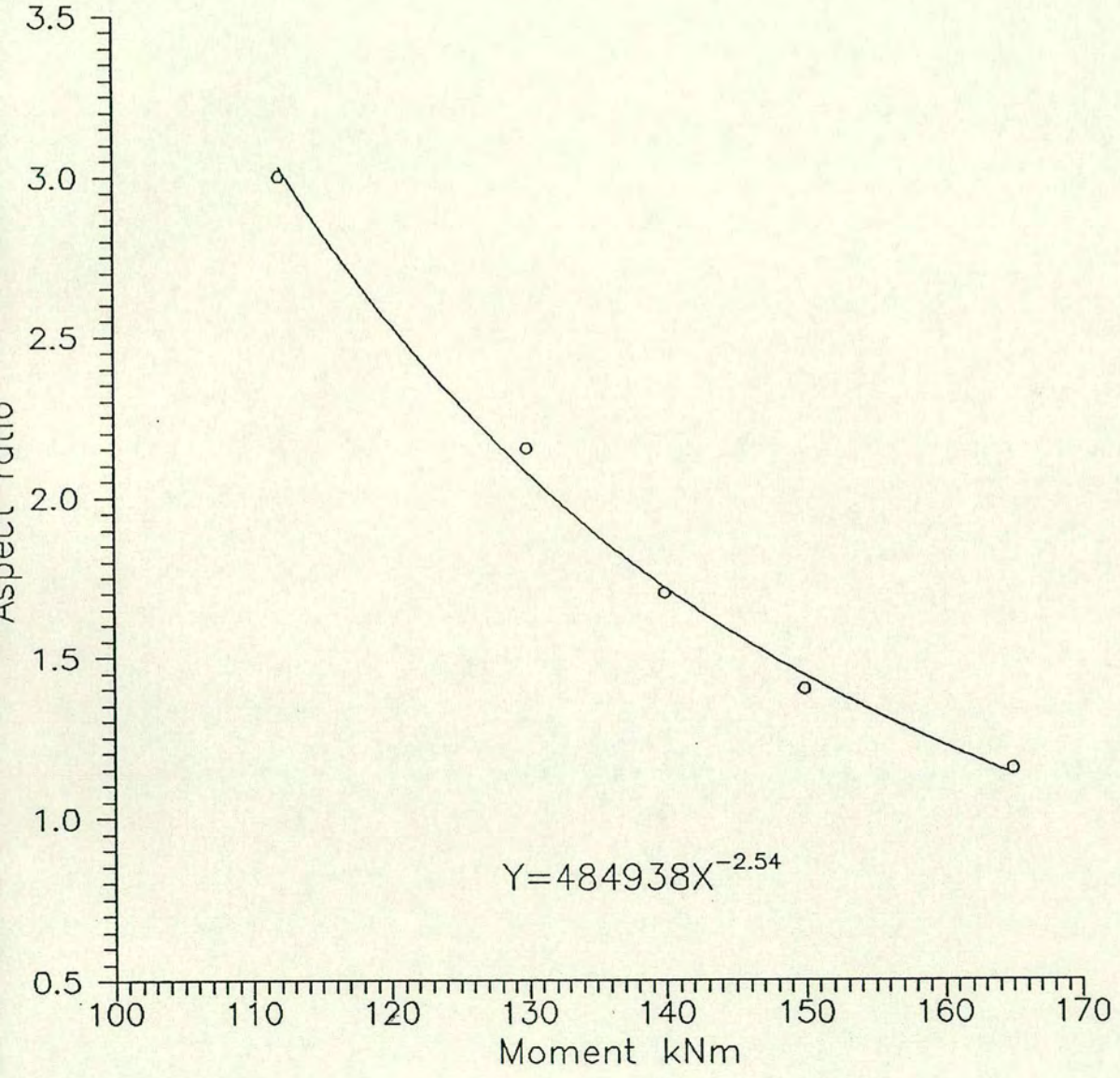

Aspect ratio – ultimate moment relationship for walls (H=3000 & h=215).

Figure 7–5

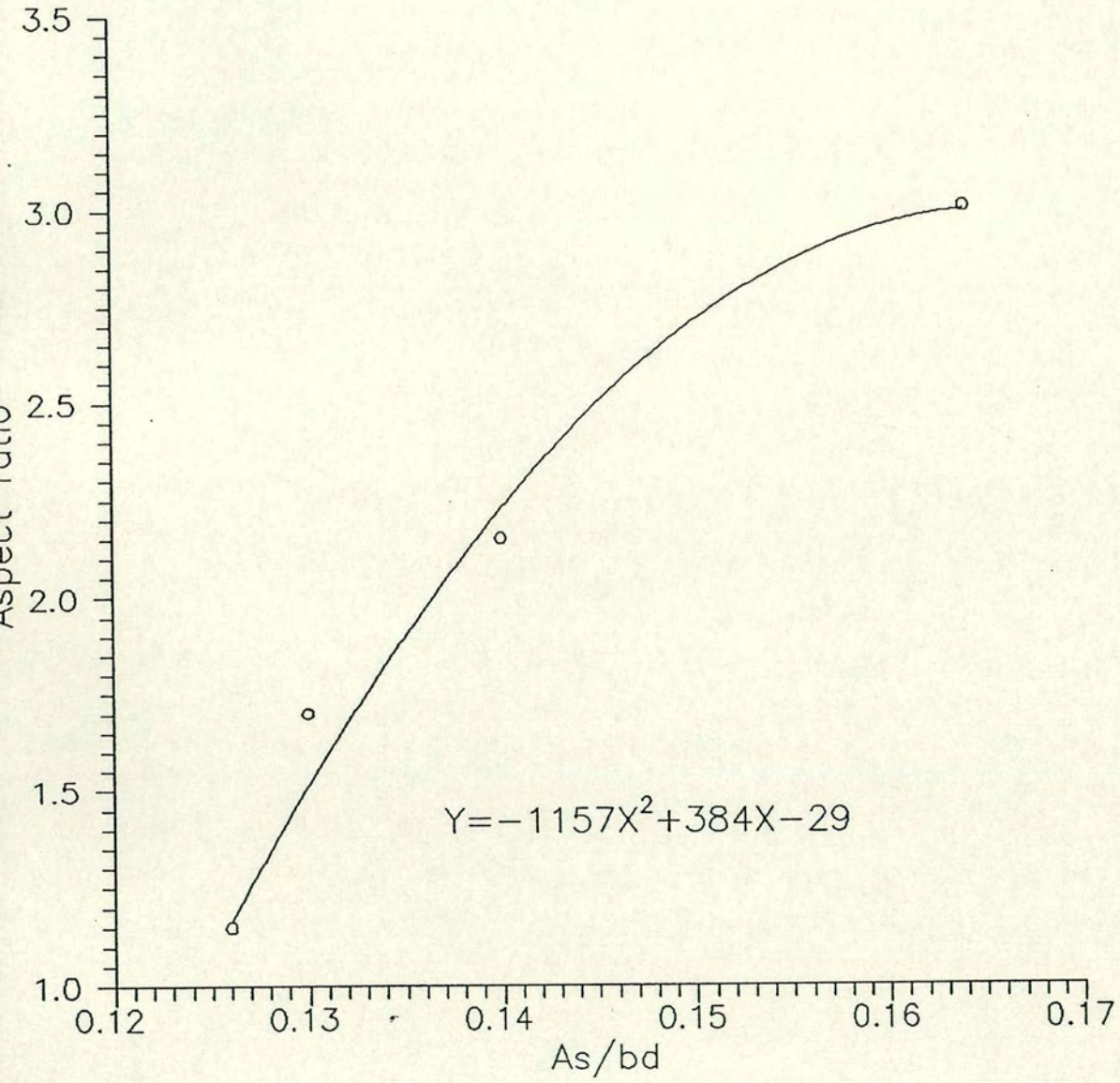

Aspect ratio – steel % relationship for walls (H=3000 & h=330).

Figure 7–6

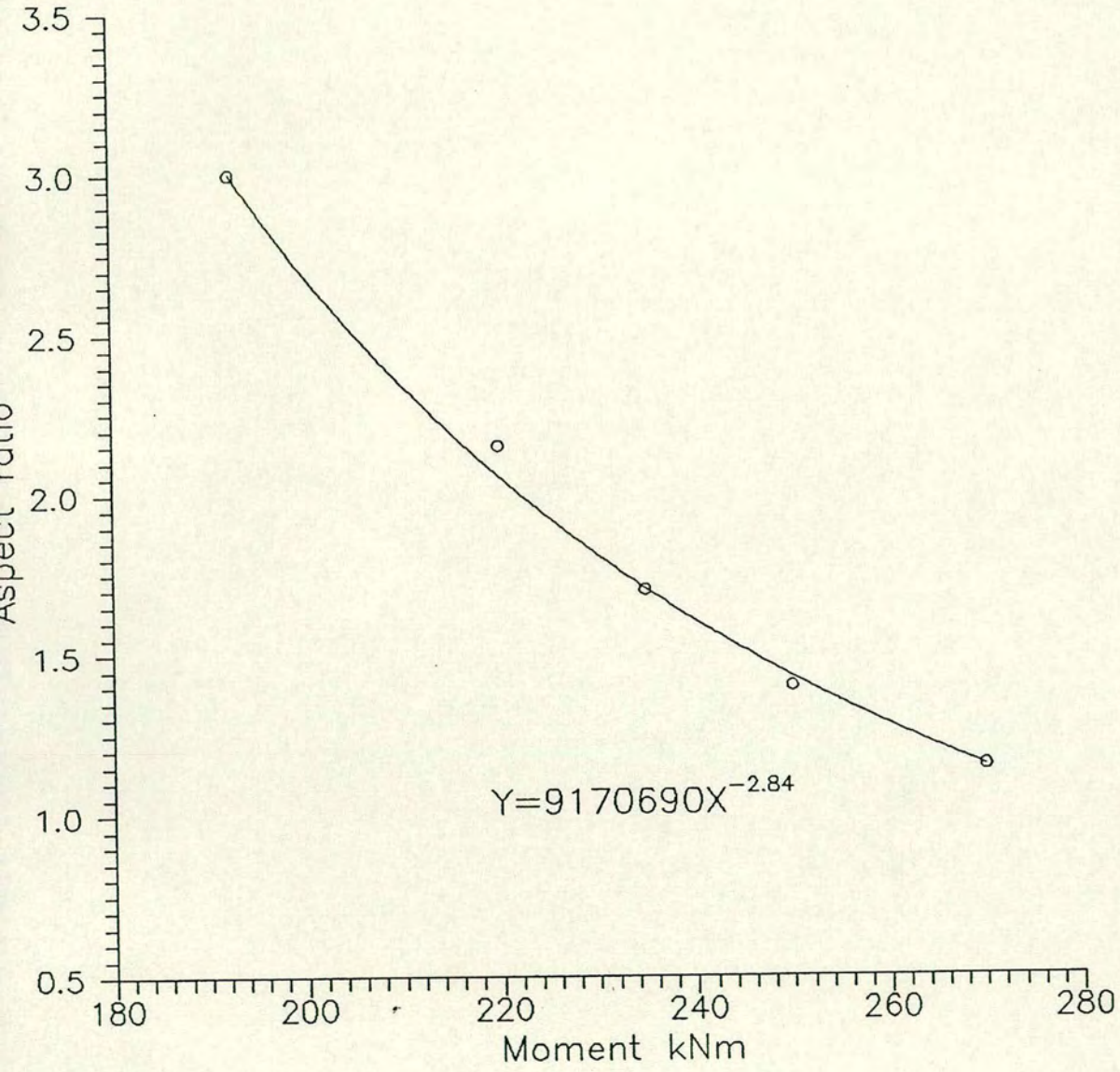

Aspect ratio – ultimate moment relationship for walls (H=3000 & h=330).

Figure 7–7

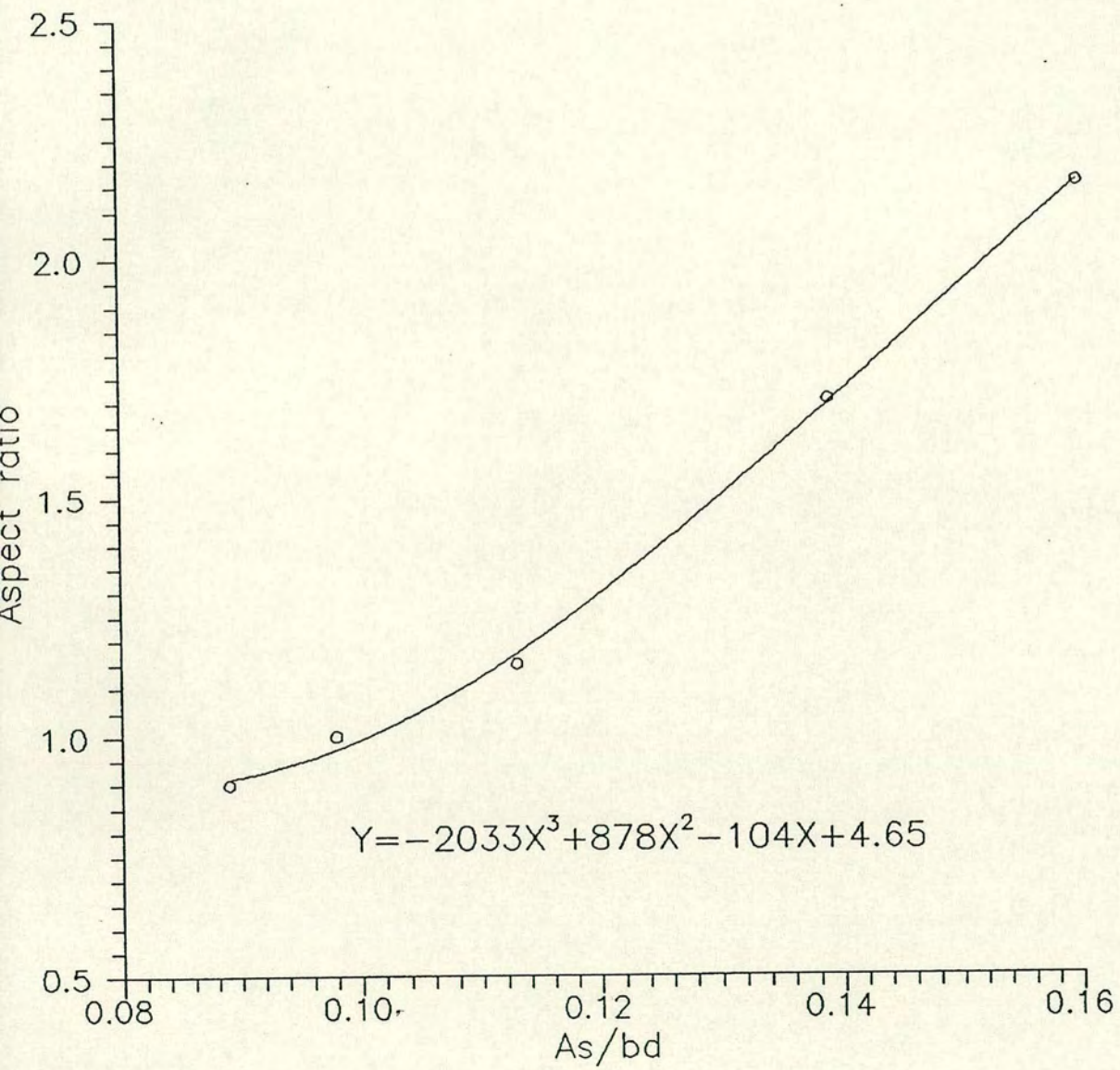

Aspect ratio – steel % relationship for walls (H=3000 & h=440).

Figure 7–8

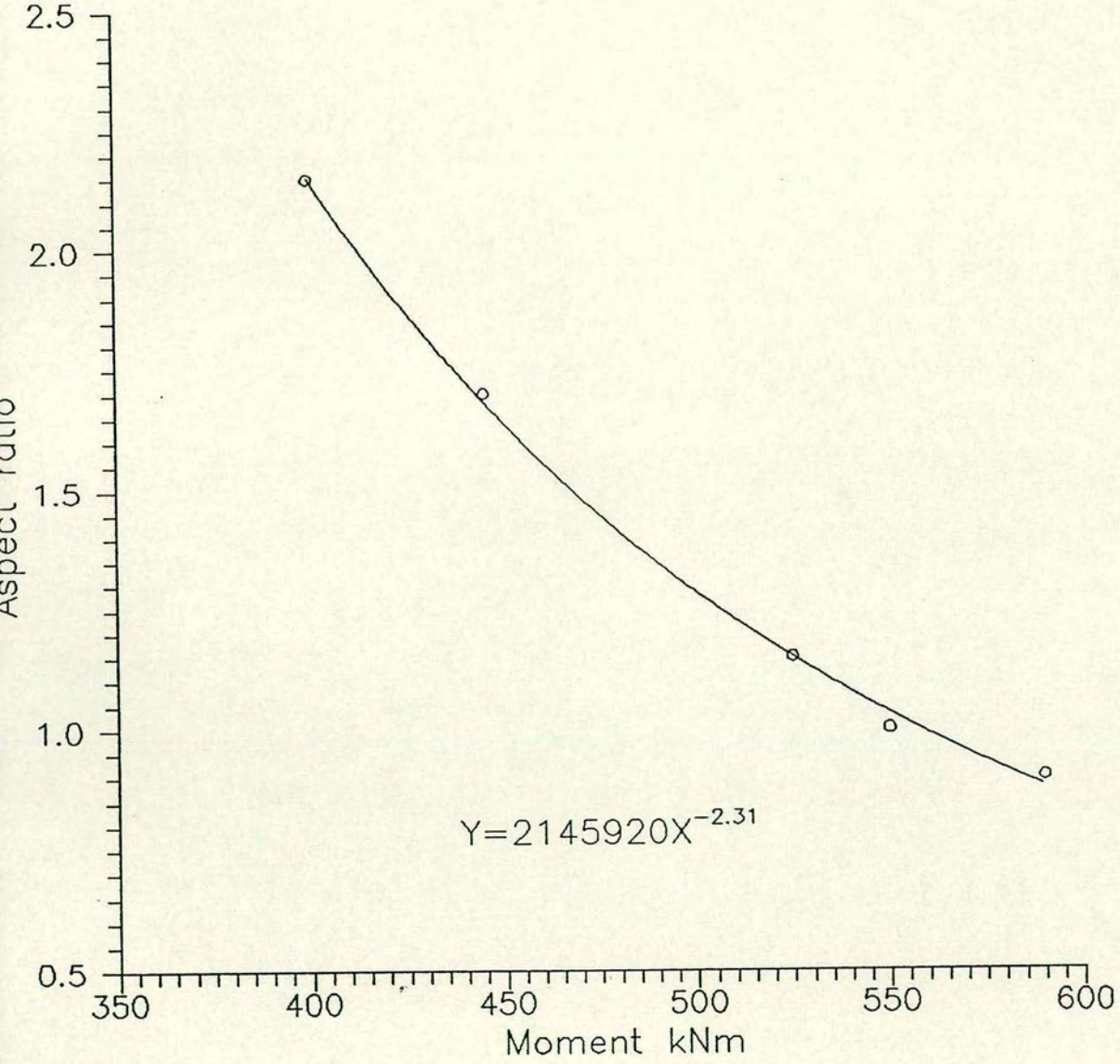

Aspect ratio – ultimate moment relationship for walls (H=3000 & h=440).

Figure 7–9

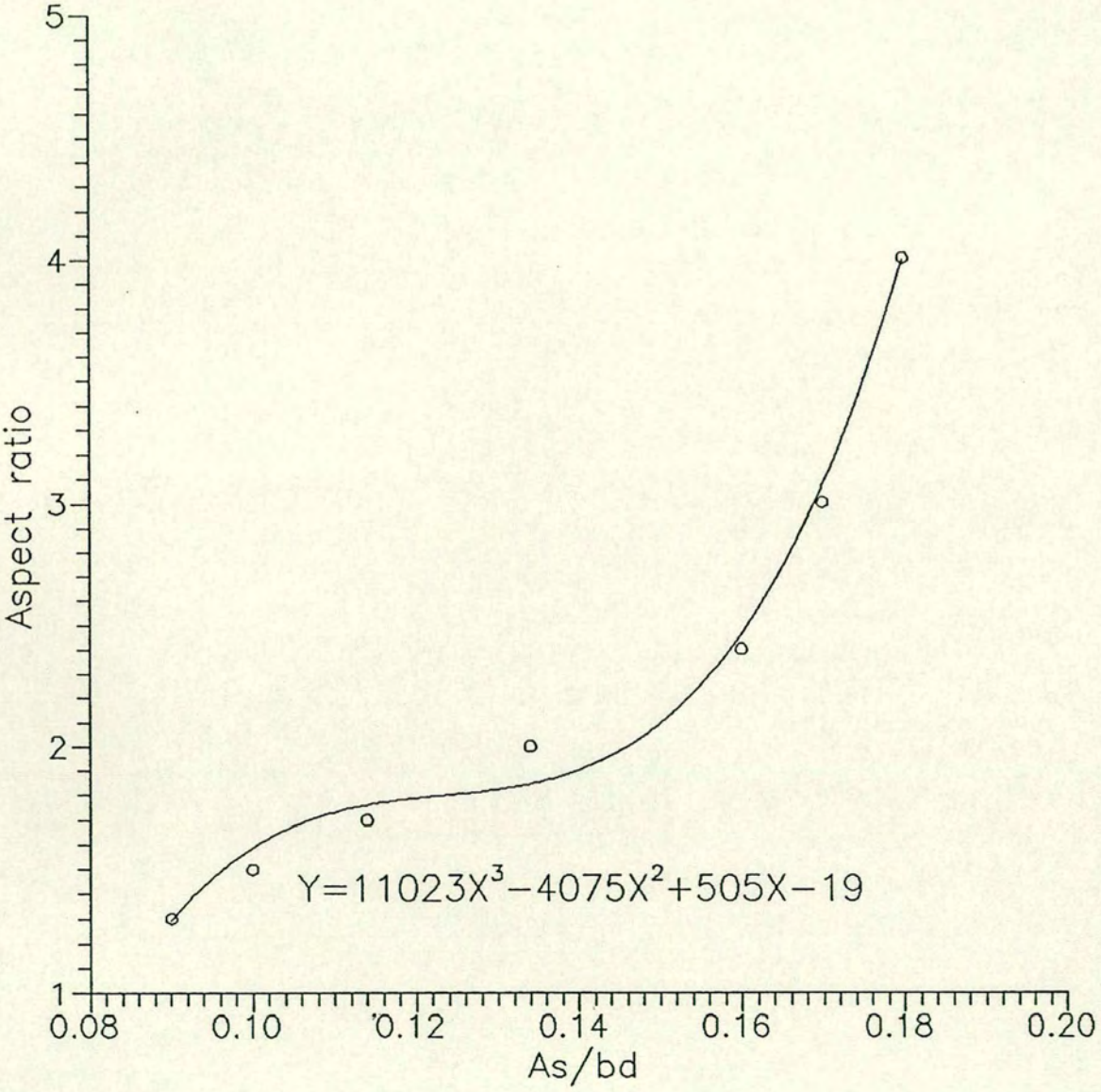

Aspect ratio – steel % relationship for walls (H=4500 & h=215).

Figure 7–10

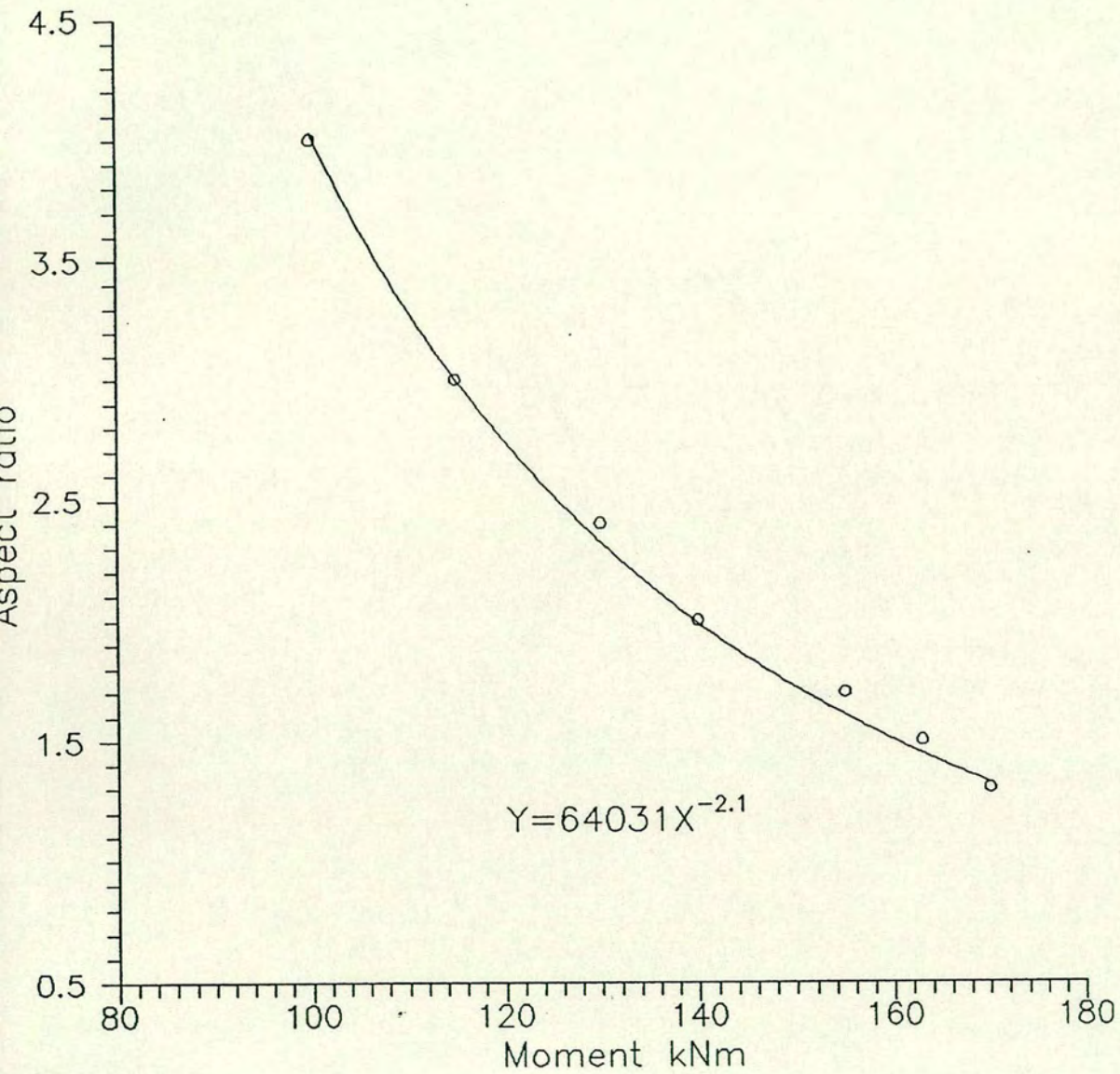

Aspect ratio – ultimate moment relationship for walls (H=4500 & h=215).

Figure 7–11

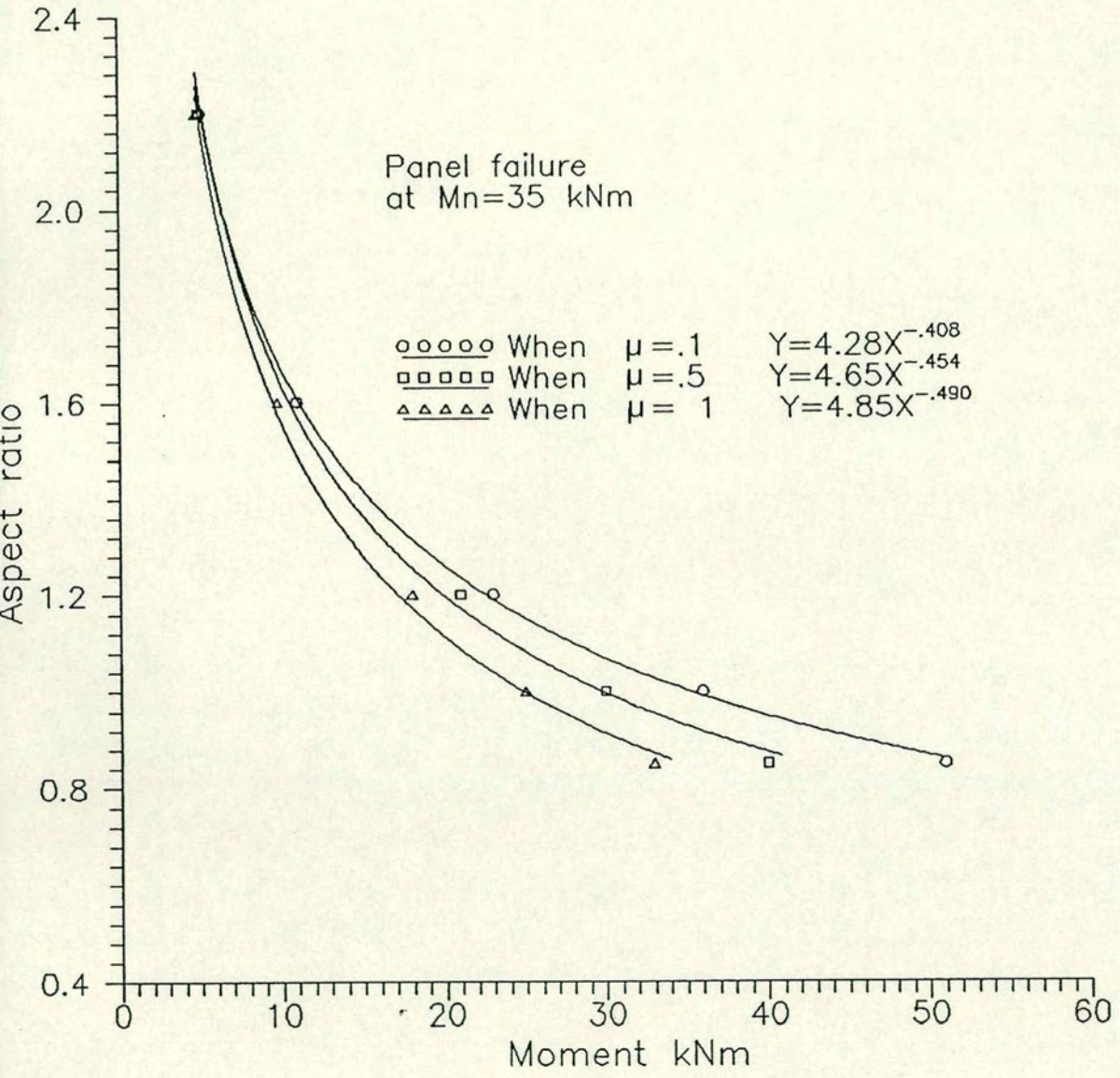

Aspect ratio – ultimate moment relationship for walls (H=2200 & h=215).

Figure 7–12

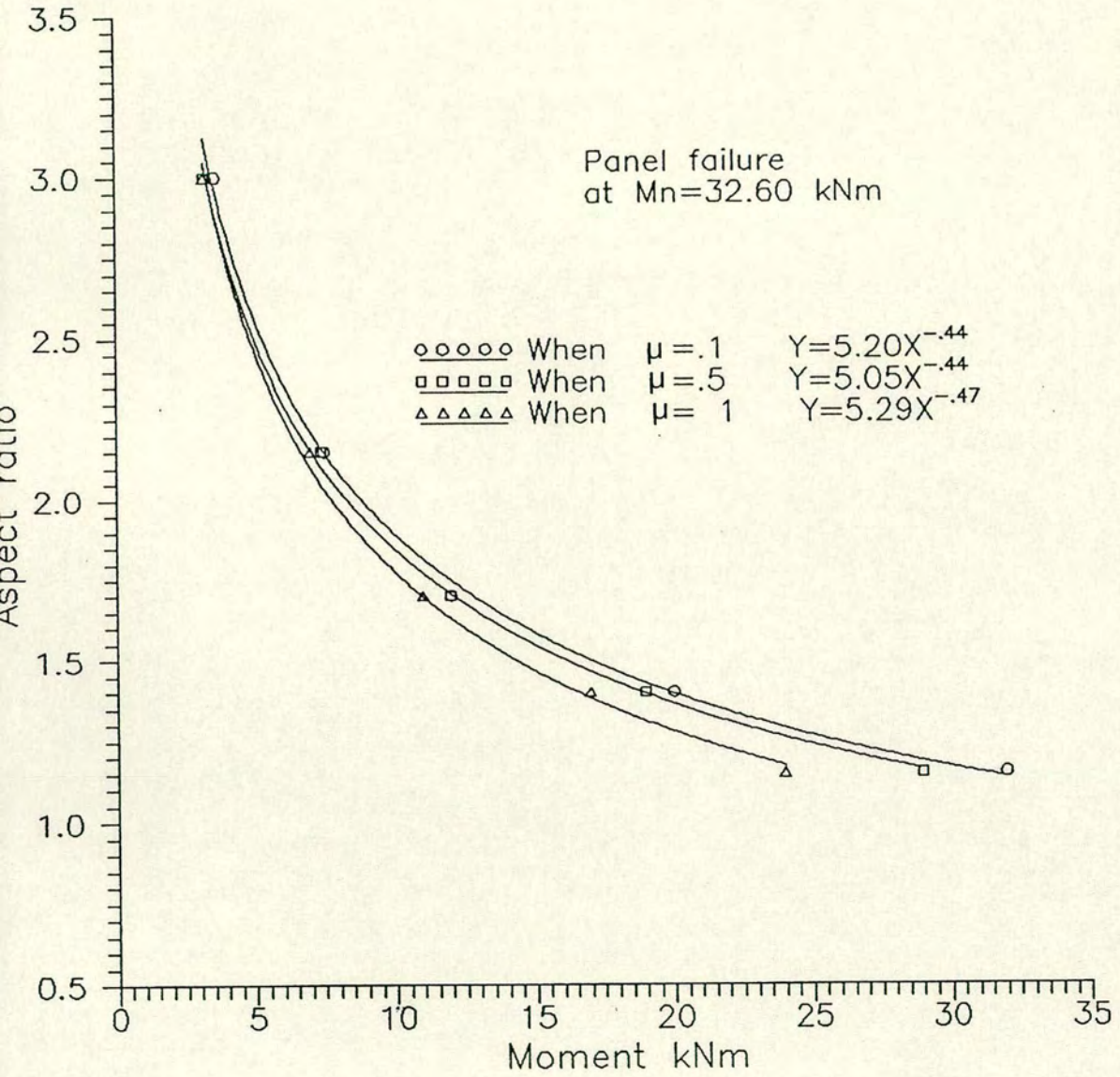

Aspect ratio – ultimate moment relationship for walls (H=3000 & h=215).

Figure 7–13

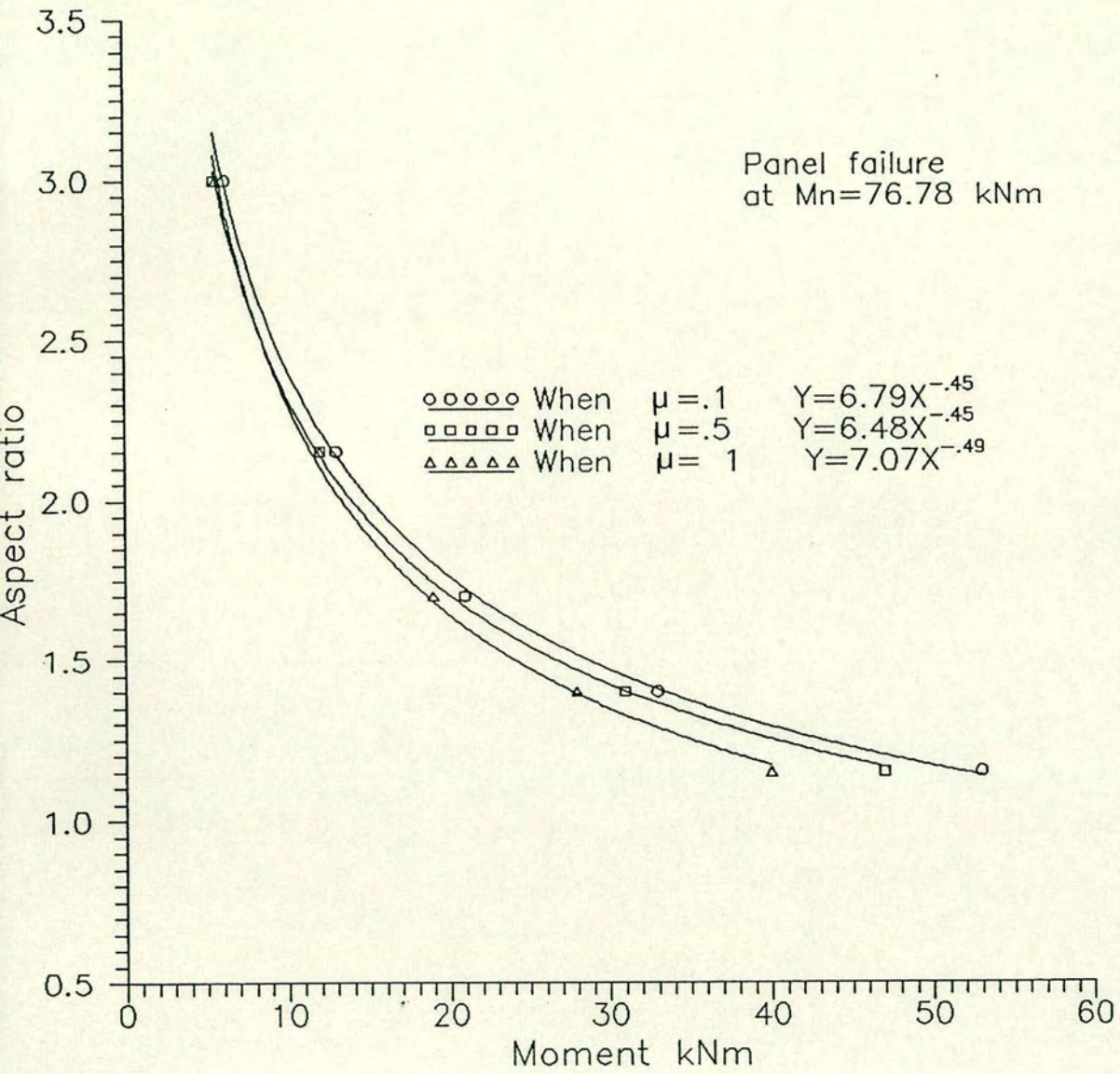

Aspect ratio – ultimate moment relationship for walls (H=3000 & h=330).

Figure 7–14

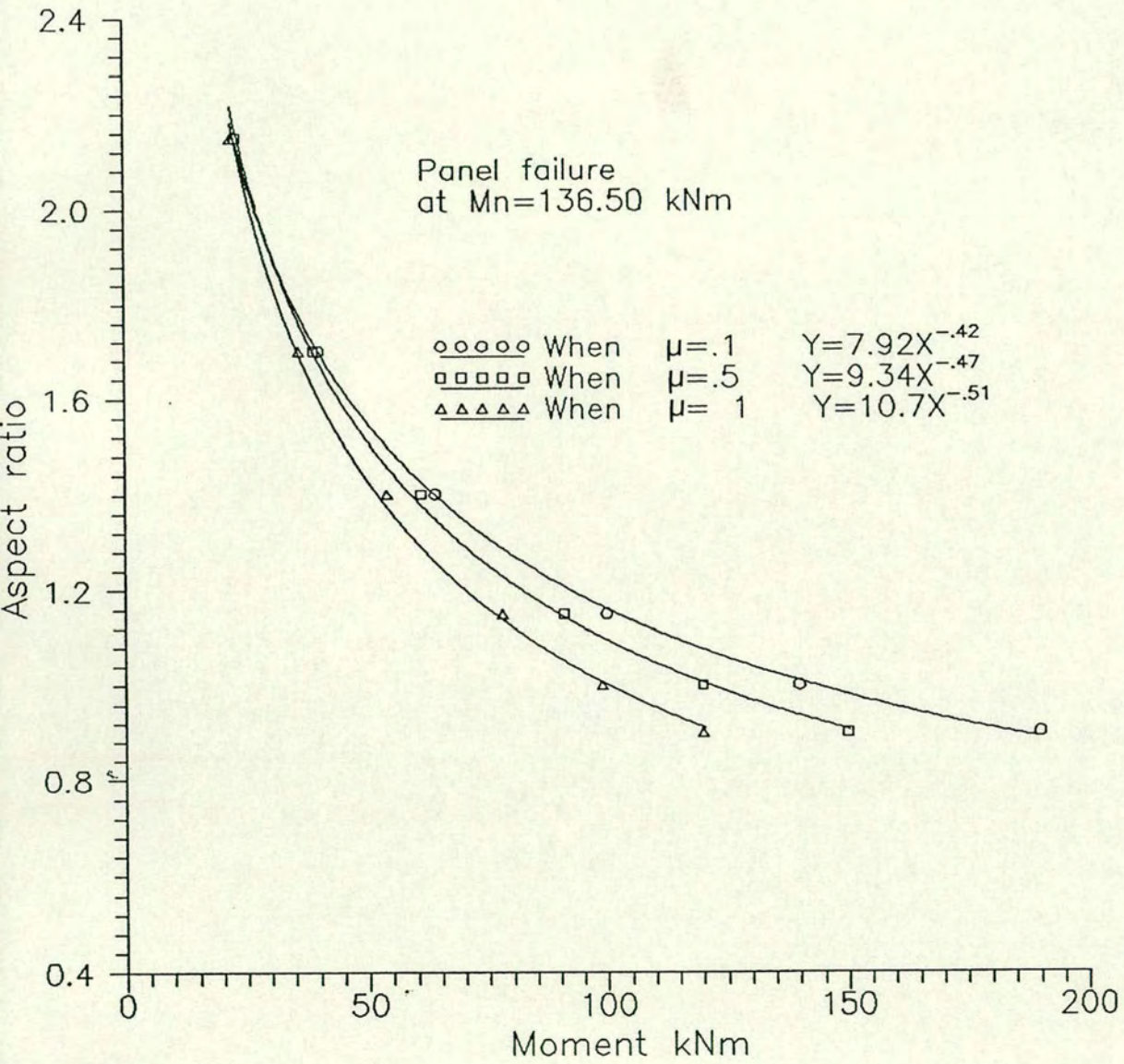

Aspect ratio – ultimate moment relationship for walls (H=3000 & h=440).

Figure 7–15

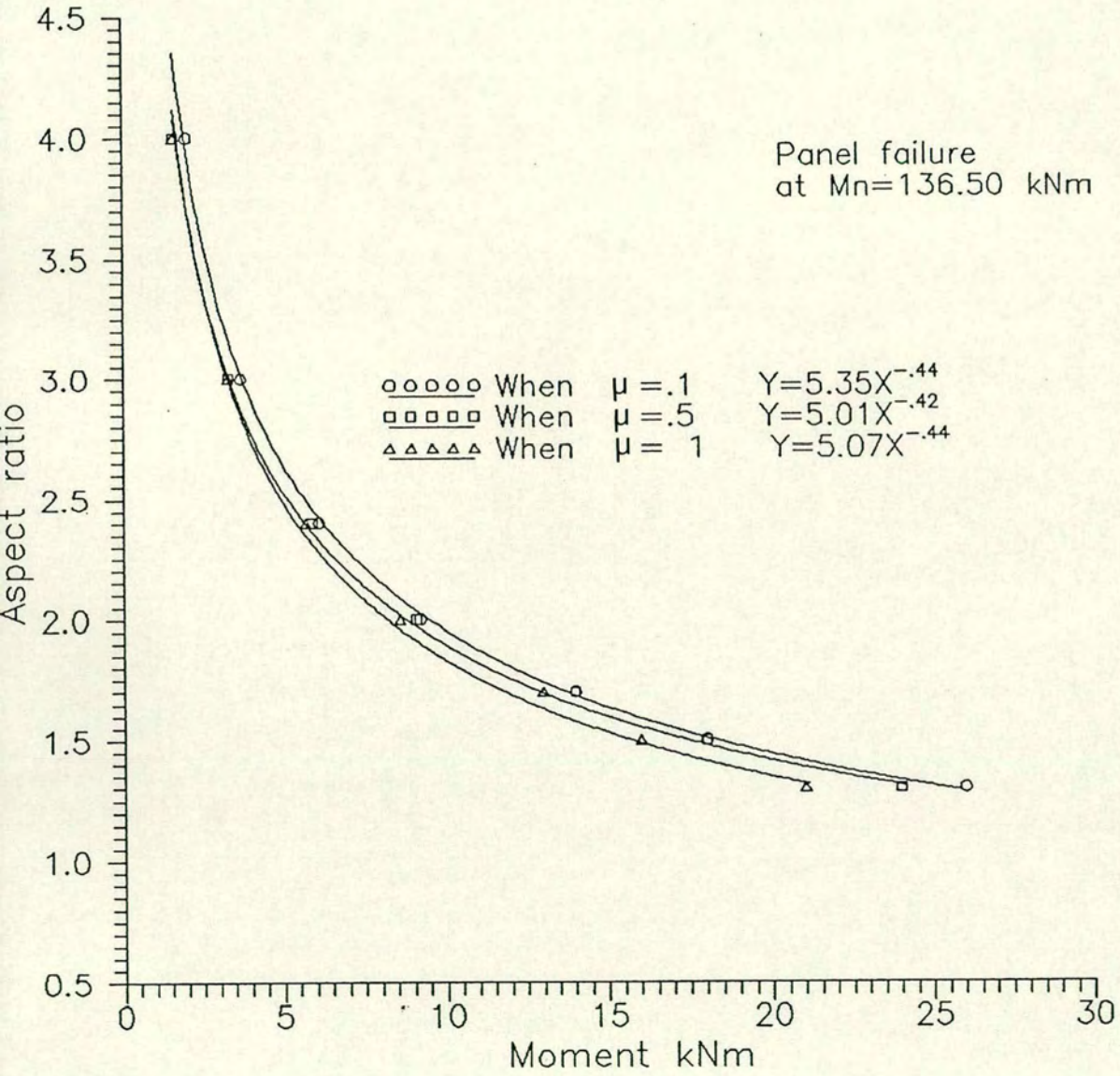

Aspect ratio – ultimate moment relationship for walls (H=4500 & h=215).

Figure 7–16

7.4 Summary and Conclusions

A finite element analysis, based on non-linear geometric and material properties, was employed to study the complex bi-axial bending behaviour of a prestressed retaining wall spanning vertically from the base while the brickwork panels span horizontally between the pockets.

Thirty-nine wall tests were carried out in the parametric analysis. The variables selected for examination were the pocket spacing and the wall slenderness. The results presented in this chapter are qualitative rather than quantitative as the analysis was based on a numerical procedure. The direct method and yield line analysis were also utilised to provide results for comparison with the finite element analysis. The conclusions reached from the theoretical investigation presented in this chapter are summarised as follows:-

1. The effective width of the interior and exterior panels should be assumed to be h/3 where the panel length is the distance between the centre-line of the formed pockets.
2. To prevent panel failure, all wall panels should have an aspect ratio greater than 1.15, irrespective of wall slenderness.
3. Increasing the aspect ratio produces a corresponding increase in the flexural strength, and decrease in the deflection and cracking.
4. All the walls failed in a flexural ductile mode due to either yielding of the steel, crushing of the brickwork or panel failure. There was no indication of arching of the panel or that shear failure took place.
5. The strength of the wall predicted using the direct method of analysis was 20 - 30% less than that given by the finite element analysis. This is because the finite element analysis takes into

account the gain in nominal strength provided by the overlap prestressing forces and the performance of the wall as a homogeneous structure.

6. Yield line analysis gave a good assessment of the strength of unreinforced brickwork panels for walls with an aspect ratio smaller than 1.15.

7. The balanced area of steel, predicted by stress block analysis was in good agreement with the obtained results.

8. Comparison of results with those given by the Code for flexure and shear indicate that the Code recommendations and design formulae are unduly conservative.

CHAPTER 8

CONCLUSIONS

8.1 GENERAL

This thesis has presented a comprehensive study of the behaviour of post-tensioned pocket-type brickwork retaining walls which are cantilever type structures consisting of a vertical assembly rigidly joined to a reinforced concrete base. The assembly is brick masonry with vertical openings on the tension face which contain vertical prestressed tendons and bonding concrete infill. Seventeen full-scale tets and six half-scale tests were investigated. An additional series of control tests were also undertaken to determine the non-linear deformation characteristics and compressive strengths of the materials used in the experimental tests and theoretical analysis. The non-linear deformation characteristics and compressive strengths were determined from tests on individual mortar and grout specimens, prisms and small wallettes. The theoretical investigation was based on the following methods:-

(i) Finite element analysis

(ii) Direct method

(iii) Stress block analysis

(iv) Yield line analysis.

Results provided by the theoretical investigation were compared with those based on recommedations in the Code of Practice. The programme of work was set out to examine the effect of the following four parameters on the performance of the wall:-

(i) Vertical concentrated eccentric load

(ii) Percentage area of steel

(iii) Pocket spacing and wall slenderness

(iv) Type of wall bond.

On the basis of the experimental and theoretical investigations, the following conclusions were drawn:-

1. The failure mode for open pocket brick masonry is fundamentally different from solid masonry subjected to a concentrated load, so that the theories and design methods applicable to concentrated loads on solid masonry may not apply to open pocket brick masonry.

2, The failure mode for concrete infill pocket brick masonry is comparable to solid masonry under concentrated load, so that the theories and design methods for concentrated loads on solid masonry may apply to concrete infill pocket brick masonry.

3. The dispersion angle under the bearing plate for eccentric concentrated loading of open pocket and concrete infill pocket brick masonry is approximately 60 degrees to the horizontal.

4. The minimum spacing between pockets in prestressed brickwork retaining walls should be limited to H/3, where the panel length is the distance between centre lines of adjacent formed pockets.

5. To prevent panel failure, all wall panels should have an aspect ratio greater than 1.15, irrespective of wall slenderness.

6. The balanced area of steel in prestressed brickwork retaining walls can be estimated from the stress block analysis, as outlined in section 5.2.2.

7. The flexural behaviour and ultimate strength of prestressed brickwork walls can be assessed using the non-linear deformation characteristics and compressive strength obtained from tests on single course prisms and small wallettes.

8. Flexural cracks in prestressed brickwork walls propagate at the final brick/mortar interface, horizontally along the base. As the load increases several cracks form along the bed joints at approximately equal heights up the wall. After cracking, the wall remains stable and retains a ductile safe capacity.

9. All the walls failed in flexure in a ductile mode, due either to the reinforcement reaching its yield stress or the brickwork crushing. There was no indication that arching of the brickwork panels or vertical tensile splitting of the wall between the pockets took place.

10. The results indicated that prestressed brickwork retaining walls are unlikely to fail in shear, even when heavily reinforced.

11. Increasing the steel area and aspect ratio in prestressed brickwork walls produces corresponding increases in the flexural strength and shear strength, and reductions in the cracking, curvature and deflection.

12. The results from this research indicate that a prestressed brickwork retaining wall can be analysed and designed as a cantilever structure where the wall panels have an aspect ratio greater than 1.15.

13. The strengths predicted by the finite element analysis were in closer agreement with the experimental results than those predicted by the the direct method of analysis or by the recommendations of B.S.5628 i.e. the stress block analysis. This was because the finite element analysis takes into account the gain in nominal strength due to the overlap prestressing forces and the behaviour of the wall as a homogeneous cantilever.

14. Yield line analysis gives a good assessment of the strength of unreinforced brickwork panels for walls with aspect ratios smaller than 1.15.

15. The results obtained indicate that the Code design formulae for flexural and shear strength are unduly conservative.

16. All Codes presently assume that brick masonry is a brittle material. The author's results indicate that post-tensioned masonry panels behave as a ductile structure.

17. The orientation of the bedjoint in brick masonry in relation to the induced prestressing load has an insignificant effect on the ultimate flexural strength of the structure.

18. The results of this research has favourably confirmed the applicability of prestressed brick masonry as slabs and retaining walls for different types of brickwork.

8.2 Suggestions for Future Research

Based on the research work carried out on this thesis, the following suggestions are recommended for further work:

1. The results obtained from the yield-line and finite element analysis in the parametric study were rational. Therefore, an experimental investigation on full scale walls should be carried out to verify the failure modes of the wall panels. The analysis should also take into account out of plane shear stresses.

2. The author recommends the use of post-tensioned pocket type brickwork retaining walls as retaining walls for large water storage tanks or oil reservoirs. Therefore an investigation should be carried out to study the behaviour of these walls under repeated loading, and the prevention of corrosion of the steel .

3. Research should now be carried out on other types of retaining wall such as a diaphragm wall, Quetta bond, grouted cavity, etc.

4. Further theoretical work is required to develop a finite element material model that will simulate the highly anistropic behaviour of brick/block masonry.

REFERENCES

Abel, C.R. and M.R. Cochrane, (1971) "Reinforced Brick Masonry Retaining Wall with Reinforcement Pockets" SIBMAC proceedings, dited by H.W.H. West and K.H. Speed, British Ceram. Res. Assoc., Stoke-on-Trent.

Abeles, P.W., (1064) "An Introduction to Prestressed Concrete Vol. 1", Concrete Publication Ltd., London.

Al-Manaseer, A.A. and Neis, V.V., (1988) "Load Tests on Post-tensioned Masonry Wall Panels", ACI Structural Journal, September-October. pp 467- Title No. 84.548.

Ali, S.K.S., (1987) "Concentrated Loads on Solid Masonry", Ph.D. Thesis, University of Newcastle, Australia.

Ambrose, R.J., Hulse, R. and S. Mohajery, (1988) "Cantilevered Prestressed Diaphragm Walling Subjected to Lateral Loading". Proceedings of the Eighth International Brick/Block Masonry Conference, Dublin, Sept. 1988, Vol. 2, pp 665-675.

Arora, S.K., (1986) "Performance of Masonry Walls under Concentrated Load, Garston, BRS Publ.. Draft No. 158/86.

Baker, L.R., (1981) "Lateral Loading of Masonry Panels - A State of the Art Report", presented at Symposium on Loadbearing Brickwork held in Bombay, India, pp 20, November 1981.

Baker, L.R., (1981) "Lateral Loading of Masonry Panels - A State of the Art Report", Seminar/Workshop on Planning, Design, Construction of

Load Bearing Brick Buildings for Developing Countries (Delhi) (Department of Civil Engineering & Building Science, University of Edinburgh, 1981) pp 168-188.

Baker, L.R., (1981) "Flexural Strength of Masonry Structures under Lateral Load", PhD Thesis, Deakin University, Victoria, .

Barnard, P.R. and Johnson, R.P., (1965) "Ultimate Strength of Composite Beams". Proc. I.C.E., Vol. 32, Oct.

Beard, R. (1973) "The Compressive Strength of some Grouted Cavity Walls", Proc. Br. Ceram. Soc. 21 113-40.

Bradshaw, R.E., Drinkwater, J. and S.E. Bell, (1982) "A Multi-Purpose Farm Building Incorporating Prestressed Brickwork Diaphragm Walling", proc. of British Ceramic Society, Load Bearing Brickwork, ed., H.W.H. West, Stoke-on-Trent, September 1982, pp 308-315.

Bradshaw R.E. and Hendry A.W., (1968) "Further Crushing Tests on Storey Height Walls 4.5" Thick", Proc. Br. Ceram. Soc., 11 (1968) 25-54.

British Standards Institution, (1970) "Structural Recommendations of Load Bearing Walls", C.P.111, London.

British Standards Institution, "Code of Practice for the Structural Use of Concrete", C.P.110, London 1972.

British Standards Institution, (1985) "Structural Use of Concrete, Code of Practice for Design and Construction", B.S. 8110: Part 1: 1985.

British Standards Institution (1985): British Standard Code of Practice for Use of Masonry, Part 2, Structural Use of Reinforced and Prestressed Masonry, BS 5628, Part 2, 1985.

Cadjert, A. (1980)Loaded Masonry Walls", Chalmers University of Technology, Division of Concrete Structures, Publication No. 80:5. Gottenberg, Sweden.

Clay Prod. Tech. Bur. (1968) Loading Tests on Brick Walls Built in Stretcher Bond", Res. Note (Lond.), 1.

Curtin, W.G., Adams,S. and Shaw,G., (1975) 'The use of Post-Tensioned Brickwork in the SCD System'. British Ceramic Society, 1975.

Curtin, W.G. and Phipps, M.E., (1982) Prestressed Masonry Diaphragm Walls". Proceedings of the Sixth International Brick Masonry Conference, Rome, May 1982, pp 971-980.

Curtin, W.G., (1986) "An Investigation into the Structural Behaviour of Post-tensioned Brick Diaphragm Walls", The Structural Engineer 64B Dec. pp 77-84.

Curtin, W.G. and Howard, J. (1988) "Lateral Loading Tests on Tall Post-Tensioned Brick Diaphragm Walls". Proceedings of the Eighth International Brick/Block Masonry Conference, Dublin, Sep. 1988, Vol. 2, pp 595-605.

Curtin, W.G., Shaw, G. and Beck, J.K., (1988) "Design of Reinforced and Prestressed Masonry", 1st edn. Thomas Telford Ltd., London.

Curtin, W.G., Shaw, G., Beck, J.K. and J. Howard, (1989) "Design of Post-Tensioned Brickwork", Brick Development Association, Windsor, England.

Dawe, J.L. and C.K. Seah, (1988) "Lateral Load Resistance of Masonry Panels in Flexible Steel Frames". Proceedings of the Eighth International Brick/Block Masonry Conference, Dublin, Sept. 1988, Vol. 2, pp 606-616.

Drinkwater, J.P. and Bradshaw, R.E., (1982) "Reinforced and Prestressed Masonry in Agriculture", Reinforced and Prestressed Masonry, Proc. of Conf. held on 5 May 1982, Thomas Telford Ltd., London.

Foster, D., (1970)"Design and Construction of a Prestressed Brickwork Water Tank", In West, H.W.H. and K.H. Speed (Eds) proceedings of the Second International Brick Masonry Conference, Stoke-on--Trent, April 1970, pp 287-294.

Garrity, S.W. and T.G. Garwood, (1989) "The Construction and Testing of a Full Scale Prestressed Clay Brickwork Diaphragm Wall Bridge Abutment", Second International Masonry Conference Proceedings of the British Masonry Society 4, London, Oct. 1989.

Garrity, S.W., and M.E. Phipps, (1988) "An Experimental Study of the Influence of Vertical Prestress on the Horizontal Flexural Strength of Clay Brickwork". Proceedings of the Eighth International Brick/Blockwork Masonry Conference, Dublin, Sept. 1988, Vol. 2, pp 642-652.

Garwood, T.G., (1983) "The Construction and Test Performance of Four Prestressed Brickwork Beams", The Eighth International Symposium on Loadbearing Brickwork, London.

Ghali, A. and Neville, A.M. (1971) "Structural Analysis: A Unified Approach", Chapman and Hall, London.

Haseltine, B.A. and J.W. Tutt, (1977) "Brickwork Retaining Walls", Brick Development Association Publication, Westerham Press.

Hendry, A.W., (1990) "Structural Masonry", 1st edn. Macmillan Education Ltd., London.

Hendry, A.W.,ed(1991) "Reinforced and Prestressed Masonry", 1st edn. Longman Group UK Ltd., England.

Hendry, A.W., Bradshaw R.E. and D.J. Rutherford, (1968) "Tests on Cavity Walls and the Effect of Concentrated Loads and Joint Thickness on the Strength of Brickwork", Rees. Note Clay prod. Tech. Bur. (Lond.).

Hobbs, B., and Y. Daou, (1988) "Post-tensioned T-section Brickwork Retaining Walls". Proceedings of the Eighth International Brick/Block Masonry Conference, Dublin, Sept. 1988, Vol. 2, pp 665-675.

Hodgkinson H.R. and S. Davies S., (1982) "The Stress Strain Relationships of Brickwork when Stressed in Directions other than Normal to the Bed Face", Proceedings of the Sixth International Brick Masonry Conference (Rome) 1982, pp 290-6.

James, J.A. (1972) "Investigation of the Behaviour of Single Leaf 9" and 11" Cavity Storey Height Walls under Axial Load", Report W/3/A (Building Development Laboratories, Morley, W. Australia 1972).

James, J.A. (1973) "Investigation of the Behaviour of Storey Height Single Leaf Walls, 9" Walls and 11" Cavity Walls under Eccentric Compressive Load", Report W/4/4 (Building Development Laboratories, Morley, W. Austrialia, 1973).

Johansen, K.W., (1972) "Yield-line Formula for Slabs", Translated from Danish by Cement and Concrete Association, Wexham Springs.

Jones, L.L., (1965) "Ultimate Load Analysis of Reinforced and Prestressed Concrete Structures". 2nd edn. Chatto & Windus Ltd., U.K.

Kheir, A.M.A., (1975) "Brickwork Panels under Lateral Loading", MPhil Thesis, University of Edinburgh, 1975.

Leonardt, F., (1964) "Prestressed Concrete", Wilhelm Ernst and Sohn, Berlin.

Malek, M.H., (1987) "Compressive Strength of Brickwork Masonry with Special Reference to Concentrated Load", Ph.D. Thesis, University of Edinburgh.

Maurenbrecher, A.H.P., Bird, A.B., Sutherland, R.J.M. and R.D. Foster, (1976) "Reinforced Brickwork Vertical Cantilevers", Vol. 1,, Structural Clay products Ltd., SCP10, Hertford, England.

Mehta, K.C. and D. Fincher, (1971) "Structural Behaviour of Pre-tensioned Prestressed Masonry Beams". Proceedings of the 2nd International Brick Masonry Conference, edited by H.W.H. West and K.H. Speed, Stoke-on-Trent, BCRA, pp 215-219.

Montague, T.I. and M.E. Phipps, (1984) "The Behaviour of Post-Tensioned Masonry in Flexure and Shear", International Symposium on Reinforced and Prestressed Masonry, Edinburgh.

Neil, J.S., (1966) "Post-tensioned Brickwork", Clay Products Technical Bureau, Technical Note, Vol. 1, No. 9.

Page, A.W., Shrive, N.G., and Jessop, E.L., (1987) "Concentrated Loads on Hollow Masonry - A Pilot Study", Masonry International 1, No. 2, 36-70, pp 58-61.

Page, A.W. and Hendry, A.W. (1988) "Design Rules for Concentrated Loads on Masonry", The Structural Engineer, Vol. 66, No. 17/6, pp 273-281.

Page, A.W. and N.G. Shrive", (1990) Concentrated Loads on Hollow Concrete Masonry", ACI Structural Journal, V.87, No. 4, July 1990, pp 436-444.

Pedreschi, R.F. and B.P. Sinha, (1982) "Development and Ultimate Load Behaviour of Prestressed Brickwork Beams", Struct. Engnr. (Sept. 1982) pp 63-67.

Pedreschi, R.F. and B.P. Sinha, (1985) "Deformation and Cracking of Prestressed Brickwork Beams", Struct. Engrn. (Dec. 1985).

Pedreschi, R.F. (1983) "A Study of the Behaviour fo Post-Tensioned Brickwork Beams", Ph.D. Thesis, University of Edinburgh, U.K.

Phipps, M.E. and T.I. Montague, (1986) "Concrete Blockwork Diaphragm Walls - Prestressed and Under Prestressed". In practical Design of Masonry Structures, Thomas Telford, London pp 265-276.

Phipps, M.E. and T.I. Montague, (1987) "The Design of Prestressed Concrete Blockwork Diaphragm Walls", Aggregate Concrete Block Association, Leicester, England.

Phipps, M.E., (1986) Discussion on paper 19. In Practical Design of Masonry Structures, Thomas Telford, London, pp 277-284.

Phipps, M.E., and T.I. Montague, (1987) "The Testing of Plain and Prestressed Concrete Blockwork Beams and Walls of Geometric Cross-section", Masonry International 1(3), pp 71-108.

Plowman, J.M., Sutherland, R.J.M. and M.L. Cousins, (1967) "The Testing of Reinforced Brickwork and Concrete Slabs Forming Box Beams", The Structural Engineer, Vol. 45, No. 11, November, 1967, pp 379-394.

Plummer, H.C. and J.A. Blume, (1953) "Reinforced Brick Masonry and Lateral Force Design". Publ. Structural Clay Products Ltd., Washington D.C.

Reddy, V.M., (1968) "The Ultimate Load Behaviour of Composite Steel-Concrete Bridge Deck Structures", PhD Thesis, Department of Civil Engineering and Building Science, The University of Edinburgh.

Roberts, J.J., Tovey, A.K., Cranston, W.B. and Beeby, A.W., (1983) "Concrete Masonry Designer's Handbook", 1st edn. Viewpoint Publications, Surrey.

Robson, I.J., Ambrose, R.J. Hulse, R. and J. Morton, (1986) "Post-tensioned Prestressed Brickwork Beam", Proceedings of the British Masonry Society, No. 1, November, 1986, pp 100-105.

Roumani, N.A., and M.E. Phipps, (1988) "The Ultimate Shear Strength of Unbonded Prestressed Brickwork I and T section Members", Proceedings of the British Masonry Society Masonry 2, April 1988.

Roumani, N. and M.E. Phipps, (1985) "The Ultimate Shear Strength of Unbonded Prestressed Brickwork I and T Section", Proceedings of the 7th International Brick Masonry Conference, Edited by T. McNeilly and J.C. Scrivener, Melbourne, Australia, Vol. 2, pp 1001-1004.

Rutherford, D.J., (1968) "Stress Concentrations in Loadbearing Brickwork Details", PhD Thesis, University of Edinburgh.

Samarasinghe, W., Page A.W. & Hendry A.W., (1982) "A Finite Element Model for the In-Plane Behaviour of Brickwork", Proc. Instn. Civ. Engrs., Part 2, Vol. 73, March 1982.

Satti, K.M.H., (1972) "Model Brickwork Panels under Lateral Loading", PhD Thesis, University of Edinburgh.

Schneider,, R.R. and W.L. Dickey, (1980) "Reinforced Masonry Design", Publ. Prentice Hall, New Jersey.

Siess, C.P., Viest, I.M. and Newmark, N.M., "Studies of Slab and Highway Bridges, Part III. Small scale Tests of Shear Connectors and Composite T-Beams", University of Illinois Engineering Experimental Station Bulletin 396.

Sinha, B.P., (1982) "Reinforced Grouted Cavity Brickwork", Building Research and Practice, Vol. 10, No. 4, July 1982, pp 226-243.

Sinha, B.P., (1978) "A Simplified Ultimate Load Analysis of Laterally Loaded Model Orthotropic Brickwork Panels of Low Tensile Strength", Struct. Engr., 56(4) pp 81-84.

Sinha B.P. and A.W. Hendry, (1968) "The Effect of Brickwork Bond on the Load Bearing Capacity of Model Brick Walls", Proc. Br. Ceram. Soc., 11 55-68.

Suter, G.T. and Hendry, A.W., (1975) "Shear Strength of Reinforced Brickwork Beams", The Structural Engineer, Vol. 53, No. 6, pp 249-253.

Tasker, H.E., (1964) "Recommendations for the Use of Prestressed Brick or Block Walls on Reactive Soils". Technical Record 52:75:3439, Department of Works, Commonwealth Experimental Building Station.

Tellett, J., (1984) "Pocket-type Reinforced Brickwork Retaining Walls". Ph.D. thesis, University of Warwick, U.K.

Thomas, K. (1969) "Current Post-tensioned and Prestressed Brickwork and Ceramics in Great Britain". In Johnson, F.B. (ed) Designing, Engineering and Constructing with Masonry Products, Gulf Publishing Co., Houston, Texas, p 285.

Thurlimann, B. and R. Gauggisberg, (1988) "Failure Criterion for Laterally Loaded Masonry Walls: Experimental Investigations". Proceedings of the Eighth International Brick/Block Masonry Conference, Dublin, Sept. 1988, Vol. 2, pp 699-706.

Uduehi, J., (1989). "A Comparative Study of the Structural Behaviour of Prestressed Beams of Brickwork and Concrete and the Shear Strength of Brickwork Beams". Ph.D. Thesis, University of Edinburgh, U.K.

Walker, P.J., (1987) "A Study of the Behaviour of Partially Prestressed Brickwork Beams", PhD Thesis, Department of Civil Engineering and Building Science, The University of Edinburgh.

Williams, E.O.L. and M. Phipps, (1982) "Bending Behaviour of Prestressed Masonry Box Beams", Proc. 6th International Brick Masonry Conference, ed. Later Consult, Rome, pp 981-994.

APPENDIX A

GENERAL GRAPHICAL DISPLAY OF THE FINITE ELEMENT RESULTS

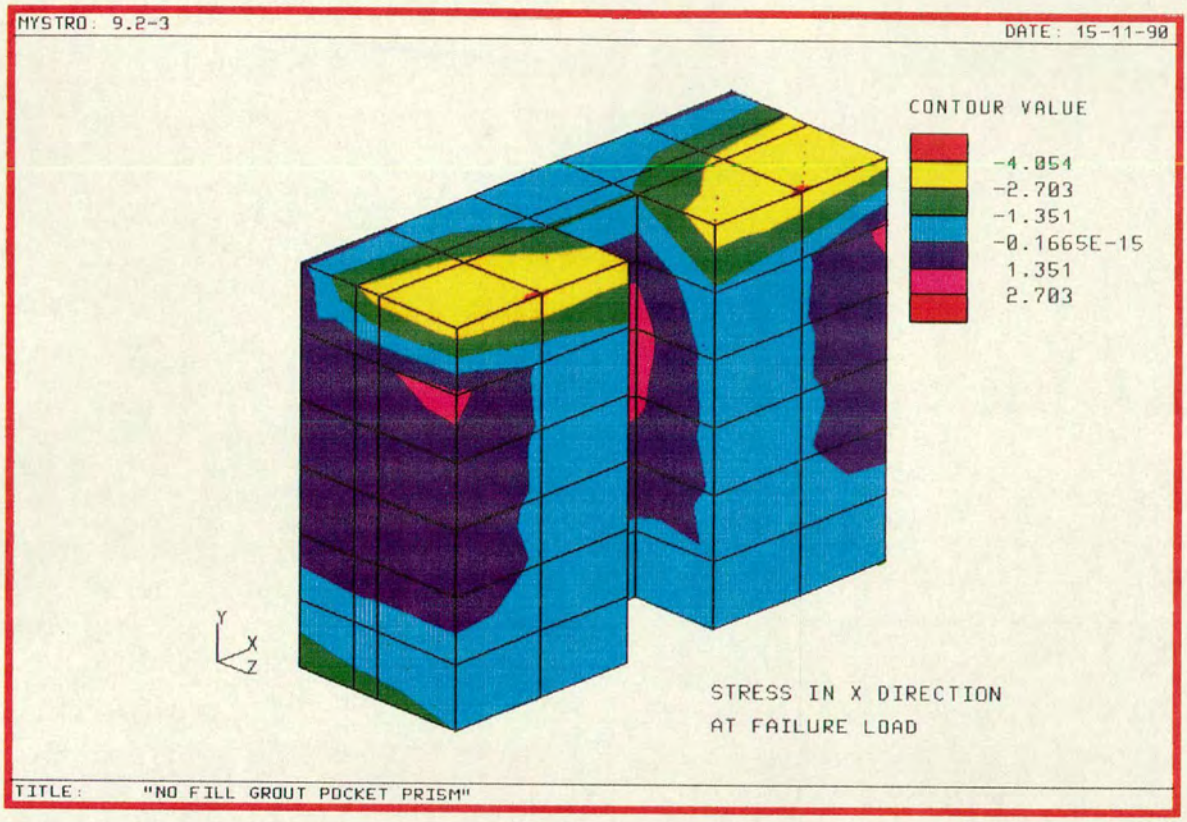
MYSTRO: 9.2-3
DATE: 15-11-90
CONTOUR VALUE
-4.054
-2.703
-1.351
-0.1665E-15
1.351
2.703
Y
X
Z
STRESS IN X DIRECTION
AT FAILURE LOAD
TITLE: "NO FILL GROUT POCKET PRISM"

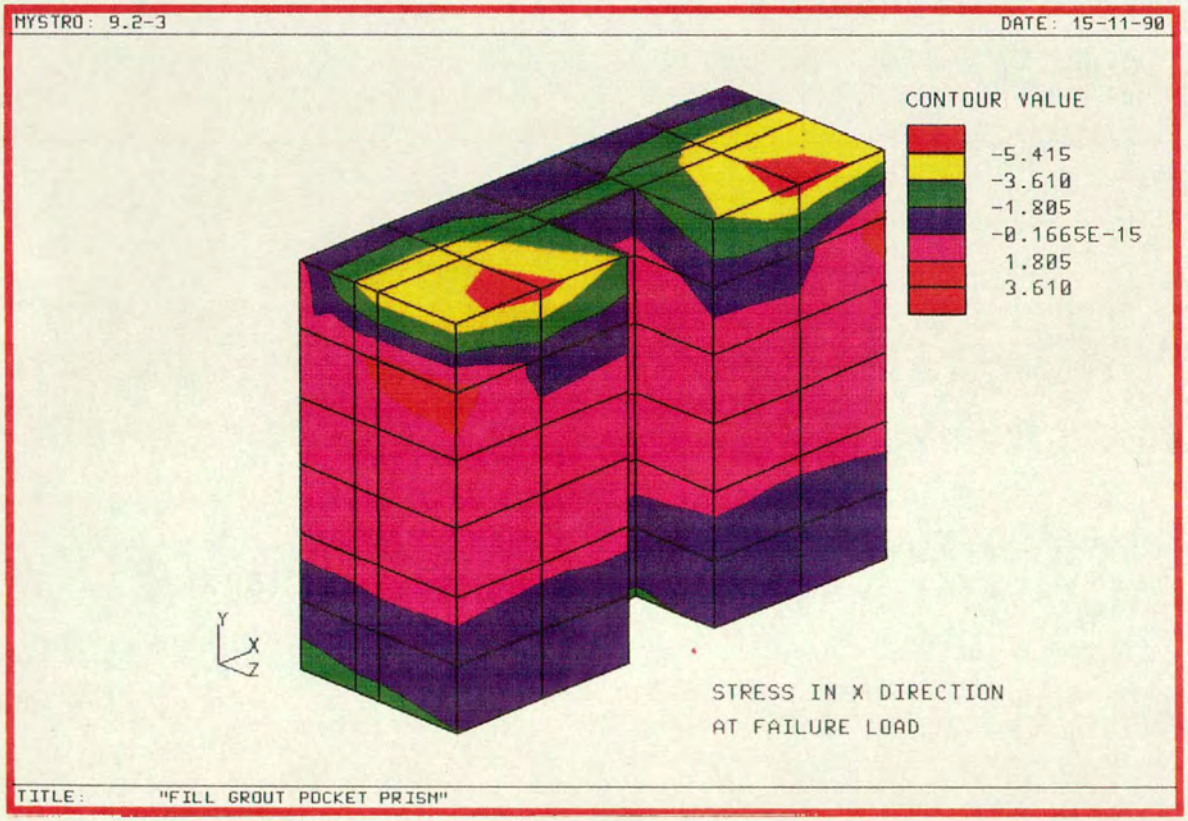
MYSTRO: 9.2-3
DATE: 15-11-90
CONTOUR VALUE
-5.415
-3.610
-1.805
-0.1665E-15
1.805
3.610
Y
X
Z
STRESS IN X DIRECTION
AT FAILURE LOAD
TITLE: "FILL GROUT POCKET PRISM"

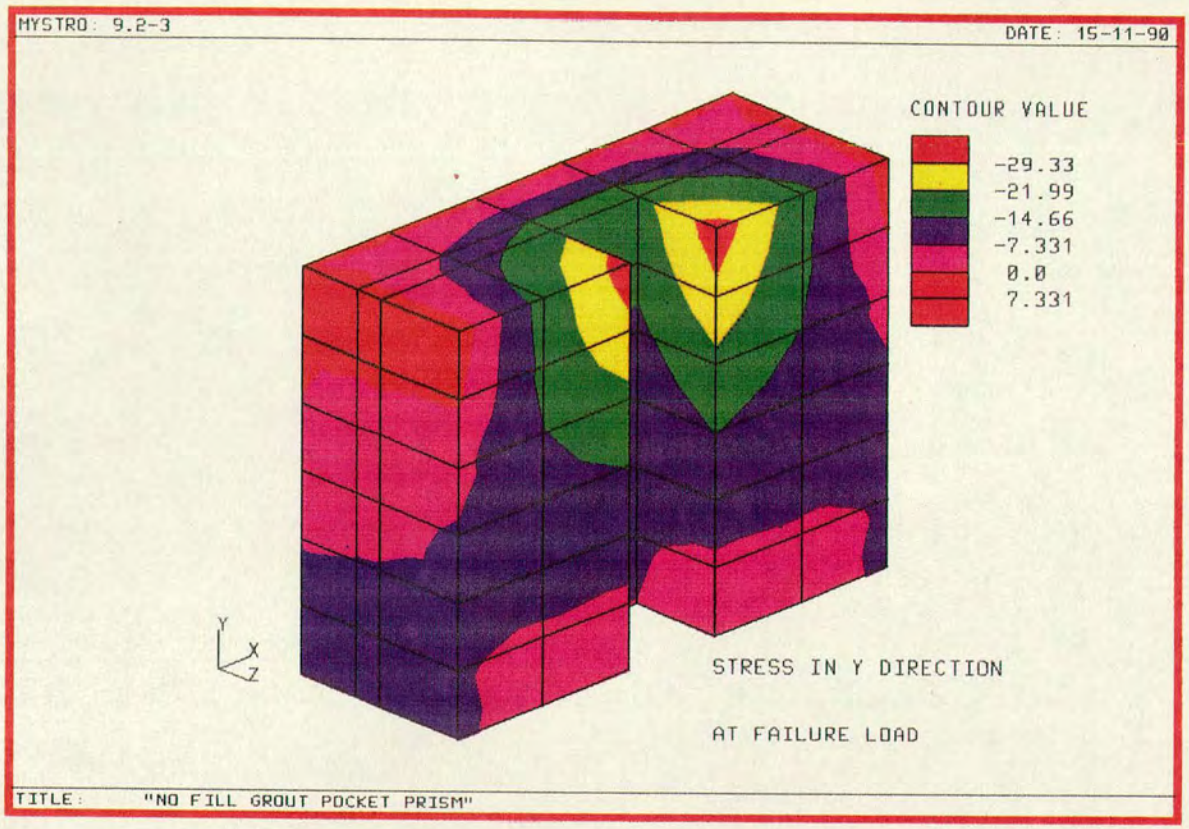
MYSTRO: 9.2-3
DATE: 15-11-90
CONTOUR VALUE
-29.33
-21.99
-14.66
-7.331
0.0
7.331
Y
X
Z
STRESS IN Y DIRECTION
AT FAILURE LOAD
TITLE: "NO FILL GROUT POCKET PRISM"

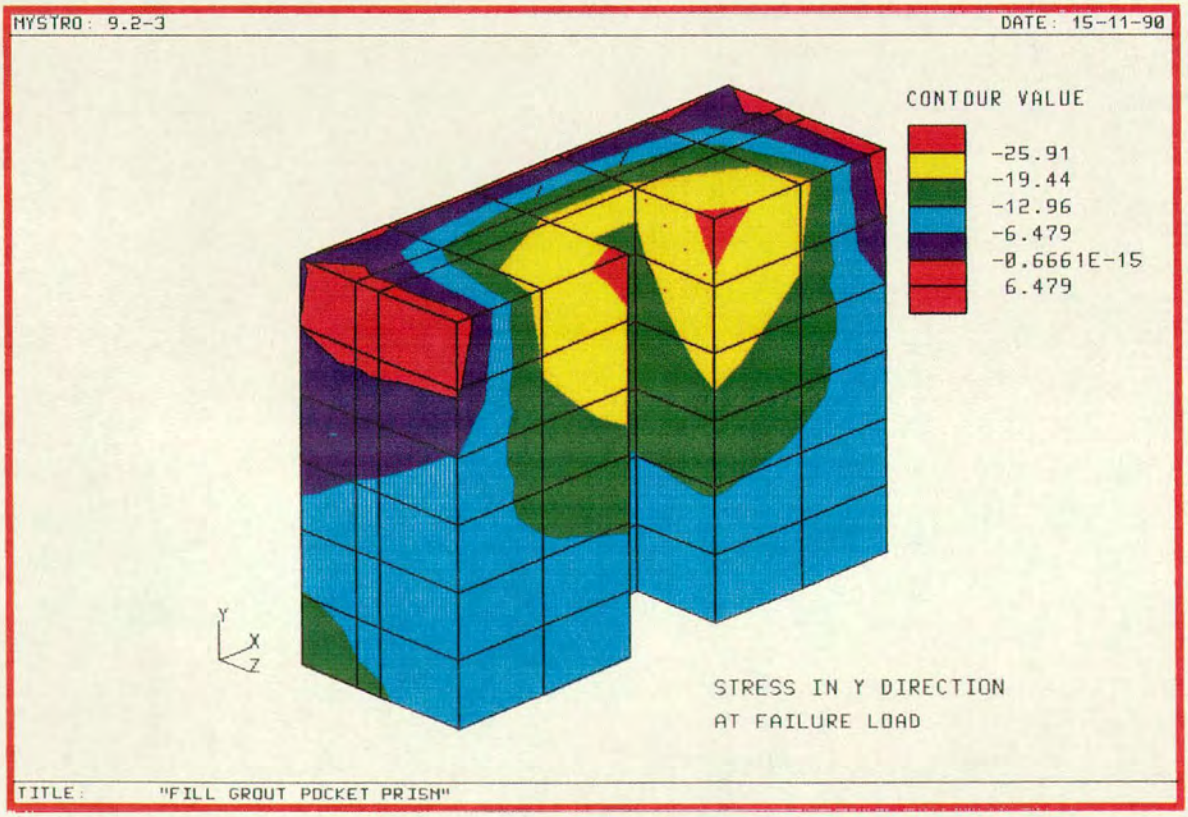
MYSTRO: 9.2-3
DATE: 15-11-90
CONTOUR VALUE
-25.91
-19.44
-12.96
-6.479
-0.6661E-15
6.479
Y
X
Z
STRESS IN Y DIRECTION
AT FAILURE LOAD
TITLE: "FILL GROUT POCKET PRISM"

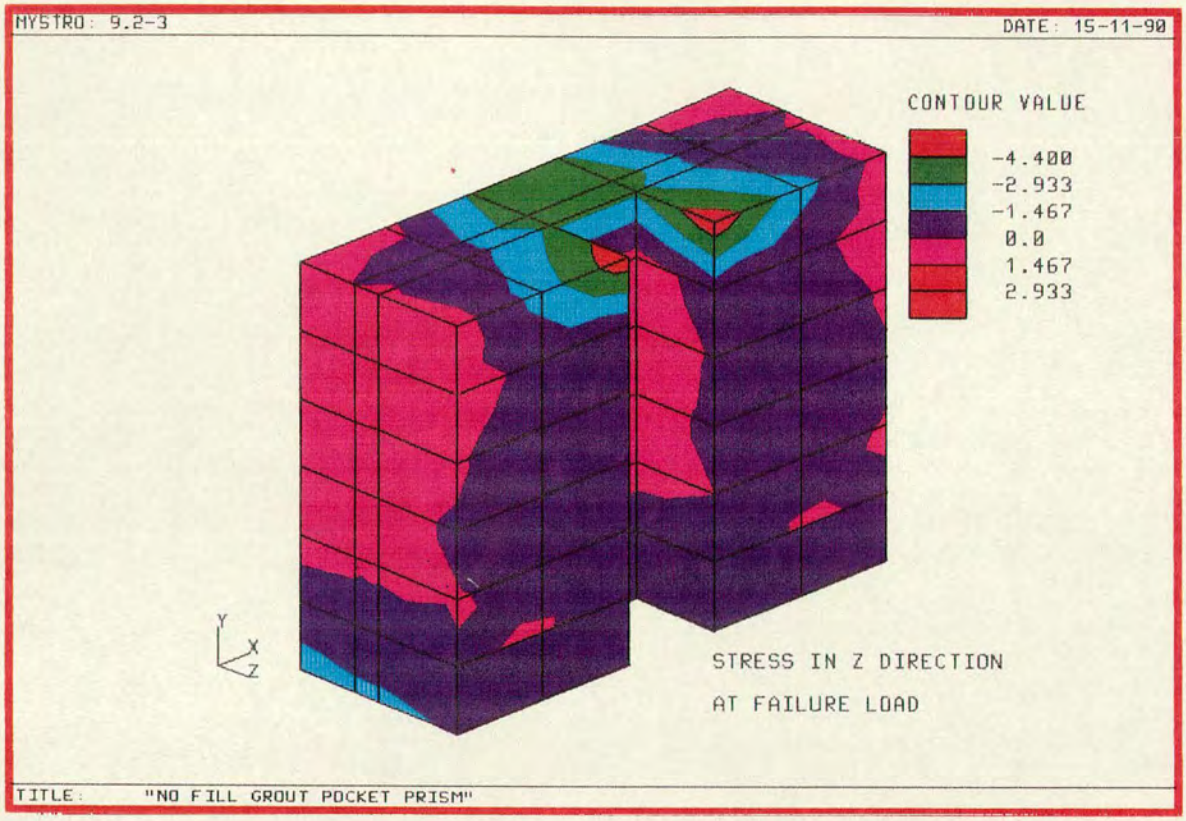
MYSTRO: 9.2-3
DATE: 15-11-90
CONTOUR VALUE
-4.400
-2.933
-1.467
0.0
1.467
2.933
Y
X
Z
STRESS IN Z DIRECTION
AT FAILURE LOAD
TITLE: "NO FILL GROUT POCKET PRISM"

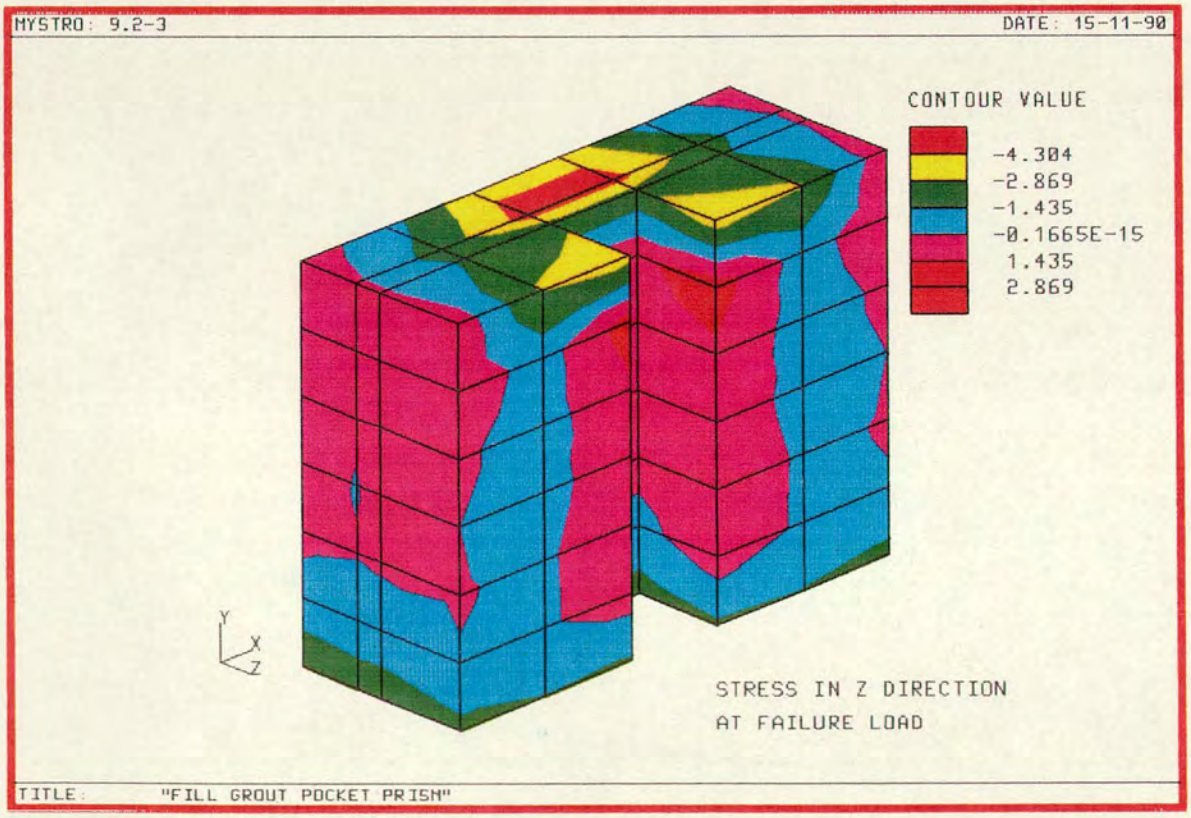
MYSTRO: 9.2-3
DATE: 15-11-90
CONTOUR VALUE
-4.304
-2.869
-1.435
-0.1665E-15
1.435
2.869
Y
X
Z
STRESS IN Z DIRECTION
AT FAILURE LOAD
TITLE: "FILL GROUT POCKET PRISM"

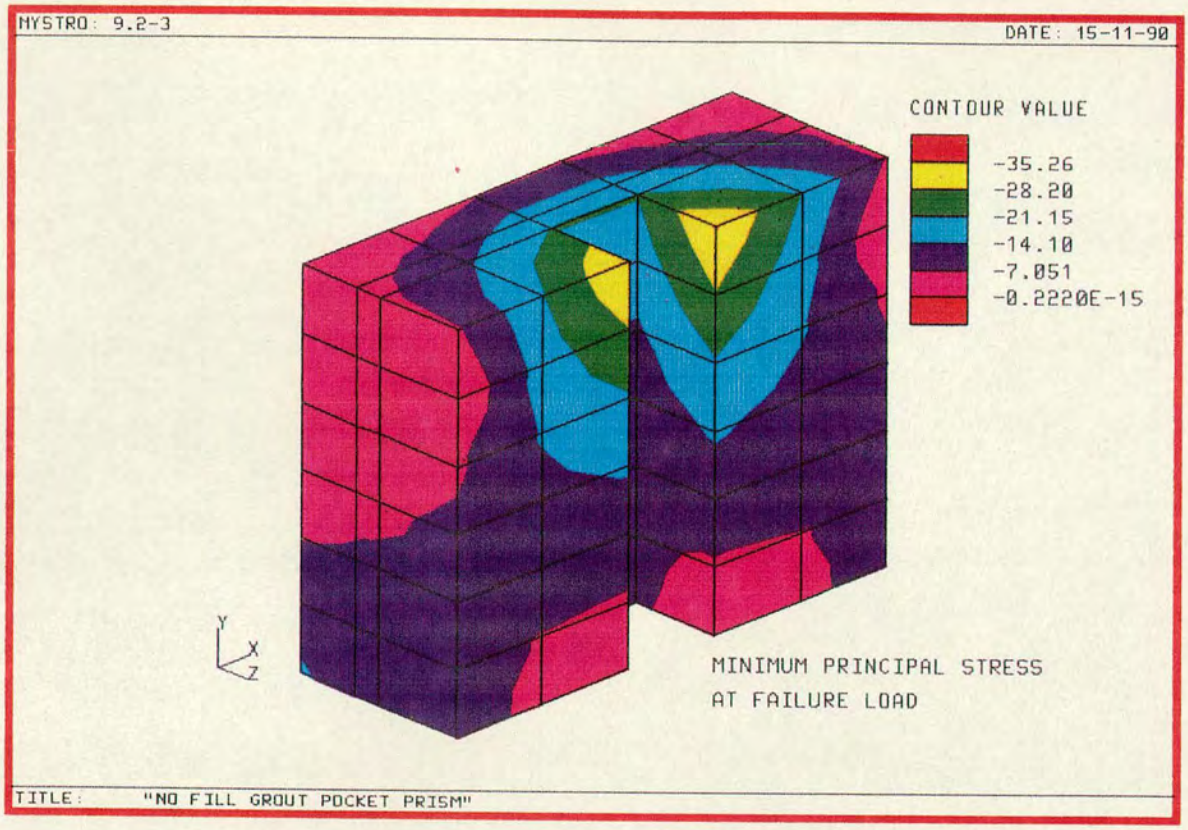
MYSTRO: 9.2-3
DATE: 15-11-90
CONTOUR VALUE
-35.26
-28.20
-21.15
-14.10
-7.051
-0.2220E-15
Y
X
Z
MINIMUM PRINCIPAL STRESS
AT FAILURE LOAD
TITLE: "NO FILL GROUT POCKET PRISM"

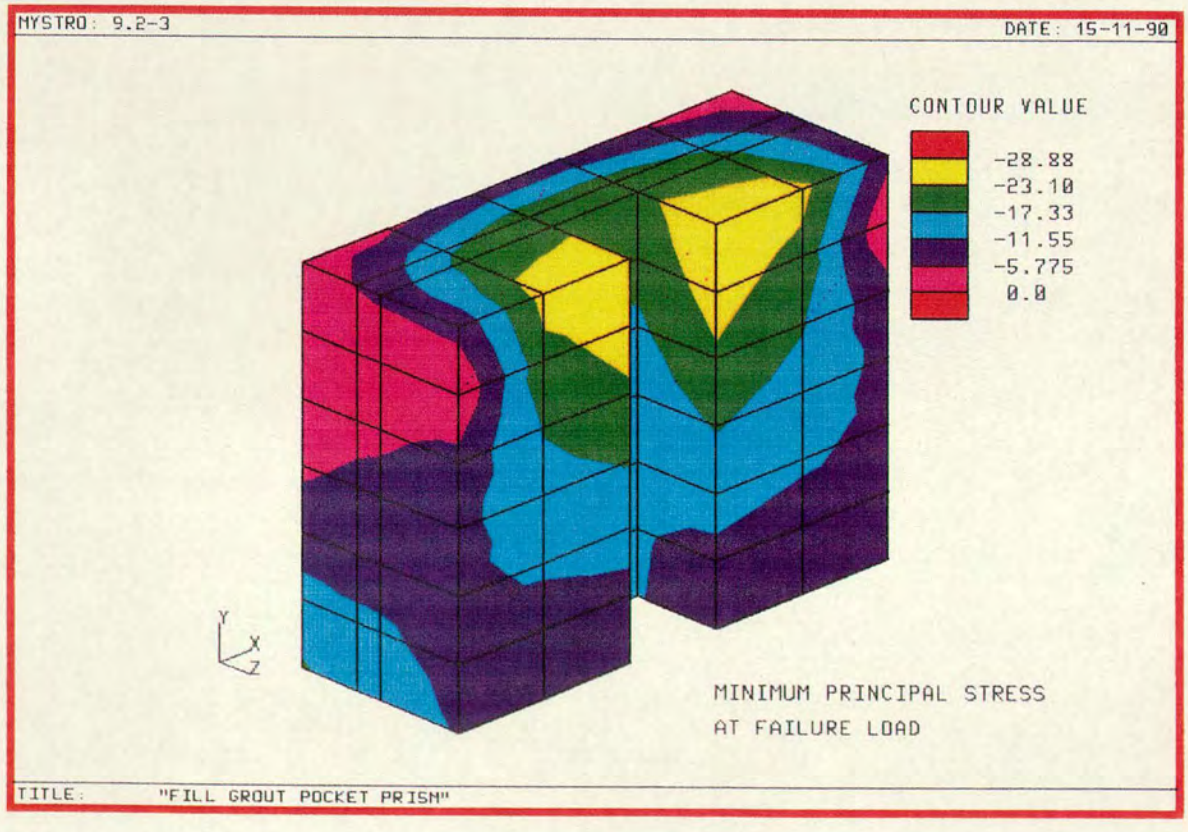
MYSTRO: 9.2-3
DATE: 15-11-90
CONTOUR VALUE
-28.88
-23.10
-17.33
-11.55
-5.775
0.0
Y
X
Z
MINIMUM PRINCIPAL STRESS
AT FAILURE LOAD
TITLE: "FILL GROUT POCKET PRISM"

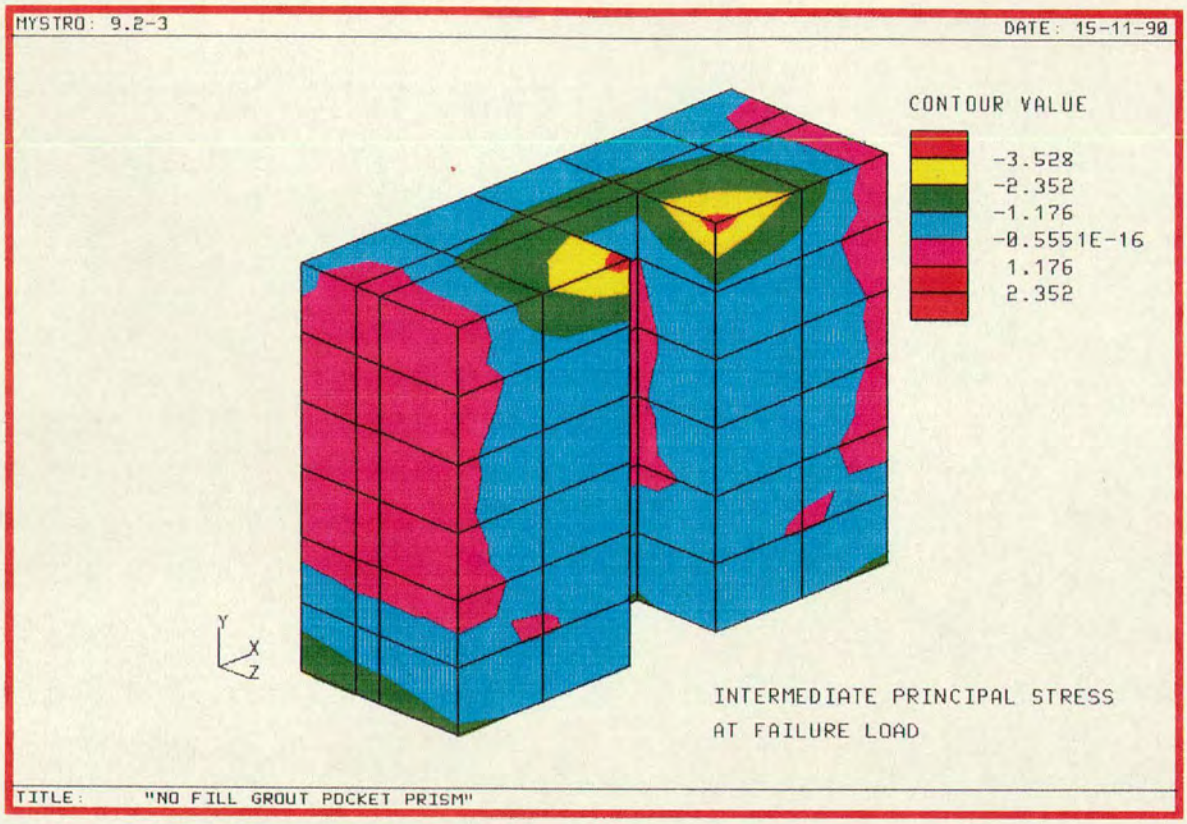
MYSTRO: 9.2-3
DATE: 15-11-90
CONTOUR VALUE
-3.528
-2.352
-1.176
-0.5551E-16
1.176
2.352
Y
X
Z
INTERMEDIATE PRINCIPAL STRESS
AT FAILURE LOAD
TITLE: "NO FILL GROUT POCKET PRISM"

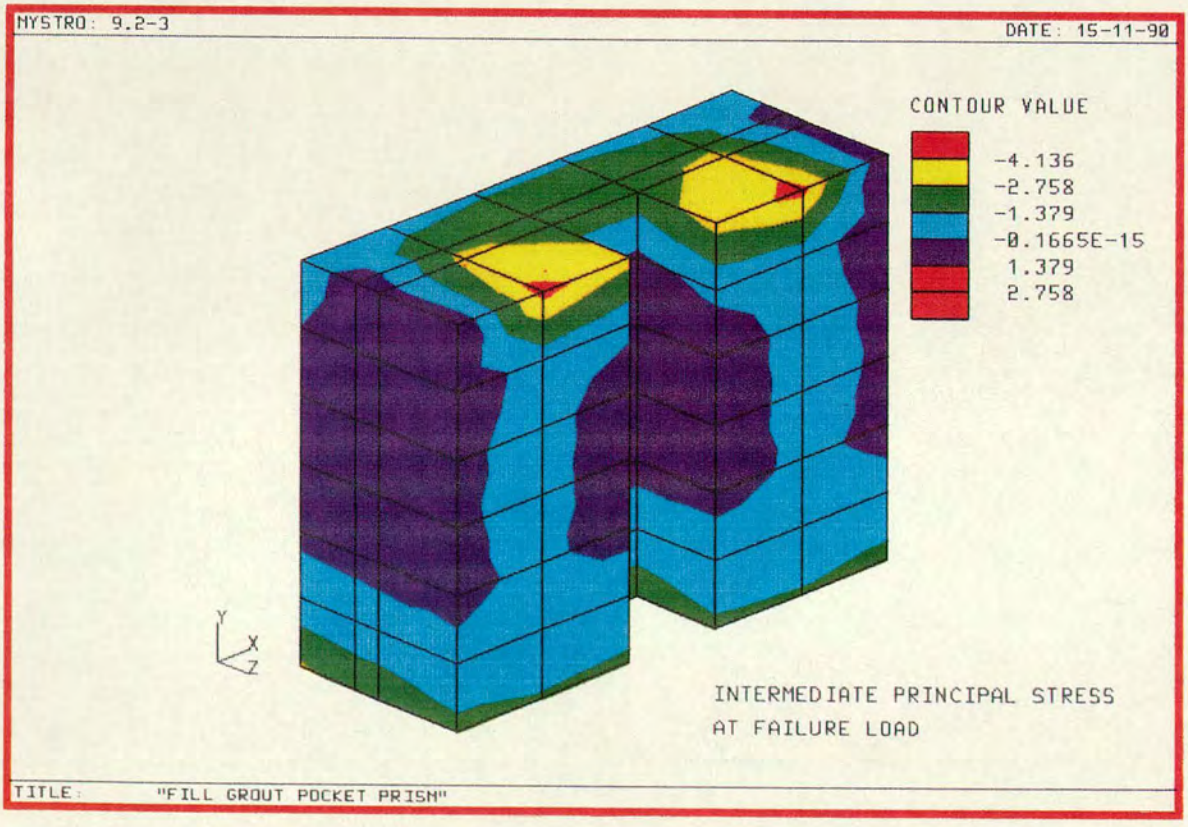
MYSTRO: 9.2-3
DATE: 15-11-90
CONTOUR VALUE
-4.136
-2.758
-1.379
-0.1665E-15
1.379
2.758
Y
X
Z
INTERMEDIATE PRINCIPAL STRESS
AT FAILURE LOAD
TITLE: "FILL GROUT POCKET PRISM"

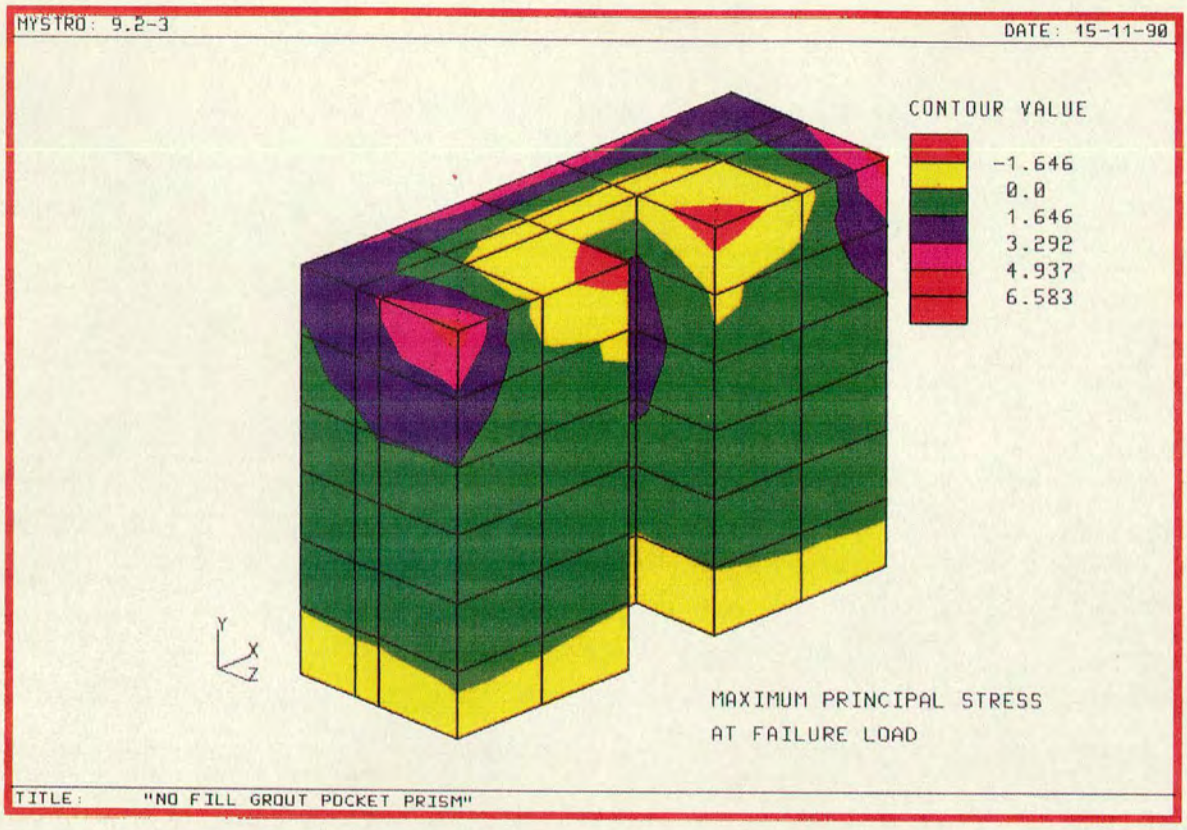
MYSTRO: 9.2-3
DATE: 15-11-90
CONTOUR VALUE
-1.646
0.0
1.646
3.292
4.937
6.583
Y
X
Z
MAXIMUM PRINCIPAL STRESS
AT FAILURE LOAD
TITLE: "NO FILL GROUT POCKET PRISM"

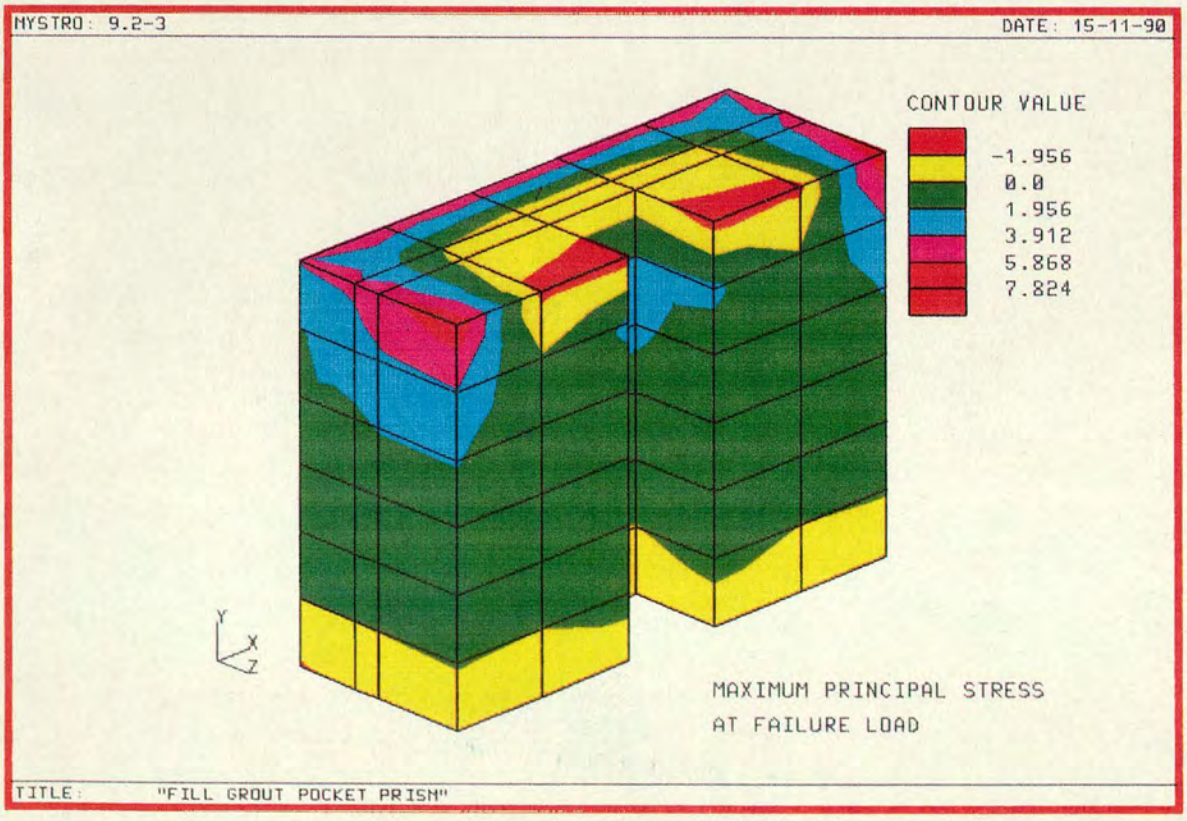
MYSTRO: 9.2-3
DATE: 15-11-90
CONTOUR VALUE
-1.956
0.0
1.956
3.912
5.868
7.824
Y
X
Z
MAXIMUM PRINCIPAL STRESS
AT FAILURE LOAD
TITLE: "FILL GROUT POCKET PRISM"

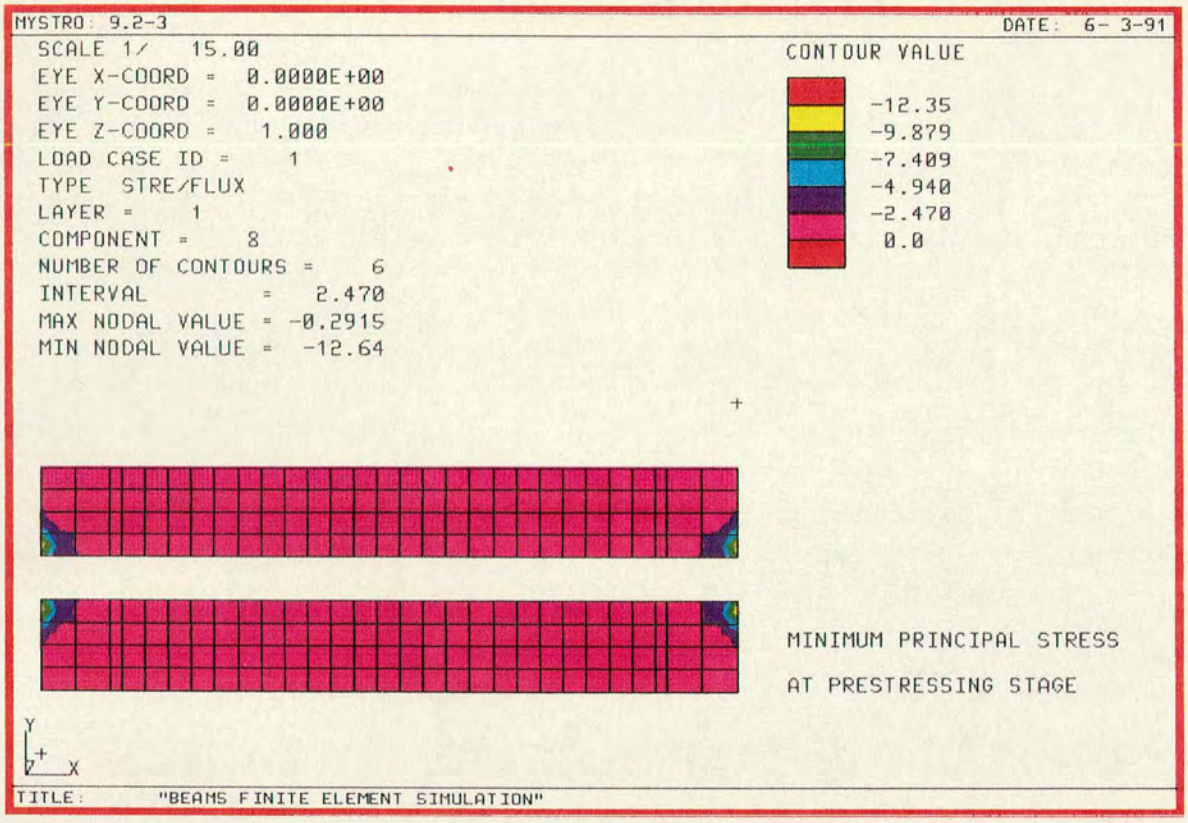
MYSTRO: 9.2-3
DATE: 6- 3-91
SCALE 1/ 15.00
EYE X-COORD = 0.0000E+00
EYE Y-COORD = 0.0000E+00
EYE Z-COORD = 1.000
LOAD CASE ID = 1
TYPE STRE/FLUX
LAYER = 1
COMPONENT = 8
NUMBER OF CONTOURS = 6
INTERVAL = 2.470
MAX NODAL VALUE = -0.2915
MIN NODAL VALUE = -12.64
CONTOUR VALUE
-12.35
-9.879
-7.409
-4.940
-2.470
0.0
MINIMUM PRINCIPAL STRESS
AT PRESTRESSING STAGE
Y
X
TITLE: "BEAMS FINITE ELEMENT SIMULATION"

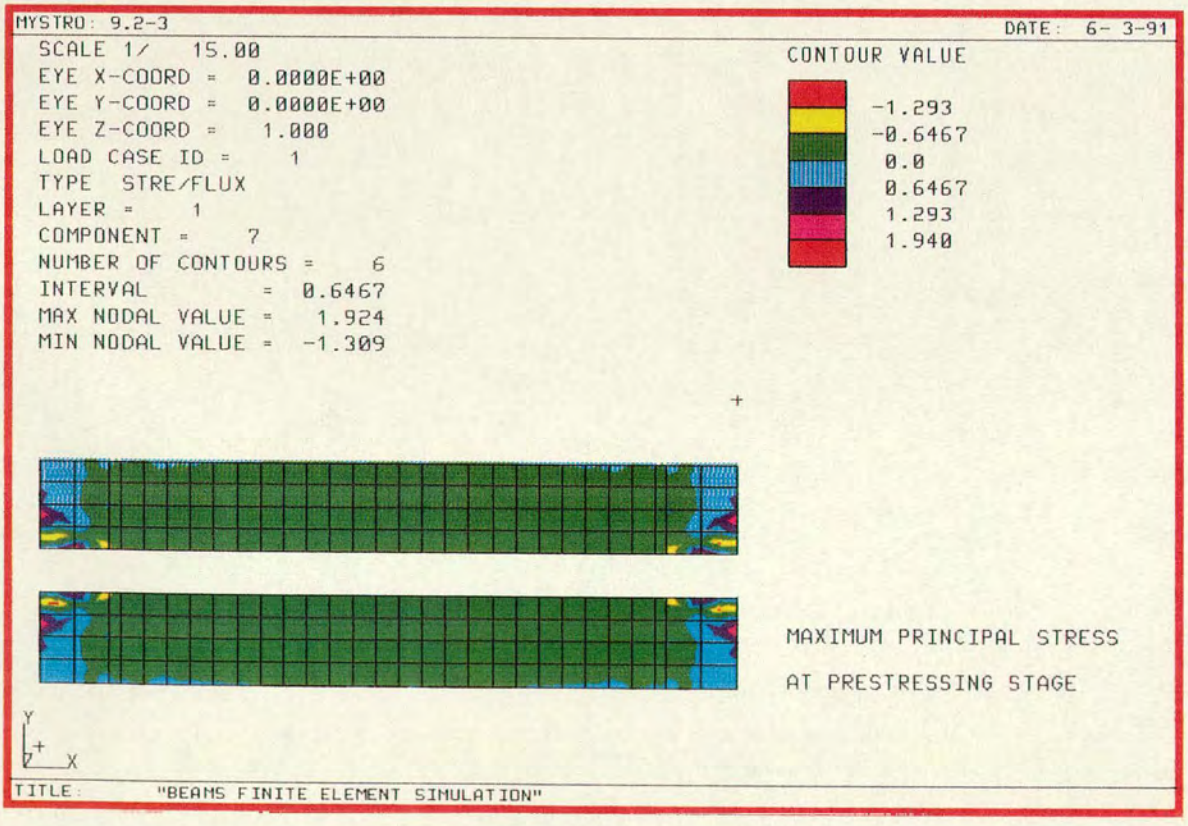
MYSTRO: 9.2-3
DATE: 6- 3-91
SCALE 1/ 15.00
EYE X-COORD = 0.0000E+00
EYE Y-COORD = 0.0000E+00
EYE Z-COORD = 1.000
LOAD CASE ID = 1
TYPE STRE/FLUX
LAYER = 1
COMPONENT = 7
NUMBER OF CONTOURS = 6
INTERVAL = 0.6467
MAX NODAL VALUE = 1.924
MIN NODAL VALUE = -1.309
CONTOUR VALUE
-1.293
-0.6467
0.0
0.6467
1.293
1.940
MAXIMUM PRINCIPAL STRESS
AT PRESTRESSING STAGE
Y
X
TITLE: "BEAMS FINITE ELEMENT SIMULATION"

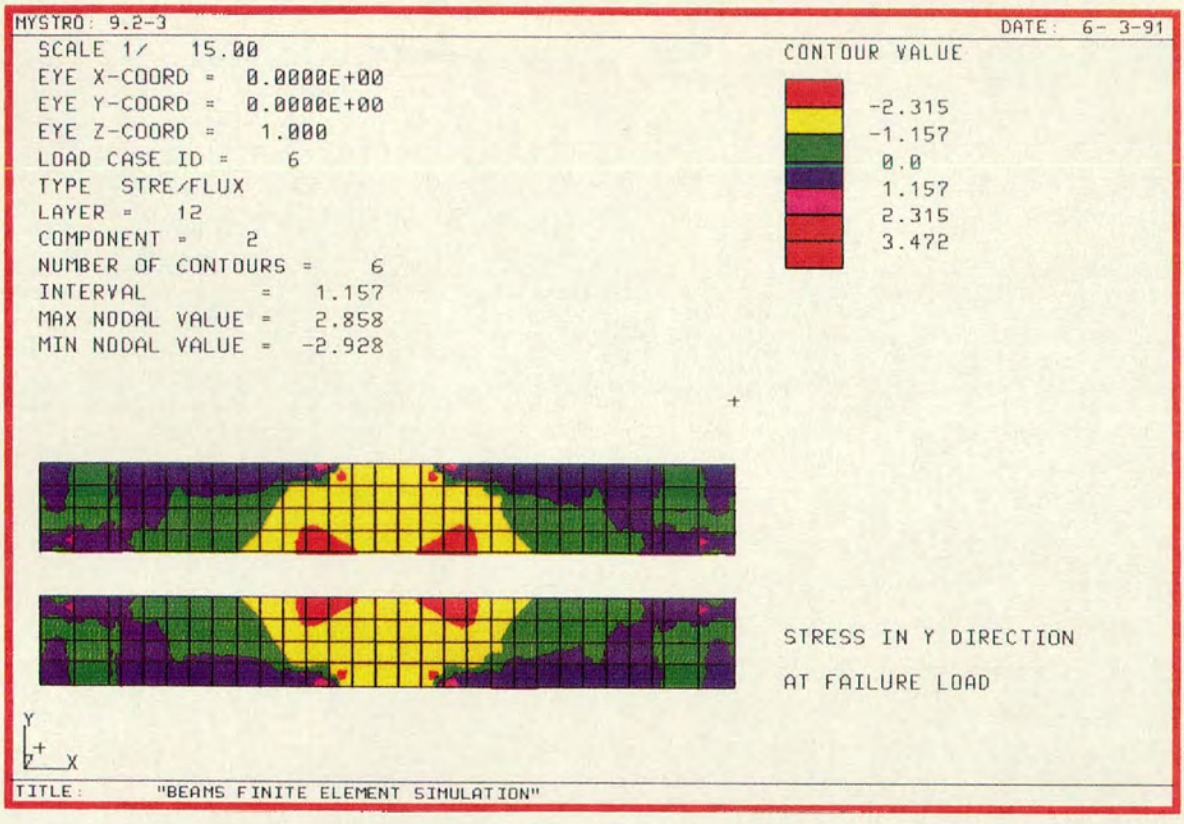
MYSTRO: 9.2-3
DATE: 6- 3-91
SCALE 1/ 15.00
EYE X-COORD = 0.0000E+00
EYE Y-COORD = 0.0000E+00
EYE Z-COORD = 1.000
LOAD CASE ID = 6
TYPE STRE/FLUX
LAYER = 12
COMPONENT = 2
NUMBER OF CONTOURS = 6
INTERVAL = 1.157
MAX NODAL VALUE = 2.858
MIN NODAL VALUE = -2.928
CONTOUR VALUE
-2.315
-1.157
0.0
1.157
2.315
3.472
STRESS IN Y DIRECTION
AT FAILURE LOAD
Y
Z
X
TITLE: "BEAMS FINITE ELEMENT SIMULATION"

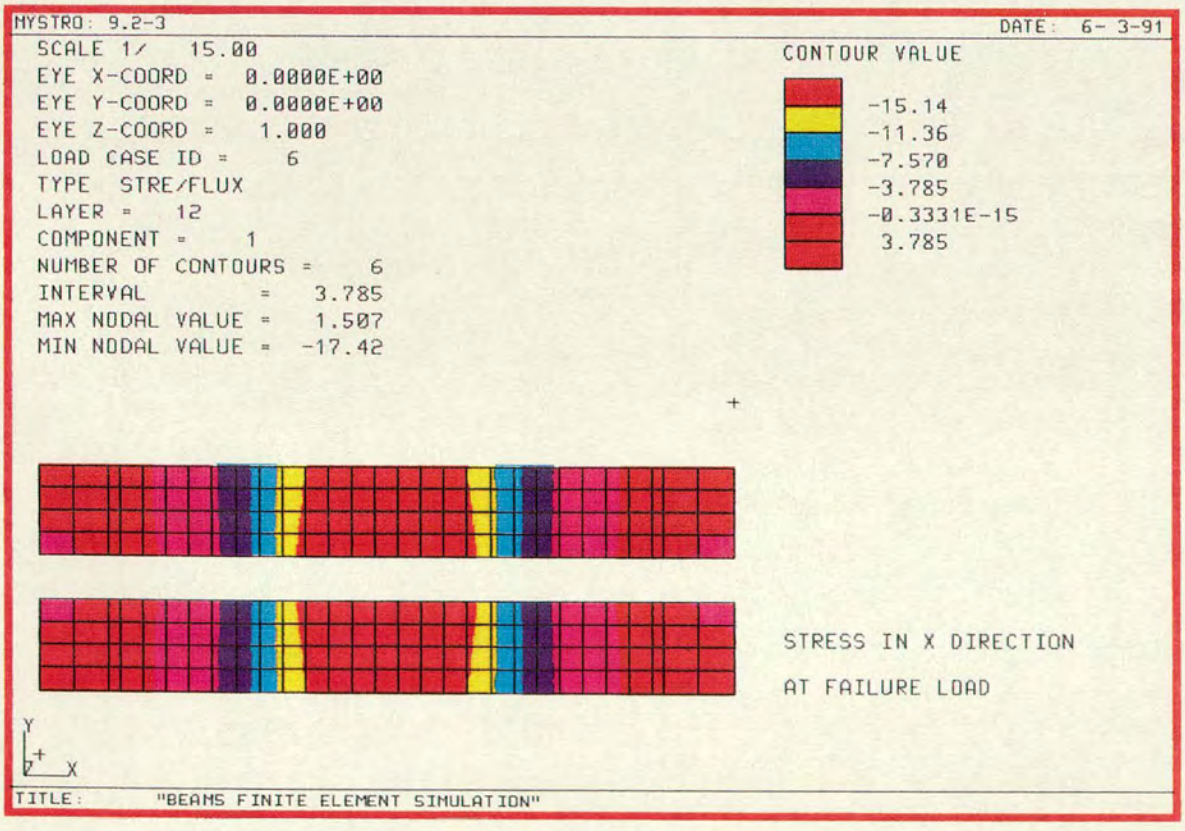
MYSTRO: 9.2-3
DATE: 6- 3-91
SCALE 1/ 15.00
EYE X-COORD = 0.0000E+00
EYE Y-COORD = 0.0000E+00
EYE Z-COORD = 1.000
LOAD CASE ID = 6
TYPE STRE/FLUX
LAYER = 12
COMPONENT = 1
NUMBER OF CONTOURS = 6
INTERVAL = 3.785
MAX NODAL VALUE = 1.507
MIN NODAL VALUE = -17.42
CONTOUR VALUE
-15.14
-11.36
-7.570
-3.785
-0.3331E-15
3.785
STRESS IN X DIRECTION
AT FAILURE LOAD
Y
Z
X
TITLE: "BEAMS FINITE ELEMENT SIMULATION"

MYSTRO: 9.2-3 DATE: 6- 3-91

SCALE 1/ 15.00
EYE X-COORD = 0.0000E+00
EYE Y-COORD = 0.0000E+00
EYE Z-COORD = 1.000
LOAD CASE ID = 6
TYPE STRE/FLUX
LAYER = 12
COMPONENT = 8
NUMBER OF CONTOURS = 6
INTERVAL = 3.625
MAX NODAL VALUE = 0.5856
MIN NODAL VALUE = -17.54

CONTOUR VALUE

-14.50
-10.87
-7.250
-3.625
-0.3331E-15
3.625

MINIMUM PRINCIPAL STRESS

AT FAILURE LOAD

TITLE: "BEAMS FINITE ELEMENT SIMULATION"

MYSTRO: 9.2-3 DATE: 6- 3-91

SCALE 1/ 15.00
EYE X-COORD = 0.0000E+00
EYE Y-COORD = 0.0000E+00
EYE Z-COORD = 1.000
LOAD CASE ID = 6
TYPE STRE/FLUX
LAYER = 12
COMPONENT = 7
NUMBER OF CONTOURS = 6
INTERVAL = 0.7297
MAX NODAL VALUE = 2.130
MIN NODAL VALUE = -1.518

CONTOUR VALUE

-1.459
-0.7297
-0.2776E-16
0.7297
1.459
2.189

MAXIMUM PRINCIPAL STRESS

AT FAILURE LOAD

TITLE: "BEAMS FINITE ELEMENT SIMULATION"

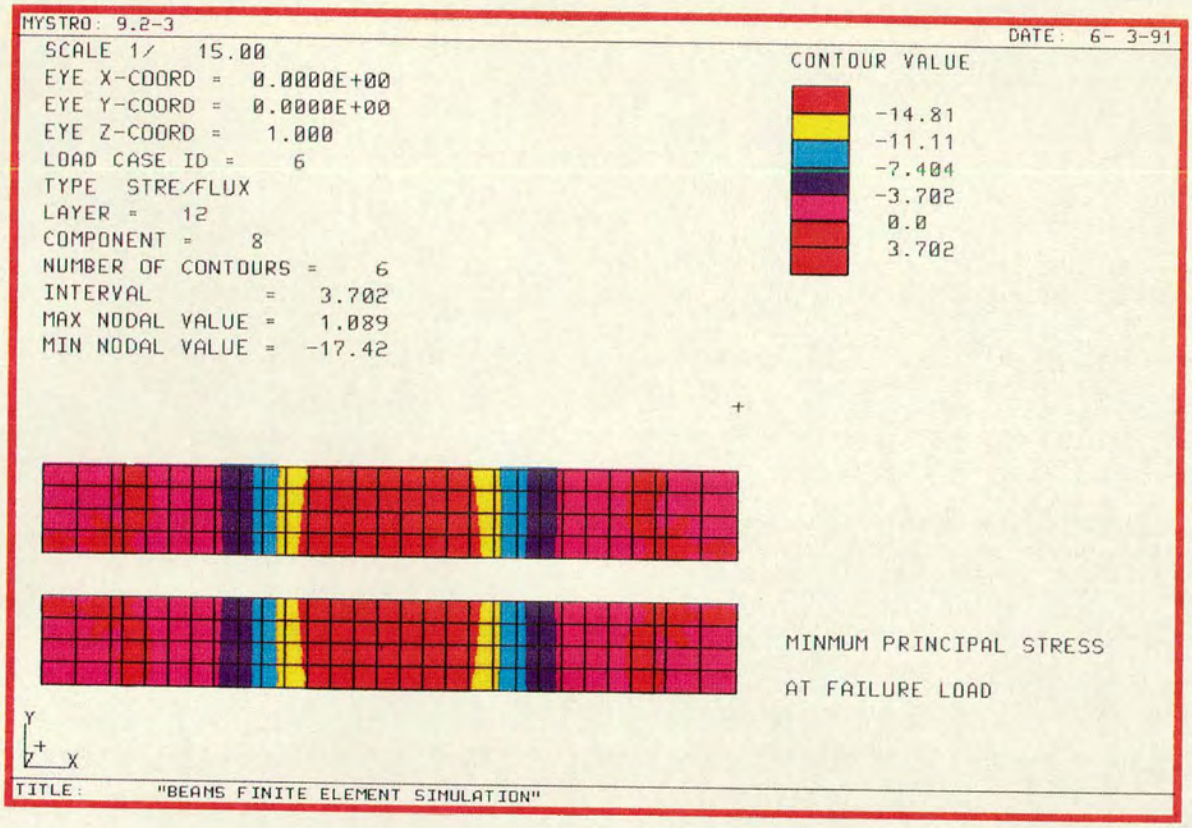
MYSTRO: 9.2-3
DATE: 6- 3-91
SCALE 1/ 15.00
EYE X-COORD = 0.0000E+00
EYE Y-COORD = 0.0000E+00
EYE Z-COORD = 1.000
LOAD CASE ID = 6
TYPE STRE/FLUX
LAYER = 12
COMPONENT = 8
NUMBER OF CONTOURS = 6
INTERVAL = 3.702
MAX NODAL VALUE = 1.089
MIN NODAL VALUE = -17.42
CONTOUR VALUE
-14.81
-11.11
-7.404
-3.702
0.0
3.702
MINMUM PRINCIPAL STRESS
AT FAILURE LOAD
Y
X
TITLE: "BEAMS FINITE ELEMENT SIMULATION"

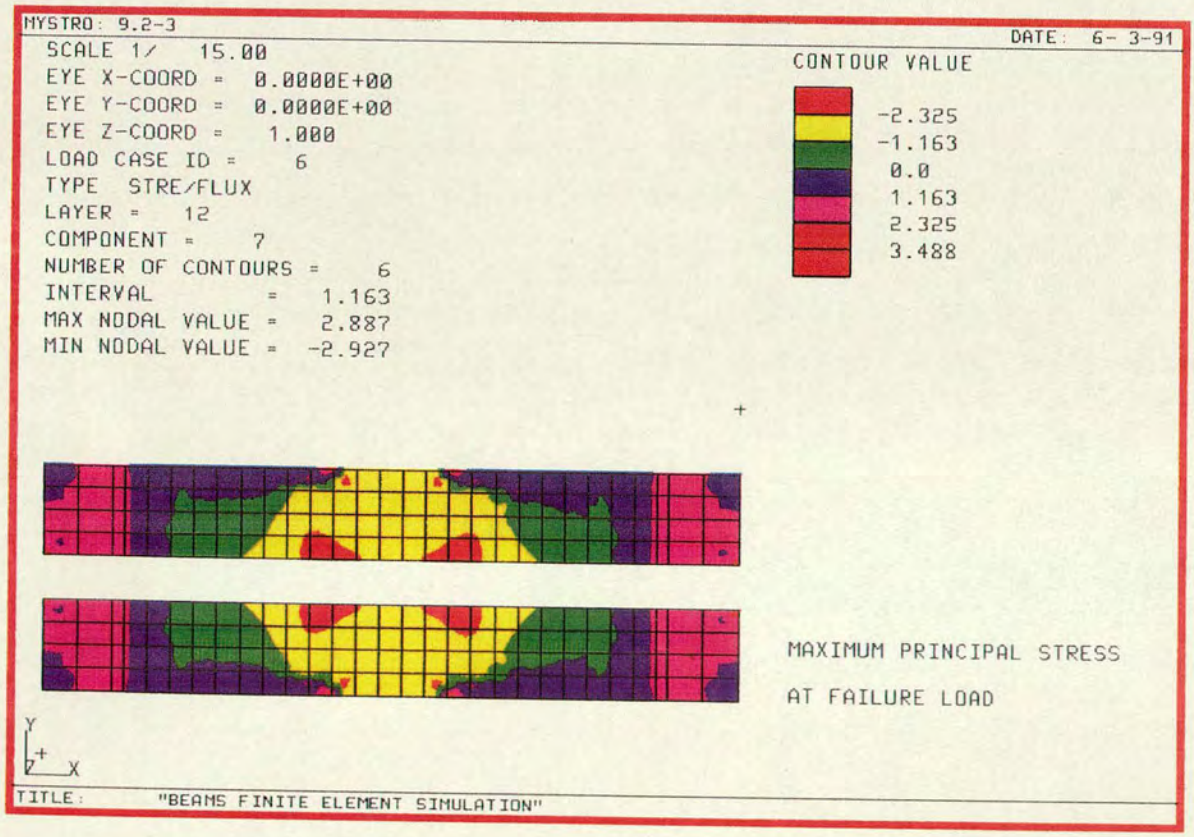
MYSTRO: 9.2-3
DATE: 6- 3-91
SCALE 1/ 15.00
EYE X-COORD = 0.0000E+00
EYE Y-COORD = 0.0000E+00
EYE Z-COORD = 1.000
LOAD CASE ID = 6
TYPE STRE/FLUX
LAYER = 12
COMPONENT = 7
NUMBER OF CONTOURS = 6
INTERVAL = 1.163
MAX NODAL VALUE = 2.887
MIN NODAL VALUE = -2.927
CONTOUR VALUE
-2.325
-1.163
0.0
1.163
2.325
3.488
MAXIMUM PRINCIPAL STRESS
AT FAILURE LOAD
Y
X
TITLE: "BEAMS FINITE ELEMENT SIMULATION"

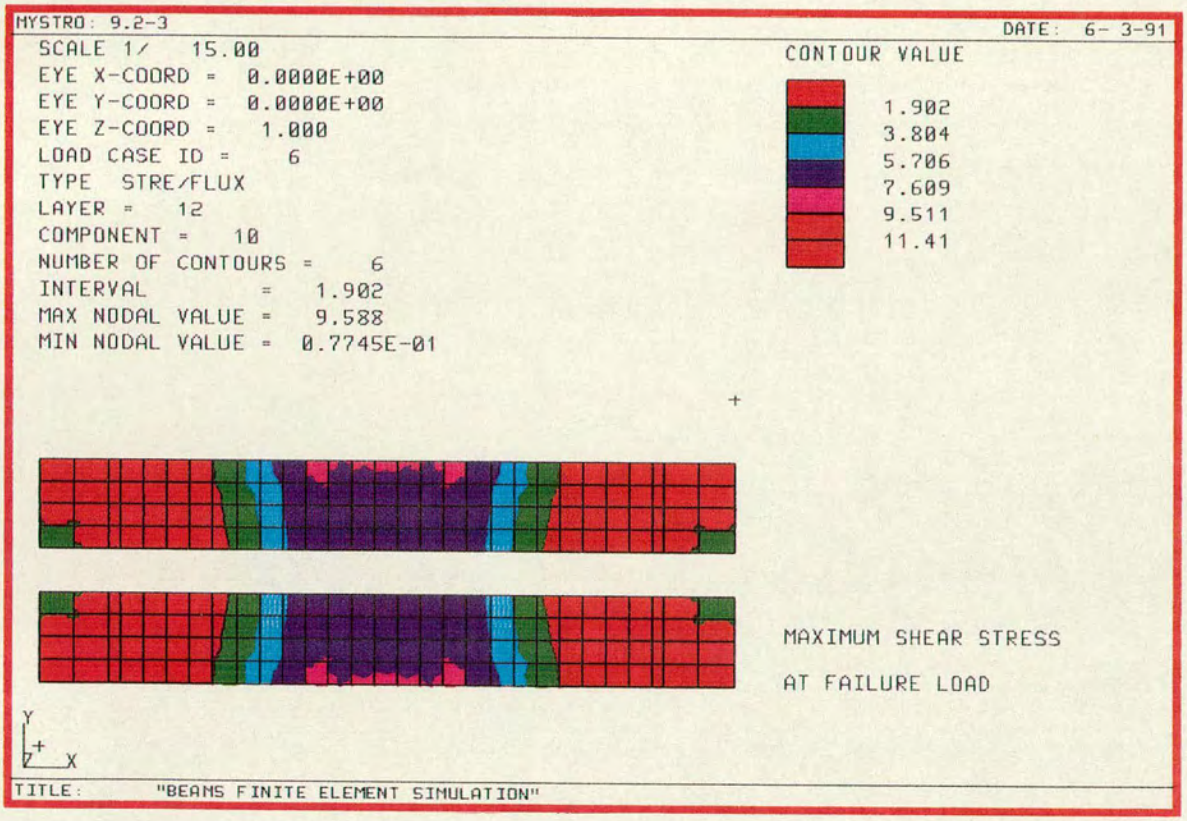
MYSTRO: 9.2-3
DATE: 6- 3-91
SCALE 1/ 15.00
EYE X-COORD = 0.0000E+00
EYE Y-COORD = 0.0000E+00
EYE Z-COORD = 1.000
LOAD CASE ID = 6
TYPE STRE/FLUX
LAYER = 12
COMPONENT = 10
NUMBER OF CONTOURS = 6
INTERVAL = 1.902
MAX NODAL VALUE = 9.588
MIN NODAL VALUE = 0.7745E-01
CONTOUR VALUE
1.902
3.804
5.706
7.609
9.511
11.41
MAXIMUM SHEAR STRESS
AT FAILURE LOAD
Y
Z
X
TITLE: "BEAMS FINITE ELEMENT SIMULATION"

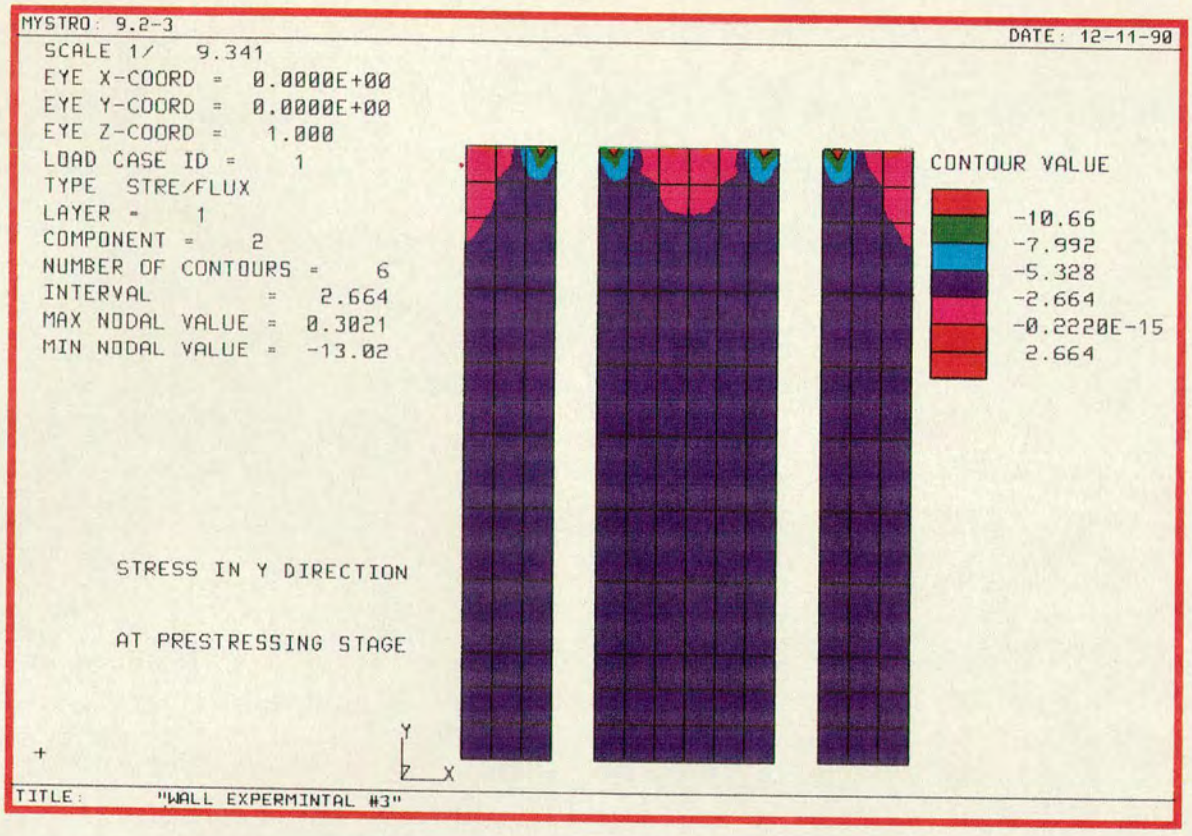
MYSTRO: 9.2-3
DATE: 12-11-90
SCALE 1/ 9.341
EYE X-COORD = 0.0000E+00
EYE Y-COORD = 0.0000E+00
EYE Z-COORD = 1.000
LOAD CASE ID = 1
TYPE STRE/FLUX
LAYER = 1
COMPONENT = 2
NUMBER OF CONTOURS = 6
INTERVAL = 2.664
MAX NODAL VALUE = 0.3021
MIN NODAL VALUE = -13.02
CONTOUR VALUE
-10.66
-7.992
-5.328
-2.664
-0.2220E-15
2.664
STRESS IN Y DIRECTION
AT PRESTRESSING STAGE
Y
Z
X
TITLE: "WALL EXPERMINTAL #3"

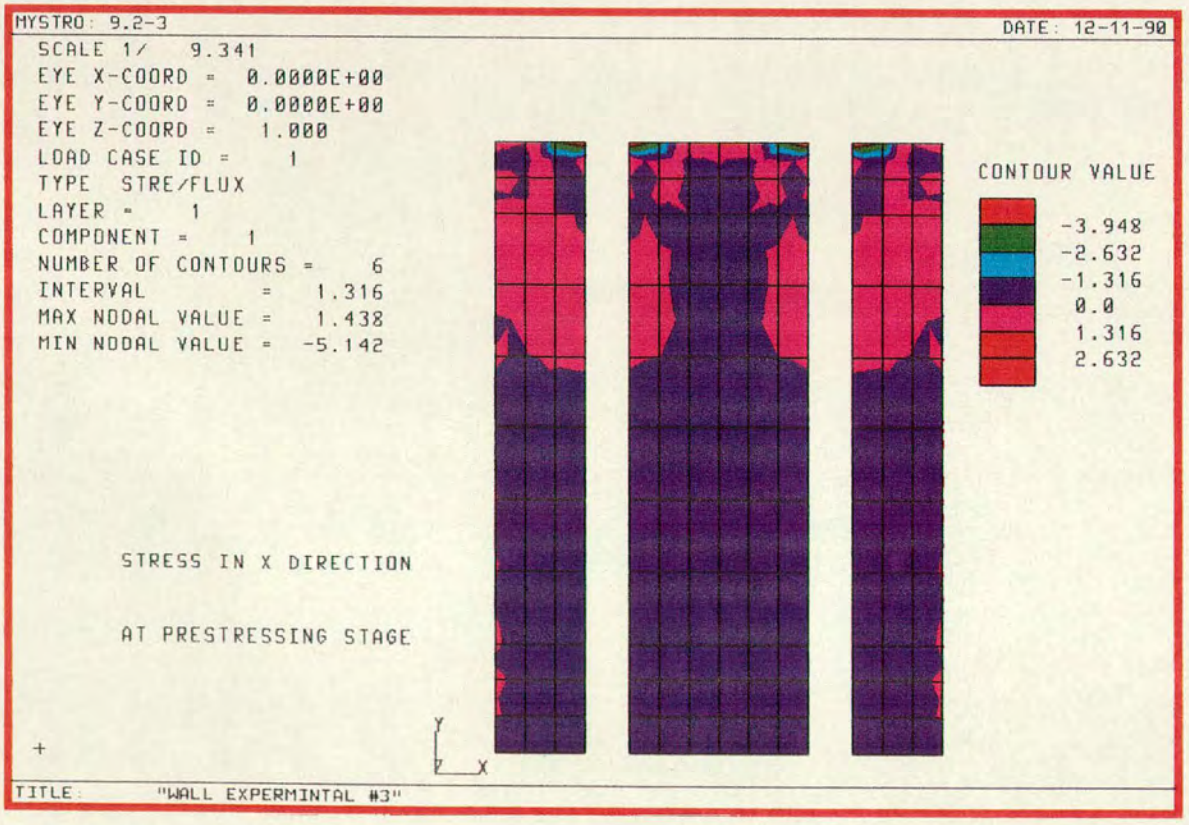
MYSTRO: 9.2-3
DATE: 12-11-90
SCALE 1/ 9.341
EYE X-COORD = 0.0000E+00
EYE Y-COORD = 0.0000E+00
EYE Z-COORD = 1.000
LOAD CASE ID = 1
TYPE STRE/FLUX
LAYER = 1
COMPONENT = 1
NUMBER OF CONTOURS = 6
INTERVAL = 1.316
MAX NODAL VALUE = 1.438
MIN NODAL VALUE = -5.142
CONTOUR VALUE
-3.948
-2.632
-1.316
0.0
1.316
2.632
STRESS IN X DIRECTION
AT PRESTRESSING STAGE
Y
Z
X
TITLE: "WALL EXPERMINTAL #3"

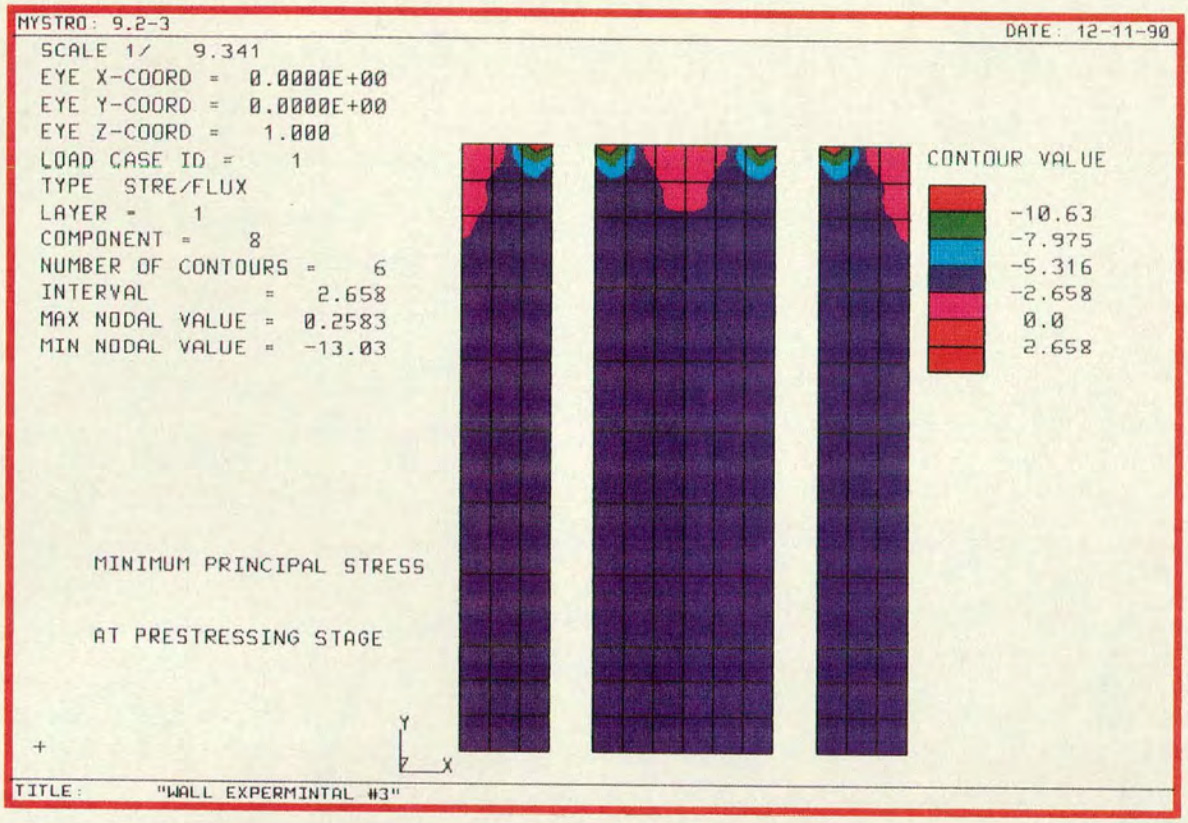
MYSTRO: 9.2-3
DATE: 12-11-90
SCALE 1/ 9.341
EYE X-COORD = 0.0000E+00
EYE Y-COORD = 0.0000E+00
EYE Z-COORD = 1.000
LOAD CASE ID = 1
TYPE STRE/FLUX
LAYER = 1
COMPONENT = 8
NUMBER OF CONTOURS = 6
INTERVAL = 2.658
MAX NODAL VALUE = 0.2583
MIN NODAL VALUE = -13.03
CONTOUR VALUE
-10.63
-7.975
-5.316
-2.658
0.0
2.658
MINIMUM PRINCIPAL STRESS
AT PRESTRESSING STAGE
Y
X
TITLE: "WALL EXPERMINTAL #3"

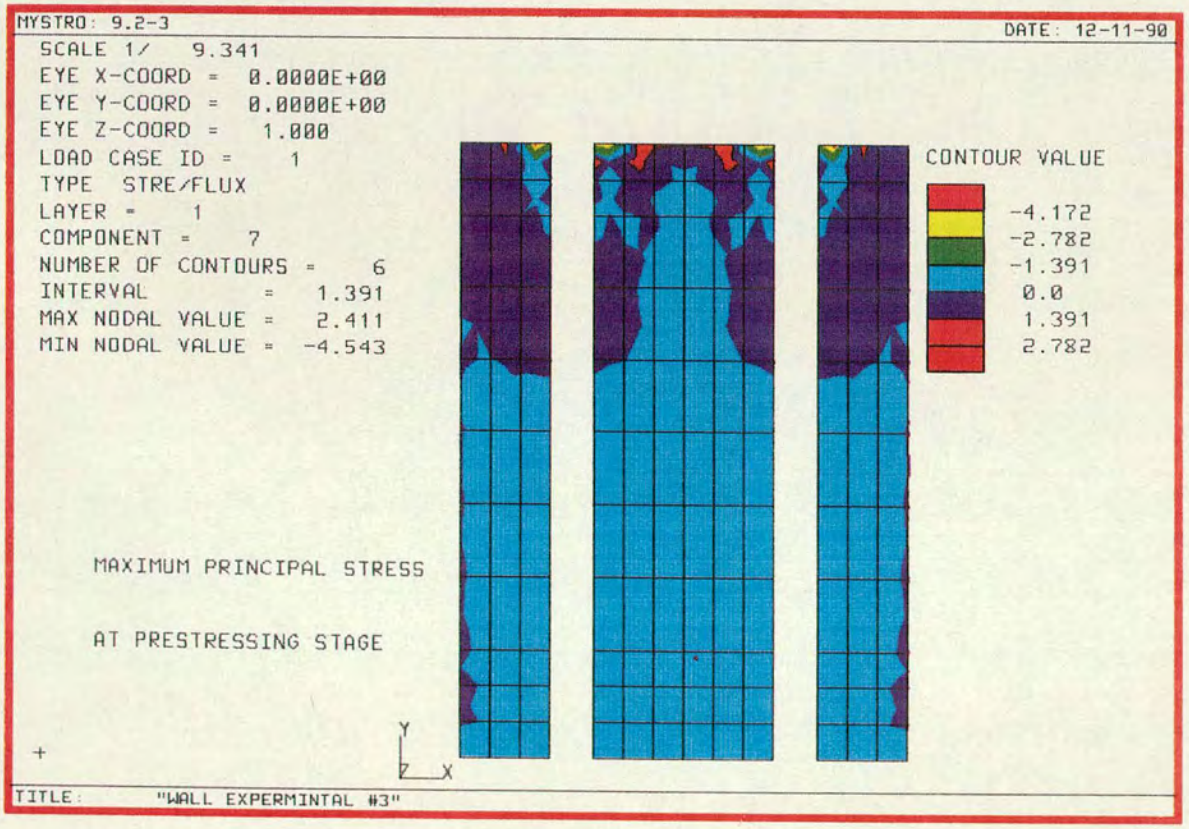
MYSTRO: 9.2-3
DATE: 12-11-90
SCALE 1/ 9.341
EYE X-COORD = 0.0000E+00
EYE Y-COORD = 0.0000E+00
EYE Z-COORD = 1.000
LOAD CASE ID = 1
TYPE STRE/FLUX
LAYER = 1
COMPONENT = 7
NUMBER OF CONTOURS = 6
INTERVAL = 1.391
MAX NODAL VALUE = 2.411
MIN NODAL VALUE = -4.543
CONTOUR VALUE
-4.172
-2.782
-1.391
0.0
1.391
2.782
MAXIMUM PRINCIPAL STRESS
AT PRESTRESSING STAGE
Y
X
TITLE: "WALL EXPERMINTAL #3"

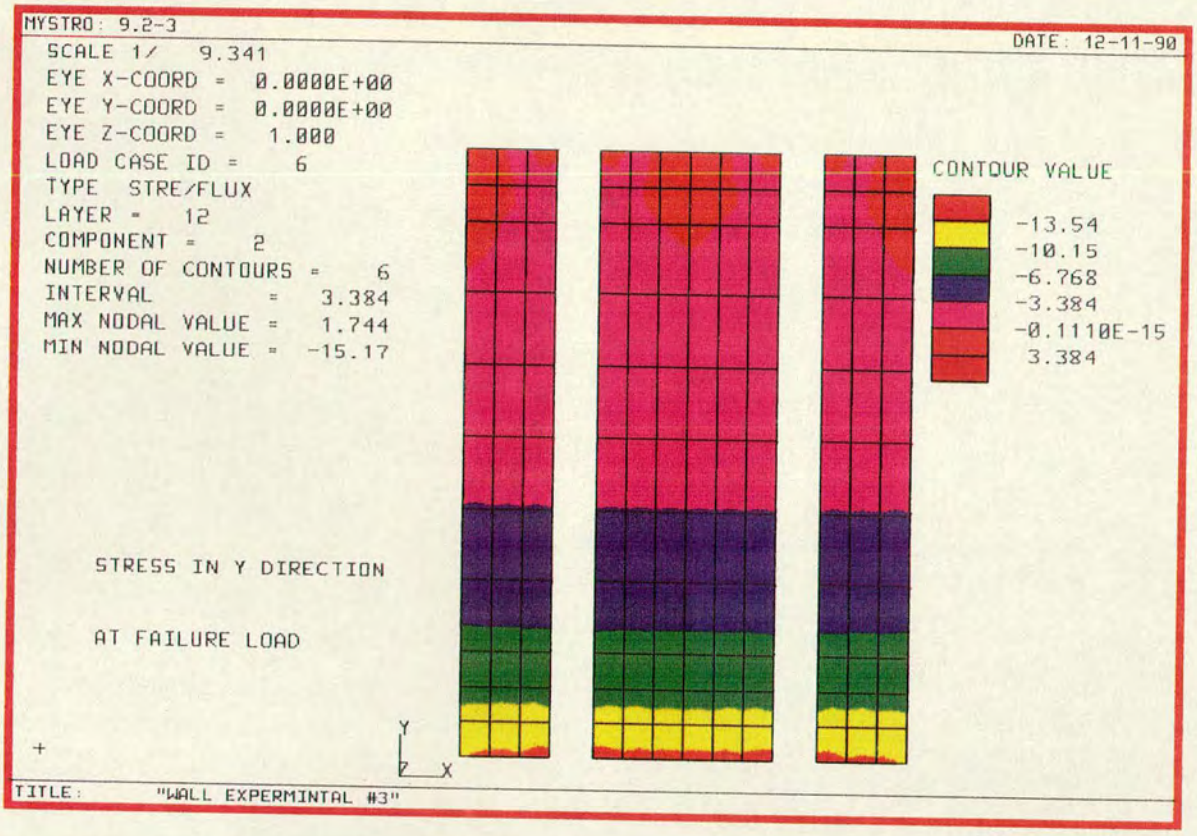
MYSTRO: 9.2-3
DATE: 12-11-90
SCALE 1/ 9.341
EYE X-COORD = 0.0000E+00
EYE Y-COORD = 0.0000E+00
EYE Z-COORD = 1.000
LOAD CASE ID = 6
TYPE STRE/FLUX
LAYER = 12
COMPONENT = 2
NUMBER OF CONTOURS = 6
INTERVAL = 3.384
MAX NODAL VALUE = 1.744
MIN NODAL VALUE = -15.17
STRESS IN Y DIRECTION
AT FAILURE LOAD
CONTOUR VALUE
-13.54
-10.15
-6.768
-3.384
-0.1110E-15
3.384
Y
X
TITLE: "WALL EXPERMINTAL #3"

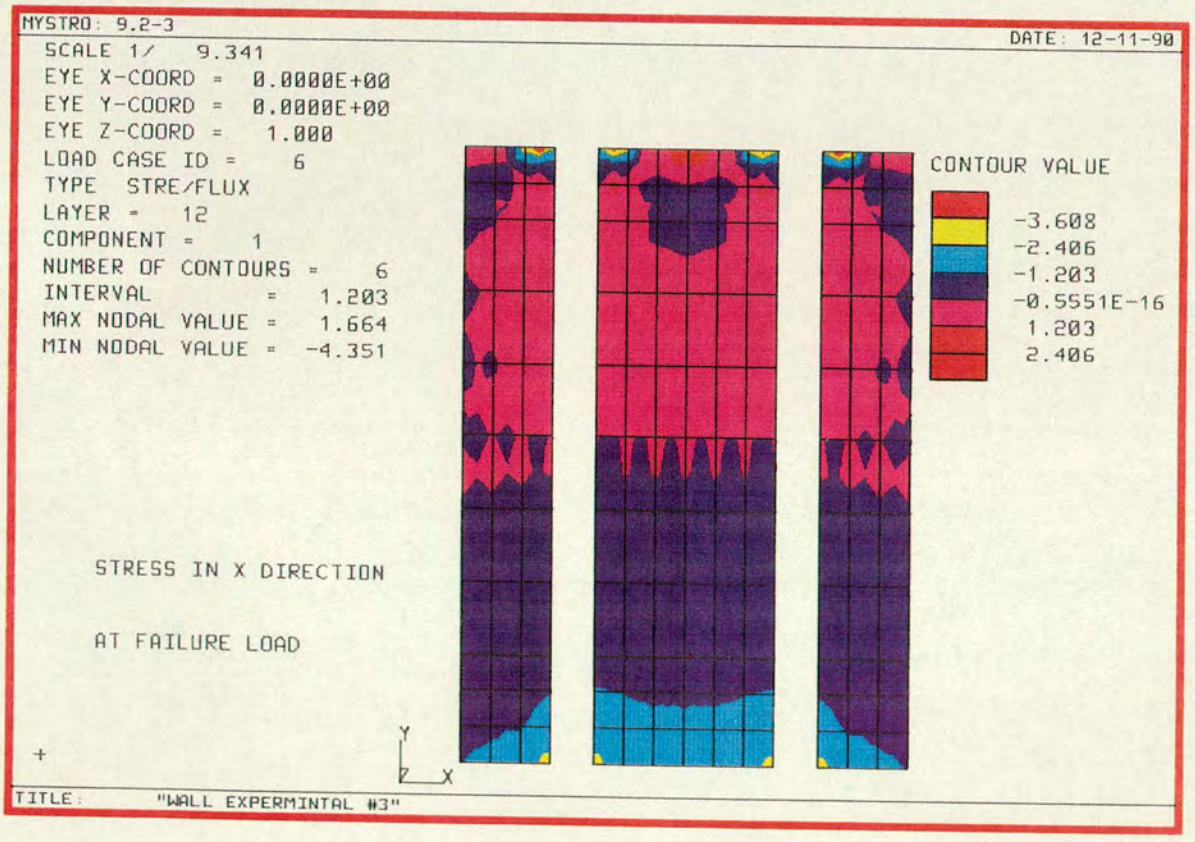
MYSTRO: 9.2-3
DATE: 12-11-90
SCALE 1/ 9.341
EYE X-COORD = 0.0000E+00
EYE Y-COORD = 0.0000E+00
EYE Z-COORD = 1.000
LOAD CASE ID = 6
TYPE STRE/FLUX
LAYER = 12
COMPONENT = 1
NUMBER OF CONTOURS = 6
INTERVAL = 1.203
MAX NODAL VALUE = 1.664
MIN NODAL VALUE = -4.351
STRESS IN X DIRECTION
AT FAILURE LOAD
CONTOUR VALUE
-3.608
-2.406
-1.203
-0.5551E-16
1.203
2.406
Y
X
TITLE: "WALL EXPERMINTAL #3"

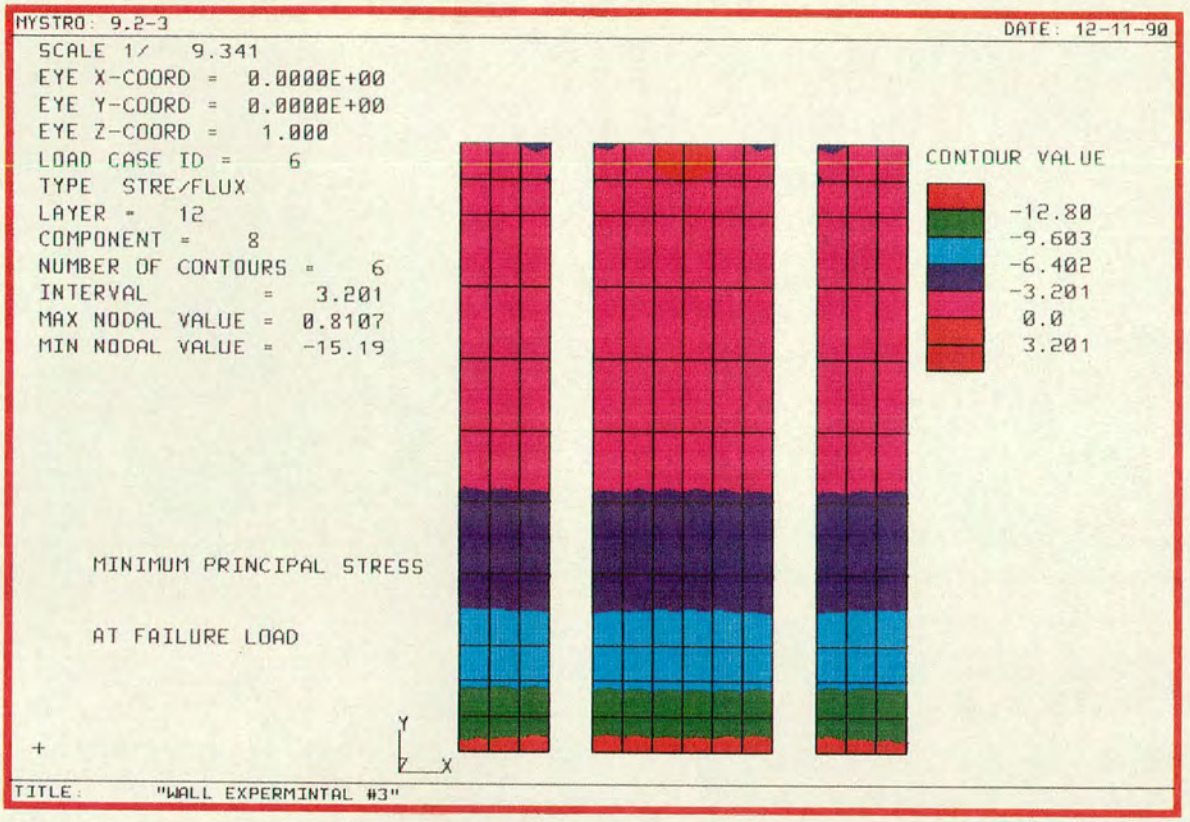
MYSTRO: 9.2-3
DATE: 12-11-90
SCALE 1/ 9.341
EYE X-COORD = 0.0000E+00
EYE Y-COORD = 0.0000E+00
EYE Z-COORD = 1.000
LOAD CASE ID = 6
TYPE STRE/FLUX
LAYER = 12
COMPONENT = 8
NUMBER OF CONTOURS = 6
INTERVAL = 3.201
MAX NODAL VALUE = 0.8107
MIN NODAL VALUE = -15.19
CONTOUR VALUE
-12.80
-9.603
-6.402
-3.201
0.0
3.201
MINIMUM PRINCIPAL STRESS
AT FAILURE LOAD
Y
Z X
TITLE: "WALL EXPERMINTAL #3"

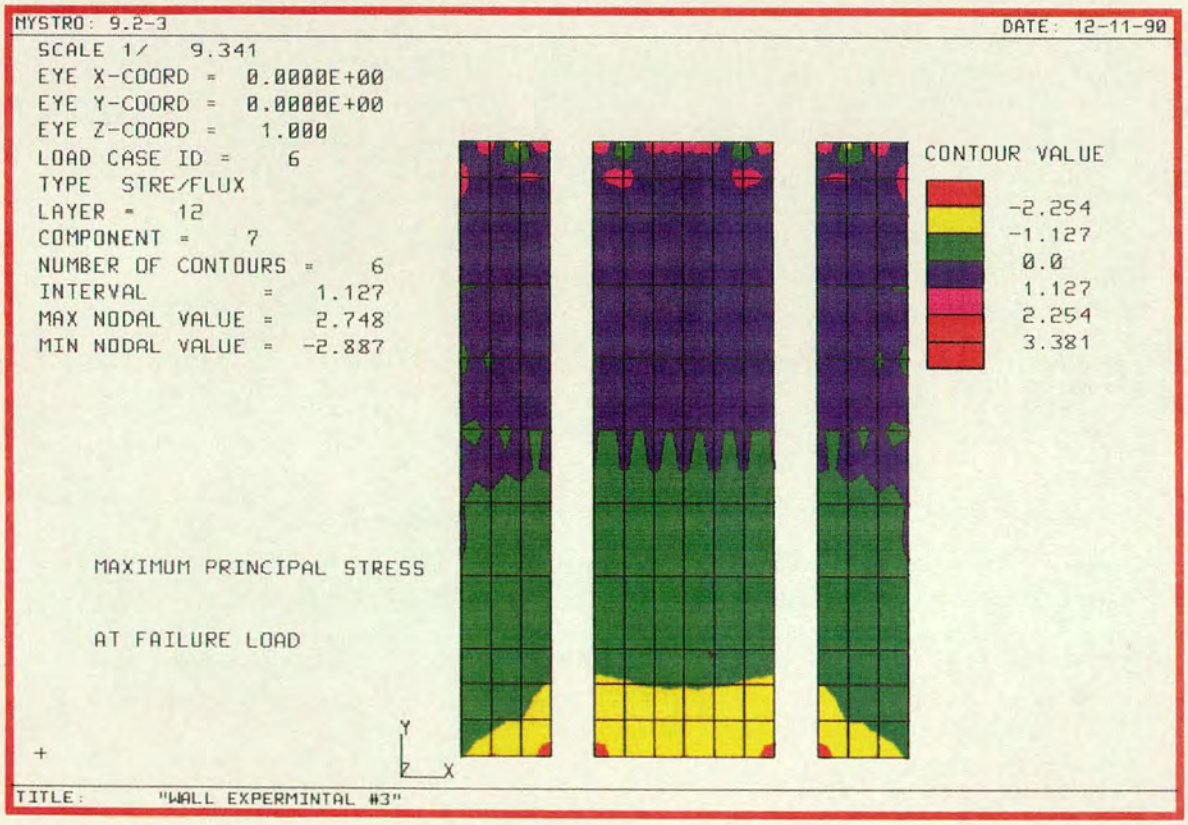
MYSTRO: 9.2-3
DATE: 12-11-90
SCALE 1/ 9.341
EYE X-COORD = 0.0000E+00
EYE Y-COORD = 0.0000E+00
EYE Z-COORD = 1.000
LOAD CASE ID = 6
TYPE STRE/FLUX
LAYER = 12
COMPONENT = 7
NUMBER OF CONTOURS = 6
INTERVAL = 1.127
MAX NODAL VALUE = 2.748
MIN NODAL VALUE = -2.887
CONTOUR VALUE
-2.254
-1.127
0.0
1.127
2.254
3.381
MAXIMUM PRINCIPAL STRESS
AT FAILURE LOAD
Y
Z X
TITLE: "WALL EXPERMINTAL #3"

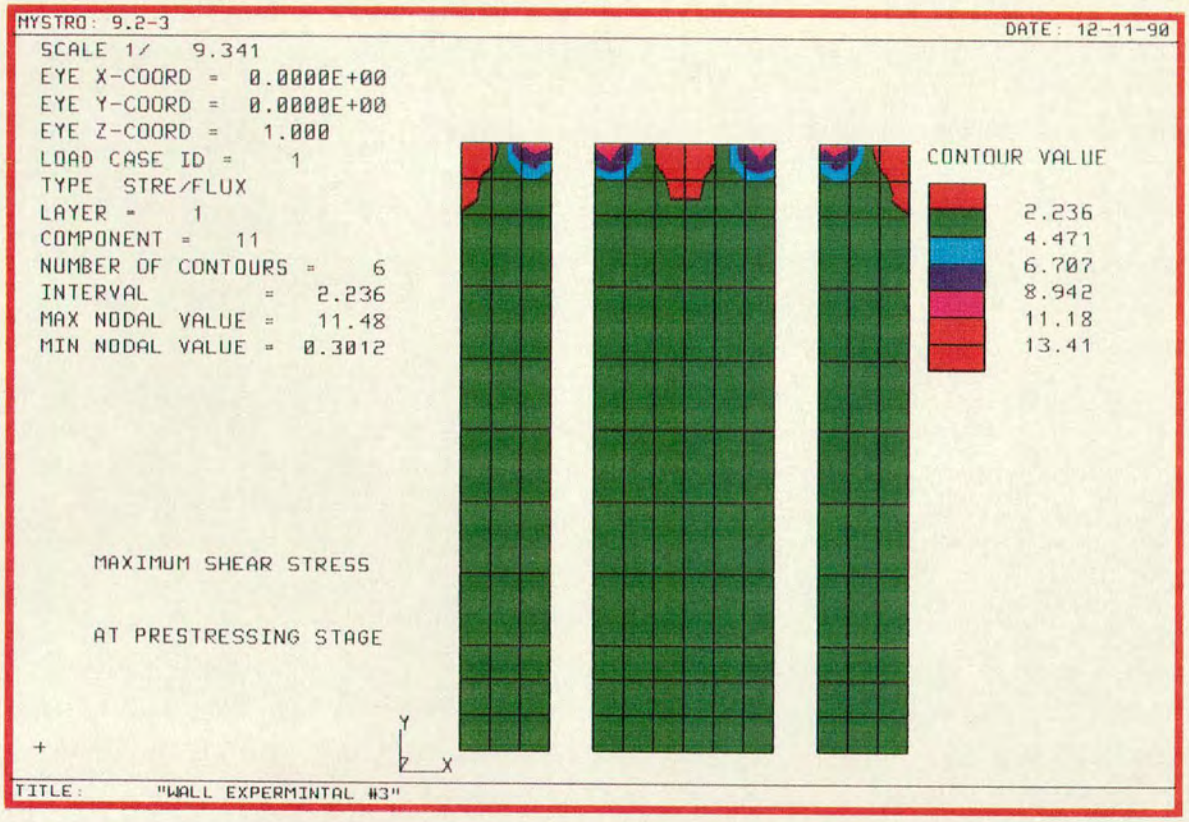
MYSTRO: 9.2-3
DATE: 12-11-90
SCALE 1/ 9.341
EYE X-COORD = 0.0000E+00
EYE Y-COORD = 0.0000E+00
EYE Z-COORD = 1.000
LOAD CASE ID = 1
TYPE STRE/FLUX
LAYER = 1
COMPONENT = 11
NUMBER OF CONTOURS = 6
INTERVAL = 2.236
MAX NODAL VALUE = 11.48
MIN NODAL VALUE = 0.3012
MAXIMUM SHEAR STRESS
AT PRESTRESSING STAGE
CONTOUR VALUE
2.236
4.471
6.707
8.942
11.18
13.41
Y
Z
X
TITLE: "WALL EXPERMINTAL #3"

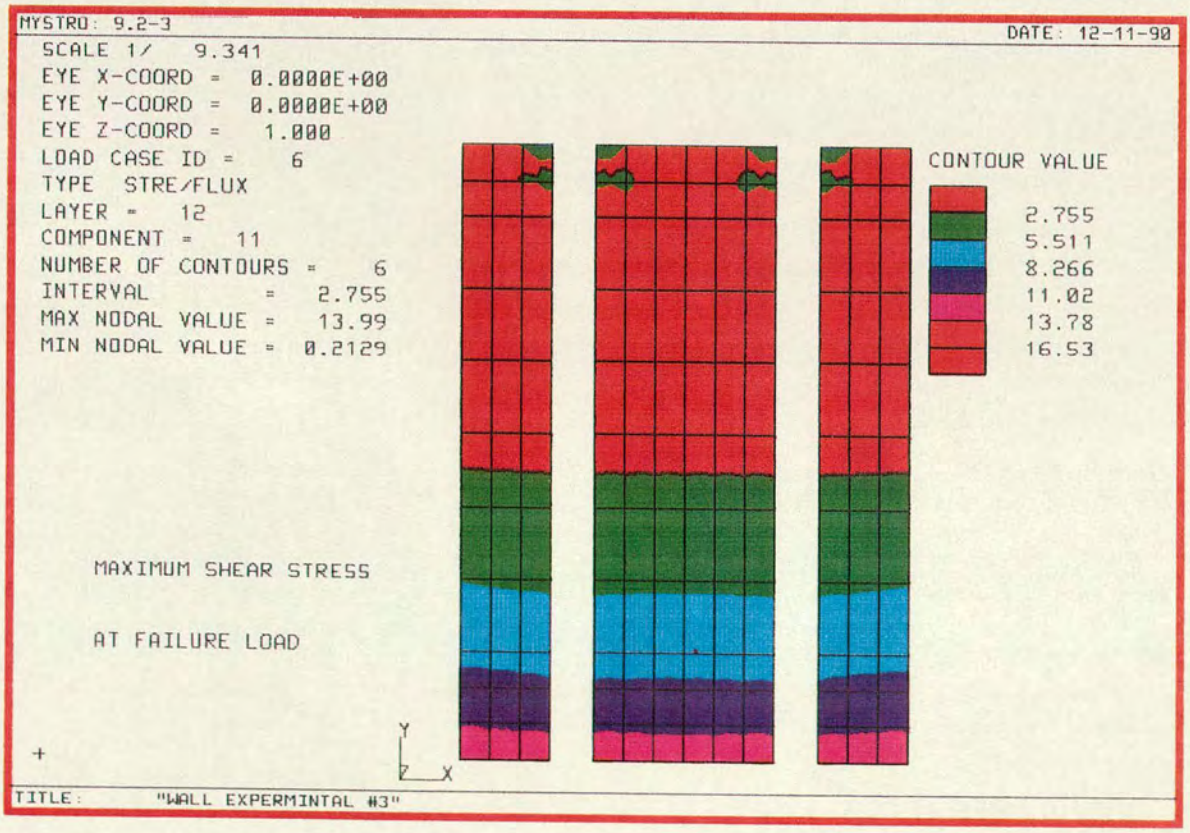
MYSTRO: 9.2-3
DATE: 12-11-90
SCALE 1/ 9.341
EYE X-COORD = 0.0000E+00
EYE Y-COORD = 0.0000E+00
EYE Z-COORD = 1.000
LOAD CASE ID = 6
TYPE STRE/FLUX
LAYER = 12
COMPONENT = 11
NUMBER OF CONTOURS = 6
INTERVAL = 2.755
MAX NODAL VALUE = 13.99
MIN NODAL VALUE = 0.2129
MAXIMUM SHEAR STRESS
AT FAILURE LOAD
CONTOUR VALUE
2.755
5.511
8.266
11.02
13.78
16.53
Y
Z
X
TITLE: "WALL EXPERMINTAL #3"

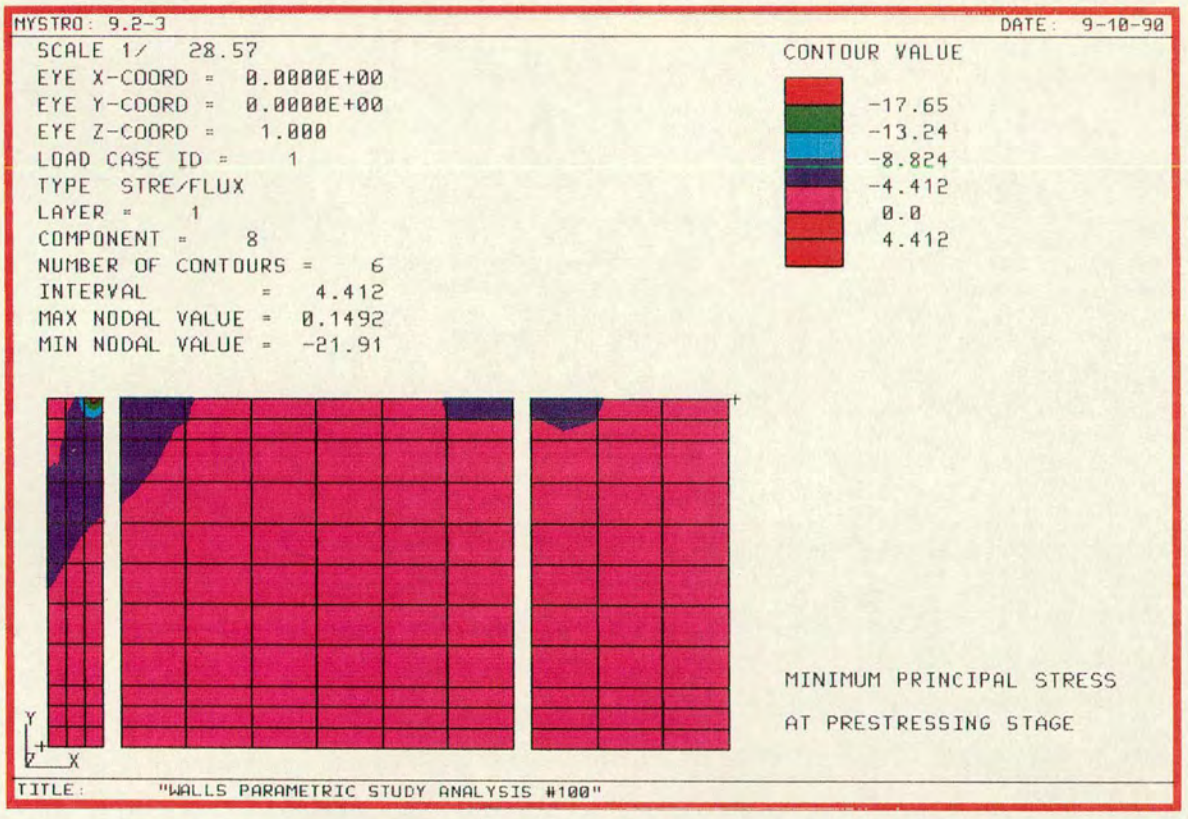
MYSTRO: 9.2-3
DATE: 9-10-90
SCALE 1/ 28.57
EYE X-COORD = 0.0000E+00
EYE Y-COORD = 0.0000E+00
EYE Z-COORD = 1.000
LOAD CASE ID = 1
TYPE STRE/FLUX
LAYER = 1
COMPONENT = 8
NUMBER OF CONTOURS = 6
INTERVAL = 4.412
MAX NODAL VALUE = 0.1492
MIN NODAL VALUE = -21.91
CONTOUR VALUE
-17.65
-13.24
-8.824
-4.412
0.0
4.412
Y
Z
X
MINIMUM PRINCIPAL STRESS
AT PRESTRESSING STAGE
TITLE: "WALLS PARAMETRIC STUDY ANALYSIS #100"

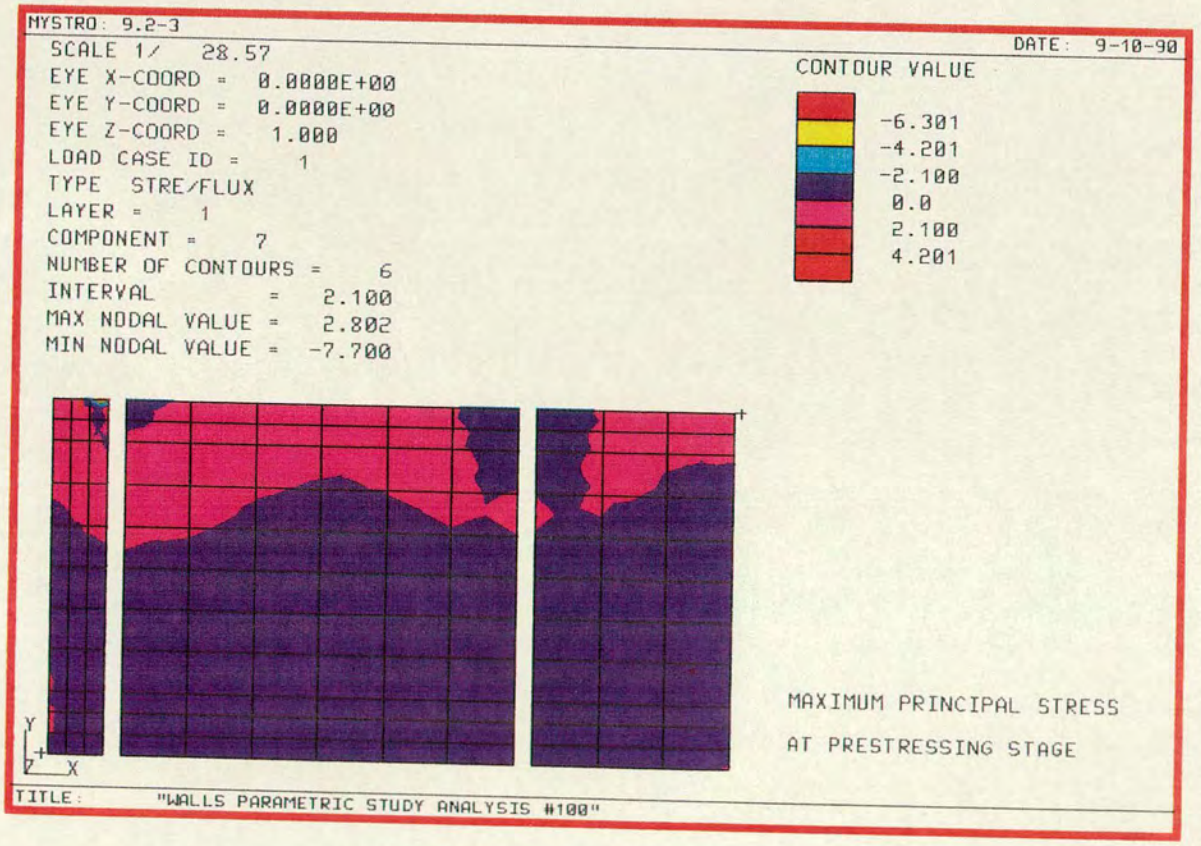
MYSTRO: 9.2-3
DATE: 9-10-90
SCALE 1/ 28.57
EYE X-COORD = 0.0000E+00
EYE Y-COORD = 0.0000E+00
EYE Z-COORD = 1.000
LOAD CASE ID = 1
TYPE STRE/FLUX
LAYER = 1
COMPONENT = 7
NUMBER OF CONTOURS = 6
INTERVAL = 2.100
MAX NODAL VALUE = 2.802
MIN NODAL VALUE = -7.700
CONTOUR VALUE
-6.301
-4.201
-2.100
0.0
2.100
4.201
Y
Z
X
MAXIMUM PRINCIPAL STRESS
AT PRESTRESSING STAGE
TITLE: "WALLS PARAMETRIC STUDY ANALYSIS #100"

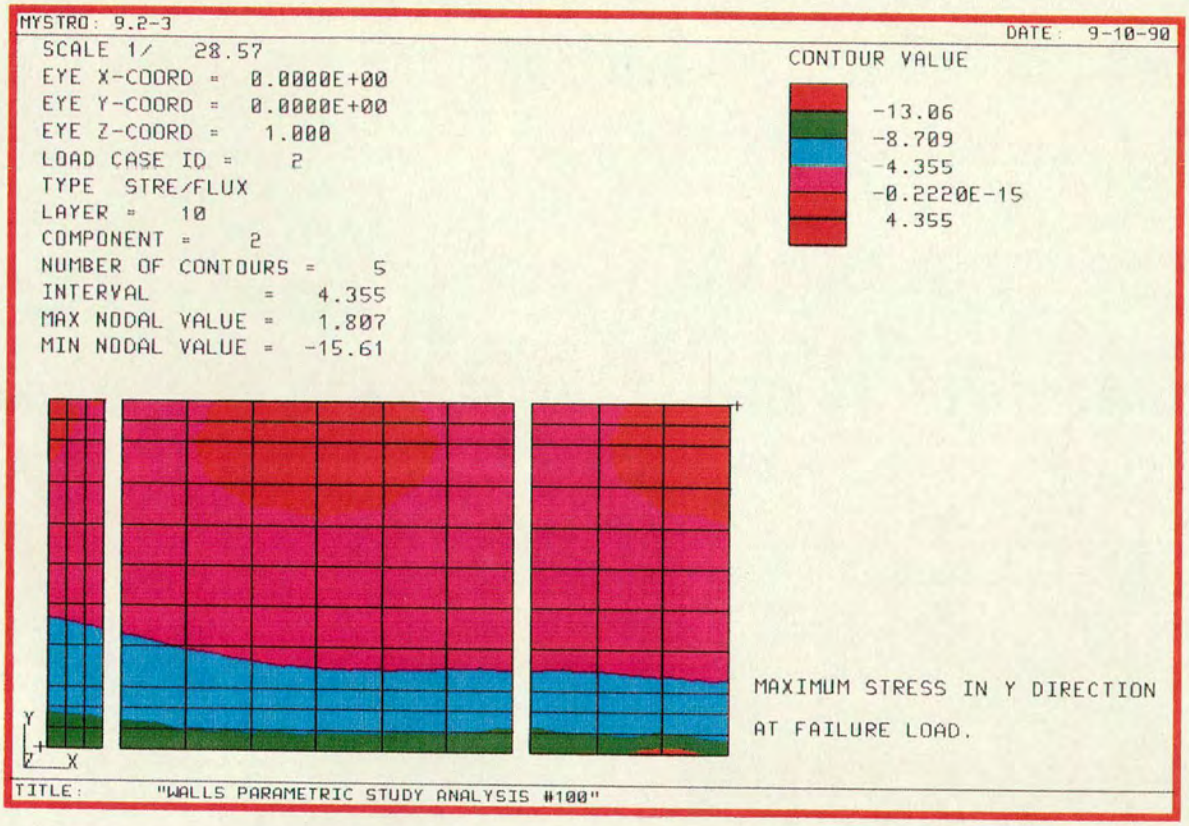
MYSTRO: 9.2-3
DATE: 9-10-90
SCALE 1/ 28.57
EYE X-COORD = 0.0000E+00
EYE Y-COORD = 0.0000E+00
EYE Z-COORD = 1.000
LOAD CASE ID = 2
TYPE STRE/FLUX
LAYER = 10
COMPONENT = 2
NUMBER OF CONTOURS = 5
INTERVAL = 4.355
MAX NODAL VALUE = 1.807
MIN NODAL VALUE = -15.61
CONTOUR VALUE
-13.06
-8.709
-4.355
-0.2220E-15
4.355
Y
Z
X
MAXIMUM STRESS IN Y DIRECTION
AT FAILURE LOAD.
TITLE: "WALLS PARAMETRIC STUDY ANALYSIS #100"

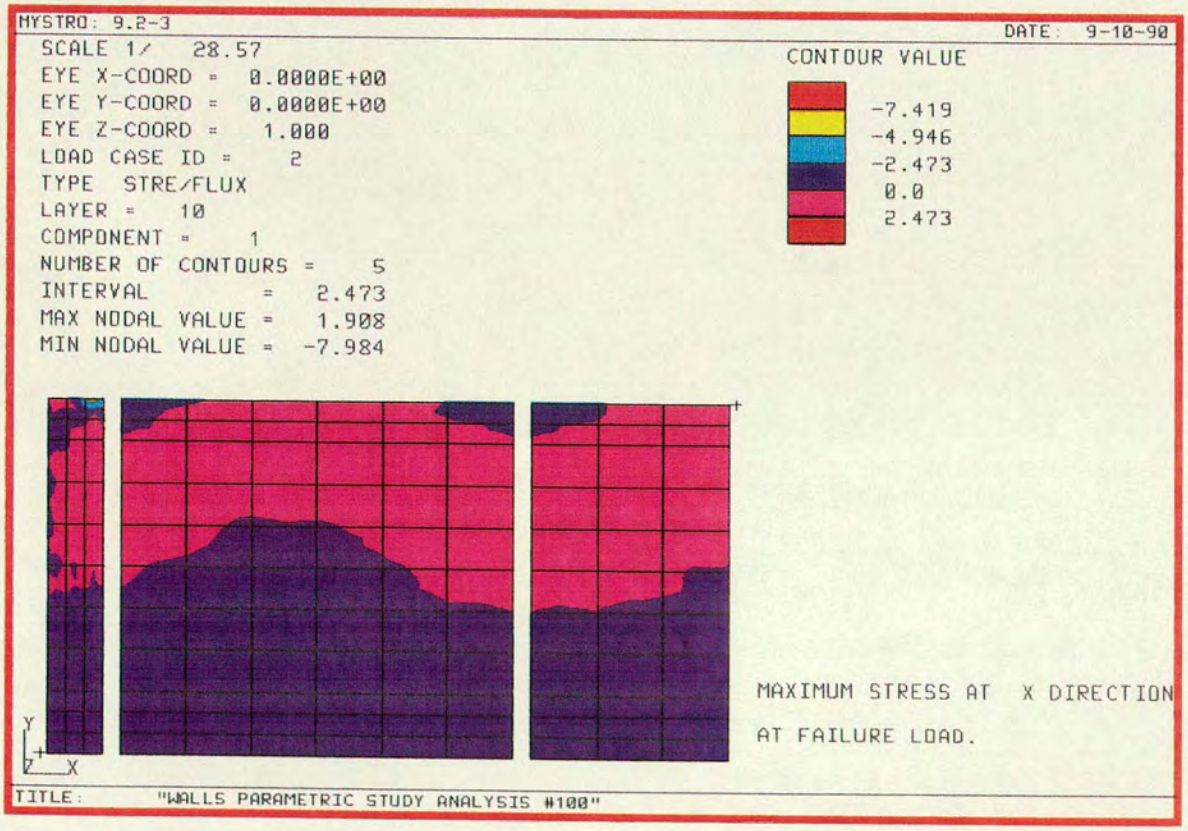
MYSTRO: 9.2-3
DATE: 9-10-90
SCALE 1/ 28.57
EYE X-COORD = 0.0000E+00
EYE Y-COORD = 0.0000E+00
EYE Z-COORD = 1.000
LOAD CASE ID = 2
TYPE STRE/FLUX
LAYER = 10
COMPONENT = 1
NUMBER OF CONTOURS = 5
INTERVAL = 2.473
MAX NODAL VALUE = 1.908
MIN NODAL VALUE = -7.984
CONTOUR VALUE
-7.419
-4.946
-2.473
0.0
2.473
Y
Z
X
MAXIMUM STRESS AT X DIRECTION
AT FAILURE LOAD.
TITLE: "WALLS PARAMETRIC STUDY ANALYSIS #100"

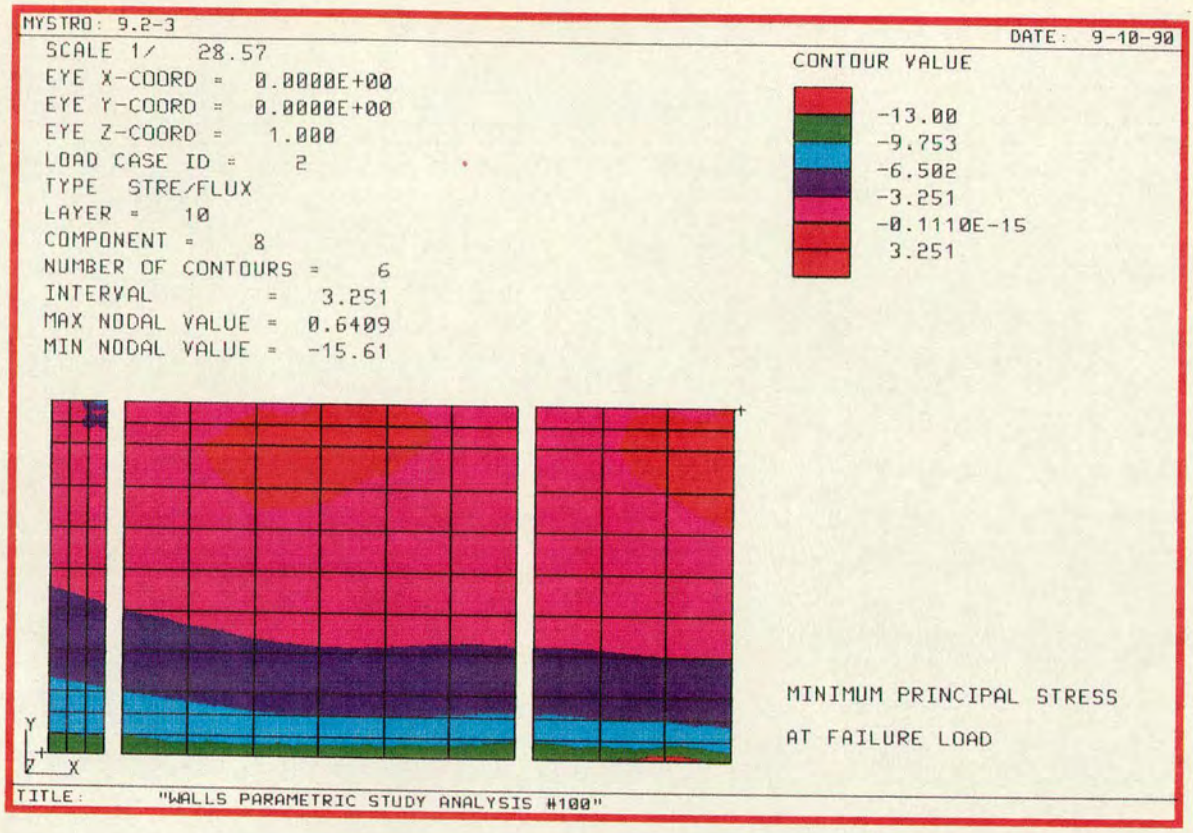
MYSTRO: 9.2-3
DATE: 9-10-90
SCALE 1/ 28.57
EYE X-COORD = 0.0000E+00
EYE Y-COORD = 0.0000E+00
EYE Z-COORD = 1.000
LOAD CASE ID = 2
TYPE STRE/FLUX
LAYER = 10
COMPONENT = 8
NUMBER OF CONTOURS = 6
INTERVAL = 3.251
MAX NODAL VALUE = 0.6409
MIN NODAL VALUE = -15.61
CONTOUR VALUE
-13.00
-9.753
-6.502
-3.251
-0.1110E-15
3.251
Y
Z
X
MINIMUM PRINCIPAL STRESS
AT FAILURE LOAD
TITLE: "WALLS PARAMETRIC STUDY ANALYSIS #100"

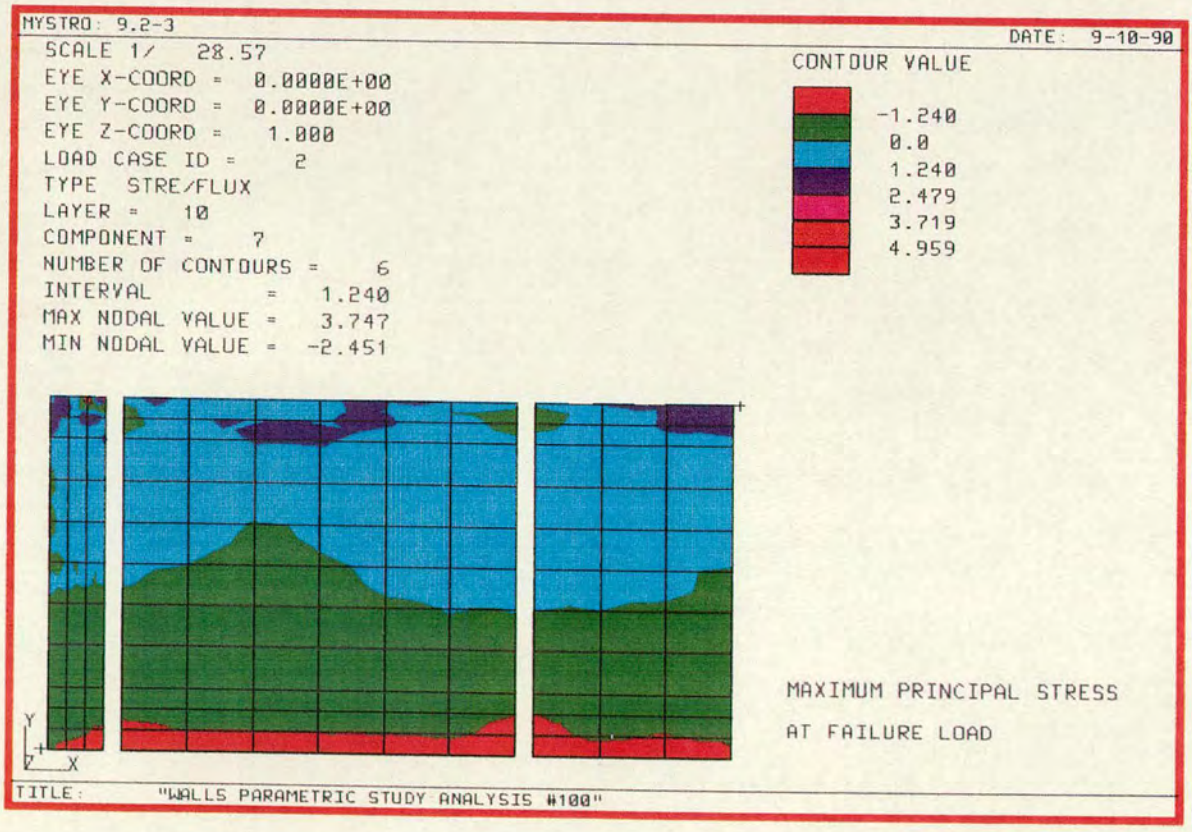
MYSTRO: 9.2-3
DATE: 9-10-90
SCALE 1/ 28.57
EYE X-COORD = 0.0000E+00
EYE Y-COORD = 0.0000E+00
EYE Z-COORD = 1.000
LOAD CASE ID = 2
TYPE STRE/FLUX
LAYER = 10
COMPONENT = 7
NUMBER OF CONTOURS = 6
INTERVAL = 1.240
MAX NODAL VALUE = 3.747
MIN NODAL VALUE = -2.451
CONTOUR VALUE
-1.240
0.0
1.240
2.479
3.719
4.959
Y
Z
X
MAXIMUM PRINCIPAL STRESS
AT FAILURE LOAD
TITLE: "WALLS PARAMETRIC STUDY ANALYSIS #100"

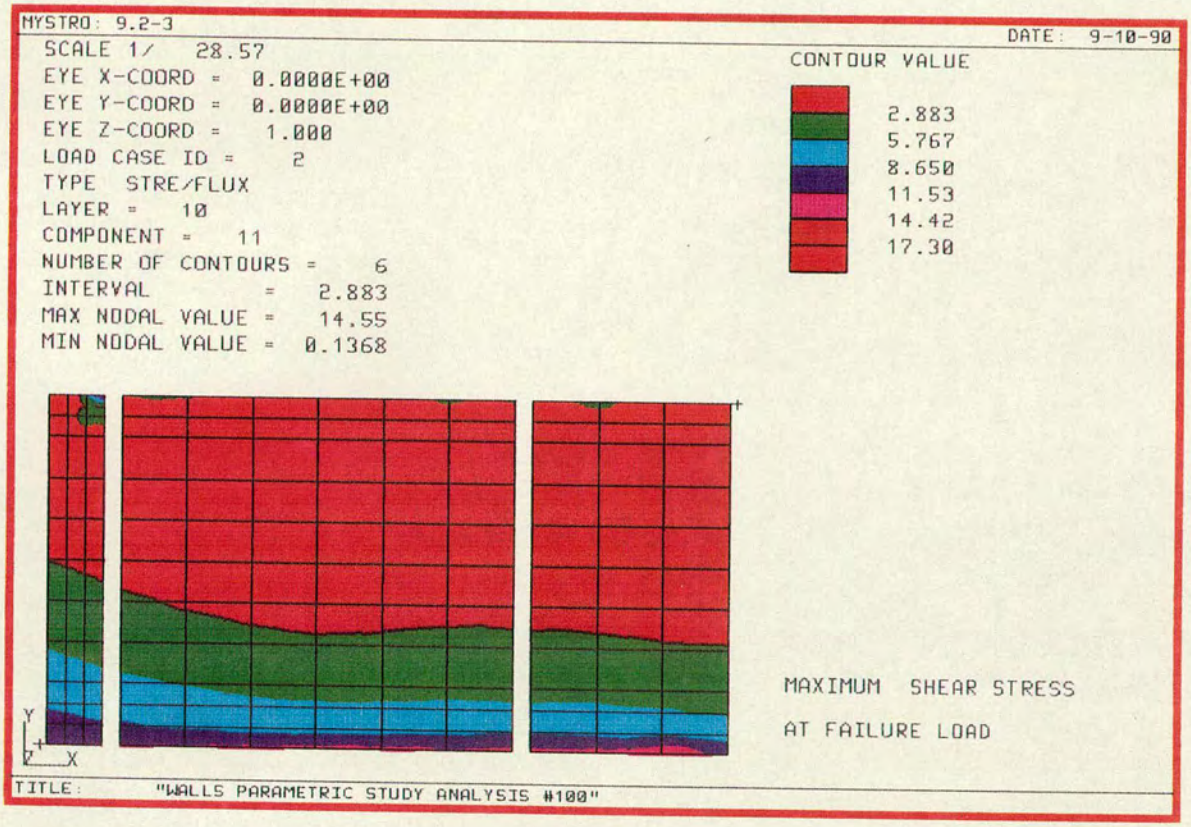
MYSTRO: 9.2-3
DATE: 9-10-90
SCALE 1/ 28.57
EYE X-COORD = 0.0000E+00
EYE Y-COORD = 0.0000E+00
EYE Z-COORD = 1.000
LOAD CASE ID = 2
TYPE STRE/FLUX
LAYER = 10
COMPONENT = 11
NUMBER OF CONTOURS = 6
INTERVAL = 2.883
MAX NODAL VALUE = 14.55
MIN NODAL VALUE = 0.1368
CONTOUR VALUE
2.883
5.767
8.650
11.53
14.42
17.30
Y
Z
X
MAXIMUM SHEAR STRESS
AT FAILURE LOAD
TITLE: "WALLS PARAMETRIC STUDY ANALYSIS #100"

APPENDIX B

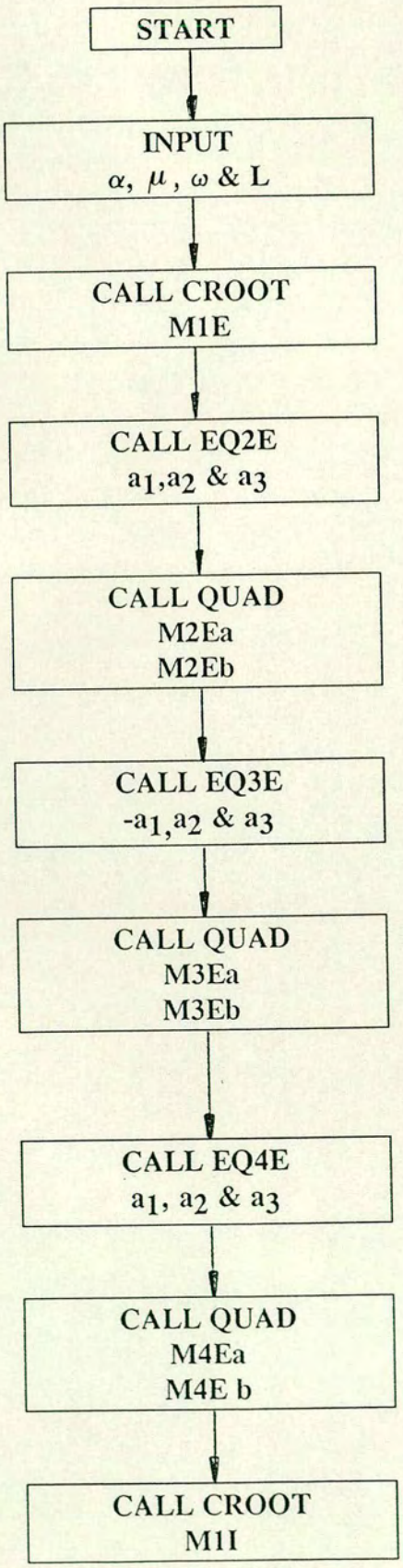
START
INPUT
α, μ, ω & L
CALL CROOT
M1E
CALL EQ2E
a1,a2 & a3
CALL QUAD
M2Ea
M2Eb
CALL EQ3E
-a1,a2 & a3
CALL QUAD
M3Ea
M3Eb
CALL EQ4E
a1, a2 & a3
CALL QUAD
M4Ea
M4E b
CALL CROOT
M1I

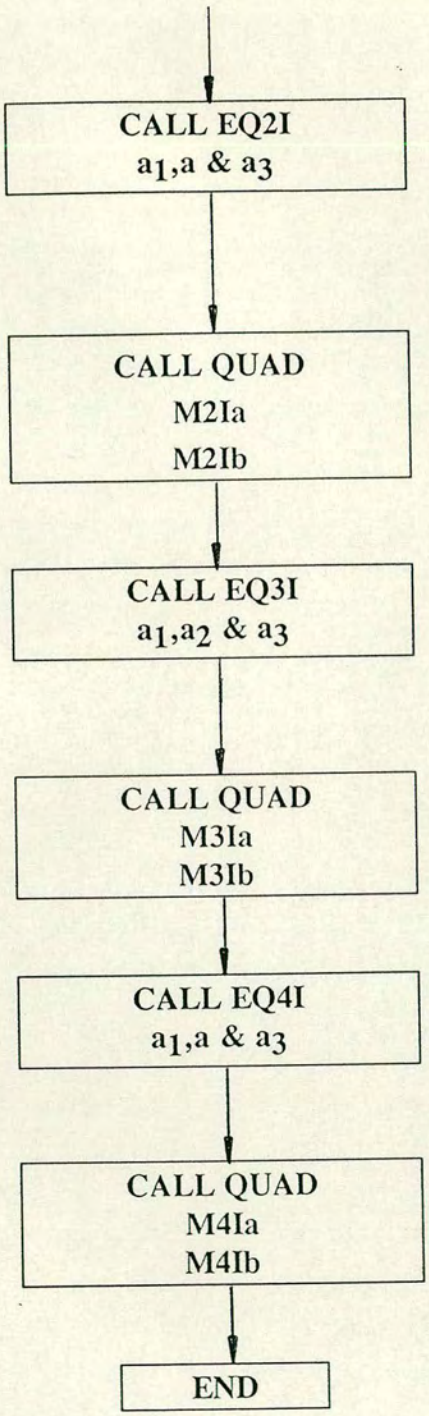

FLOW CHART OF THE PANEL MAIN PROGRAM

APPENDIX C

FORMULA FOR CALCULATING THE MOMENT-CURVATURE AND THE LOAD-DEFLECTION RELATIONSHIPS (PEDRESCHI, 1983)

I CALCULATION OF MOMENT-CURVATURE

1) At Prestressing

$$\phi_p = \frac{\varepsilon_{p1} - \varepsilon_{p2}}{h}$$

2) M-ϕ Relationship up to cracking

$$M_{cr} = C.Ia - Ts(h-d) - Tm(h-n)/3$$

$$\phi = \frac{\varepsilon_1 - \varepsilon_2}{h}$$

3) M-ϕ Relationship after cracking at a crack

$$M_{cr} = C.Ia - Ts(h-d)$$

$$\phi_{av} = \frac{\varepsilon_1 - \varepsilon_{sam}}{d}$$

II CALCULATION OF LOAD-DEFLECTION

Once the moment and average curvature relationship was obtained the load-deflection relationship of the prestressed brickwork beams was determined using the finite difference method.

APPENDIX D

PAPERS

The work from this thesis has led to several papers by the author in collaboration with Dr. Fairbairn. The titles of the papers under the process of being published are as follows:-

1. The behaviour of post-tensioned pocket-type brickwork retaining walls up to failure load.

2. The influence of bonding patterns on the performance of prestressed brick/masonry.